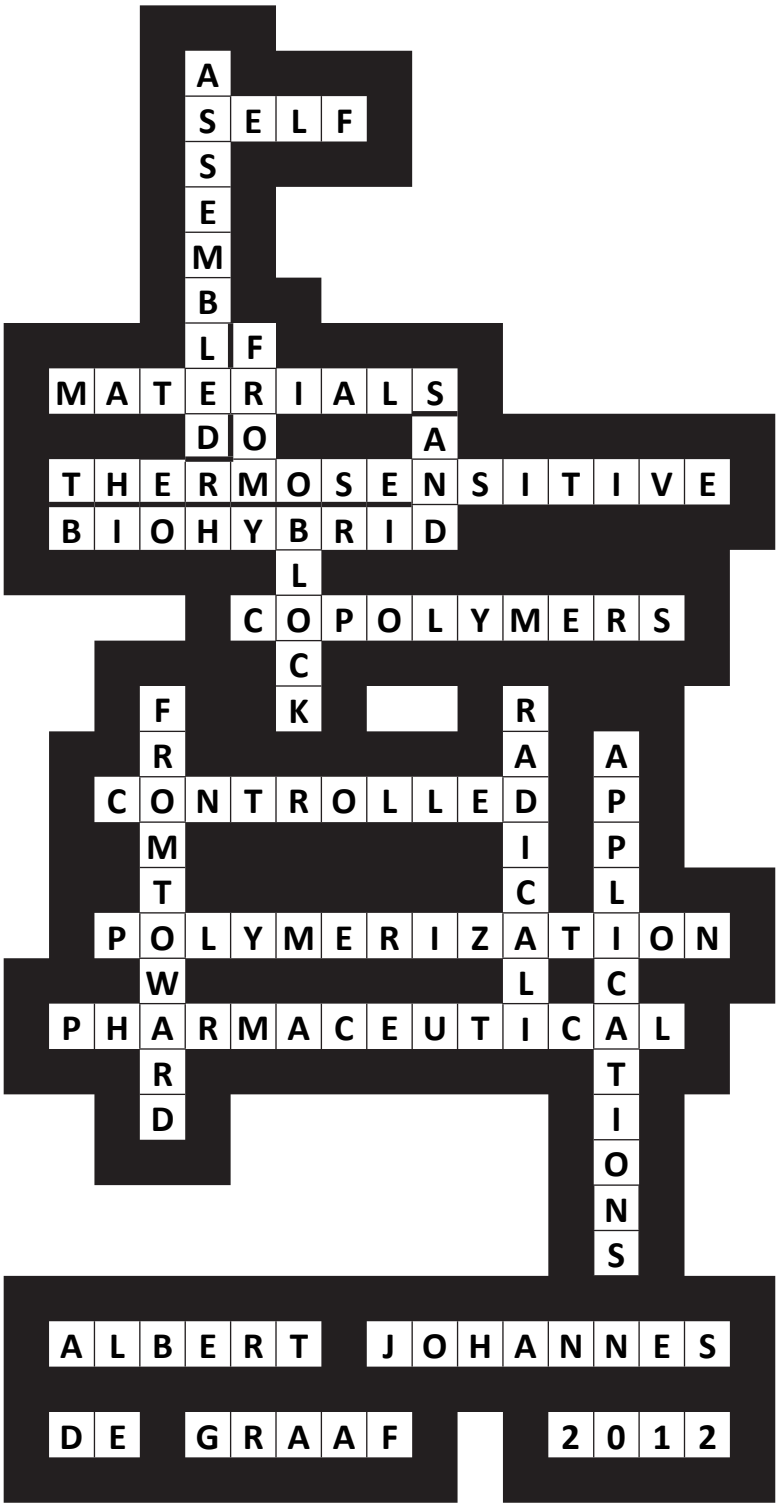
A
SELF
SSEMBL
F
MATERIALS
DO
A
THERMOSENSITIVE
BIOHYBRID
L
COPOLYMERS
C
FK
R
RA
A
CONTROLLED
P
M
I
P
TC
L
POLYMERIZATION
WL
C
PHARMACEUTICAL
R
T
D
I
O
N
S
ALBERT JOHANNES
DE GRAAF
2012

ISBN: 978-90-393-5753-8

© 2012 A.J. de Graaf, Utrecht

The printing of this thesis was financially supported by MSD Oss B.V.

Printed by CPI Koninklijke Wöhrmann Print Service

Self-assembled materials from thermosensitive and biohybrid block copolymers

From controlled radical polymerization toward pharmaceutical applications

Zelfassemblerende materialen van thermosensitieve en biohybride blok copolymeren

Van gecontroleerde radicaalpolymerisatie tot farmaceutische toepassingen

(met een samenvatting in het Nederlands)

Proefschrift

ter verkrijging van de graad van doctor aan de Universiteit Utrecht
op gezag van de rector magnificus, prof. dr. G. J. van der Zwaan,
ingevolge het besluit van het college voor promoties in het openbaar te verdedigen op
woensdag 28 maart 2012 des middags te 2.30 uur

door

Albert Johannes de Graaf

geboren op 29 januari 1983
te Delft

Promotor:	Prof. dr. ir. W. E. Hennink
Co-promotoren:	Dr. E. Mastrobattista Dr. ir. T. Vermonden

Voor mijn moeder

Table of Contents

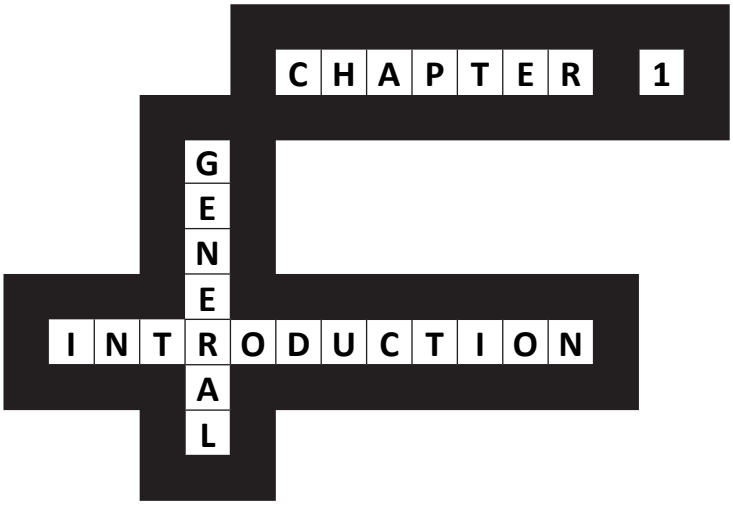
CHAPTER 1
GENERAL
INTRODUCTION

1.1. Drug delivery systems

1.1.1. Nanoparticles in medicine

Nanoparticles, *i.e.* particles with a diameter of less than 1 μm (and preferable <100 nm), are extensively being studied as formulations for a wide range of experimental and existing therapeutic drugs.[1] Several nanoparticulate formulations have already entered the market.[2] The reason for the interest in "nanomedicine" is that formulation in nanoparticles has been shown to significantly decrease the rates of degradation and excretion of a drug as well as alter its distribution in the body, which can lead to reduced side effects in non-target tissues and organs.[3]

Degradation of substances formulated in nanoparticles is prevented simply by the fact that nanoparticles are generally poorly penetrable by enzymes that are present in blood. Especially the new classes of therapeutics, like peptides, proteins, DNA and RNA, are in their naked form often very rapidly degraded and thus benefit from being packaged in nanoparticles.

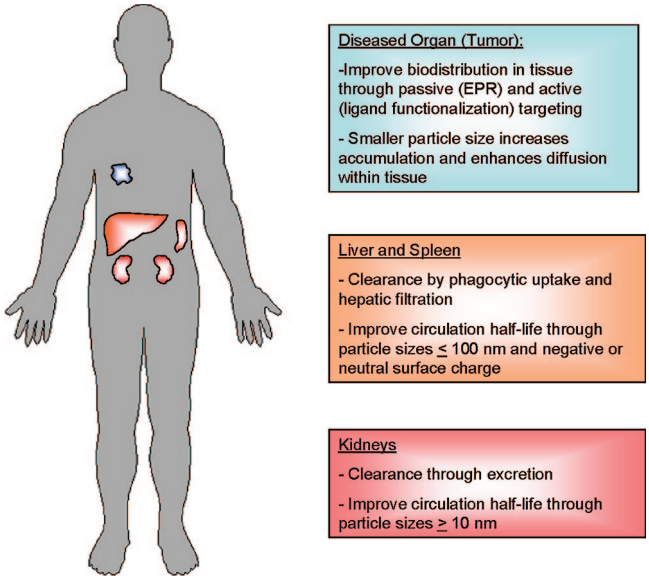

Figure 1. Effect of nanoparticle characteristics on their biodistribution. Reprinted with permission from Alexis et al.[4] Copyright 2008 by the American Chemical Society.

Furthermore, the rate of renal excretion of any molecule or particle from the circulation is dependent on their size. In general, particles with a diameter larger than 7 nm (the size of albumin; a long circulating plasma protein) are hardly excreted by the kidneys.[4] On the other hand, particles with a diameter larger than 100 nm are effectively removed from the circulation by filtration in the spleen and by the mononuclear phagocyte system (MPS), also known as the reticuloendothelial system (RES).[4] Consequently, it is clear that formulating therapeutic molecules in nanoparticles with a diameter between 10 and 100 nm will lead to the longest blood residence time (Figure 1).

Apart from their size, the surface characteristics such as the charge (ζ-potential) of nanoparticles have also been shown to significantly affect the recognition and uptake by the MPS.[5] Particles with a positive surface charge are cleared significantly faster than neutral or negatively charged particles.[6] Furthermore, covering nanoparticles with a layer of hydrophilic, highly hydrated polymer greatly reduces the attachment of opsonins to the particles, which would otherwise 'label' the particle for being cleared by the MPS.[7,8] The most widely studied polymers for this purpose are poly(*N*-(2-hydroxypropyl) methacrylamide) (pHPMAm) and poly(ethylene glycol) (PEG).[4] Especially PEG is a very effective protein repellant due to its high level of hydration and its high flexibility, even when it is tethered to a surface.[8-11]

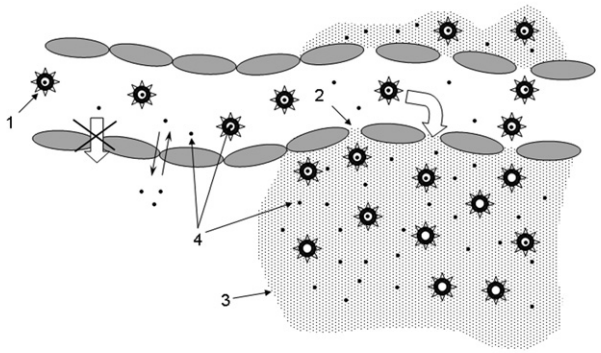

Figure 2. The enhanced permeability and retention (EPR) effect. Nanoparticles (1) cannot leave normal blood vessels but do penetrate through the leaky pathological vasculature (2) into the tumor interstitium (3) and release their payload (4) over time. Reprinted with permission from Torchilin.[14] Copyright 2007 by the American Association of Pharmaceutical Scientists.

Apart from different degradation and excretion kinetics, nanoparticles may also have altered distribution patterns in the body compared to free drug molecules. Nanoparticles, and any drugs which are stably entrapped inside them, cannot diffuse out of the blood stream into healthy tissues. However, as first described by Maeda *et al.*, the vasculature in chronically inflamed tissue (*e.g.* in rheumatoid arthritis and tumors) contains large (up to several hundred nm) discontinuities. This "leakiness" enables nanoparticles to penetrate significantly more into such diseased tissues than in healthy tissues (Figure 2).[12] Furthermore, especially in tumors the lymphatic system is underdeveloped leading to reduced drainage of nanoparticles that accumulated from the circulation in tumors. Together, these effects have been coined the "enhanced permeability and retention (EPR) effect".[13] It must be noted, however, that some organs (mainly the liver and spleen) also have an open vasculature and nanoparticles may also accumulate in these organs.

1.1.2. Polymeric micelles

One important class of nanoparticles that is currently under investigation for use as drug carrier systems are polymeric micelles.[14-19] At concentrations above their critical micelle concentration (CMC), amphiphilic block copolymers can self-assemble into such micelles having a dense, hydrophobic core and a hydrated corona (Figure 3).[20] Hydrophobic molecules can be loaded in the core, whereas the hydrated corona stabilizes the micelles (by preventing their aggregation) and reduces adsorption of

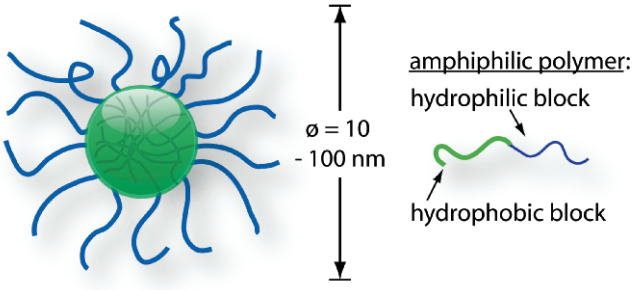

Figure 3. Schematic representation of a polymeric micelle (without payload). Reprinted with permission from Blanco *et al.*[15] Copyright 2009 by the Society for Experimental Biology and Medicine.

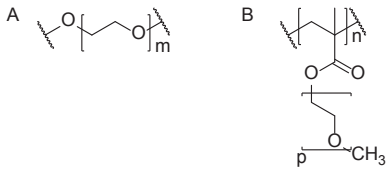

Figure 4. Chemical structures of PEG (A) and pOEGMA (B).

opsonins.[7] Advantages of polymeric micelles above low molecular weight surfactant micelles include their lower CMC[21] and their comparatively larger size which allows more drug molecules to be incorporated.

Since PEG is highly hydrated and has excellent protein repellent properties, micelles with PEG as corona are commonly referred to as "stealth" micelles.[16, 22] Furthermore, PEG is readily available, making it one of the most frequently used corona-forming polymers. Throughout this thesis PEG and its brush-shaped derivative poly(oligo(ethylene glycol) methyl ether methacrylate (pOEGMA), a brush-shaped derivative of PEG which can be prepared by (controlled) radical polymerization[23-26] are used as the corona forming blocks of polymeric micelles (Figure 4).

1.1.3. Thermosensitive polymers and micelles

An interesting class of polymers is that of thermosensitive polymers which are water-soluble at low temperature, but precipitate above a certain temperature, called the cloud point (CP). Below the CP the polymer chains are hydrated by the formation of hydrogen

Figure 5. A solution of thermosensitive polymer at low (left) and high (right) temperature.

bonds with water molecules. Hydrogen bonds, however, weaken as the temperature is raised, causing the polymer to be dehydrated and to become predominantly hydrophobic above the CP (Figure 5).

For biomedical applications, several thermosensitive polymers have been developed which have a CP below body temperature.[27] When a thermosensitive polymer with a CP below body temperature is combined with a permanently hydrophilic polymer (*e.g.* PEG) in the form of a block copolymer, micelles (or other structures) will be formed spontaneously when an aqueous solution of such a block copolymer is heated to body temperature.[28-30]

A frequently used thermosensitive polymer for biomedical and pharmaceutical applications is poly(*N*-isopropylacrylamide) (pNIPAm).[31, 32] Its popularity is mainly due to the fact that its CP is around 32 °C, meaning that it is water-soluble at room temperature but water-insoluble at body temperature.[33, 34] Another thermosensitive polymer, developed in our group, is a random copolymer of HMPAm-monolactate and HPMAm-dilactate.[29,35] This polymer has two advantages over pNIPAm. Firstly, its CP can be tuned by varying the percentage of the two monomers. Secondly, when this polymer is used *in vivo*, over time the lactate units will be hydrolyzed.[36] This hydrolysis causes the polymer to become more hydrophilic and even water-soluble at body temperature when its CP will reach 37 °C or higher.

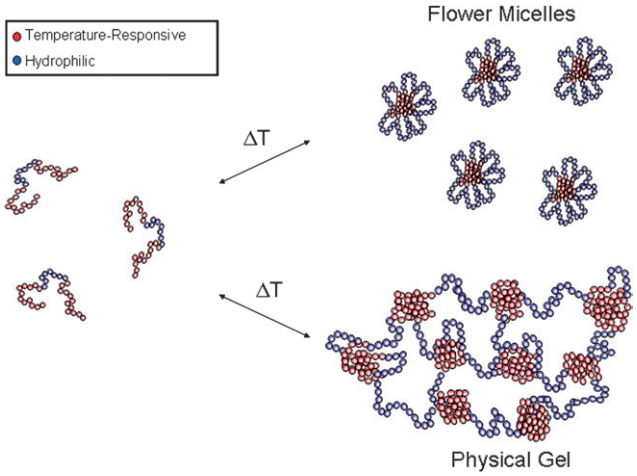

Figure 6. Self-assembly of thermosensitive BAB block copolymers. Reprinted with permission from McCormick *et al.*[47] Copyright 2008 by the Royal Society of Chemistry.

1.1.4. Flower-like micelles and hydrogels

Amphiphilic diblock copolymers are commonly referred to as AB-type polymers, Apart from these diblock copolymers, amphiphilic triblock copolymers are also studied for biomedical applications. These triblock copolymers can either have an ABA architecture with a hydrophobic B block flanked by two hydrophilic A blocks, or a BAB architecture with a hydrophilic block between two hydrophobic blocks. Whereas amphiphilic ABA block copolymers can form micelles that are very similar to micelles of AB block copolymers,[37] the BAB block copolymers are different. At concentrations not too far above the CMC these polymers can be expected to form "flower-like" micelles, in which the corona-forming polymer blocks are looped (Figure 6).[38-42]

Furthermore, at concentrations much above the CMC, amphiphilic block copolymers can also form hydrogels.[43] These gels are composed of packed micelles which, in the case of BAB block copolymers, are held together by "bridging" chains (Figure 6). In a number of studies it has been shown that there is always an equilibrium between free micelles and bridged micelles (gel).[44-47] This implies that micelles are slowly released from a BAB block copolymer hydrogel when it is put in an aqueous medium.

1.2. Radical polymerization techniques

As opposed to many anionic, cationic and condensation polymerizations, radical polymerizations are generally tolerant of water and many functional groups. Therefore, a wide variety of functional polymers can be prepared by radical polymerizations. Furthermore, radical polymerizations allow for the preparation of polymers in the presence of (or even attached to) biomolecules such as proteins.

1.2.1. Free radical polymerization

In a simplified description of conventional free radical polymerization, radicals are continuously formed by dissociation of initiator molecules; each of these radicals then propagate with a random number of monomer molecules before terminating after a certain time (usually in

the order of a second).[48] Due to this termination, no block copolymers can be synthesized. Furthermore, the random nature of this termination process leads to a broad distribution of polymer molecular weights.

The average molecular weight M of polymer chains produced at a certain time point is proportional to the ratio between the rate of propagation (R_P) and the rate of termination (R_T):

$$M \propto \frac{R_P}{R_T} \quad \textbf{(1)}$$

Since propagation is a process between a radical (P*) and a monomer (M) its rate is dependent on the concentrations of these two species:

$$R_P \propto [\mathrm{P}^*][\mathrm{M}] \quad \textbf{(2)}$$

Similarly, if we assume that termination is largely caused by processes between two growing polymer chains (either by combination or disproportionation):

$$R_P \propto [\mathrm{P}^*]^2 \quad \textbf{(3)}$$

Combining equations **(1)** – **(3)**, for free radical polymerization it follows that

$$M \propto \frac{[\mathrm{M}]}{[\mathrm{P}^*]} \quad \textbf{(4)}$$

During a batch free radical polymerization it is generally ensured that [P*] decreases (much) slower than [M] as otherwise, according to equation **(2)**, R_P would decrease impractically fast. It then follows from equation **(4)** that in the beginning of the polymerization much longer polymer chains will be produced than at the end, which is the second cause why free radical polymerizations yield broad molecular weight distributions.

Another characteristic of free radical polymerization is composition drift, which occurs during the copolymerization of two or more monomers of unequal reactivity. The chains that are produced at the beginning of the reaction will consist mainly of the more reactive monomer, whereas the chains that are produced in a later stage consist mainly of the less reactive one.

1.2.2. Controlled radical polymerization

To overcome the problems pointed out above, a number of so-called controlled (or "living") radical polymerizations have been developed.[49, 50] The three main examples of such techniques are atom transfer radical polymerization (ATRP),[51-53] reversible addition-fragmentation chain transfer (RAFT)[54-56] polymerization and stable free radical polymerization (SFRP), commonly known as nitroxide mediated polymerization (NMP).[57-59] Their common feature is continuous reversible deactivation of the propagating radicals into what is called a "dormant" species, with the equilibrium being strongly on the side of this dormant species. This method makes it possible to initiate all chains at the same time without obtaining a too high radical concentration. Thus, all chains will grow at the same time (Figure 7): in other words the number-averaged molecular weight M_n ideally is a linear function of the monomer conversion. Furthermore, growing chains will negligibly combine with each other (unless the polymerization is driven to very high conversion), leading to polymers with a very narrow molecular weight distribution. Together, the instantaneous initiation of all chains and the very low rate of termination lead to a constant [P*], which results in an exponentially decreasing [M].

When monomers with different reactivities are copolymerized in a controlled radical polymerization, no composition drift is observed but instead gradient copolymers are produced. In other words, the composition of all chains will in this case be the same but in every chain the monomer composition gradually changes going from one end to the other.

A final and important aspect of controlled radical polymerizations is the fact that after polymerization all chains are still "dormant" and not "dead". This means that after a first block, a second block of a different monomer can be polymerized (Figure 7).

Together, the properties outlined above have led to an enormous current interest in controlled radical polymerizations for the preparation of biomedical and pharmaceutical polymers.[60] The high level of control over the molecular weight and the low dispersity that can be attained enables the production of well-defined pharmaceutical products with predictable properties (*e.g.* renal clearance rate). Furthermore, the facile preparation of block- and gradient copolymers of various architectures allows for the

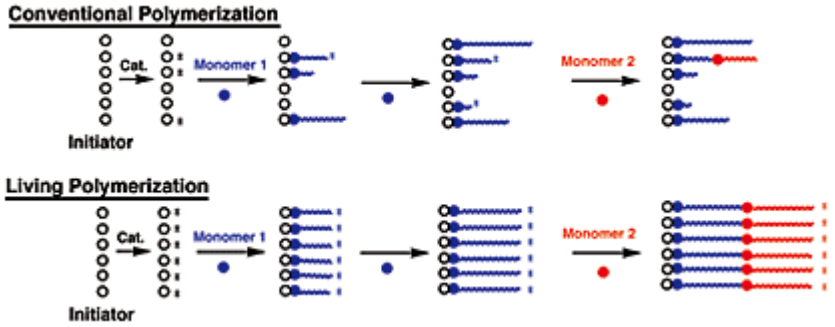

Figure 7. Comparison of conventional and living polymerization, showing that living polymerization yields polymers with narrow molecular weight distribution and allows for the preparation of block copolymers. o: initiator, *: radical.

design of a wide range of self-assembling biomaterials such as polymeric micelles and hydrogels. Finally, the compatibility of controlled radical polymerizations with proteins in aqueous environment and (especially for ATRP) the possibility of coupling functional molecules to the living chain end, enable the generation of functional polymers and polymer-protein hybrids.

1.2.3. Atom transfer radical polymerization

Since its discovery in 1995,[61] ATRP has been one of the most widely employed techniques of controlled radical polymerization. In the ATRP process, both the initiator and the dormant chain are "capped" with a halogen atom. The bond between the halogen and the carbon to which it is attached, can be broken homolytically by a transition metal in its lower oxidation state, most commonly Cu^{+} (Scheme 1). This process leaves a radical on the carbon atom and the transition metal changes to

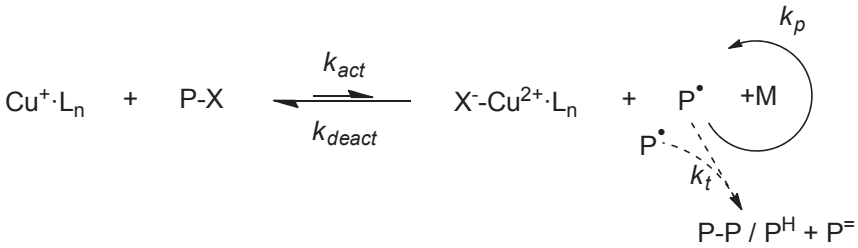

Scheme 1. The catalytic equilibrium in copper-catalyzed ATRP. L: complexing ligand, P: polymer chain, X: Cl or Br, M: monomer, P^{H}: hydrogen-terminated chain, $P^{=}$: double bond-terminated chain, k_{act}: activation rate constant, k_{deact}: deactivation rate constant, k_p: polymerization rate constant, k_t: termination rate constant.

its higher oxidation state (*e.g.* Cu^{2+}). It is the reversibility of this process (with the equilibrium lying strongly to the side of the halogen-capped polymer) that leads to the high level of control in ATRP polymerizations.[62]

1.3. Conjugates of polymers and peptides or proteins

It is has been shown in many publications that by coupling of water-soluble polymers (particularly PEG) to therapeutic proteins, their blood residence time can be significantly increased due to an increase of hydrodynamic volume and consequently reduced renal filtration.[63-69] Several therapeutic PEG-protein conjugates that benefit from this feature are already on the market.[70] PEGylated therapeutic proteins are often less immunogenic than native proteins;[71] on the other hand there is a growing number of reports of patients developing specific anti-PEG antibodies.[72]

The most common chemistries for conjugating water-soluble polymers (or any other moieties) to proteins target cysteine or lysine residues. In case multiple of such residues are present, exact control over the attachment site(s) and number of attachments per protein is difficult. Therefore, a number of methods to achieve site-specific coupling have been, and are being, developed (see also **Chapter 2** of this thesis).[73-75]

Outside the field of therapeutic proteins, there is also much interest in polymer-protein or polymer-peptide conjugates as these conjugates may have (combinations of) material properties that are unattainable by polymer-only or peptide/protein-only materials.[76, 77] Such "biohybrid" materials are under investigation for a wide range of applications, such as biohybrid hydrogels for tissue engineering or sustained drug release or biohybrid micelles for targeted drug delivery.[78-82] Reactive, well-defined biohybrid polymers can be obtained by controlled radical polymerization, while the peptide or protein part of these materials may render them sensitive to pH, redox potential or temperature, or may contain cell adhesion sequences or specific enzymatic cleavage sites.[79-81]

1.4. Aim and outline of this thesis

The aim of the work described in this thesis was to design and synthesize several self-assembling block copolymers to be used as nanocarriers in drug delivery. Block copolymers were synthesized by ATRP, their self-assembling properties were investigated and conjugates of the polymers with a peptide for enzyme-controlled destabilization were made. All block copolymers were based on the thermosensitive pNIPAm and either PEG or poly(oligo(ethylene glycol) methyl ether methacrylate) (pOEGMA).

Chapter 2 gives an overview of current literature on site-specific coupling of polymers or other molecules to proteins by incorporating non-natural amino acids with orthogonal reactivities into these proteins.

After this perspective on the functionalization of proteins, **Chapter 3** describes the development of a novel method to end-functionalize polymers synthesized by ATRP using the copper-catalyzed azide-alkyne cycloaddition 'click' reaction in a one-pot reaction post polymerization.

In **Chapter 4**, a novel method is presented to incorporate a peptide into block copolymers. Two polymer blocks are grown from a peptide, leading to a peptide-hybrid block copolymer having a peptide as the junction between a hydrophilic and a thermosensitive block. The resulting polymers self-assemble into micelles at body temperature which can be enzymatically cleaved by tumor-specific enzymes.

In **Chapter 5** proof is presented that pNIPAm-PEG-pNIPAm triblock copolymers, as opposed to PEG-pNIPAm diblock copolymers, self-assemble into structures referred to as flower-like micelles. In these flower-like micelles, the hydrophilic polymer blocks are looped. It is demonstrated that this looping leads to a decreased aggregation number as compared to star-like micelles. Furthermore, ^{1}H NMR relaxation measurements show that that this looping leads to strain in the hydrophilic polymer blocks.

Chapter 6 describes the ability of the mentioned triblock copolymers to self-assemble into physically crosslinked hydrogels that can shed flowerlike micelles into their aqueous surroundings. Furthermore, the possibility of exploiting this mechanism to make a drug depot from which the hydrophobic anticancer drug paclitaxel is released in the form of micelles, is explored.

In **Chapter 7**, a summarizing discussion of this thesis is given. Some possible future applications of the developed technologies are suggested, *e.g.* the preparation of synthetic vaccines consisting of polymer-peptide hybrid materials.

References

(1) Zhang, L.; Gu, F. X.; Chan, J. M.; Wang, A. Z.; Langer, R. S.; Farokhzad, O. C. *Clin. Pharmacol. Ther.* **2007**, *5*, 761-769.

(2) Bawa, R. *Nanotechnology Law & Business* **2008**, 135-155.

(3) Emerich, D. F.; Thanos, C. G. *J. Drug Target.* **2007**, 3, 163-183.

(4) Alexis, F.; Pridgen, E.; Molnar, L. K.; Farokhzad, O. C. *Mol. Pharm.* **2008**, *4*, 505-515.

(5) Moghimi, S. M.; Hunter, A. C.; Murray, J. C. *Pharmacol. Rev.* **2001**, *2*, 283-318.

(6) Roser, M.; Fischer, D.; Kissel, T. E. *J. Pharm. Biopharm.* **1998**, *3*, 255-263.

(7) Owens, D. E.,3rd; Peppas, N. A. *Int. J. Pharm.* **2006**, *1*, 93-102.

(8) Vittaz, M.; Bazile, D.; Spenlehauer, G.; Verrecchia, T.; Veillard, M.; Puisieux, F.; Labarre, D. *Biomaterials* **1996**, *16*, 1575-1581.

(9) Otsuka, H.; Nagasaki, Y.; Kataoka, K. *Adv. Drug Deliv. Rev.* **2003**, *3*, 403-419.

(10) Gref, R.; Lück, M.; Quellec, P.; Marchand, M.; Dellacherie, E.; Harnisch, S.; Blunk, T.; Müller, R. H. *Colloids Surf., B* **2000**, *3-4*, 301-313.

(11) Crielaard, B. J.; Yousefi, A.; Schillemans, J. P.; Vermehren, C.; Buyens, K.; Braeckmans, K.; Lammers, T.; Storm, G. *J. Controlled Release* **2011**, *156*, 307-314.

(12) Matsumura, Y.; Maeda, H. *Cancer Res.* **1986**, *12 Pt 1*, 6387-6392.

(13) Maeda, H.; Wu, J.; Sawa, T.; Matsumura, Y.; Hori, K. *J. Controlled Release* **2000**, *1-2*, 271-284.

(14) Torchilin, V. P. *AAPS J.* **2007**, *2*, E128-E147.

(15) Blanco, E.; Kessinger, C. W.; Sumer, B. D.; Gao, *J. Exp. Biol. Med. (Maywood, NJ, U. S.)* **2009**, *2*, 123-131.

(16) Torchilin, V. P. *Pharm. Res.* **2007**, *1*, 1-16.

(17) Torchilin, V. P. *Cell Mol. Life Sci.* **2004**, *19-20*, 2549-2559.

(18) Hu, X.; Jing, X. *Expert Opin. Drug Deliv.* **2009**, *10*, 1079-1090.

(19) Oerlemans, C.; Bult, W.; Bos, M.; Storm, G.; Nijsen, J.F.W.; Hennink, W.E. *Pharm. Res.* **2010**, 2569-2589.

(20) Kumar, N.; Ravikumar, M. N.; Domb, A. *J. Adv. Drug Deliv. Rev.* **2001**, *1*, 23-44.

(21) le Maire, M.; Champeil, P.; Møller, J. V. *Biochim. Biophys. Acta – Biomembr.* **2000**, *1-2*, 86-111.

(22) Attwood, D.; Zhou, Z.; Booth, C. *Expert Opin. Drug Deliv.* **2007**, *5*, 533-546.

(23) Wang, X.; Armes, S. P. *Macromolecules* **2000**, *18*, 6640-6647.

(24) Lutz, J. -F.; Hoth, A. *Macromolecules* **2006**, *2*, 893-896.

(25) Ishizone, T.; Seki, A.; Hagiwara, M.; Han, S.; Yokoyama, H.; Oyane, A.; Deffieux, A.; Carlotti, S. *Macromolecules* **2008**, *8*, 2963-2967.

(26) Badi, N.; Lutz, J. -F. *J. Controlled Release* **2009**, *3*, 224-229.

(27) Ward, M. A.; Georgiou, T. K. *Polymers* **2011**, *3*, 1215-1242.

(28) Talelli, M.; Hennink, W. E. *Nanomedicine* **2011**, *7*, 1245-1255.

(29) Talelli, M.; Rijcken, C. J.; van Nostrum, C. F.; Storm, G.; Hennink, W. E. *Adv. Drug Deliv. Rev.* **2010**, *2*, 231-239.

(30) Wang, B.; Shao, P.; Wang, Y.; Li, J.; Zhang, Y. *J. Nanomater.* **2011**.

(31) Wei, H.; Cheng, S.; Zhang, X.; Zhuo, R. *Prog. Polym. Sci.* **2009**, *9*, 893-910.

(32) Rzaev, Z. M. O.; Dinçer, S.; Pişkin, E. *Prog. Polym. Sci.* **2007**, *5*, 534-595.

(33) Graziano, G. *Int. J. Biol. Macromol.* **2000**, *1*, 89-97.

(34) Wang, X.; Qiu, X.; Wu, C. *Macromolecules* **1998**, *9*, 2972-2976.

(35) Soga, O.; van Nostrum, C. F.; Hennink, W. E. *Biomacromolecules* **2004**, *3*, 818-821.

(36) Soga, O.; van Nostrum, C. F.; Fens, M.; Rijcken, C. J.; Schiffelers, R. M.; Storm, G.; Hennink, W. E. *J. Controlled Release* **2005**, *2*, 341-53.

(37) Alexandridis, P.; Holzwarth, J. F.; Hatton, T. A. *Macromolecules* **1994**, *9*, 2414-2425.

(38) Zhou, Z.; Chu, B. *Macromolecules* **1994**, *8*, 2025-2033.

(39) Chang, G.; Li, C.; Lu, W.; Ding, *J. Macromol. Biosci*. **2010**, *10*, 1248-1256.

(40) Honda, S.; Yamamoto, T.; Tezuka, Y. *J. Am. Chem. Soc*. **2010**, *30*, 10251-10253.

(41) Hua, S.; Li, Y.; Liu, Y.; Xiao, W.; Li, C.; Huang, F.; Zhang, X.; Zhuo, R. *Macromol. Rapid Commun*. **2010**, *1*, 81-86.

(42) Lee, E. S.; Oh, K. T.; Kim, D.; Youn, Y. S.; Bae, Y. H. *J. Controlled Release* **2007**, *1*, 19-26.

(43) Bae, S. J.; Suh, J. M.; Sohn, Y. S.; Bae, Y. H.; Kim, S. W.; Jeong, B. *Macromolecules* **2005**, *12*, 5260-5265.

(44) Semenov, A. N.; Joanny, J.; Khokhlov, A. R. *Macromolecules* **1995**, *4*, 1066-1075.

(45) Fumihiko, T. *J. Non-Cryst. Solids* **2002**, *0*, 688-697.

(46) Kujawa, P.; Watanabe, H.; Tanaka, F.; Winnik, F. M. *Eur. Phys. J. E: Soft Matter* **2005**, *2*, 129-137.

(47) McCormick, C. L.; Sumerlin, B. S.; Lokitz, B. S.; Stempka, J. E. *Soft Matter* **2008**, *9*, 1760-1773.

(48) Flory, P. J. Principles of polymer chemistry; Cornell University Press: New York, 1992.

(49) Braunecker, W. A.; Matyjaszewski, K. *Prog. Polym. Sci*. **2007**, *1*, 93-146.

(50) Matyjaszewski, K. *Curr. Opin. Solid State Mater. Sci*. **1996**, *6*, 769-776.

(51) Pintauer, T.; Matyjaszewski, K. *Chem. Soc. Rev.* **2008**, *6*, 1087-1097.

(52) Fristrup, C. J.; Jankova, K.; Hvilsted, S. *Soft Matter* **2009**, *23*, 4623-4634.

(53) Min, K.; Matyjaszewski, K. *Cent. Eur. J. Chem.* **2009**, *4*, 657-674.

(54) Boyer, C.; Bulmus, V.; Davis, T. P.; Ladmiral, V.; Liu, J.; Perrier, S. *Chem. Rev*. **2009**, *11*, 5402-5436.

(55) Gregory, A.; Stenzel, M. H. *Expert Opin. Drug Delivery* **2011**, *2*, 237-269.

(56) Stenzel, M. H. *Chem. Commun. (Cambridge, U. K.)* **2008**, *30*, 3486-3503.

(57) Studer, A.; Schulte, T. *Chem. Rec.* **2005**, *1*, 27-35.

(58) Brinks, M. K.; Studer, A. *Macromol. Rapid Commun*. **2009**, *13*, 1043-1057.

(59) Bertin, D.; Gigmes, D.; Marque, S. R. A.; Tordo, P. *Chem. Soc. Rev*. **2011**, *5*, 2189-2198.

(60) Matyjaszewski, K.; Tsarevsky, N. V. *Nat. Chem*. **2009**, *4*, 276-288.

(61) Wang, J.; Matyjaszewski, K. *J. Am. Chem. Soc.* **1995**, *20*, 5614-5615.

(62) Matyjaszewski, K.; Xia, J. *Chem. Rev*. **2001**, *9*, 2921-2990.

(63) Chen, C.; Constantinou, A.; Deonarain, M. *Expert Opin. Drug Delivery* **2011**, *8*, 1221-1236.

(64) Alconcel, S. N. S., Baas, A. S., Maynard, H. D. *Polym. Chem*. **2011**, *2*, 1442-1448.

(65) Veronese, F. M.; Mero, A. *BioDrugs* **2008**, *22*, 315-329.

(66) Monfardini, C.; Veronese, F. M. *Bioconjugate Chem*. **1998**, *4*, 418-450.

(67) Veronese, F. M.; Morpurgo, M. *Il Farmaco* **1999**, *8*, 497-516.

(68) Nucci, M. L.; Shorr, R.; Abuchowski, A. *Adv. Drug Deliv. Rev*. **1991**, *2*, 133-151.

(69) Maeda, H. *Adv. Drug Deliv. Rev*. **1991**, *2*, 181-202.

(70) Pasut, G.; Veronese, F. M. *Adv. Drug Deliv. Rev*. **2009**, *13*, 1177-1188.

(71) Sehon, A. H. *Adv. Drug Deliv. Rev*. **1991**, *2*, 203-217.

(72) Garay, R. P.; Labaune, J. P. *Open Conf. Proc. J*. **2011**, 104-107.

(73) Cazalis, C. S.; Haller, C. A.; Sease-Cargo, L.; Chaikof, E. L. *Bioconjugate Chem*. **2004**, *5*, 1005-1009.

(74) Gaertner, H. F.; Offord, R. E. *Bioconjugate Chem*. **1996**, *1*, 38-44.

(75) Broyer, R. M.; Quaker, G. M.; Maynard, H. D. *J. Am. Chem. Soc*. **2007**, *3*, 1041-1047.

(76) Ruiz-Hitzky, E.; Darder, M.; Aranda, P.; Ariga, K. *Adv. Mater*. **2010**, *3*, 323-336.

(77) Venkatesh, S.; Byrne, M. E.; Peppas, N. A.; Hilt, J. Z. *Expert Opin. Drug Deliv*. **2005**, *6*, 1085-1096.

(78) Tsurkan, M. V.; Chwalek, K.; Levental, K. R.; Freudenberg, U.; Werner, C. *Macromol. Rapid Commun*. **2010**, *17*, 1529-1533.

(79) Seliktar, D.; Zisch, A. H.; Lutolf, M. P.; Wrana, J. L.; Hubbell, J. A. *J. Biomed. Mater. Res. A.* **2004**, *4*, 704-716.

(80) Fuks, G.; Mayap Talom, R.; Gauffre, F. *Chem. Soc. Rev*. **2011**, *5*, 2475-2493.

(81) Xun, W.; Wu, D. Q.; Li, Z. Y.; Wang, H. Y.; Huang, F. W.; Cheng, S. X.; Zhang, X. Z.; Zhuo, R. X. *Macromol. Biosci.* **2009**, *12*, 1219-1226.

(82) Habraken, G. J.; Peeters, M.; Thornton, P. D.; Koning, C. E.; Heise, A. *Biomacromolecules* **2011**.

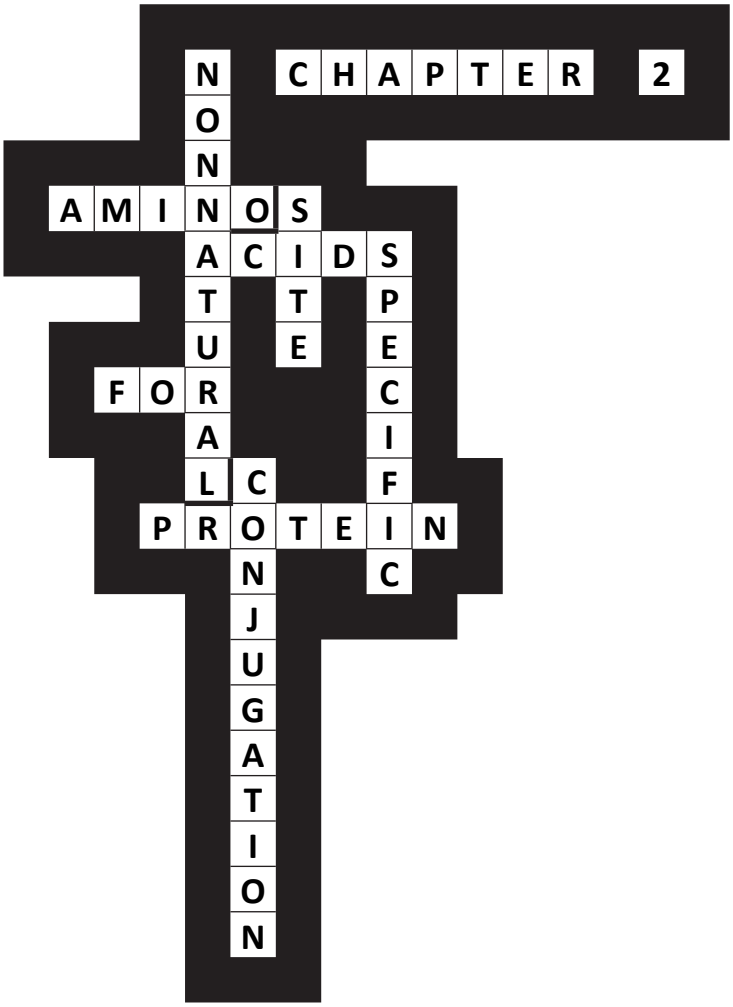

Nonnatural amino acids for site specific protein conjugation
Albert J. de Graaf, Marlous Kooijman,
Wim E. Hennink and Enrico Mastrobattista
Bioconjugate Chemistry, **2009**, *20* (7), pp 1281-1295
Copyright 2009, the Amertican Chemical Society

Abstract

Over the years, several chemical reactions have been developed that enable the covalent conjugation of synthetic molecules to natural proteins. The resulting bioconjugates have become important tools in the study of natural proteins. Furthermore, they form a new class of protein-based pharmaceuticals and biomaterials. However, classical bioconjugation reactions to natural amino acids suffer from poor site-specificity. To overcome this problem, a variety of uniquely reactive non-natural amino acids have recently been designed. These can be incorporated into proteins by specifically engineered bacterial strains. Such reactive non-natural amino acids create new possibilities for bio-orthogonal conjugation to proteins. This review first gives an overview of the various methods for site-specific introduction of non-natural amino acids into proteins. Both semisynthetic and entirely recombinant methods are addressed. Then, a detailed description is given of the reactive non-natural amino acids that have already been recombinantly introduced into proteins. The bio-orthogonal reactions that can be used for conjugation to these reactive non-natural amino acids are also discussed. These include the alkyne/azide 'click' reaction, carbonyl condensations, Michael-type additions, and Mizoroki-Heck substitutions.

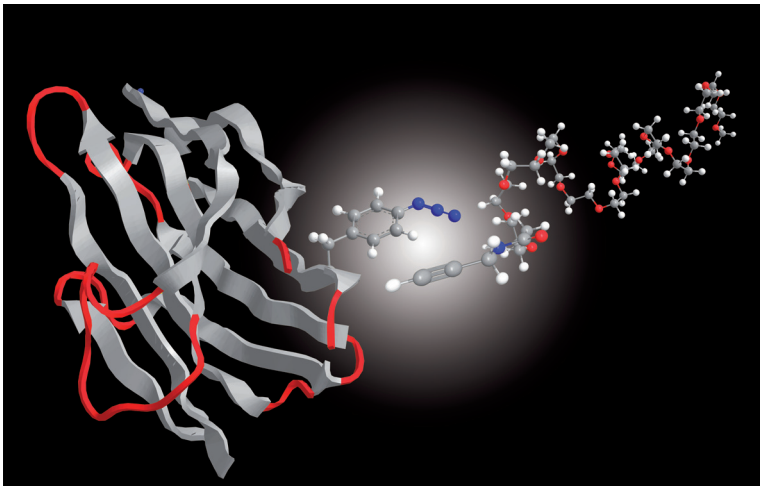

2.1. Introduction

Proteins are responsible for the majority of functional attributes of all living organisms. They act as building blocks of the cell structure and as catalysts in the metabolism of cells. Furthermore, signal transduction within and between cells, as well as cell morphology and stability, are dependent on a large number of proteins. Many of these functions are dependent on post-translational modifications (*e.g.*, glycosylation or lipidation) at specific sites of the proteins involved.

Scientists have long been inspired by the mechanisms of nature to couple different molecules to proteins and have explored them in order to synthesize (nonnatural) protein bioconjugates. As a result of this research, different chemoselective conjugation methods have been developed in the last decades. These chemoselective conjugation methods have proven to be very useful, *e.g.*, to attach probes or drugs to proteins. Another application is the attachment of hydrophilic polymers (*e.g.*, poly(ethylene glycol) (PEG)) to therapeutic proteins. PEGylation reduces the immunogenicity and antibody recognition of therapeutic proteins. This leads to increased stability and body residence time. PEGylation has also improved the targeting and tissue penetration of protein pharmaceuticals.[1-5]

Furthermore, fusion proteins and proteins with new functionalities have been developed using bioconjugation reactions.[2-8] Finally, chemoselective conjugation reactions are useful tools for the design of new biomaterials .[9-12]

A drawback of the conventional chemoselective bioconjugation reactions is the heterogeneity of the product that is formed. This is due to the fact that more than one residue of the targeted amino acid species may be present in a protein. To overcome this limitation, orthogonally reactive nonnatural amino acids can be introduced into proteins. Various methods to incorporate nonnatural amino acids into proteins are outlined below. Being able to attach molecules only to the introduced nonnatural amino acid, without derivatizing the natural amino acids in the protein, one can achieve exact control over the site and number of conjugations to a protein. In this way, highly defined products can be obtained. In principle, such bio-orthogonal conjugation reactions can be carried out in the presence of other proteins that contain only natural amino acids.

This review analyzes the potential of bio-orthogonal conjugation reactions to proteins containing nonnatural amino acids. First, the most common techniques for incorporation of nonnatural amino acids into proteins are discussed. Then, an overview is given of chemically reactive nonnatural amino acids that have been introduced into proteins, together with a discussion of the reactions that can be used for conjugation to these amino acids.

2.2. Conjugation to natural amino acids

Most bioconjugation reactions make use of the reactivities of natural amino acids. Though not the scope of this review, a short account of these reactions is given here to clarify the need for nonnatural amino acids with bio-orthogonal reactivities.

There are nine canonical amino acids that may in principle be derivatized at their side chains, since these amino acids possess functional groups (Table 1).

Nucleophile-to-electrophile attacks are the most common protein conjugation reactions. The strongest nucleophile present in natural proteins is the cysteine thiol group. However, this amino acid is relatively rare, and when it is present in a protein, it is often involved in the catalytic center or in disulfide bridges. Cysteine residues are therefore not always optimal as sites for conjugation reactions. Consequently, the main targets of protein conjugation are the ε-lysil amino groups (together with the N-terminal (α-) amino group). The natural occurrence of lysine residues in mammalian proteins is around 6%.[13] Therefore, site-specificity can be difficult to achieve. When there are no lysine residues available, or lysine residues form part of the active site of a protein, conjugation to carboxylic acid groups can be considered. However, it is then difficult to avoid cross-linking with the amino groups of the protein itself.[1]

In nature, the range of functions of proteins is extended by posttranslational modifications of amino acid residues. Other functional groups, peptides, or proteins can be attached and structural changes can be made. Even the very chemical nature of an amino acid residue can be changed.[14] The enzymes that naturally induce such posttranslational modifications can be used for bioconjugation as well. Transglutaminase can, for example, be used for polyamination;[15] farnesyltransferase and geranylgeranyltransferase

Table 1. Reactive Natural Amino Acid Side Chains.

Amino acid	Side chain	pKa
Aspartic acid	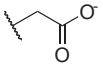	3.7 - 4.0
Glutamic acid	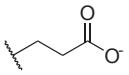	4.2 - 4.5
Histidine	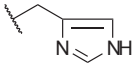	6.7 - 7.1
Lysine	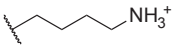	9.3 - 9.5
Arginine	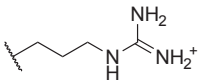	> 12
Tyrosine	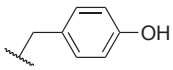	9.7 - 10.1
Cysteine		8.8 - 9.1
Methionine	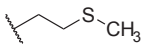	
Tryptophan	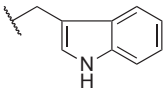	
C-terminus		2.1 - 2.4
N-terminus		7.6 - 8.0

can be used for prenylation;[16, 17] and *N*-myristoyltransferase can be used for myristoylation.[18, 19] Once again, the limitation of these reactions is that the essential amino acid residues must be available and the modification of an amino acid residue should not induce loss of structural integrity and functionality.

In general, due to the abundance of amino acids containing functional side groups within proteins, site-specific conjugation reactions to canonical amino acids are often difficult to achieve. Conjugations at undesired sites within the protein may induce loss of structural integrity and functionality.

2.3. Translational incorporation of nonnatural amino acids

With the recent developments in synthetic biology, it has become possible to engineer bacteria and yeast in such a way that they can incorporate nonnatural amino acids with selective reactivities into proteins. With this technique, the possibilities for site-specific conjugation to functionally active proteins can be substantially increased. Several methods that currently exist for the translational incorporation of nonnatural amino acids are discussed here.

2.3.1. Use of auxotrophic strains

The simplest and oldest method for incorporation of nonnatural amino acids into recombinantly produced proteins makes use of *Escherichia coli* strains that are auxotrophic for a certain amino acid. This means they are unable to synthesize it and therefore dependent on uptake from the growth medium. In the growth medium, this particular amino acid can be replaced by a structurally similar nonnatural analogue. The bacteria then build in this analogue. For this substitution method, the gene encoding the protein of interest has to be under tight inducible control. The bacteria can then first be grown in normal medium, followed by washing and transfer to medium containing the nonnatural analogue instead of the natural amino acid. After allowing the bacteria some time to deplete their intracellular stocks of the natural amino acid, production of the target protein is induced. Virtually, all copies of the target protein will then contain the nonnatural amino acid.

Incorporation efficiency can be greatly enhanced by overexpressing the relevant aminoacyl tRNA transferase and by somewhat relaxing the substrate specificity of its synthetase and proofreading active sites.[20-23]

Codons for leucine,[24] isoleucine,[25] phenylalanine,[26] tryptophan,[27, 28] proline,[29] and especially methionine[20, 30-35] have been reassigned in order to incorporate nonnatural amino acids using this method. Methionine is a frequently used amino acid for this technique, since it is one of the least common natural amino acids. Global replacement of methionine by nonnatural amino acids can therefore be expected to have less impact on protein structure and function than substitution of other amino acids. Furthermore, due to its hydrophobicity methionine is usually not located at the surface of natural

proteins. This makes it possible to introduce, *e.g.*, an alkyne or azide methionine analogue in a unique and well-defined place on the outside of a protein, accessible for subsequent modification by the azide/alkyne 'click' reaction.

Obviously, the major drawback of the substitution technique is that it leads to incorporation of the nonnatural amino acid at every site where the substituted amino acid is encoded. This may impair the protein's structure and function. Furthermore, incorporation in the cell's own proteins may lead to toxic effects. Finally, it is not possible to incorporate both the nonnatural amino acid and the substituted natural amino acid.

2.3.2. Stop codon suppressor tRNAs

To overcome the above-mentioned problems, Noren *et al.* (1989) developed a different method to translationally incorporate nonnatural amino acids into proteins. They used a tRNA that specifically recognizes one of the three stop codons. By chemically aminoacylating this tRNA and injecting it into *Xenopus* oocytes, a nonnatural 21st amino acid could be incorporated into proteins in response to the stop codon[36] (Figure 1).

tRNAs that efficiently recognize the amber (UAG) stop codon occur naturally in yeast. Such amber-suppressor tRNAs prevent release factor I (RF-I) from binding to the UAG codon. Therefore, the ribosome will continue elongating the protein. Because the ribosome does not proofread amino acids during translation, the cell does not recognize this "error" in the protein and therefore does not destroy it.[37] By aminoacylating

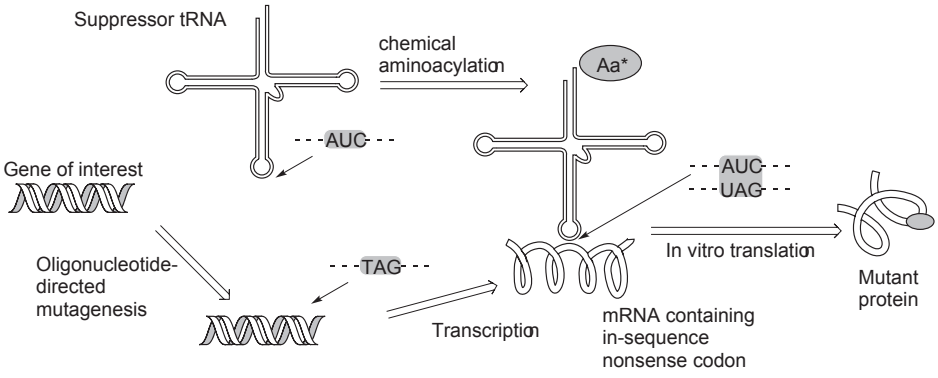

Figure 1. tRNA suppressing the amber codon.

such a suppressor tRNA with a desired nonnatural amino acid (*e.g.*, through chemical aminoacylation), it becomes possible to site-specifically incorporate a 21st amino acid in response to the amber codon.[36-39]

The main advantage of the termination readthrough mechanism is that nonnatural amino acids are only incorporated at the amber codon and therefore can be incorporated in addition to the 20 standard amino acids. Due to this characteristic, amber suppression has become a popular tool for incorporation of nonnatural amino acids.[40] Since the elongation factor and peptidyltransferase show relatively broad substrate specificity, site-specific insertion of any desired amino acid may in principle be achieved.[36]

To achieve high product yield and homogeneity, the suppressor tRNA must efficiently insert the amino acid in response to the UAG codon. Furthermore, it must be neither acylated nor deacylated by any of the naturally occurring aminoacyl-tRNA synthetases (AARS) of the host organism.[36, 37]

2.3.1. Orthogonal aminoacyl-tRNA synthetases

A major drawback of the above-mentioned approach is that tRNAs are too large to be taken up by the host cell after chemical aminoacylation. Therefore, they have to be microinjected.[41, 42] This limits the applicability of this technique to large cells such as *Xenopus* oocytes.[43, 44] A variant to this approach is *in vitro* protein translation in cell free extracts.[45, 46] However, these two methods are only applicable on a very small scale. To overcome this problem, the host cell can be genetically engineered to produce the suppressor tRNA and a corresponding AARS itself.[47] This AARS/tRNA pair has to be orthogonal to the host AARS/tRNA pairs. This means that the introduced tRNA should function efficiently in protein translation but should not be a substrate for any of the host AARS. Furthermore, the introduced AARS should not aminoacylate any of the endogenous host tRNAs.[37, 40] There are two methods to develop an orthogonal AARS/tRNA pair: it can be borrowed from unrelated organisms,[48] or it can be designed.[37, 49] Figure 2 illustrates the general selection method to develop orthogonal AARS/tRNA pairs.[37]

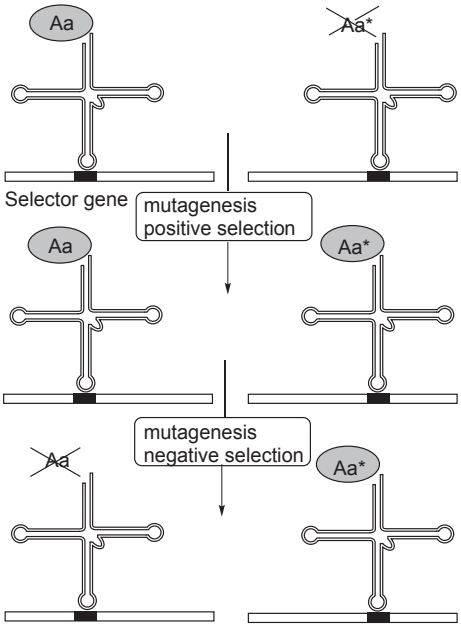

Figure 2. Strategy to select for an orthogonal AARS pair. (A) The starting AARS charges the suppressor tRNA with a natural amino acid Aa but not with the nonnatural amino acid Aa*. An amber codon (UAG) is inserted into a gene that codes for a selectable marker such as antibiotic resistance, GFP, or the Gal4 repressor. (B) A positive selection yields AARS* variants that incorporate both the natural and nonnatural amino acids. (C) Negative screening or selection yields an AARS** variant that rejects the natural amino acid.

When using orthogonal AARS/tRNA pairs, the nonnatural amino acid has to be available in the cytoplasm of the host. Therefore, the nonnatural amino acid has to be designed such that it can be passively or actively transported into the host cell. It is even possible to genetically modify *E. coli*, giving it the capability of biosynthesizing a nonnatural amino acid itself.[50]

Although successful, incorporating nonnatural amino acids by tRNA suppression of nonsense codons is somewhat limited by its low efficiency. The efficiency of the incorporation of one nonnatural amino acid per protein by amber suppression is dependent on the host organism, but on average, an efficiency of 20–30% (defined as the ratio of full-length protein to truncated protein) can be achieved. The low efficiency is a result of two factors. First, the acylation of suppressor tRNAs is sometimes a problem. Second, RF-1 will always compete with the suppressor tRNA for the stop codon.[37, 38, 40, 51] If the number of amber codons in a

gene increases, the efficiency decreases multiplicatively.[51] Consequently, multiple incorporations of nonnatural amino acids by using more than one amber codon are not feasible. Combining the suppression of another stop codon with amber codon supression is not feasible either, since the suppression efficiency of the other stop codons (UAA and UGA) is even smaller.[52] Apart from these limitations, it has also been observed that charged amino acids are incorporated less efficiently than hydrophobic ones. *d*- and β-amino acids are not compatible with stop codon suppression.[53]

Apart from bacteria, mammalian cells are also used for the production of certain proteins. Whether the method of stop codon suppression can ever be exploited for the introduction of nonnatural amino acids in these systems is uncertain, because the occurrence of the amber termination codon is higher in mammals than in *E. coli*. In human genes, for example, 23% of stop codons is UAG. It is therefore likely that amber suppression will be toxic, since essential proteins are not terminated correctly. The use of the other termination codons seems even less promising because their occurrence is even higher (UAA, 30%; UGA, 47%).[51, 54]

An exciting recent variation to stop codon reassignment is the reassignment of degenerate sense codons. Kwon *et al.* (2003) demonstrated the feasibility of this approach by breaking the degeneracy of the phenylalanine codons UUU and UUC. The anticodon sequence of $tRNA_{Phe}$ is AAG, but this tRNA also binds to the UUU codon by "wobbling". Kwon *et al.* introduced a heterologous tRNA having the anticodon AAA into an *E. coli* host. At the same time, they introduced an AARS that specifically loaded this tRNA with 2-naphtylalanine. By doing so, they were able to reach an incorporation efficiency of 80% for 2-naphtylalanine in response to UUU, while all UUC was still translated as phenylalanine.[55]

Another recent addition to the technique of stop codon suppression is the development of an orthogonal ribosome–mRNA pair.[51, 56] In this technique, the mRNA encoding for the protein of interest is given a modified Shine–Dalgarno (SD) sequence. The SD sequence is the part of the mRNA that initiates binding to the ribosome. The modified SD sequence is not recognized by natural ribosomes. The used expression strain is therefore given two sets of ribosomes: one that only recognizes

normal SD sequences and one that only recognizes the modified SD sequence. In this way, the production of the cell's own proteins is separated from the production of the desired protein containing the nonnatural amino acid. Furthermore, the mutant ribosome has an adjusted structure that rejects RF-1 (Figure 3). The use of such an orthogonal ribosome–mRNA pair therefore increases the suppression efficiency. Using this technique, a readthrough efficiency of 60% has been achieved.[51]

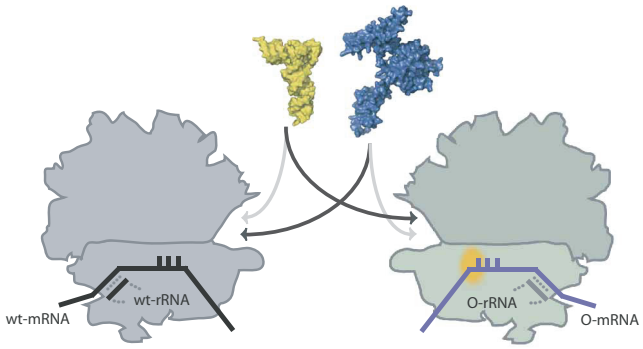

Figure 3. Orthogonal ribosome-tRNA pairs. The natural ribosome (left) and the orthogonal ribosome (right) translate wild-type (black) and orthogonal (purple) mRNAs, respectively. RF-1 (blue) cannot compete efficiently for UAG codons in the modified A-site (orange) of the orthogonal ribosome. Therefore, the orthogonal ribosome efficiently accepts the suppressor tRNA (yellow). Translation of the cell's own mRNAs is unaffected because the orthogonal ribosome does not read mRNAs with a normal SD sequence, but the natural ribosome is unaltered. Reprinted by permission from Macmillan Publishers Ltd.: *Nature Biotechnology* 25(7) p771, copyright 2007.

2.3.2. Expanding the size of codons

The number of different amino acids that can be incorporated into one protein is ultimately limited by the fact that natural codons consist of only three bases. The discovery of frameshift suppressor tRNAs, together with the ability of ribosomes to handle a wide variety of codon/anticodon pairs, has made it possible to create new codons by expanding the size of codons from triplets to quadruplets or even quintets.[52, 57, 58] This method was pioneered by Hohsaka and Sisido (2000).[57] It has created the possibility to develop additional codons and thereby has made incorporation of several different nonnatural amino acids at a time possible.[59]

Figure 4 illustrates the basic principle of this frameshift suppressor tRNA strategy. The gene containing the quadruplet or the quintet is generated by PCR.[57] During this process, an extra nucleotide is inserted at a specific place to create the quadruplet codon. In the case of a quintet, two nucleotides are inserted. Besides the modified DNA, the relevant orthogonal tRNA as well as a corresponding AARS are required for this method. When the frameshift suppressor tRNA successfully reads the concerning quadruplet/quintet, a frameshift will take place as planned and the protein will be completed to a full-length protein containing the nonnatural amino acid. However, if the concerning sequence is read by a naturally occurring tRNA, the planned frameshift does not occur. The reading frame is then shifted backward by one or two bases, which results in truncation of the protein at the next occurring stop codon.[52, 57]

Many four-base codons have been examined in *E. coli*. Hohsaka *et al.* (2001) found that five quadruplet codon/anticodon pairs (AGGU, CGGU, CCCU, CUCU, and GGGU) are orthogonal and very efficient (*e.g.*, GGGU has an efficiency of 80% with respect to the wild-type protein).[58] Several different quadruplets can in principle be used to incorporate more

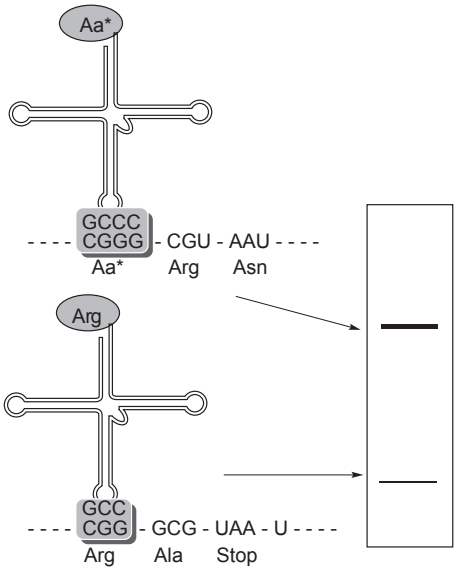

Figure 4. Priniciple of the four-base codon strategy. The target protein (right, upper band) can easily be separated by gel electrophoresis from the byproduct resulting from insertion of a natural amino acid (lower band).

than one nonnatural amino acid into one protein. Hohsaka and Sisido (2000) also examined the quintet codons $CGGN_1N_2$. The suppression efficiency was comparable for all the different quintets and was estimated at 16% for the incorporation of nitrophenylalanine in cell-free extracts. This is comparable to the efficiency of the amber suppression method with the same nonnatural amino acid.[57] Other amino acid analogues that have been introduced using this technique are homoglycine[59] and 2-hydroxy-3-(4-hydroxyphenyl)propionic acid, which introduces a hydrolyzable ester bond instead of an amide bond into the protein backbone.[60]

Efforts have been undertaken to use frameshift suppression *in vivo*, but these have not been very successful until now.[37, 59]

2.3.3. Nonnatural base pairs

A challenging method to expand the genetic code is to develop nonnatural base pairs. Creating a new base pair that is orthogonal to the naturally occurring base pairs generates great opportunities. With an additional base pair, the genetic code can be expanded from 64 coding triplets to 216 coding triplets. The basic principle behind this approach is illustrated in Figure 5.

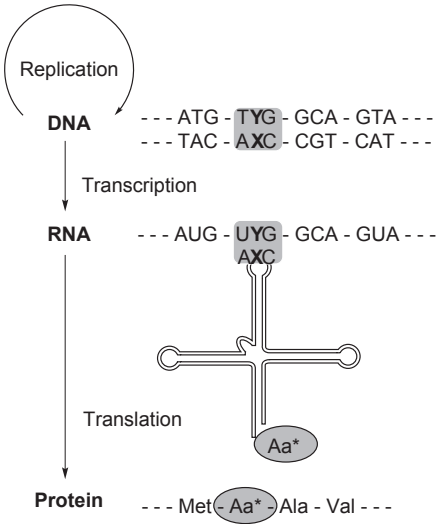

Figure 5. The expansion of the genetic alphabet with a nonnatural base pair X and Y.

Switzer *et al.* developed the first new base pair and thereby a 65th codon in 1989.[61] They incorporated the base pair isoC and isoG into DNA and managed to transcribe the DNA containing these nonnatural bases into mRNA, which in turn was successfully translated with the help of a synthetic tRNA into a protein containing a nonnatural amino acid. This approach seemed very promising, but the main problem was that the DNA containing the nonnatural base pairs had a limited stability.[62] Apart from the stability of the DNA, the success of a nonnatural nucleotide base pair is dependent on many other factors. The base pair must be completely orthogonal to the other nucleotide bases, but they must couple to each other with high affinity and high fidelity. In addition, the artificial base pair must be accepted and recognized by the DNA polymerase and RNA polymerase to make replication and transcription possible.[52, 63, 64] Despite the fact that it is not easy to satisfy these requirements, Ohtsuki *et al.*,[65] Hirao *et al.*,[66, 67] and the group of Romesberg[63, 64] succeeded to develop several nonnatural nucleotide base pairs which are promising candidates for expanding the genetic code. However, the orthogonality, fidelity, and DNA synthesis efficiency of these nonnatural base pairs is still insufficient for practical application.

2.4. Semisynthetic incorporation of nonnatural amino acids

Through the progression in solid-phase peptide synthesis (SPPS) methodology, the synthesis of peptides and small proteins has become routine. With SPPS, it is easy to incorporate all sorts of nonnatural amino acids into peptides. However, the solid-phase methodology has some drawbacks. These include accumulation of side products arising from incomplete deprotection or coupling reactions, the difficulty of synthesizing highly hydrophobic peptides, and nonnative folding of the products. Therefore, the method is limited to the synthesis of polypeptides not larger than 50 amino acid residues. In contrast, the average length of a natural protein is about 250 amino acid residues.

To circumvent these size limitations of the solid-phase methodology, several semisynthetic approaches have been developed to incorporate nonnatural amino acids.[68] The principal strategy encompasses synthesizing the desired protein in two parts. The part that contains the nonnatural

amino acid(s) is synthesized by SPPS. The rest of the target protein is produced by recombinant techniques. The two fragments are then modified at their termini with mutually reactive, bio-orthogonal groups. Finally, the two fragments are linked to each other to yield a full-length semisynthetic protein containing one or more nonnatural amino acids.[69] Schnolzer and Kent (1992) were among the first to prove this powerful concept through the chemoselective synthesis of a human immunodeficiency virus 1 (HIV-1) protease analogue having a modified backbone. They used this analogue for the study of backbone involvement in inhibitor binding.[70, 71]

A variety of chemoselective protein ligation reactions have been developed.[70] Some of these reactions generate a nonnatural structure at the ligation site. Examples include the thioester and thioether ligations[72-75] and the imine/pseudoproline ligation (discussed below). In addition to these, there are now a number of ligation reactions available that generate a native peptide bond. Generally, these consist of a two-step sequence (Scheme 1). The first step is a chemoselective capture between an electrophile at the C-terminus of peptide **1** and a nucleophile at the N-terminus of peptide **2**. The type of bond that is formed depends on the nucleophile and electrophile used in the capture reaction. If the formed bond is an ester or a thioester, a spontaneous intramolecular acyl shift will occur (through the five-membered intermediate **3**) to form an amide bond in the product **4**.[69, 76]

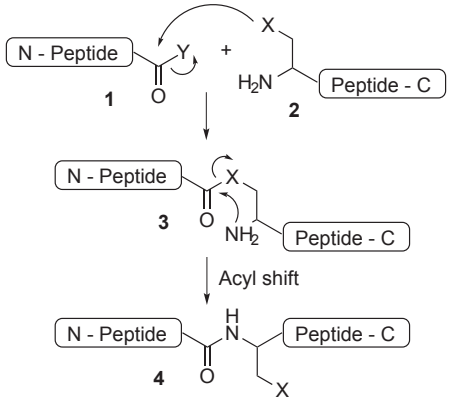

Scheme 1. General concept of orthogonal peptide ligation. X and Y represent a good nucleophile and a good leaving group, respectively. For example, in native chemical ligation X = SH and Y = SR.

2.4.1. Native chemical ligation

The native chemical ligation approach of Dawson *et al.* (1994) was the first approach that did not cause a nonnatural structure at the ligation site.[77] The principle behind this method is that each peptide fragment has a unique, mutually reactive functionality which enables a chemoselective reaction. Because of this chemoselectivity, the ligation can take place with unprotected peptide fragments in aqueous solution. In the native chemical ligation approach, the peptide **2** bears an N-terminal cysteine and the peptide **1** bears a C-terminal thioester. There are several solid-phase methods and recombinant strategies based on protein splicing to synthesize a C-terminal thioester.[77, 78] The first step of the ligation is a chemoselective transthioesterification reaction involving the thiol group of the N-terminal cysteine of peptide **2** and the C-terminal thioester moiety of peptide **1**. The intermediate product **3** then undergoes a rapid intramolecular S→N acyl shift, which results in an amide bond at the ligation site in the final product **4**.[68]

This reaction is applicable to peptides with all (non-) canonical amino acid residues, as long as one of the peptides bears a thioester at the C-terminus and the other peptide has an N-terminal cysteine residue. The nature of the thioester leaving group and the pH both influence the rate and the efficiency of the reaction.[68] The most important limitation of this method is that a cysteine residue always results at the ligation site. In a semisynthetic approach, the location of cysteines in the desired product therefore dictates the length of the recombinantly and synthetically produced parts. Since the occurrence of cysteine is only 1.7%, this can lead to impractically long sequences that have to be produced by SPPS.

Several alternative methods have been developed to overcome this problem.[79] For example, Tam and Yu (1998) devised a route that leads to a methionine at the ligation site.[80] This approach is illustrated in Scheme 2. Instead of a cysteine, the peptide **5** has an N-terminal homocysteine residue. The start of the reaction is the same as for the native chemical ligation, but the intermediate product **6** is different: the intramolecular S→N acyl shift occurs through a six-membered ring instead of a five-membered ring. After the ligation reaction, the homocysteine residue can be converted to a methionine by methylation. Comparable ligation reactions can be executed with selenocysteine and the imidazole side chain of histidine.[68]

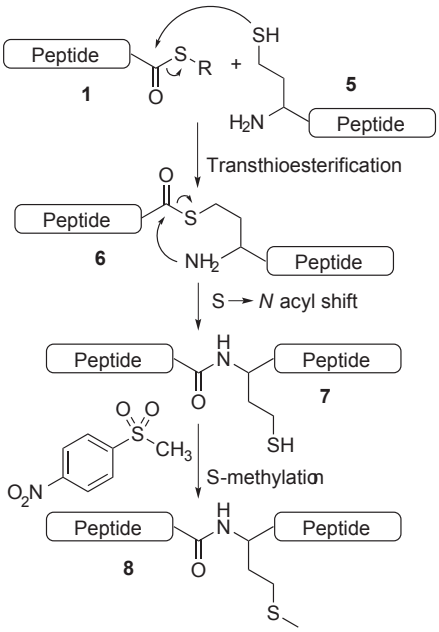

Scheme 2. Native chemical ligation with homocysteine.

Another versatile method to overcome the requirement of an N-terminal cysteine residue is to mimic the characteristics of the cysteine residue through the use of a removable auxiliary. Several types of auxiliaries have been developed. These are shown in Scheme 3. Several researchers have replaced the N-terminal cysteine residue by 2-mercaptobenzylamine **9**.[68, 81] Canne *et al.* (1996) used oxyethanethiol **10**[82] and Kawakami and Aimoto (2003) used the photoremovable *o*-nitrobenzyl scaffold **11** to substitute the N-terminal cysteine residue.[83] The principle behind this method is that, by mimicking the characteristics of the cysteine residue, it is possible to ligate the peptides by native chemical ligation regardless of the kind of amino acid residue at the N-terminus of peptides **9**–**11**. The reaction is the same except that there is one additional step at the end to remove the N-terminal substitute.[83] A significant limitation of all auxiliaries is, however, that they are currently only applicable to synthetic C-terminal peptides.[84]

Use of recombinantly produced protein fragments in (native) chemical ligation reactions requires that they possess either an N-terminal cysteine residue or a C-terminal thioester. The latter has become possible due to the expressed protein ligation method developed by Muir and co-

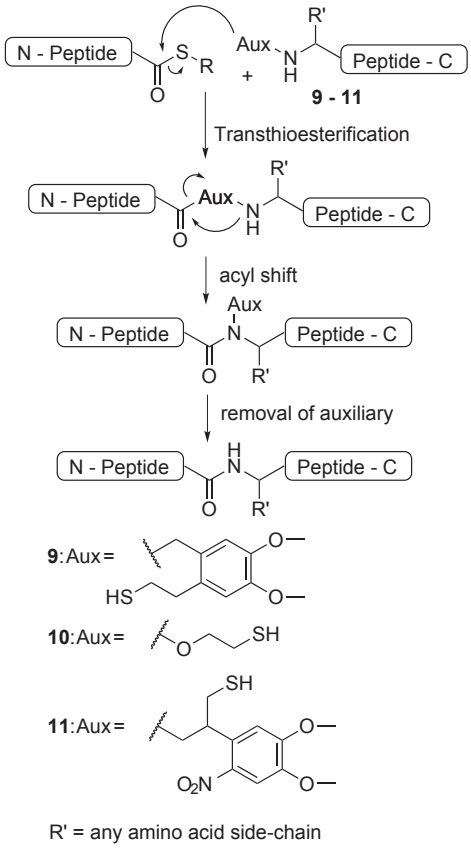

Scheme 3. Chemical ligation using removable auxiliaries.

workers. They used intein-mediated posttranscriptional protein splicing (Scheme 4). This is a naturally occurring process whereby a protein **12** undergoes an intramolecular rearrangement resulting in the extrusion of an internal sequence (intein **15**) and the joining of the lateral sequences (exteins) to form the protein **14**. This reaction is autocatalyzed by the intein domain. An intermediate product of the reaction is thioester **13**. By mutating the site between the intein and the C-terminal protein from arginine to alanine, the splicing reaction can be stopped halfway. Addition of a thiol then results in the natural protein **16** having a C-terminal thioester.[78,85,86] This product can subsequently be used for native chemical ligation.[87]

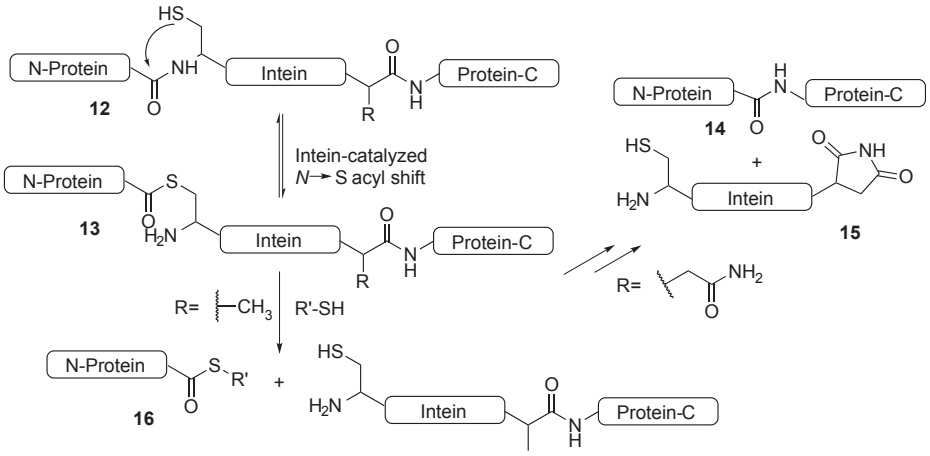

Scheme 4. Intein-mediated production of a C-terminal thioester.

2.4.2. Staudinger ligation

The groups of Raines and Bertozzi independently developed an elegant method to overcome the limitation of the original native chemical ligation method.[88, 89] Their approach is based on the Staudinger reaction.[90] Scheme 5 illustrates the ligation of two peptides by this modified Staudinger reaction. The C-terminus of peptide **17** needs to bear a phophinothioester group, and the second peptide **18** needs to bear an N-terminal azide group.

Like in the classical Staudinger reaction, the first step is the reaction between the C-terminal phophinothioester **17** and the N-terminal azide **18** to form the intermediate iminophosphorane **19**. **19** then undergoes an intramolecular S→N acyl shift leading to the amidophosphonium salt **20**. Through hydrolysis, this salt is converted to the amide product **21** and the phosphine **22**.

The disadvantages of this method are that the peptide chains must be fully protected because of the high reactivity of the intermediate aza-ylide and that diphenyl phosphine oxide traces always remain in the product.[68, 91] To overcome the latter disadvantage, a "traceless" Staudinger ligation has also been developed.[89, 91]

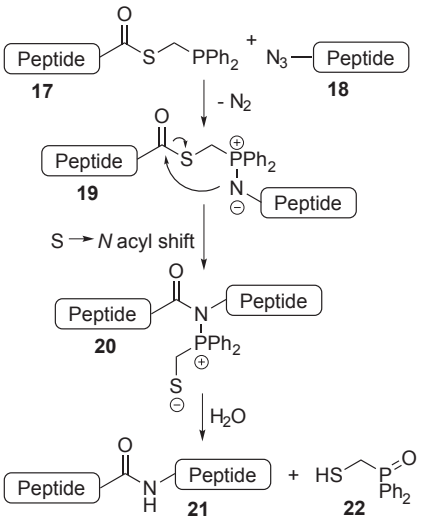

Scheme 5. Staudinger ligation.

In biochemistry, these reactions are particularly valuable because the azide function is (i) virtually absent in biological macromolecules, (ii) exhibits a high intrinsic reactivity with a very limited number of reactants, and (iii) can be easily introduced in peptides or proteins using either organic chemistry or recombinant techniques.[91]

2.5. Bio-orthogonal conjugation to nonnatural amino acids

Several classes of nonnatural amino acids have been successfully incorporated into proteins by the methods described above. The following section describes the nonnatural amino acids that have bio-orthogonal reactivities which can be used in bioconjugation reactions. Most of these nonnatural amino acids have been incorporated using either the substitution method or the termination readthrough method.[92]

2.5.1. 'Click' chemistry

Many of the bioconjugation reactions that are discussed below can be referred to as 'click' reactions. In a narrow sense, this term is often used specifically for the Huisgen 1,3-dipolar cycloaddition (discussed below). However, the term is used here in its original, much broader sense. 'Click'

chemistry is a synthetic approach inspired by the simplicity and efficiency of the chemistry of nature.[91] Nature prefers building its products from simple building blocks linked by carbon-heteroatom bonds rather than carbon–carbon bonds.[93, 94] The Sharpless group has identified a set of reactions that they termed 'click' reactions. These reactions mimic nature in "[being] modular, wide in scope, give very high yields, generate only inoffensive byproducts that can be removed by nonchromatographic methods, and [being] stereo-specific (but not necessarily enantioselective)".[94] Furthermore, the process should have simple reaction conditions, have readily available starting materials and reagents, and require no or easily removable solvents. The term 'click' reaction refers to the high rate and high selectivity of these reactions.[94] Examples of such reactions are given in Scheme 6 and Table 2.

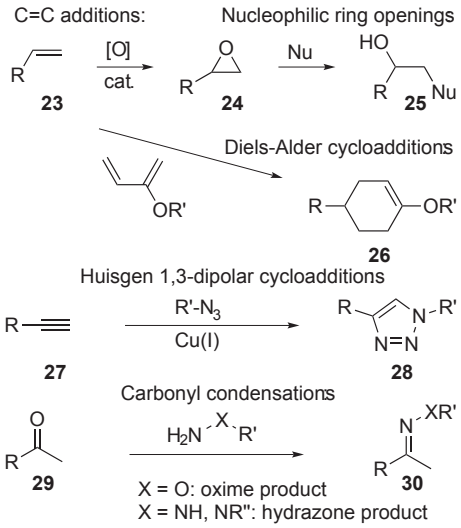

Scheme 6. A selection of 'click' reactions.

Alkyne and azide functionalities

The most frequently applied 'click' reaction is the Huisgen 1,3-dipolar cycloaddition reaction of alkynes and azides catalyzed by copper(I).[93] The general principle of this reaction is outlined in Scheme 6 (**27** to **28**). This is a straightforward reaction which can be performed at room or body temperature and in a variety of solvents. Furthermore, the reaction is compatible with several other functional groups.[91]

Table 2. Applications of 'click' reactions.

Reaction	Examples	Examples of applications	Restrictions
Cycloaddition reactions	Huisgen 1,3-dipolar cycloaddition[95]	• Glyco-polycycles and macrocycles • Glycopeptides	• Glycosylation efficiency • Stereo- and regio-control
	Diels-Alder reaction[96]	• Polyketides • Alkaloids	• Product inhibition if a catalyst is used
Nucleophilic ring-opening reactions	Aziridine reactions[97]	• Dopamine antagonist AS-811223 • (*R*)-1-(benzofuran-2-yl)-2- propyl-aminopentane	• Harsh conditions for subsequent *N*-deprotection
	Aziridinium ion reactions[97]	• Ecopipam • Antitumor agent R-116010	
Carbonyl condensation reactions	Oxime ligation[98, 99]	• Aminooxy-peptides • Neoglycolipid probes	• *N*-overacylation • Stability at low pH
	Hydrazone ligation[100, 101]	• Lipopeptides • R-Melanocyte-stimulating hormone	
Addition to carbon–carbon multiple bonds	Michael additions[102]	• Reaction between cysteine and PEG-maleimide	• All nucleophiles in a protein may react to some extent
	Epoxidation addition[103]	• Polyetherpolyols	• Side reactions of H_2O_2 with cysteine and methionine

As a result of the popularity of the azide/alkyne 'click' reaction, many attempts have been undertaken to incorporate nonnatural amino acids containing azide or alkyne functionalities into proteins. The nonnatural amino acids azidohomoalanine **31** and homopropargylglycine **33** have been designed to closely mimic the natural amino acid methionine. Indeed, they have been shown to be effectively introduced into proteins by methionine auxotrophic bacterial strains. Strable *et al.* (2008) proved this concept by first incorporating **31** or **33** into hepatitis B virus by reassigning the methionine sense codon. Subsequently, the azide or alkyne containing virus particles were successfully labeled using alkyne or azide functionalized fluorescein, rhodamine, biotin, or gadolinium-tetraazacyclododecanetetraacetic acid (Gd-DOTA).[104] 'Click' reactions to incorporated nonnatural amino acids **31** and **33** have also been successfully used to PEGylate proteins,[105] glycosylate proteins,[106, 107] label proteins with fluorophore tags[108, 109] and cross-link several proteins into supramolecular structures.[33, 104] Even live *E. coli* cells have been biotinylated at their outer membrane proteins using this method.[110]

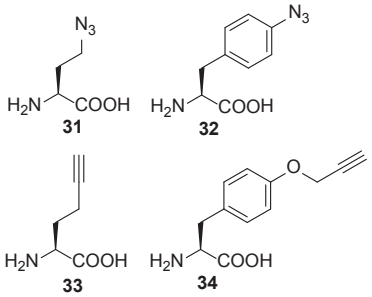

Figure 6. Nonnatural amino acids having azide and alkyne functionalities.

The aromatic amino acids *p*-azidophenylalanine **32** and *p*-propargyloxyphenylalanine **34** have been incorporated site-specifically into proteins by reassigning the UAG stop codon. In *Saccharomyces cerevisiae*, this has been achieved by introducing an *E. coli* mutant tyrosyl-tRNA synthetase[111] and in *E. coli* by using a mutant *Methanococcus jannaschii* tyrosyl-tRNA synthetase.[112] By means of the azide/alkyne 'click' reaction, has been used to site-specifically functionalize cytochrome c3 with the electron donor azidoviologen.[113] **32** has been used for site-specific PEGylation of proteins by reaction with alkyne-functionalized PEG segments.[114]

Apart from azide/alkyne 'click' chemistry, bio-orthogonal conjugation to peptides can also be achieved using Staudinger ligation at azide-containing nonnatural amino acids such as **31** and **32**.[115, 116] Another interesting application of **31** is its ability to be cleaved by a phosphine or dithiol. This reaction yields a reactive C-terminal homoserine lactone in a fashion similar to cyanogen bromide cleavage but under very mild conditions.[117]

Keto/aldehyde functionalities

Another class of 'click' reactions that are gaining interest are certain nucleophilic additions to carbonyl groups. Carbonyl groups do not occur in natural proteins. They have a slightly acidic α-hydrogen due to keto–enol tautomerization and are easily attacked by nucleophiles (Scheme 6: **29**–**30**). If carbonyl groups are introduced into recombinant proteins, some imine formation with the ε-amino groups of lysine residues will therefore occur. However, this reaction is reversible and at physiological pH the equilibrium lies toward the free carbonyl and amine.[118]

Hydrazides, alkoxyamines, and semicarbazides react rapidly and quantitatively with carbonyl groups to form hydrazones, oximes, and semicarbazones, respectively.[119-121] These reaction products are stable under physiological conditions. An additional advantage of these reactions is that they occur in only slightly acidic aqueous medium and require no auxiliaries or catalysts.

The oxime ligation method involves an imine capture between an ester, an aldehyde, or a ketone **29** and an aminooxy nucleophile, yielding the oxime **30**.[122, 123] The hydrazone ligation method is one of the oldest ligation methods and is comparable with the oxime ligation method. However, a hydrazide rather than an aminooxy is used for the ligation, and therefore, a hydrazone bond is formed in the product **30**.[124] No side chain protection is needed for these ligation methods, because on one hand aminooxy and hydrazide groups are more nucleophilic than natural amino acid side chains, and on the other hand the carbonyl groups are more electrophilic than natural side chains.

Another useful carbonyl reaction is imine ligation (Scheme 7), which produces a proline-like structure at the ligation site. This reaction can be used for conjugation to a nucleophilic N-terminal amino acid **36**. The carbonyl group of the conjugating agent **35** is attacked by the

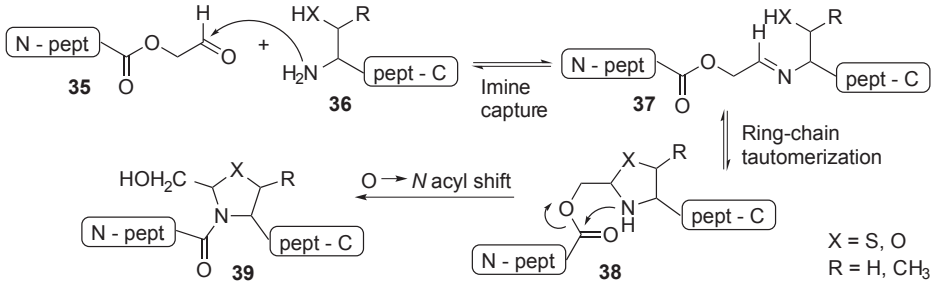

Scheme 7. Imine ligation of N-terminal Cys-, Ser-, and Thr-containing peptides to form pseudoprolines through thiazolidine and oxazolidine ring formation

nucleophilic N-terminal amino acid **36**, forming the imine **37**. **37** subsequently undergoes a rapid ring–chain tautomerization, which results in the heterocycle **38**. This intermediate product facilitates an acyl transfer, forming a proline-like imidic bond in the product **39**. This reaction is well-represented by ligation methods using cysteine, threonine, tryptophan, histidine, or asparagine as N-terminal nucleophiles, yielding a variety of mono-, bi-, and tricyclic side chains at the ligation site.[76] The ring–chain tautomerization in the formation of the heterocyclic ring **38** affords the specificity of the imine ligation.[122] The central feature of imine capture is that the reaction is driven by the weakly basic N-terminus of **36**, which induces the formation of a heterocyclic ring. Given that imine ligation is performed under slightly acidic aqueous conditions, lysine and arginine side chains will be protonated and are therefore not reactive.[122]

Although the ketones and aldehydes that are required for these reactions do not occur in natural proteins, they can be introduced into proteins by sodium periodate oxidation of an N-terminal threonine or serine, respectively. Serine-derived aldehydes have been used to attach a hydrazide-functionalized biotin tag and aminooxy-functionalized PEG chain to the N-terminus of proteins.[119, 125] Furthermore, they have been used to couple two peptide or protein segments by hydrazone or oxime linkages.[120, 121, 126, 127]

The method of sodium periodate oxidation is, however, hampered by the fact that it is only applicable to the N-terminus of a protein. Therefore, several groups have developed carbonyl-containing nonnatural amino acids. The nonnatural amino acids *p*-acetylphenylalanine **40** and *m*-acetylphenylalanine **41** have been introduced site-specifically into

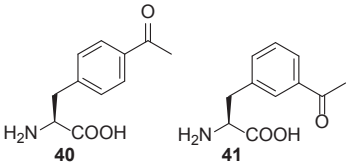

Figure 7. Nonnatural amino acids having carbonyl functionalities.

recombinantly produced proteins by the amber suppression method.[129-133] In addition, **40** has also been introduced using a phenylalanine auxotrophic bacterial strain.[128] The resulting proteins were successfully reacted *in vitro* and *in vivo* with biotin hydrazide[128-130] or fluorescein hydrazide.[129-131] In addition, **40** has also been coupled to aminooxy-functionalized biotin.[132] Another published application of **40** involves recombinant incorporation followed by reaction with aminooxy-functionalized saccharides. In this way, proteins have been site-specifically glycosylated.[133]

The β-diketone analogue **42** has also been genetically incorporated into proteins using stop codon suppression. Subsequently, it was labeled with aminooxy-functionalized biotin and Alexa Fluor 488.[127] Furthermore, **42** is expected to have a number of other reactivities (Scheme 8). For example, the hydrogen atoms between the two keto groups are relatively acidic. The

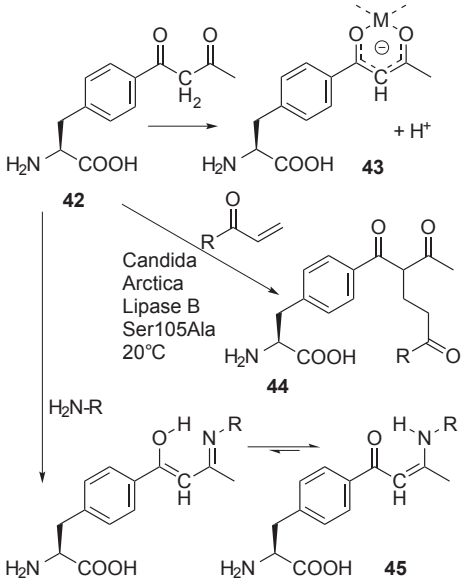

Scheme 8. Possible bioconjugation reactions to the diketone-containing nonnatural amino acid **42**.

deprotonated **43** may therefore be able to chelate metal ions. **42** is also expected to react enzymatically with α,β-unsaturated carbonyl compounds in a carbon–carbon bond forming Michael reaction yielding **44**.[127, 134] Finally, **42** can form the enamine adduct **45** by reacting with a primary amine. **45** is stable at physiological pH due to a six-membered intramolecular hydrogen bridge.[127,135]

Alkenes

A fourth functional group that is very common to synthetic organic and polymer chemistry but rare in natural proteins is the carbon–carbon double bond. The simplest amino acid containing an alkene functionality is dehydroalanine **48**, which occurs sometimes as a posttranslational modification of cysteine.[136] This amino acid has not been introduced directly into recombinant proteins. Instead, its precursors phenylselenocysteine **46** and selenalysine **47** have been used. For the incorporation of **46**, the amber suppression strategy was used.[138] **47** was substituted for lysine in a cell-free translation system.[137] Upon mild oxidative elimination, these two nonnatural amino acids yield **48**, which has been reacted in a Michael addition reaction with various thiol reagents.[137, 138]

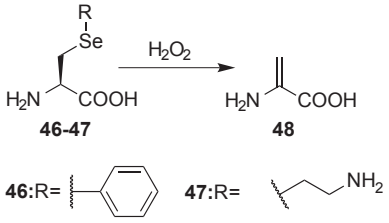

Scheme 9. Conversion of selenium-containing nonnatural amino acids into dehydroalanine.

Two alkene-containing amino acids that have been directly incorporated into proteins are homoallylglycine **49**[34] and *O*-allyltyrosine **50**.[139] **49** was incorporated by a methionine auxotrophic strain. In another experiment, it was

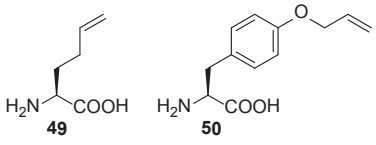

Figure 8. Nonnatural amino acids having vinyl functionalities.

used for cyclization of peptides by ruthenium-catalyzed alkene metathesis.[140] **50** was incorporated by stop codon suppression. Bioconjugation reactions involving **50** have not yet been described to our knowledge. However, it can be expected to have the same reactivity as the other alkene-containing amino acids.

p-Halophenylalanines

Using a palladium catalyst in aqueous environment, aryl halides can undergo a Mizoroki–Heck substitution reaction with alkenes or alkynes. This has been exploited by the incorporation of *p*-iodophenylalanine **51** into proteins in a cell-free translation system, followed by reaction with vinylated biotin.[141] *p*-Bromophenylalanine **52** has been incorporated into recombinant proteins by both the stop codon suppression method and the substitution method, using a phenylalanine auxotrophic *E. coli* strain.[22, 142] However, a subsequent coupling to an alkene or alkyne has, to our knowledge, not yet been described for this amino acid.

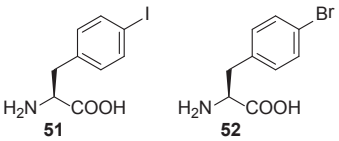

Figure 9. Nonnatural amino acids having aryl halide functionalities.

Radical polymerization initiators and chain transfer agents

One particularly challenging field of bioconjugation chemistry is the chemical synthesis of polymers starting from a protein as macroinitiator or macro-chain-transfer agent (the so-called "grafting from" approach).[143] The ribosomal incorporation of nonnatural amino acids that can give proteins these functionalities would give this field of research a considerable impulse.

Recent progress in this direction is the successful use of *p*-(1-chloroethyl)phenylalanine **53** and *O*-(2-bromoisubutyryl)serine **54** as ATRP initiators. However, these have at present only been incorporated into solid-phase synthesized peptides.[144] The depicted stable radical containing cysteine derivative **55** has been incorporated into proteins by stop codon suppression in *E. coli* and *Xenopus* oocytes.[145, 146] In these experiments, it was used as a spin label. However, **55** might also be used as a chain transfer agent in nitroxide-mediated controlled radical polymerization.

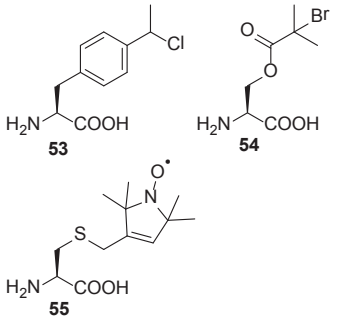

Figure 10. Nonnatural amino acids having ATRP initiator functionalities (**53** and **54**) and nitroxide chain transfer capability (**55**).

Other functional nonnatural amino acids

Apart from the above-mentioned chemically reactive amino acids, many amino acids with other functionalities have been site-specifically introduced into proteins. This makes it possible to incorporate a certain functionality directly into the protein of interest, without having to perform a bioconjugation reaction after protein production. So, whereas some nonnatural amino acids expand the possibilities for bioconjugation, others even make bioconjugation superfluous. To illustrate this vast potential of nonnatural amino acids, a short overview of the functionalities that have been incorporated is given here.

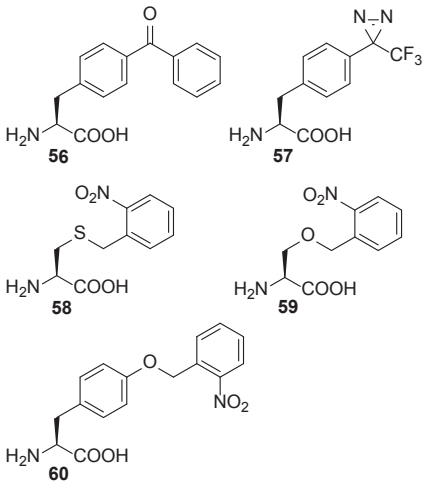

Figure 11. Nonnatural amino acids carrying photoreactive groups.

Amino acids carrying photoreactive groups such as *p*-benzoylphenylalanine **56** and *p*-(3-trifluoromethyl-3H-diazirin-3-yl)-phenylalanine **57**, but also *p*-azidophenylalanine **32**, can be used as probes of protein interactions, protein structure, and protein dynamics *in vitro* and *in vivo*. They can therefore be useful in identifying receptors for ligands.[147-155] Other types of photoreactive amino acids are the photocaged cysteine, serine, and tyrosine analogues **58**, **59**, and **60**. Substituted nitrobenzyl groups block the side-chain hydroxy or thiol groups of these amino acids. These protective groups can be cleaved off by irradiation with 365 nm light *in vitro* or *in vivo*, making it possible to "switch proteins on" by illumination.[156, 157]

The fluorescent probes **61** and **62**,[158, 159] the distance probe **63** (a tryptophan autofluorescence quencher),[160] the site-selective ^{15}N NMR probe **64**,[161] and the infrared probes **65** and **66**[162] are all examples of recombinantly incorporated nonnatural amino acids carrying biophysical probes. These functional groups can visualize protein conformational changes, localization, protein dynamics, local environment, and intermolecular interactions. The amino acids **51** and **52** also belong to this class, as their heavy halogen atoms induce single-wavelength anomalous diffraction.[163]

Electron transfers are involved in a large number of biological processes such as enzyme catalysis and the primary charge separation processes in photosynthesis. To aid in studying these phenomena, the

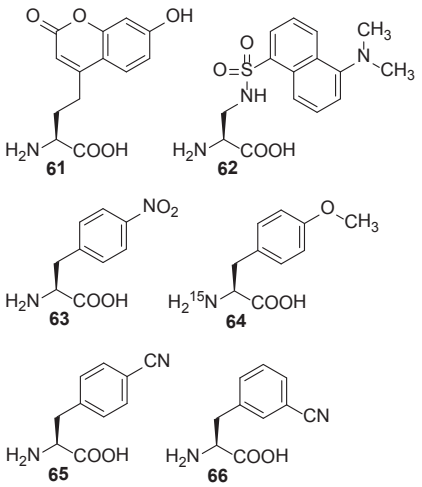

Figure 12. Nonnatural amino acids carrying biophysical probes.

redox-active nonnatural amino acids dihydroxyphenylalanine **67** and 3-aminol-tyrosine **68** have been site-specifically incorporated into proteins.[38, 39, 164] Both can be used to probe and manipulate electron-transfer processes in proteins because they can undergo a two-electron oxidation.

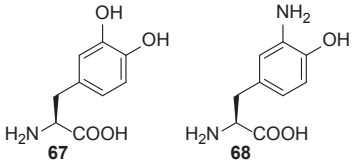

Figure 13. Redox-active nonnatural amino acids.

2.6. Conclusion and future prospects

The research areas of bioconjugation to proteins and incorporation of nonnatural amino acids into proteins are both growing at a fast pace. This is driven by the need for innovative ways of probing protein structure and interactions and the rapid increase in the number of potential therapeutic proteins.

The field of recombinant introduction of nonnatural amino acids is relatively new. The possibilities in this field are actively being expanded at present. In the near future, this may lead to the incorporation of metal-chelating amino acids, amino acids carrying electron-transfer mediators, near-infrared probes, and long-chain alkanes, as well as amino acids with altered backbones (*e.g.*, β-amino acids). It might eventually become possible to create biopolymers with ester rather than amide linkages in the backbone or even generate multicellular organisms that contain nonnatural amino acids.[92] In addition, research into bioconjugation to nonnatural amino acids is currently emerging.

As shown in this review, several reactive nonnatural amino acids have already been incorporated into proteins. A significant number of conjugation reactions to these amino acids have been described. These include the alkyne/azide 'click' reaction, carbonyl condensations, Michael-type additions, and Mizoroki–Heck substitutions. More examples can be expected in the near future. Further elaboration of this field will lead to the creation of powerful strategies to synthesize complex nonnatural proteins by combining methods to incorporate nonnatural amino acids with bio-orthogonal conjugation methods.

We anticipate that this as-yet relatively unexplored field of bioconjugation holds a great potential and will fast-forward developments in the design of, *e.g.*, therapeutic protein derivatives and semisynthetic biomaterials.

References

(1) Veronese, F. M. and Morpurgo, M. (**1999**) Bioconjugation in pharmaceutical chemistry. *Il Farmaco. 54*, 497-516

(2) Monfardini, C. and Veronese, F. M. (**1998**) Stabilization of substances in circulation. *Bioconjugate Chem. 9*, 418-450

(3) Nucci, M. L., Shorr, R. and Abuchowski, A. (**1991**) The therapeutic value of poly(ethylene glycol)-modified proteins. *Adv. Drug Delivery Rev. 6*, 133-151

(4) Maeda, H. (**1991**) SMANCS and polymer-conjugated macromolecular drugs: Advantages in cancer chemotherapy. *Adv. Drug Delivery Rev. 6*, 181-202

(5) Sehon, A. H. (**1991**) Suppression of antibody responses by conjugates of antigens and monomethoxypoly(ethylene glycol). *Adv. Drug Delivery Rev. 6*, 203-217

(6) Yeo, D. S., Srinivasan, R., Chen, G. Y. and Yao, S. Q. (**2004**) Expanded utility of the native chemical ligation reaction. *Chemistry. 10*, 4664-72

(7) Gaertner, H. F., Offord, R. E., Cotton, R., Timms, D., Camble, R. and Rose, K. (**1994**) Chemo-enzymic backbone engineering of proteins. Site-specific incorporation of synthetic peptides that mimic the 64-74 disulfide loop of granulocyte colony-stimulating factor. *J Biol Chem. 269*, 7224-30

(8) Kratz, F. Albumin as a drug carrier: Design of prodrugs, drug conjugates and nanoparticles. *J. Controlled Release*. In Press, Corrected Proof

(9) Wang, C., Stewart, R. J. and Kopecek, J. (**1999**) Hybrid hydrogels assembled from synthetic polymers and coiled-coil protein domains. *Nature. 397*, 417-20

(10) Yang, J., Xu, C., Kopeckova, P. and Kopecek, J. (**2006**) Hybrid hydrogels self-assembled from HPMA copolymers containing peptide grafts. *Macromol. Biosci. 6*, 201-9

(11) Hentschel, J., ten Cate, M. G. J. and Borner, H. G. (**2007**) Peptide-guided organization of peptide-polymer conjugates: Expanding the approach from oligo- to polymers. *Macromolecules. 40*, 9224-9232

(12) Wu, K., Yang, J., Konák, C., Kopecková, P. and Kopecek, J. (**2008**) Novel synthesis of HPMA copolymers containing peptide grafts and their self-assembly into hybrid hydrogels. *Macromol. Chem. Phys. 209*, 467-475

(13) Wu, G., Ott, T. L., Knabe, D. A. and Bazer, F. W. (**1999**) Amino acid composition of the fetal pig. *J. Nutr. 129*, 1031-1038

(14) Mann, M. and Jensen, O. N. (**2003**) Proteomic analysis of post-translational modifications. *Nat Biotech. 21*, 255-261

(15) Lentini, A., Abbruzzese, A., Caraglia, M., Marra, M. and Beninati, S. (**2004**) Protein-polyamine conjugation by transglutaminase in cancer cell differentiation: Review article. *Amino Acids. 26*, 331-337

(16) Basso, A. D., Kirschmeier, P. and Bishop, W. R. (**2006**) Thematic review series: Lipid posttranslational modifications. farnesyl transferase inhibitors. *J. Lipid Res. 47*, 15-31

(17) Casey, P. J. and Seabra, M. C. (**1996**) Protein prenyltransferases. *J. Biol. Chem. 271*, 5289-5292

(18) Farazi, T. A., Waksman, G. and Gordon, J. I. (**2001**) The biology and enzymology of protein N-myristoylation. *J. Biol. Chem. 276*, 39501-39504

(19) Raju, R. V. S., Datla, R. S. S., Moyana, T. N., Kakkar, R., Carlsen, S. A. and Sharma, R. K. (**2000**) N-myristoyltransferase. *Mol. Cell. Biochem. 204*, 135-155

(20) Kiick, K. L., Weberskirch, R. and Tirrell, D. A. (**2001**) Identification of an expanded set of translationally active methionine analogues in *Escherichia coli*. *FEBS Lett. 502*, 25-30

(21) Ibba, M. and Hennecke, H. (**1995**) Relaxing the substrate specificity of an aminoacyl-tRNA synthetase allows *in vitro* and *in vivo synthesis* of proteins containing unnatural amino acids. *FEBS Lett. 364*, 272-275

(22) Sharma, N., Furter, R., Kast, P. and Tirrell, D. A. (**2000**) Efficient introduction of aryl bromide functionality into proteins *in vivo*. *FEBS Lett. 467*, 37-40

(23) Tang, Y. and Tirrell, D. A. (**2002**) Attenuation of the editing activity of the *Escherichia coli* leucyl-tRNA synthetase allows incorporation of novel amino acids into proteins *in vivo*. *Biochemistry. 41*, 10635-10645

(24) Tang, Y. and Tirrell, D. A. (**2001**) Biosynthesis of a highly stable coiled-coil protein containing hexafluoroleucine in an engineered bacterial host. *J. Am. Chem. Soc. 123*, 11089-11090

(25) Wang, Q., Chan, T. R., Hilgraf, R., Fokin, V. V., Sharpless, K. B. and Finn, M. G. (**2003**) Bioconjugation by copper(I)-catalyzed azide-alkyne [3 + 2] cycloaddition. *J. Am. Chem. Soc. 125*, 3192-3193

(26) Yoshikawa, E., Fournier, M. J., Mason, T. L. and Tirrell, D. A. (**1994**) Genetically engineered fluoropolymers. synthesis of repetitive polypeptides containing *p*-fluorophenylalanine residues. *Macromolecules. 27*, 5471-5475

(27) Budisa, N., Alefelder, S., Bae, J. H., Golbik, R., Minks, C., Huber, R. and Moroder, L. (**2001**) Proteins with β-(thienopyrrolyl)alanines as alternative chromophores and pharmaceutically active amino acids. *Protein Sci. 10*, 1281-1292

(28) Bae, J. H., Alefelder, S., Kaiser, J. T., Friedrich, R., Moroder, L., Huber, R. and Budisa, N. (**2001**) Incorporation of β-selenolo[3,2-b] pyrrolyl-alanine into proteins for phase determination in protein X-ray crystallography. *J. Mol. Biol. 309*, 925-936

(29) Renner, C., Alefelder, S., Bae, J. H., Budisa, N., Huber, R. and Moroder, L. (**2001**) Fluoroprolines as tools for protein design and Engineering. *Angew. Chem., Int. Ed. 40*, 923-925

(30) Kiick, K. L. and Tirrell, D. A. (**2000**) Protein engineering by *in vivo* incorporation of non-natural amino acids: Control of incorporation of methionine analogues by methionyl-tRNA synthetase. *Tetrahedron. 56*, 9487-9493

(31) Kiick, K. L., Saxon, E., Tirrell, D. A. and Bertozzi, C. R. (**2002**) Incorporation of azides into recombinant proteins for chemoselective modification by the Staudinger ligation. *Proc. Natl. Acad. Sci. U.S.A. 99*, 19-24

(32) Link, A. J. and Tirrell, D. A. (**2003**) Cell surface labeling of *Escherichia coli* via copper(I)-catalyzed [3+2] cycloaddition. *J. Am. Chem. Soc. 125*, 11164-11165

(33) Link, A. J., Vink, M. K. S. and Tirrell, D. A. (**2004**) Presentation and detection of azide functionality in bacterial cell surface proteins. *J. Am. Chem. Soc. 126*, 10598-10602

(34) van Hest, J. C. M. and Tirrell, D. A. (**1998**) Efficient introduction of alkene functionality into proteins *in vivo*. *FEBS Lett. 428*, 68-70

(35) Kiick, K. L., van Hest, J. C. M. and Tirrell, D. A. (**2000**) Expanding the scope of protein biosynthesis by altering the methionyl-tRNA synthetase activity of a bacterial expression host. *Angew. Chem., Int. Ed. 39*, 2148-2152

(36) Noren, C. J., Anthony-Cahill, S. J., Griffith, M. C. and Schultz, P. G. (**1989**) A general method for site-specific incorporation of unnatural amino acids into proteins. *Science. 244*, 182-188

(37) Hendrickson, T. L., De Crécy-Lagard, V. and Schimmel, P. (**2004**) Incorporation of nonnatural amino acids into proteins. *Annu. Rev. Biochem. 73*, 147-176

(38) Hohsaka, T. and Sisido, M. (**2002**) Incorporation of non-natural amino acids into proteins. *Curr. Opin. Chem. Biol. 6*, 809-815

(39) Hecht, S. M., Alford, B. L., Kuroda, Y. and Kitano, S. (**1978**) "Chemical aminoacylation" of tRNA's. *J. Biol. Chem. 253*, 4517-4520

(40) Wiltschi, B. and Budisa, N. (**2007**) Natural history and experimental evolution of the genetic code. *Appl. Microbiol. Biotechnol. 74*, 739-753

(41) Wang, L. and Schultz, P. G. (**2002**) Expanding the genetic code. *Chem. Commun. (Cambridge). 1*, 1-11

(42) Rodriguez, E. A., Lester, H. A. and Dougherty, D. A. (**2007**) Improved amber and opal suppressor tRNAs for incorporation of unnatural amino acids *in vivo*. Part 2: Evaluating suppression efficiency. *RNA. 13*, 1715-1722

(43) Nowak, M. W., Kearney, P. C., Sampson, J. R., Saks, M. E., Labarca, C. G., Silverman, S. K., Zhong, W., Thorson, J., Abelson, J. N. and Davidson, N. (**1995**) Nicotinic receptor binding site probed with unnatural amino acid incorporation in intact cells. *Science. 268*, 439-442

(44) Turcatti, G., Nemeth, K., Edgerton, M. D., Meseth, U., Talabot, F., Peitsch, M., Knowles, J., Vogel, H. and Chollet, A. (**1996**) Probing the structure and function of the tachykinin neurokinin-2 receptor through biosynthetic incorporation of fluorescent amino acids at specific sites. *J. Biol. Chem. 271*, 19991-19998

(45) Kiga, D., Sakamoto, K., Kodama, K., Kigawa, T., Matsuda, T., Yabuki, T., Shirouzu, M., Harada, Y., Nakayama, H., Takio, K., Hasegawa, Y., Endo, Y., Hirao, I. and Yokoyama, S. (**2002**) An engineered *Escherichia coli* tyrosyl-tRNA synthetase for site-specific incorporation of an unnatural amino acid into proteins in eukaryotic translation and its application in a wheat germ cell-free system. *Proc. Natl. Acad. Sci. U.S.A. 99*, 9715-9720

(46) Swartz, J. R., Jewett, M. C. and Woodrow, K. A. (**2004**) Cell-free protein synthesis with prokaryotic combined transcription-translation. *Methods Mol. Biol. 267*, 169-182

(47) Xie, J. and Schultz, P. G. (**2005**) Adding amino acids to the genetic repertoire. *Curr. Opin. Chem. Biol. 9*, 548-554

(48) Wang, L. and Schultz, P. G. (**2001**) A general approach for the generation of orthogonal tRNAs. *Chem. Biol. 8*, 883-890

(49) Sakamoto, K., Hayashi, A., Sakamoto, A., Kiga, D., Nakayama, H., Soma, A., Kobayashi, T., Kitabatake, M., Takio, K., Saito, K., Shirouzu, M., Hirao, I. and Yokoyama, S. (**2002**) Site-specific incorporation of an unnatural amino acid into proteins in mammalian cells. *Nucleic Acids Res. 30*, 4692-4699

(50) Mehl, R. A., Anderson, J. C., Santoro, S. W., Wang, L., Martin, A. B., King, D. S., Horn, D. M. and Schultz, P. G. (**2003**) Generation of a bacterium with a 21 amino acid genetic code. *J. Am. Chem. Soc. 125*, 935-939

(51) Wang, K., Neumann, H., Peak-Chew, S. Y. and Chin, J. W. (**2007**) Evolved orthogonal ribosomes enhance the efficiency of synthetic genetic code expansion. *Nat. Biotechnol. 25*, 770-777

(52) Sisido, M. and Hohsaka, T. (**2001**) Introduction of specialty functions by the position-specific incorporation of nonnatural amino acids into proteins through four-base codon/anticodon pairs. *Appl. Microbiol. Biotechnol. 57*, 274-281

(53) Dougherty, D. A. (**2000**) Unnatural amino acids as probes of protein structure and function. *Curr. Opin. Chem. Biol. 4*, 645-652

(54) Liu, W., Brock, A., Chen, S., Chen, S. and Schultz, P. G. (**2007**) Genetic incorporation of unnatural amino acids into proteins in mammalian cells. *Nat. Methods. 4*, 239-244

(55) Kwon, I., Kirshenbaum, K. and Tirrell, D. A. (**2003**) Breaking the degeneracy of the genetic code. *J. Am. Chem. Soc. 125*, 7512-7513

(56) Rackham, O. and Chin, J. W. (**2005**) A network of orthogonal ribosome × mRNA pairs. *Nat. Chem. Biol. 1*, 159-166

(57) Hohsaka, T. and Sisido, M. (**2000**) Incorporation of nonnatural amino acids into proteins by using five-base codon-anticodon pairs. *Nucleic Acids Symp. Ser. 44*, 99-100

(58) Hohsaka, T., Ashizuka, Y., Taira, H., Murakami, H. and Sisido, M. (**2001**) Incorporation of nonnatural amino acids into proteins by using various four-base codons in an *Escherichia coli in vitro* translation system. *Biochemistry. 40*, 11060-11064

(59) Rodriguez, E. A., Lester, H. A. and Dougherty, D. A. (**2006**) *In vivo* incorporation of multiple unnatural amino acids through nonsense and frameshift suppression. *Proc. Natl. Acad. Sci. U.S.A. 103*, 8650-8655

(60) Taki, M., Hohsaka, T. and Sisido, M. (**2001**) Site-specific cleavage of a protein via introducing a hydroxy acid derivative in the main chain by using four-base codon/anticodon pairs. *Nucleic Acids Symp. Ser. 1*, 227-228

(61) Switzer, C., Moroney, S. E. and Benner, S. A. (**1989**) Enzymatic incorporation of a new base pair into DNA and RNA. *J. Am. Chem. Soc. 111*, 8322-8323

(62) Bain, J. D., Switzer, C., Chamberlin, R. and Bennert, S. A. (**1992**) Ribosome-mediated incorporation of a non-standard amino acid into a peptide through expansion of the genetic code. *Nature. 356*, 537-539

(63) Matsuda, S., Fillo, J. D., Henry, A. A., Rai, P., Wilkens, S. J., Dwyer, T. J., Geierstanger, B. H., Wemmer, D. E., Schultz, P. G., Spraggon, G. and Romesberg, F. E. (**2007**) Efforts toward expansion of the genetic alphabet: Structure and replication of unnatural base pairs. *J. Am. Chem. Soc. 129*, 10466-10473

(64) Leconte, A. M., Hwang, G. T., Matsuda, S., Capek, P., Hari, Y. and Romesberg, F. E. (**2008**) Discovery, characterization, and optimization of an unnatural base pair for expansion of the genetic alphabet. *J. Am. Chem. Soc. 130*, 2336-2343

(65) Ohtsuki, T., Kimoto, M., Ishikawa, M., Mitsui, T. O., Hirao, I. and Yokoyama, S. (**2001**) Unnatural base pairs for specific transcription. *Proc. Natl. Acad. Sci. U.S.A. 98*, 4922-4925

(66) Hirao, I., Kimoto, M., Mitsui, T., Fujiwara, T., Kawai, R., Sato, A., Harada, Y. and Yokoyama, S. (**2006**) An unnatural base pair system for *in vitro* replication and transcription. *Nucleic Acids Symp. Ser. 50*, 33-34

(67) Hirao, I. (**2006**) Unnatural base pair systems for DNA/RNA-based biotechnology. *Curr. Opin. Chem. Biol. 10*, 622-627

(68) Kimmerlin, T. and Seebach, D. (**2005**) '100 years of peptide synthesis': Ligation methods for peptide and protein synthesis with applications to β-peptide assemblies. *J. Pept. Res. 65*, 229-260

(69) Han, S. and Viola, R. E. (**2004**) Splicing of unnatural amino acids into proteins: A peptide model study. *Protein Pept. Lett. 11*, 107-114

(70) Lemieux, G. A. and Bertozzi, C. R. (**1998**) Chemoselective ligation reactions with proteins, oligosaccharides and cells. *Trends Biotechnol. 16*, 506-513

(71) Schnolzer, M. and Kent, S. B. H. (**1992**) Constructing proteins by dovetailing unprotected synthetic peptides: *Backbone-engineered HIV protease. Science. 256*, 221-225

(72) Rademann, J. (**2004**) Organic protein chemistry: Drug discovery through the chemical modification of proteins. *Angew. Chem., Int. Ed. 43*, 4554-4556

(73) Borgia, J. A. and Fields, G. B. (**2000**) Chemical synthesis of proteins. *Trends Biotechnol. 18*, 243-251

(74) Englebretsen, D. R., Choma, C. T. and Robillard, G. T. (**1998**) Synthesis of a designed transmembrane protein by thioether ligation of solubilised segments: Nα-haloacetylated peptides survived resin cleavage using TFA with EDT as scavenger. *Tetrahedron Lett. 39*, 4929-4932

(75) Brunel, F. M. and Dawson, P. E. (**2005**) Synthesis of constrained helical peptides by thioether ligation: Application to analogs of gp41. *Chem.Commun. (Cambridge). 20*, 2552-2554

(76) Tam, J. P., Xu, J. and Eom, K. D. (**2001**) Methods and strategies of peptide ligation. *Pept. Sci. 60*, 194-205

(77) Dawson, P. E., Muir, T. W., Clark-Lewis, I. and Kent, S. B. H. (**1994**) Synthesis of proteins by native chemical ligation. *Science. 266*, 776-779

(78) Severinov, K. and Muir, T. W. (**1998**) Expressed protein ligation, a novel method for studying protein-protein interactions in transcription. *J. Biol. Chem. 273*, 16205-16209

(79) Nilsson, B. L., Soellner, M. B. and Raines, R. T. (**2005**) Chemical synthesis of proteins. *Annu. Rev. Biophys. Biomol. Struct. 34*, 91-118

(80) Tam, J. P. and Yu, Q. (**1998**) Methionine ligation strategy in the biomimetic synthesis of parathyroid hormones. *Biopolymers. 46*, 319-327

(81) Offer, J. and Dawson, P. E. (**2000**) Nα-2-mercaptobenzylamine-assisted chemical ligation. *Org. Lett. 2*, 23-26

(82) Canne, L. E., Bark, S. J. and Kent, S. B. H. (**1996**) Extending the applicability of native chemical ligation. *J. Am. Chem. Soc. 118*, 5891-5896

(83) Kawakami, T. and Aimoto, S. (**2003**) A photoremovable ligation auxiliary for use in polypeptide synthesis. *Tetrahedron Lett. 44*, 6059-6061

(84) Macmillan, D. (**2006**) Evolving strategies for protein synthesis converge on native chemical ligation. *Angew. Chem., Int. Ed. 45*, 7668-7672

(85) Muir, T. W., Sondhi, D. and Cole, P. A. (**1998**) Expressed protein ligation: A general method for protein engineering. *Proc. Natl. Acad. Sci. U.S.A. 95*, 6705-6710

(86) Muir, T. W. (**2003**) Semisynhesis of proteins by expressed protein ligation. *Annu. Rev. Biochem. 72*, 249-289

(87) Buskas, T., Ingale, S. and Boons, G. J. (**2006**) Glycopeptides as versatile tools for glycobiology. *Glycobiology. 16*, 113R-136

(88) Nilsson, B. L., Kiessling, L. L. and Raines, R. T. (**2000**) Staudinger ligation: A peptide from a thioester and azide. *Org. Lett. 2*, 1939-1941

(89) Saxon, E., Armstrong, J. I. and Bertozzi, C. R. (**2000**) A "traceless" Staudinger ligation for the chemoselective synthesis of amide bonds. *Org. Lett. 2*, 2141-2143

(90) Staudinger, H. and Meyer, J. (**1919**) New organic compounds of phosphorus. III. Phosphinemethylene derivatives and phosphinimines. *Helv. Chim. Acta. 2*, 635-646

(91) Lutz, J. F. and Borner, H. G. (**2008**) Modern trends in polymer bioconjugates design. *Prog. Polym. Sci. 33*, 1-39

(92) Xie, J. and Schultz, P. G. (**2006**) A chemical toolkit for proteins - an expanded genetic code. *Nat. Rev. Mol. Cell Biol. 7*, 775-782

(93) Moses, J. E. and Moorhouse, A. D. (**2007**) The growing applications of click chemistry. *Chem. Soc. Rev. 36*, 1249-1262

(94) Kolb, H. C., Finn, M. G. and Sharpless, K. F. (**2001**) Click chemistry: Diverse chemical function from a few good reactions. *Angew. Chem., Int. Ed. 40*, 2004-2021

(95) Dedola, S., Nepogodiev, S. A. and Field, R. A. (**2007**) Recent applications of the Cu(I)-catalyzed Huisgen azide-alkyne 1,3-dipolar cycloaddition reaction in carbohydrate chemistry. *Org. Biomol. Chem. 5*, 1006-1017

(96) Stocking, E. M. and Williams, R. M. (**2003**) Chemistry and biology of biosynthetic Diels-Alder reactions. *Angew. Chem., Int. Ed. 42*, 3078-3115

(97) Dahanukar, V. and Zavialov, L. (**2002**) Aziridines and aziridinium ions in the practical synthesis of pharmaceutical intermediates - A perspective. *Curr. Opin. Drug Discov. Devel. 5*, 918-927

(98) Foillard, S., Rasmussen, M. O., Razkin, J., Boturyn, D. and Dumy, P. (**2008**) 1-ethoxyethylidene, a new group for the stepwise SPPS of aminooxyacetic acid containing peptides. *J. Org. Chem. 73*, 983-991

(99) Liu, Y., Feizi, T., Campanero-Rhodes, M. A., Childs, R. A., Zhang, Y., Mulloy, B., Evans, P. G., Osborn, H. M. I., Otto, D., Crocker, P. R. and Chai, W. (**2007**) Neoglycolipid probes prepared via oxime ligation for microarray analysis of oligosaccharide-protein interactions. *Chem. Biol. 14*, 847-859

(100) Dubs, P., Bourel-Bonnet, L., Subra, G., Blanpain, A., Melnyk, O., Pinel, A. M., Gras-masse, H. and Martinez, J. (**2007**) Parallel synthesis of a lipopeptide library by hydrazone-based chemical ligation. *J. Comb. Chem. 9*, 973-981

(101) Gras-Masse, H. (**2001**) Chemoselective ligation and antigen vectorization. *Biologicals. 29*, 183-188

(102) Mather, B. D., Viswanathan, K., Miller, K. M. and Long, T. E. (**2006**) Michael addition reactions in macromolecular design for emerging technologies. *Prog. Polym. Sci. 31*, 487-531

(103) Metzger, J. and Bornscheuer, U. (**2006**) Lipids as renewable resources: Current state of chemical and biotechnological conversion and diversification. *Appl. Microbiol. Biotechnol. 71*, 13-22

(104) Strable, E., Prasuhn, D. E., Udit, A. K., Brown, S., Link, A. J., Ngo, J. T., Lander, G., Quispe, J., Potter, C. S., Carragher, B., Tirrell, D. A. and Finn, M. G. (**2008**) Unnatural amino acid incorporation into virus-like particles. *Bioconjugate Chem. 19*, 866-875

(105) Cazalis, C. S., Haller, C. A., Sease-Cargo, L. and Chaikof, E. L. (**2004**) C-terminal site-specific PEGylation of a truncated thrombomodulin mutant with retention of full bioactivity. *Bioconjugate Chem. 15*, 1005-1009

(106) van Kasteren, S. I., Kramer, H. B., Gamblin, D. P. and Davis, B. G. (**2007**) Site-selective glycosylation of proteins: Creating synthetic glycoproteins. *Nat. Protoc. 2*, 3185-3194

(107) van Kasteren, S. I., Kramer, H. B., Jensen, H. H., Campbell, S. J., Kirkpatrick, J., Oldham, N. J., Anthony, D. C. and Davis, B. G. (**2007**) Expanding the diversity of chemical protein modification allows post-translational mimicry. *Nature. 446*, 1105-1109

(108) Beatty, K. E., Liu, J. C., Xie, F., Dieterich, D. C., Schuman, E. M., Wang, Q. and Tirrell, D. A. (**2006**) Fluorescence visualization of newly synthesized proteins in mammalian cells. *Angew. Chem., Int. Ed. 45*, 7364-7367

(109) Beatty, K. E., Xie, F., Wang, Q. and Tirrell, D. A. (**2005**) Selective dye-labeling of newly synthesized proteins in bacterial cells. *J. Am. Chem. Soc. 127*, 14150-14151

(110) Link, A. J. and Tirrell, D. A. (**2003**) Cell surface labeling of *Escherichia coli* via copper(I)-catalyzed [3+2] cycloaddition. *J. Am. Chem. Soc. 125*, 11164-11165

(111) Deiters, A., Cropp, T. A., Mukherji, M., Chin, J. W., Anderson, J. C. and Schultz, P. G. (**2003**) Adding amino acids with novel reactivity to the genetic code of *Saccharomyces cerevisiae*. *J. Am. Chem. Soc. 125*, 11782-11783

(112) Deiters, A. and Schultz, P. G. (**2005**) *In vivo* incorporation of an alkyne into proteins in *Escherichia coli. Bioorg. Med. Chem. Lett. 15*, 1521-1524

(113) Iida, S., Asakura, N., Tabata, K., Okura, I. and Kamachi, T. (**2006**) Incorporation of unnatural amino acids into cytochrome c3 and specific viologen binding to the unnatural amino acid. *ChemBioChem. 7*, 1853-1855

(114) Deiters, A., Cropp, T. A., Summerer, D., Mukherji, M. and Schultz, P. G. (**2004**) Site-specific PEGylation of proteins containing unnatural amino acids. *Bioorg. Med. Chem. Lett. 14*, 5743-5745

(115) Kiick, K. L., Saxon, E., Tirrell, D. A. and Bertozzi, C. R. (**2002**) Incorporation of azides into recombinant proteins for chemoselective modification by the staudinger ligation. *Proc. Natl. Acad. Sci. U.S.A. 99*, 19-24

(116) Tsao, M., Tian, F. and Schultz, P. G. (**2005**) Selective Staudinger modification of proteins containing *p*-azidophenylalanine. *ChemBioChem. 6*, 2147-2149

(117) Back, J. W., David, O., Kramer, G., Masson, G., Kasper, P. T., de Koning, L. J., de Jong, L., van Maarseveen, J. H. and de Koster, C. G. (**2005**) Mild and chemoselective peptide-bond cleavage of peptides and proteins at azido homoalanine. *Angew. Chem., Int. Ed. 44*, 7946-7950

(118) Godoy-Alcántar, C., Yatsimirsky, A. K. and Lehn, J. (**2005**) Structure-stability correlations for imine formation in aqueous solution. *J. Phys. Org. Chem. 18*, 979-985

(119) Geoghegan, K. F. and Stroh, J. G. (**1992**) Site-directed conjugation of nonpeptide groups to peptides and proteins via periodate oxidation of a 2-amino alcohol. Application to modification at N-terminal serine. *Bioconjugate Chem. 3*, 138-46

(120) Shao, J. and Tam, J. P. (**1995**) Unprotected peptides as building blocks for the synthesis of peptide dendrimers with oxime, hydrazone, and thiazolidine linkages. *J. Am. Chem. Soc. 117*, 3893-3899

(121) Rose, K. (**1994**) Facile synthesis of homogeneous artificial proteins. *J. Am. Chem. Soc. 116*, 30-33

(122) Tam, J. P., Yu, Q. and Miao, Z. (**1999**) Orthogonal ligation strategies for peptide and protein. *Pept. Sci. 51*, 311-332

(123) Löwik, D., Ayres, L., Smeenk, J. and Van Hest, J. (**2006**) Synthesis of bio-inspired hybrid polymers using peptide synthesis and protein engineering. *Adv. Polym. Sci. 202*, 19-52

(124) Köhn, M. and Breinbauer, R. (**2004**) The Staudinger ligation - A gift to chemical biology. *Angew. Chem., Intl. Ed. 43*, 3106-3116

(125) Gaertner, H. F. and Offord, R. E. (**1996**) Site-specific attachment of functionalized poly(ethylene glycol) to the amino terminus of proteins. *Bioconjugate Chem. 7*, 38-44

(126) Canne, L. E., Ferre - d'Amare, A. R., Burley, S. K. and Kent, S. B. H. (**1995**) Total chemical synthesis of a unique transcription factor-related protein: CMyc-max. *J. Am. Chem. Soc. 117*, 2998-3007

(127) Zeng, H., Xie, J. and Schultz, P. G. (**2006**) Genetic introduction of a diketone-containing amino acid into proteins. *Bioorg. Med. Chem. Lett. 16*, 5356-5359

(128) Datta, D., Wang, P., Carrico, I. S., Mayo, S. L. and Tirrell, D. A. (**2002**) A designed phenylalanyl-tRNA synthetase variant allows efficient *in vivo* incorporation of aryl ketone functionality into proteins. *J. Am. Chem. Soc. 124*, 5652-5653

(129) Wang, L., Zhang, Z., Brock, A. and Schultz, P. G. (**2003**) Addition of the keto functional group to the genetic code of *Escherichia coli*. *Proc. Natl. Acad. Sci. U.S.A. 100*, 56-61

(130) Zhang, Z., Smith, B. A. C., Wang, L., Brock, A., Cho, C. and Schultz, P. G. (**2003**) A new strategy for the site-specific modification of proteins *in vivo. Biochemistry. 42*, 6735-6746

(131) Ye, S., Koehrer, C., Huber, T., Kazmi, M., Sachdev, P., Yan, E. C. Y., Bhagat, A., RajBhandary, U. L. and Sakmar, T. P. (**2008**) Site-specific incorporation of keto amino acids into functional G protein-coupled receptors using unnatural amino acid mutagenesis. *J. Biol. Chem. 283*, 1525-1533

(132) Taki, M., Tokuda, Y., Ohtsuki, T. and Sisido, M. (**2006**) Design of carrier tRNAs and selection of four-base codons for efficient incorporation of various nonnatural amino acids into proteins in *Spodoptera frugiperda 21* (Sf21) insect cell-free translation system. *The Society for Biotechnology, Japan. 102*, 511-517

(133) Liu, H., Wang, L., Brock, A., Wong, C. and Schultz, P. G. (**2003**) A method for the generation of glycoprotein mimetics. *J. Am. Chem. Soc. 125*, 1702-1703

(134) Svedendahl, M., Hult, K. and Berglund, P. (**2005**) Fast carbon-carbon bond formation by a promiscuous lipase. *J. Am. Chem. Soc. 127*, 17988-17989

(135) Barbas, C. F.,3rd, Heine, A., Zhong, G., Hoffmann, T., Gramatikova, S., Bjornestedt, R., List, B., Anderson, J., Stura, E. A., Wilson, I. A. and Lerner, R. A. (**1997**) Immune versus natural selection: Antibody aldolases with enzymic rates but broader scope. *Science. 278*, 2085-2092

(136) Bar-Or, R., Rael, L. T. and Bar-Or, D. (**2008**) Dehydroalanine derived from cysteine is a common post-translational modification in human serum albumin. *Rapid Commun. Mass Spectrom. 22*, 711-716

(137) Seebeck, F. P. and Szostak, J. W. (**2006**) Ribosomal synthesis of dehydroalanine-containing peptides. *J. Am. Chem. Soc. 128*, 7150-7151

(138) Wang, J., Schiller, S. M. and Schultz, P. G. (**2007**) A biosynthetic route to dehydroalanine-containing proteins. *Angew. Chem., Int. Ed. 46*, 6849-6851

(139) Zhang, Z., Wang, L., Brock, A. and Schultz, P. G. (**2002**) The selective incorporation of alkenes into proteins in *Escherichia coli. Angew. Chem., Int. Ed. 41*, 2840-2842

(140) Clark, T. D. and Ghadiri, M. R. (**1995**) Supramolecular design by covalent capture. Design of a peptide cylinder via hydrogen-bond-promoted intermolecular olefin metathesis. *J. Am. Chem. Soc. 117*, 12364-12365

(141) Kodama, K., Fukuzawa, S., Nakayama, H., Kigawa, T., Sakamoto, K., Yabuki, T., Matsuda, N., Shirouzu, M., Takio, K., Tachibana, K. and Yokoyama, S. (**2006**) Regioselective carbon-carbon bond formation in proteins with palladium catalysis; new protein chemistry by organometallic chemistry. *ChemBioChem. 7*, 134-139

(142) Kwon, I., Wang, P. and Tirrell, D. A. (**2006**) Design of a bacterial host for site-specific incorporation of *p*-bromophenylalanine into recombinant proteins. *J. Am. Chem. Soc. 128*, 11778-11783

(143) Bontempo, D. and Maynard, H. D. (**2005**) Streptavidin as a macroinitiator for polymerization: *In situ* protein-polymer conjugate formation. *J. Am. Chem. Soc. 127*, 6508-9

(144) Broyer, R. M., Quaker, G. M. and Maynard, H. D. (**2007**) Designed amino acid ATRP initiators for the synthesis of biohybrid materials. *J. Am. Chem. Soc. 130*, 1041-1047

(145) Cornish, V. W., Benson, D. R., Altenbach, C. A., Hideg, K., Hubbell, W. L. and Schultz, P. G. (**1994**) Site-specific incorporation of biophysical probes into proteins. *Proc. Natl. Acad. Sci. U.S.A. 91*, 2910-2914

(146) Shafer, A. M., Kalai, T., Liu, S. Q. B., Hideg, K. and Voss, J. C. (**2004**) Site-specific insertion of spin-labeled L-amino acids in *Xenopus* oocytes. *Biochemistry. 43*, 8470-8482

(147) Chin, J. W., Cropp, T. A., Anderson, J. C., Mukherji, M., Zhang, Z. and Schultz, P. G. (**2003**) An expanded eukaryotic genetic code. *Science. 301*, 964-967

(148) Chin, J. W., Santoro, S. W., Martin, A. B., King, D. S., Wang, L. and Schultz, P. G. (**2002**) Addition of *p*-azido-L-phenylalanine to the genetic code of *Escherichia coli. J. Am. Chem. Soc. 124*, 9026-9027

(149) Farrell, I. S., Toroney, R., Hazen, J. L., Mehl, R. A. and Chin, J. W. (**2005**) Photo-cross-linking interacting proteins with a genetically encoded benzophenone. *Nat. Methods. 2*, 377-384

(150) Chin, J. W., Martin, A. B., King, D. S., Wang, L. and Schultz, P. G. (**2002**) Addition of a photocrosslinking amino acid to the genetic code of *Escherichia coli. Proc. Natl. Acad. Sci. U.S.A. 99*, 11020-11024

(151) Chin, J. W. and Schultz, P. G. (**2002**) *In vivo* photocrosslinking with unnatural amino acid mutagenesis. *ChemBioChem. 3*, 1135-1137

(152) Kauer, J. C., Erickson-Viitanen, S., Wolfe, H. R.,Jr and DeGrado, W. F. (**1986**) *p*-benzoyl-L-phenylalanine, a new photoreactive amino acid. Photolabeling of calmodulin with a synthetic calmodulin-binding peptide. *J. Biol. Chem. 261*, 10695-10700

(153) Schlieker, C., Weibezahn, J., Patzelt, H., Tessarz, P., Strub, C., Zeth, K., Erbse, A., Schneider-Mergener, J., Chin, J. W., Schultz, P. G., Bukau, B. and Mogk, A. (**2004**) Substrate recognition by the AAA+ chaperone ClpB. *Nat. Struct. Mol. Biol. 11*, 607-615

(154) Weibezahn, J., Tessarz, P., Schlieker, C., Zahn, R., Maglica, Z., Lee, S., Zentgraf, H., Weber-Ban, E. U., Dougan, D. A., Tsai, F. T., Mogk, A. and Bukau, B. (**2004**) Thermotolerance requires refolding of aggregated proteins by substrate translocation through the central pore of ClpB. *Cell. 119*, 653-665

(155) Hino, N., Okazaki, Y., Kobayashi, T., Hayashi, A., Sakamoto, K. and Yokoyama, S. (**2005**) Protein photo-cross-linking in mammalian cells by site-specific incorporation of a photoreactive amino acid. *Nat. Methods. 2*, 201-206

(156) Wu, N., Deiters, A., Cropp, T. A., King, D. and Schultz, P. G. (**2004**) A genetically encoded photocaged amino acid. *J. Am. Chem. Soc. 126*, 14306-14307

(157) Deiters, A., Groff, D., Ryu, Y., Xie, J. and Schultz, P. G. (**2006**) A genetically encoded photocaged tyrosine. *Angew. Chem., Int. Ed. 45*, 2728-2731

(158) Wang, J., Xie, J. and Schultz, P. G. (**2006**) A genetically encoded fluorescent amino acid. *J. Am. Chem. Soc. 128*, 8738-8739

(159) Summerer, D., Chen, S., Wu, N., Deiters, A., Chin, J. W. and Schultz, P. G. (**2006**) A genetically encoded fluorescent amino acid. *Proc. Natl. Acad. Sci. U.S.A. 103*, 9785-9789

(160) Tsao, M. L., Summerer, D., Ryu, Y. and Schultz, P. G. (**2006**) The genetic incorporation of a distance probe into proteins in *Escherichia coli. J. Am. Chem. Soc. 128*, 4572-4573

(161) Deiters, A., Geierstanger, B. H. and Schultz, P. G. (**2005**) Site-specific *in vivo* labeling of proteins for NMR studies. *ChemBioChem. 6*, 55-58

(162) Suydam, I. T. and Boxer, S. G. (**2003**) Vibrational stark effects calibrate the sensitivity of vibrational probes for electric fields in proteins. *Biochemistry. 42*, 12050-12055

(163) Xie, J., Wang, L., Wu, N., Brock, A., Spraggon, G. and Schultz, P. G. (**2004**) The site-specific incorporation of *p*-iodo-L-phenylalanine into proteins for structure determination. *Nat. Biotechnol. 22*, 1297-1301

(164) Alfonta, L., Zhang, Z., Uryu, S., Loo, J. A. and Schultz, P. G. (**2003**) Site-specific incorporation of a redox-active amino acid into proteins. *J. Am. Chem. Soc. 125*, 14662-14663

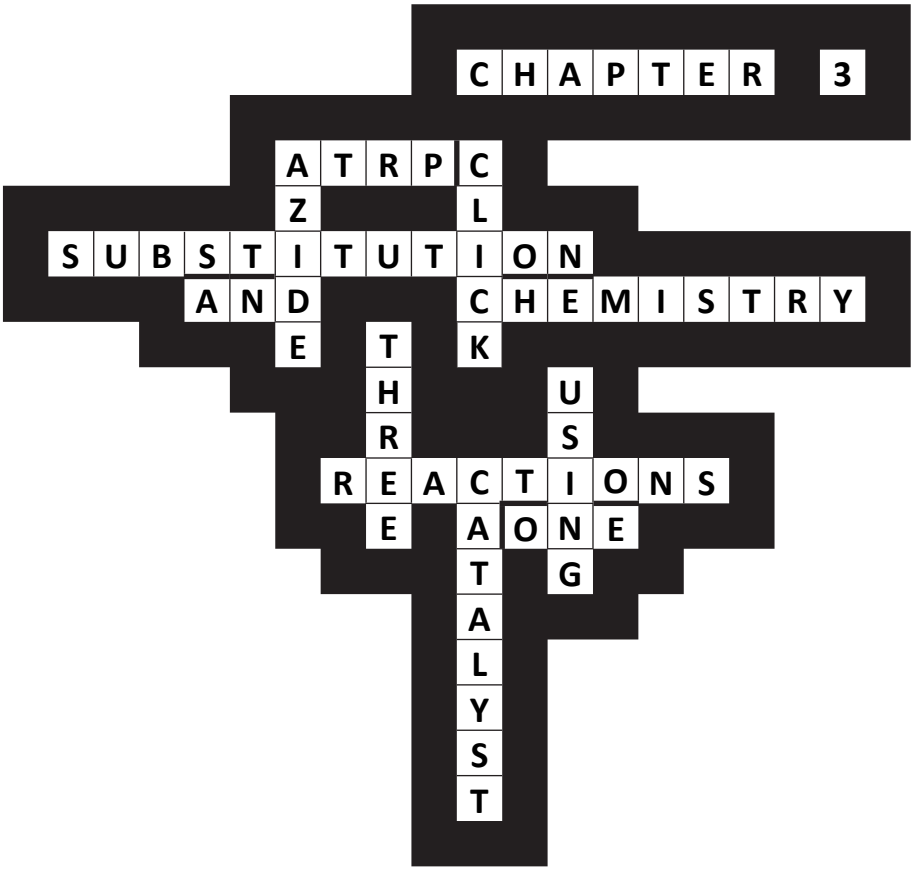

ATRP, subsequent azide substitution and 'click' chemistry:
Three reactions using one catalyst in one pot

Albert J. de Graaf, Enrico Mastrobattista, Cornelus F. van Nostrum,
Dirk T. S. Rijkers, Wim E. Hennink and Tina Vermonden

Chemical Communications, **2011**, *47*, pp. 6972-6974

Copyright 2011, the Royal Society of Chemistry

Abstract

This chapter describes a novel and fast reaction to substitute the living chain end after Atom Transfer Radical Polymerization (ATRP) by an azide functionality. The reaction is catalyzed by the ATRP catalyst at room temperature in aqueous solution and can be followed by a 'click' reaction using again the same catalyst.

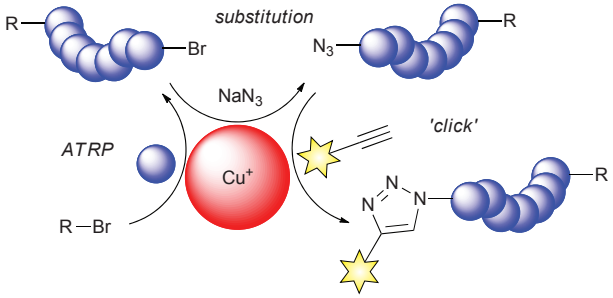

3.1. Introduction

Atom Transfer Radical Polymerization (ATRP) and Copper-catalyzed Azide–Alkyne Cycloaddition (CuAAC) 'click' chemistry have both become established techniques.[1,2] In addition, the combination of these two techniques is becoming increasingly popular.[3] This popularity is in part due to the fact that ATRP and CuAAC can be catalyzed by the same copper complexes.[3b,c,4] Using azide- or alkyne functionalized monomers and/or initiators, CuAAC and ATRP have been performed sequentially and even simultaneously.[3d,e,5] On the other hand, the highly popular approach of 'clicking' to the living ATRP chain end has not been reported in a one-pot procedure, since this approach requires conversion of the living R–Br (or, less commonly, R–Cl) chain end into R–N_3 before a CuAAC reaction can be performed.[6] This azidation is usually carried out by an S_N2 reaction using a large excess of NaN_3 in *N*,*N*-dimethylformamide (DMF) overnight and, in the case of chloride-terminated polymers, requires elevated temperatures.[6b,7]

In this chapter, we present a novel, non-S_N2 reaction for azidation of the living chain end, catalyzed by an ATRP copper catalyst. This method has several advantages over the traditional S_N2 substitution, namely a very short reaction time with only a small excess of NaN_3, compatibility with aqueous solvents and the possibility to perform ATRP, azidation of the living chain end and 'clicking' to it in a one-pot procedure with all three reactions catalyzed by the same catalyst.

3.2. Materials and methods

Macro-initiator **1** (Figure 1) was synthesized from poly(ethylene glycol) monomethyl ether (mPEG) (2 kDa) and 2-bromoisobutyrylbromide. This macro-initiator was used to demonstrate the substitution of bromide by azide, catalyzed by an ATRP catalyst.

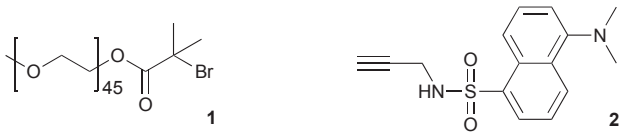

Figure 1. Structures of the ATRP macroinitiator and dansyl-propargylamide

In a typical experiment, **1**, the ATRP catalyst $CuBr/CuBr_2$/bipyridyl(Bpy) (0.6:0.4:2) and NaN_3 (1.2 eq.) were dissolved in CD_3CN/D_2O (3:7). At regular time intervals a sample was taken and diluted with air-saturated D_2O to quench the reaction. Conversion was determined using ^1H NMR by comparing the integrals of the peaks at 1.97 ppm ($–C(CH_3)_2–Br$) and 1.55 ppm ($–C(CH_3)_2–N_3$).[7b,8]

3.3. Results and discussion

Within 20 min, the reaction reached 95% conversion (k = 0.42 L mol^{-1} s^{-1}) (Figure 2 and Figure S1, Supporting Information (SI)). When a two-fold excess of NaN_3 was used, quantitative conversion to the azide was achieved within 5 min. It was shown that the conversion was <5% in 18 h in the absence of any copper species as catalyst (Figure 2), an indication that the substitution reaction is not based on an S_N2-type mechanism. The fast kinetics and mild, aqueous conditions of the copper-catalyzed substitution reaction are a significant improvement compared to the traditional substitution method which uses a large excess (10×) of NaN_3 in DMF overnight. Especially for tertiary halides (like compound **1**, or methacrylate polymers), the traditional S_N2 reaction in DMF requires extended reaction time (and/or high temperature) to reach completion.[7]

We expect the mechanism of the copper-catalyzed azidation to be similar to the process of 'halogen exchange' in ATRP (Scheme 1).[9] During the ATRP process, a copper catalyst homolytically removes a halogen from

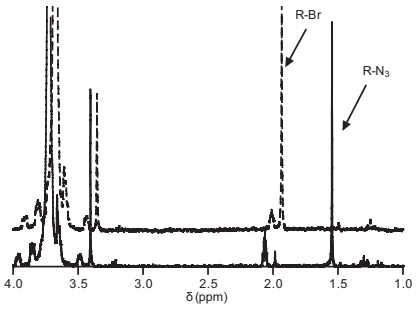

Figure 2. ^1H NMR spectra of the azidation reaction with $CuBr/CuBr_2$/Bpy catalyst after 20 min (bottom) and the control reaction without catalyst after 18 h (top, shifted by 0.05 ppm for clarity). Arrows indicate the $-C(CH_3)_2-X$ peaks.

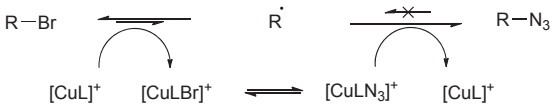

Scheme 1. Proposed reaction sequence of copper-catalyzed substitution of a bromide by an azide. L= ligand.

the living chain end, leaving a radical and allowing chain propagation, and reforms the polymer–halide bond in a dynamic equilibrium. In doing so, the catalyst can exchange different halogen species.[9] The azide ion (commonly called a pseudohalogen)[10] is readily oxidized by copper(I)[11] and thus can also participate in this exchange reaction.

Since ATRP using chloride initiators generally proceeds slower than ATRP using bromide initiators[12] it was expected that the copper-catalyzed substitution of chloride by azide would proceed slower as well. To investigate this, **1** was first incubated with a $CuCl/CuCl_2$/Bpy catalyst to obtain the chloride chain end, as evidenced by a shift of the $–C(CH_3)_2–X$ peak in the ^1H NMR spectrum from 1.97 to 1.83 ppm. Subsequent substitution of this chloride by a two-fold excess of NaN_3 proceeds to only 30% in 2 h (Figure 3). To improve the azidation reaction for chloride chain ends, the effects of increasing the azide concentration, Cu(I)/Cu(II) ratio (by addition of ascorbic acid) and temperature were examined. Figure 3 shows that increasing the temperature from room temperature to 40 °C more than doubles the conversion after 2 h. Furthermore, both increasing the concentration of azide and raising the Cu(I)/Cu(II) ratio (and thereby

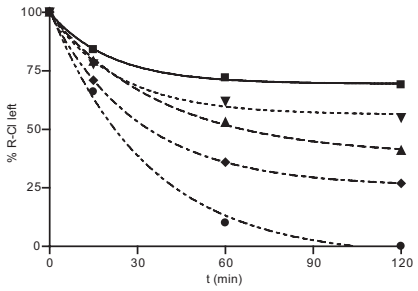

Figure 3. Optimization of chloride chain end substitution by azide: (■) 2 eq. NaN_3, (▼) 10 eq. NaN_3, (▲) 2 eq. NaN_3 + 10 eq. ascorbic acid, (♦) 2 eq. NaN_3 at 40°C, (●) 10 eq. NaN_3 + 10 eq. ascorbic acid at 40°C.

increasing the concentration of radicals) individually increase the reaction rate. These findings indicate that the reaction occurs between a polymer chain radical and an azide-containing species, consistent with Scheme 1.

Increasing the Cu(I)/Cu(II) ratio has two effects, namely an increase in radical concentration but also a decrease in the concentration of the Cu(II)–azide complex. Since the net effect is an increase in the reaction rate, it can be concluded that the radical formation is the rate-limiting step. This is corroborated by the fact that the rate increase by raising just the azide concentration is relatively small (Figure 3).

The combined effect of raising the temperature and adding excess NaN_3 and reducing agent was found effective to drive the reaction to completion within 2 h. This is still a significant improvement compared to the traditional S_N2-substitution of chlorides, which is generally slow and incomplete.[7b]

In the next experiment, the full three reactions in a one pot sequence of ATRP, azide substitution and CuAAC were carried out. Oligo(ethylene glycol) monomethyl ether methacrylate (OEGMA, M_n = 300 g mol^{-1}) was polymerized using **1** under the same conditions as the substitution experiment. At 80% monomer conversion (determined by ^{1}H NMR), 2 mol. equiv. (to chain ends) of NaN_3 was added to the reaction mixture. After 5 min, a peak at 1.57 ppm could clearly be observed by ^{1}H NMR, which corresponds to –C(CH_3)N_3–COOR (Figure S2, SI). Re-activation of the azide-substituted chain end does not occur, since the monomer conversion (determined by ^{1}H NMR) had not increased one hour after addition of azide. After substituting the living chain end with azide, without intermediate work-up, 1 mol. equiv. of the fluorophore dansyl-propargylamide **2** (Figure 1) was added to the reaction mixture and allowed to react overnight at room temperature. Then, the polymer was analyzed by Gel Permeation Chromatography (GPC) with both Refractive Index (RI) and fluorescence detection. The similar shapes of the two GPC traces as presented in Figure 4a clearly show that the pOEGMA polymer has been fluorescently labeled with **2**. From the peak integrals in Figure 4a, the yield of the 'click' reaction was calculated to be 70% (tertiary azides and bipyridyl are known to be the poorest substrates[8] and ligand,[4] respectively, for CuAAC). On the other hand, a control reaction without azide did not result

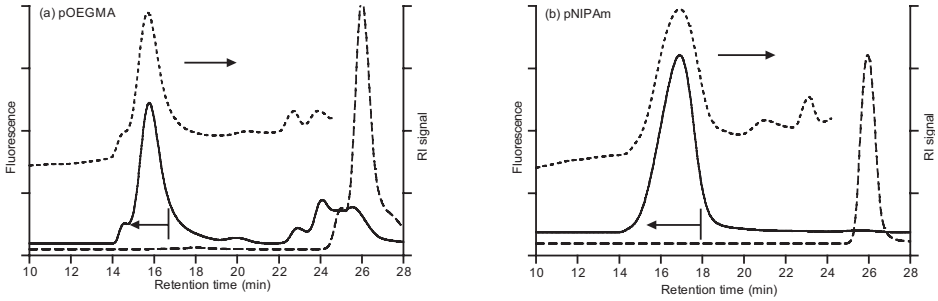

Figure 4. (a) GPC traces of fluorescently labelled pOEGMA (top and middle) and the control reaction to which no azide was added (bottom). (b) GPC traces of fluorescently labelled pNIPAm (top and middle) and the control reaction to which no azide was added (bottom).

in labeling. These findings prove that ATRP, azide substitution and CuAAC can all be catalyzed by the same copper complex, in a three reaction one pot procedure. Furthermore, addition of TEMPO inhibited the substitution by azide (Figure S3, SI), which supports the proposed radical mechanism.

To demonstrate the broad applicability of the procedure, it was also applied to a different monomer/catalyst ligand pair, namely *N*-isopropylacrylamide (NIPAm) and tris[2-(dimethylamino)ethyl]amine (Me_6tren). This combination of the monomer and catalyst resulted in quantitative labeling of the polymer (Figure 4b). We expect that the reaction is generally applicable to any monomer/catalyst pair suitable for ATRP, including hydrophobic monomers in aprotic media (see also Figure S4, SI).

3.4. Conclusion

In conclusion, this study shows that ATRP catalysts can very efficiently and irreversibly substitute a bromide or chloride on a living ATRP chain end by an azide. Furthermore, we have demonstrated for two different monomer/catalyst pairs that this reaction allows ATRP, azide substitution and CuAAC subsequently in a one-pot procedure, with all three reactions catalyzed by the same copper complex. This one-pot procedure greatly simplifies the increasingly popular procedure of 'clicking' a functional unit to a living ATRP chain end. Moreover, the compatibility with aqueous conditions makes this method ideally suitable for end-functionalization of bioconjugated polymers.

Acknowledgement

The authors thank J.C. Slootweg (Medicinal Chemistry & Chemical Biology, Utrecht University) for his kind gift of compound **2**.

References

(1) T. Pintauer and K. Matyjaszewski, *Top. Organomet. Chem.*, **2009**, *26*, 221; T. Pintauer and K. Matyjaszewski, *Chem. Soc. Rev.*, **2008**, *37*, 1087; C. J. Fristrup, K. Jankova and S. Hvilsted, *Soft Matter*, **2009**, *5*, 4623; K. Min and K. Matyjaszewski, *Cent. Eur. J. Chem.*, **2009**, *7*, 657.

(2) M. Meldal and C. W. Tomøe, *Chem. Rev.*, **2008**, *108*, 2952; M. van Dijk, D. T. S. Rijkers, R. M. J. Liskamp, C. F. van Nostrum and W. E. Hennink,. *Bioconjugate Chem.*, **2009**, *20*, 2001; K. Nwe and M. W. Brechbiel, *Cancer Biother. Radiopharm.*, **2009**, *24*, 289.

(3) (a) P. Golas and K. Matyjaszewski, *QSAR Comb. Sci.*, **2007**, *26*, 1116; (b) J. -F. Lutz, H. G. Börner and K. Weichenhan, *Macromol. Rapid Commun.*, **2005**, *26*, 514; (c) J. -F. Lutz, H. G. Börner and K. Weichenhan, *Macromolecules*, **2006**, *39*, 6376; (d) L. Mespouille, M. Vachaudez, F. Suriano, P. Gerbaux, O. Coulembier, P. Degée, R. Flammang and P. Dubois, *Macromol. Rapid Commun.*, **2007**, *28*, 2151; (e) D. Damiron, M. Desorme, R. -V. Ostaci, S. Al Akhrass, T. Hamaide and E. Drockenmuller, *J. Polym. Sci., Part A: Polym. Chem.*, **2009**, *47*, 3803.

(4) P. L. Golas, N. V. Tsarevsky, B. S. Sumerlin and K. Matyjaszewski, *Macromolecules*, **2006**, *39*, 6451.

(5) (a) J. Geng, J. Lindqvist, G. Mantovani and D. M. Haddleton, *Angew. Chem., Int. Ed.*, **2008**, *47*, 4180; (b) L. Q. Xu, F. Yao, G. D. Fu and E. T. Kang, *Biomacromolecules*, **2010**, *11*, 1810; (c) D. Damiron, R. -V. Ostaci, M. Desorme, C. Hawker and E. Drockenmuller, *Polym. Prepr. (Am. Chem. Soc., Div. Polym. Chem.)*, **2008**, *49*, 236; (d) B. Grignard, C. Calberg, C. Jerome and C. Detrembleur, *J. Supercrit. Fluids*, **2010**, *53*, 151; (e) P. D. Topham, N. Sandon, E. S. Read, J. Madsen, A. J. Ryan and S. P. Armes, *Macromolecules*, **2008**, *41*, 9542; (f) Y. Zhang, C. Li and S. Liu, *J. Polym. Sci., Part A: Polym. Chem.*, **2009**, *47*, 3066.

(6) (a) Y. -Q. Dong, Y. -Y. Tong, B. -T. Dong, F. -S. Du and Z. -C. Li, *Macromolecules*, **2009**, *42*, 2940; (b) K. Matyjaszewski, Y. Nakagawa and S. G. Gaynor, *Macromol. Rapid Commun.*, **1997**, *18*, 1057; (c) A. Hasneen, H. S. Han and H. -J. Paik, *React. Funct. Polym.*, **2009**, *69*, 681; (d) S. S. Okcu, Y. Y. Durmaz and Y. Yagci, *Des. Monomers Polym.*, **2010**, *13*, 459; (e) Y. Wang, J. Chen, J. Xiang, H. Li, Y. Shen, X. Gao and Y. Liang, *React. Funct. Polym.*, **2009**, *69*, 393; (f) J. Xu, J. Ye and S. Liu, *Macromolecules*, **2007**, **40**, 9103.

(7) (a) F. G. Bordwell and W. T. Brannen, *J. Am. Chem. Soc.*, **1964**, *86*, 4645; (b) V. Coessens and K. Matyjaszewski, *J. Macromol. Sci., Part A: Pure Appl.Chem.*, **1999**, *36*, 667.

(8) P. L. Golas, N. V. Tsarevsky and K. Matyjaszewski, *Macromol. Rapid Commun.*, **2008**, *29*, 1167.

(9) K. Matyjaszewski, D. A. Shipp, J. Wang, T. Grimaud and T. E. Patten, *Macromolecules*, **1998**, *31*, 6836.

(10) L. Birckenbach and K. Kellermann, *Ber. Dtsch. Chem. Ges. B*, **1925**, *58*, 786.

(11) B. L. Evans, *Proc. R. Soc. London, Ser. A*, **1958**, *246*, 199.

(12) (a) W. Tang, Y. Kwak, W. Braunecker, N. V. Tsarevsky, M. L. Coote and K. Matyjaszewski, *J. Am. Chem. Soc.*, **2008**, *130*, 10702; (b) W. Tang and K. Matyjaszewski, *Macromolecules*, **2007**, *40*, 1858.

3.5. Supporting information

3.5.1. Materials and Methods

Tetrahydrofuran (THF), dichloromethane, *n*-hexane, diethyl ether and *N*,*N*-dimethylformamide (DMF) were obtained from Biosolve (Valkenswaard, the Netherlands), triethylamine, acetic acid and polyethylene glycol monomethylether (mPEG, M_n = 2 kDa) were obtained from Merck (Darmstadt, Germany), toluene, CuBr and $CuBr_2$ from Acros (Geel, Belgium) and CuCl from Alfa-Aesar (Karlsruhe, Germany). $CuCl_2 \cdot 2H_2O$, 2,2'-bipyridyl (Bpy), tris(2-aminoethyl)amine, *N*,*N*,*N*',*N*",*N*"-pentamethyldiethylenetriamine (PMDETA), 2-bromoisobutyrylbromide, (1-bromoethyl)benzene, oligo(ethylene glycol) monomethyl ether methacrylate (OEGMA M_n = 300 g mol^{-1}), *N*-Isopropylacrylamide (NIPAm), NaN_3, tetrabutylammonium azide, LiCl, ascorbic acid, D_2O and CD_3CN were purchased from Sigma-Aldrich (Zwijndrecht, the Netherlands). mPEG was dried by azeotropically distilling off water using toluene. NIPAm was recrystallized twice from a mixture of n-hexane and toluene. CuBr was purified by stirring overnight in glacial acetic acid. Anisole and OEGMA were passed over a short column of basic alumina. All other chemicals were used as received. Tris[2-(dimethylamino) ethyl]amine (Me_6tren) was synthesized by Eschweiler-Clarke methylation of tris(2-aminoethyl)amine[S1] and purified by distillation under reduced pressure.

^{1}H Nuclear Magnetic Resonance (NMR) spectrometry was performed on a Gemini 300 MHz spectrometer (Varian Associates Inc., Palo Alto, CA). Chemical shift values are reported in ppm, taking the residual solvent peak as reference (δ(CHCl3) = 7.24, δ(HOD) = 4.79). Gel Permeation Chromatography (GPC) was performed on a Waters 2695 system equipped with a Refractive Index detector and Fluorescence detector, using 2 PLgel 3 μm Mixed-D columns (Polymer Laboratories). As eluent, 10 mM LiCl in DMF was used at 0.7 mL/min and 40 °C. The excitation and emission wavelengths were set to 330 and 560 nm, respectively.

3.5.2. Synthesis of macro-initiator 1

Anhydrous mPEG (5 g, 2.5 mmol) was dissolved in dry THF (100 mL) under a nitrogen atmosphere and the solution was cooled on ice. Then, triethylamine (0.37 mL, 2.7 mmol, 1.1 eq) was added followed by

2-bromoisobutyrylbromide (0.33 mL, 2.7 mmol, 1.1 eq). After stirring the reaction mixture overnight, the formed triethylammonium bromide was removed by filtration. The filtrate was concentrated at reduced pressure and the residue was redissolved in a minimal amount of dichloromethane. The product was then isolated by precipitation with ice-cold diethylether. The yield was ~80%. ^{1}H NMR ($CDCl_3$): δ 4.3 (t, 2H, OCH_2), δ 3.85 (t, 2H, OCH_2), δ 3.65 (OCH_2), δ 3.35 (t, 2H, OCH_2), δ 3.30 (s, 3H, OCH_3), δ 1.85 (s, 6H, CCH_3).

3.5.3. Typical procedure for copper-catalyzed azide substitution

A stock solution of catalyst was freshly prepared by placing 8.6 mg (60 μmol) CuBr, 8.9 mg (40 μmol) $CuBr_2$ and 31.2 mg (200 μmol) Bpy in a screw-capped septum vial which was then purged for 15 min with N_2 gas. Subsequently, 300 μL of N_2-purged acetonitrile-d_3 and 700 μl N_2-purged D_2O were added using a gas-tight syringe. Formation of the brown catalytic complex was aided by sonication.

20 mg of **1** (10 μmol) was placed in a screw-capped septum vial containing a magnetic stirrer bar, which was then purged for 15 min with N_2 gas. Subsequently, 300 μL of N_2-purged CD_3CN and 700 μL N_2-purged D_2O were added and the mixture was stirred until all initiator was dissolved. The reaction was started by addition of 100 μL of the catalyst stock solution followed by slow addition of 12 μL of an N_2-purged 1 M solution of NaN_3 in D_2O. At regular time intervals a 20 μL sample was taken and diluted

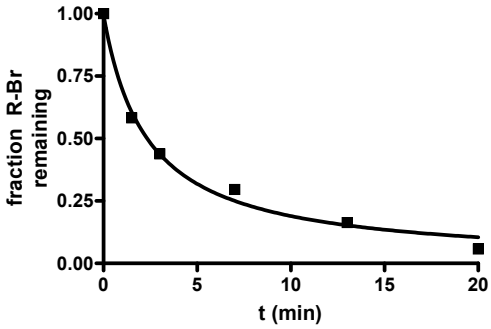

Figure S1. Plot of the bromide to azide conversion in time. **1** was incubated with 1.2 eq. NaN_3 and CuBr/$CuBr_2$/Bpy catalyst

with 700 μL of air-saturated D_2O to quench the reaction. Conversion was determined using ^1H NMR by comparing the integrals of the peaks at 1.97 ppm (-$C(CH_3)_2$-Br and 1.55 ppm (-$C(CH_3)_2$-N_3 (Figure S1).

Assuming that the reaction is first-order in both [R-Br] and [N3-], the rate constant could be calculated as 0.42 L mol^{-1} s^{-1}.

3.5.4. ATRP, azidation and fluorescent labeling of p($OEGMA_{300}$)

20 mg of **1** (10 μmol) was placed in a screw-capped septum vial containing a magnetic stirrer bar, which was then purged for 15 min with N_2 gas. Subsequently, 300 μL of N_2-purged CD_3CN, 700 μL N_2-purged D_2O and 200 μL $OEGMA_{300}$ were added and the mixture was stirred until all initiator was dissolved. The reaction was started by addition of 100 μL of the same catalyst stock as described above. Conversion was monitored by regularly taking 20 μL samples, which were diluted with 700 μL of air-saturated D_2O and analyzed using ^1H NMR. The integrals of the H_2C=C peaks between 5.5 and 6.5 ppm (2H) were compared with the integrals of the C(=O)OCH_2 peaks (2H) between 4.0 and 4.5 ppm. At 80% conversion (approx. 20 min), 20 μL 1M NaN_3 solution was slowly added. After 5 minutes, the peak at 1.57 ppm of -$C(CH_3)N_3$-COOR (2.6 H, 85% conversion) could clearly be observed in ^1H NMR (Figure S2). The monomer conversion was determined again 1 h after addition of azide. It was found that the monomer conversion had not increased further indicating that re-activation of the azide-substituted chain end is negligible. Then, an equimolar amount of dansyl-propargylamide **2** was added and allowed to react overnight at room temperature.

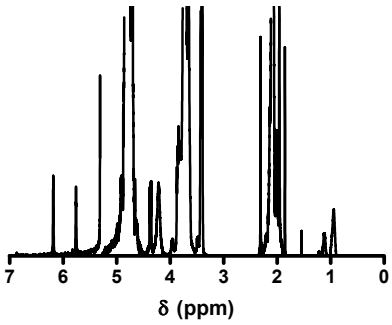

Figure S2. NMR spectrum of PEG-pOEGMA-N_3. Arrow indicates the -$C(CH_3)_2$-N_3 peak

In one control reaction, the same procedure was followed except that the addition of sodium azide was omitted. In another control reaction, 2 molar equivalents of TEMPO were added together with the addition of sodium azide. Termination was evident from fading of the brown color of the copper(I)-bipyridyl complex. An extra 100 μL of catalyst stock was added to compensate for the loss of copper(I) species, which would preclude any CuAAC 'click' reaction, before again an equimolar amount of dansyl-propargylamide was added. The next day, the reaction mixture was analyzed by GPC with fluorescence detection (Figure S3). TEMPO was able to almost completely inhibit the substitution by azide, which lends further support to the proposed radical mechanism of azide substitution.

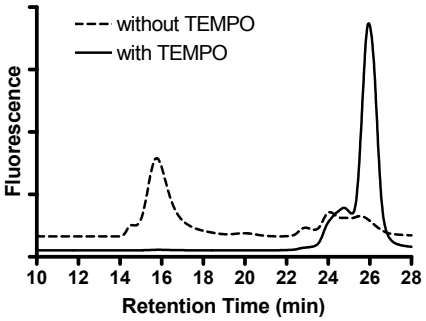

Figure S3. GPC traces of fluorescently labeled pOEGMA (dashed line) and the control reaction to which TEMPO had been added (continuous line).

3.5.5. ATRP, azidation and fluorescent labeling of pNIPAm

The procedure was very similar to the procedure for ATRP of $OEGMA_{300}$. However, Me_6tren (1:1 molar equivalent to total copper) was used instead of Bpy and the polymerization was performed in an ice bath. 160 mg of NIPAm (target M_n=16 kDa) was used and monomer conversion was determined by comparing, in the NMR spectrum, the total vinylic proton peak integral (5.4 - 6.3 ppm, 3H) to the total isopropyl methyne proton peak integral (3.6 - 3.85 ppm, 1H). After 15 min, ^{1}H NMR indicated 90% monomer conversion and 2 mol eq. NaN_3 was added. After an additional 20 minutes of stirring, a $–CHN_3$-CONHR peak could not be observed in ^{1}H NMR due to peak overlap, but the

monomer conversion had not increased, which indicated substitution of the bromide by azide which could not re-initiate. Again, dansyl-propargylamide 2 was added and allowed to react overnight at room temperature.

3.5.6. Substitution by azide in aprotic medium

In a preliminary experiment, the copper-catalyzed azide substitution reaction was also applied to (1-bromoethyl)benzene in anisole, as a model for the living chain end of polystyrene. 2.8 mg (0.02 mmol) of CuBr was placed in a screw-capped septum vial which was then purged for 15 min. with N_2. Subsequently, 800 μL of N_2 purged anisole and 2.7 μL (0.02 mmol) of (1-bromoethyl)benzene were added. A sample was taken, diluted in $CDCl_3$ and analyzed by ^{1}H NMR (Figure S4). Then, a solution of 11.4 mg (0.04 mmol) of tetrabutylammonium azide and 4.2 μL (0.02 mmol) of PMDETA in 200 μL N_2 purged anisole were added. The vial was put in an oil bath thermostated at 100 °C and after 15 min another sample was analyzed by ^{1}H NMR (Figure S4).

The disappearance of the peaks at 5.2 ppm and 2.0 ppm, characteristic of (1-bromoethyl)benzene, and the appearance of a peak at 4.6 ppm, characteristic of (1-azidoethyl)benzene,[S2] indicate that the procedure might be applicable to hydrophobic monomers in aprotic solvents as well.

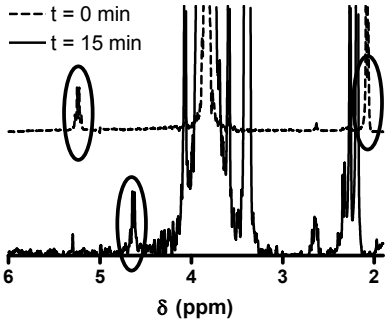

Figure S4. NMR spectra before (top) and after (bottom) azide substitution of (1-bromoethyl) benzene in anisole.

References for Supporting Information

(S1) M. Ciampolini and N. Nardi, *Inorg. Chem.*, **1966**, *5*, 41

(S2) P. L. Golas, N. V. Tsarevsky and K. Matyjaszewski, *Macromol. Rapid Commun.*, **2008**, *29*, 1167.

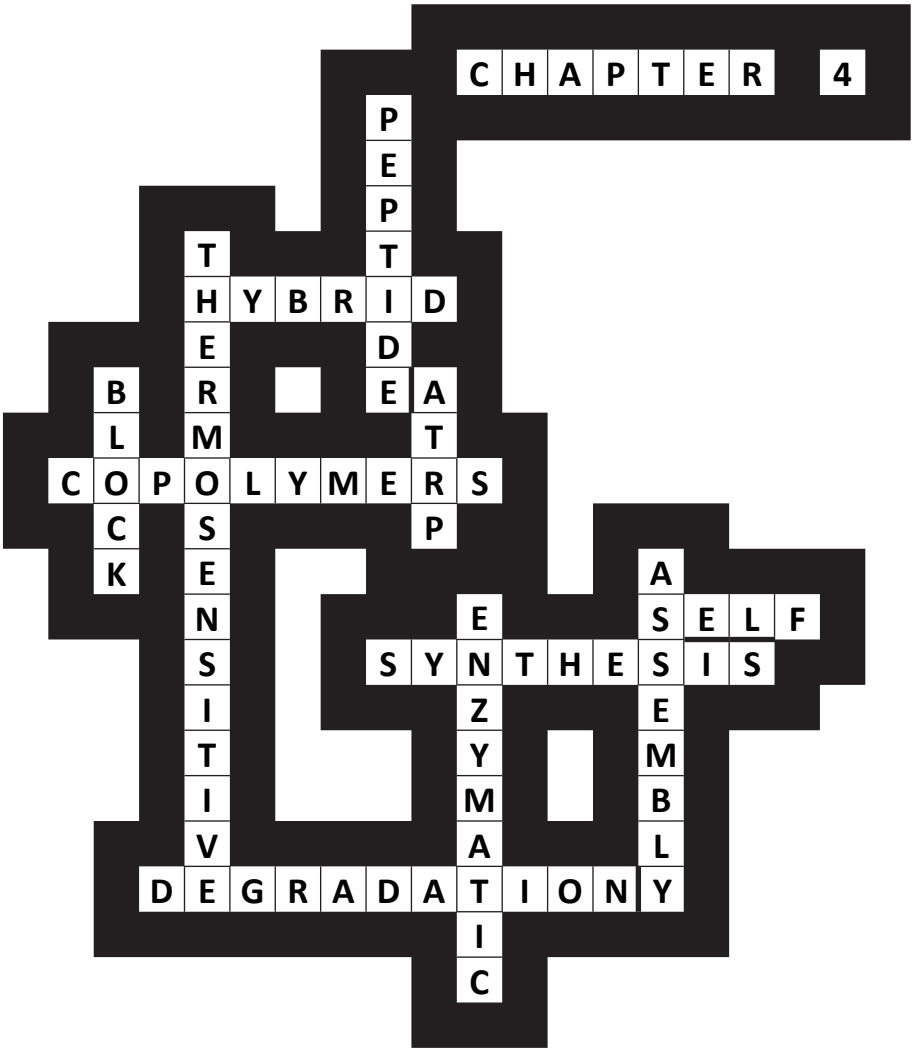

Thermosensitive peptide-hybrid ABC block copolymers obtained by ATRP: Synthesis, self-assembly, and enzymatic degradation

Albert J. de Graaf, Enrico Mastrobattista, Tina Vermonden, Cornelus F. van Nostrum,Dirk T. S. Rijkers, Rob M. J. Liskamp and Wim E. Hennink, *Macromolecules* **2012**, *45*, pp. 842-851

Copyright 2012, the American Chemical Society

Abstract

Peptide-hybrid ABC block copolymers were synthesized by growing two different polymer chains from a native peptide using atom transfer radical polymerization (ATRP). To this end, two different ATRP initiators were coupled via orthogonal methods to the N- and C-terminus of the peptide Ser-Gly-Pro-Gln-Gly-Ile-Phe-Gly-Gln-Met-Gly, a substrate for matrix metalloproteases 2 and 9. First, a hydrophilic block of poly(oligo(ethylene glycol) methyl ether methacrylate) (pOEGMA) was polymerized from the peptide's C-terminus. Before polymerization of the second block, the first living chain end was inactivated by substitution of its Cl-terminus with azide under mild conditions. Then, a thermosensitive block of poly(*N*-isopropylacrylamide) (pNIPAm) was polymerized from the peptide's N-terminus. Well-defined polymers were obtained with good control over both block sizes. The resulting polymers self-assembled into micelles above the cloud point of the pNIPAm block. As anticipated, it was shown that the peptide linkage between the polymer blocks can be cut by a metalloprotease, leading to "shedding" of the corona of the micelles which makes these systems potentially suitable for enzyme-triggered drug delivery.

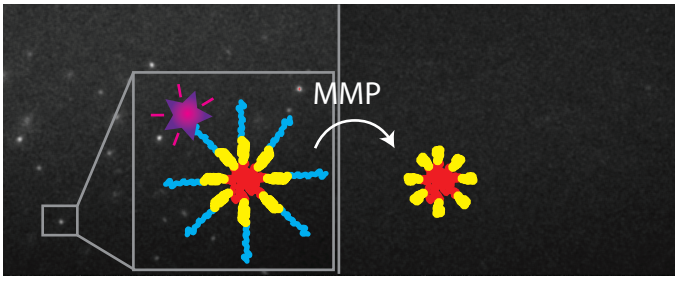

4.1. Introduction

The field of biohybrid materials (materials that consist of synthetic materials together with biomolecules or even entire cells) has been rapidly expanding over the past decade. This is due to the promises it holds for pharmaceutical, medical, and bio- and nanotechnological applications.[1, 2] Among others, biohybrid materials are under investigation for use in targeted drug delivery and for the controlled release of therapeutic (bio)molecules. For example, biohybrid hydrogels can be used as depot formulations of drugs or as scaffolds for tissue engineering, whereas biohybrid micelles and vesicles are under investigation for targeted drug delivery to inflamed tissue, *e.g.*, in cancer and rheumatoid arthritis.[3-8] In these materials, the "bio" part may *e.g.* be a peptide containing a cell adhesion site or an enzymatic cleavage site or a pH-, redox-, or temperature-responsive peptide.[4-6]

A number of techniques are presently available for the design of such peptide-hybrid polymers, including coupling a peptide to a premade polymer (the "grafting to" approach),[9, 10] polymerizing a peptide-functionalized monomer (the "grafting through" approach),[11,12] or performing a polymerization using a peptide macroinitiator (the "grafting from" approach).[13, 14]

The advent of several controlled, "living" radical polymerization techniques has greatly expanded the scope of these "grafting" techniques. Techniques such as atom transfer radical polymerization (ATRP),[15-17] reversible addition–fragmentation chain transfer (RAFT) polymerization,[18-20] and nitroxide-mediated polymerization (NMP)[21-23] allow for the synthesis of low-dispersity polymers with defined, reactive chain-ends.[24] A variety of monomers can be polymerized using these techniques, often under mild conditions. Furthermore, living radical polymerizations are compatible with many functional groups. Together, these properties render living radical polymerizations suitable for use in "grafting from" and "grafting through" strategies.[25]

In the present work we aimed at incorporating a peptide into semisynthetic amphiphilic triblock copolymers, such that the peptide is positioned between a hydrophilic and a thermosensitive block. For the hydrophilic block of the final block copolymer, oligo(ethylene glycol) methyl ether methacrylate (OEGMA, M_n = 300 Da) was chosen as

monomer. The thermosensitive block was prepared by polymerization of *N*-isopropylacrylamide (NIPAm). In aqueous solutions, these polymers likely self-assemble into micellar structures above the cloud point (CP) of the thermosensitive block as demonstrated for other thermosensitive block copolymers.[26, 27] The peptide, Ser-Gly-Pro-Gln-Gly-Ile-Phe-Gly-Gln-Met-Gly, was designed to be functionalizable by specific chemistries on both its N- and C-terminus. Furthermore, this peptide is cleavable at the Gly–Ile bond by matrix metalloproteinases (MMPs) 2 and 9,[28] which are upregulated in inflamed tissues such as in cancer and rheumatoid arthritis.[29-31] Micelles, formed by self-assembly of these amphiphilic block copolymers above the CP of the pNIPAM block, can be loaded with a drug and be administered intravenously. Because of the enhanced permeability and retention (EPR) effect, they will accumulate in the inflamed target tissue,[32] where the hydrophilic stealth corona will subsequently be selectively shed off by action of the MMPs. The exposed micellar cores may then be taken up by the target cells or aggregate and release their payload over time.[33]

In order to generate these thermosensitive block copolymers with a peptide connecting the hydrophilic and thermosensitive polymer blocks, in the present paper, two sequential polymerizations, each initiating on the other terminus of the same peptide, were carried out. Thereby, full benefit is taken from the advantages of the "grafting from" approach, mainly the high coupling efficiency and easy work-up. To the best of our knowledge, this is the first report of two sequential "grafting from" polymerizations, initiated from the C- and N-terminus of a peptide. Furthermore, we use the same polymerization technique, ATRP, for both blocks. At present, sequential "grafting from" has only been performed using a nonpeptide initiator carrying two initiating moieties each for a different polymerization chemistry.[34, 35] It is shown that well-defined amphiphilic polymers can indeed be synthesized in this way. These polymers self-assemble into micelles, having a corona which can be shed off by action of a metalloprotease.

4.2. Experimental part

4.2.1. Chemicals

All solvents were obtained from Biosolve (Valkenswaard, The Netherlands). Unless otherwise noted, the chemicals were obtained from Sigma-Aldrich (Steinheim, Germany) and were used as received. Prior to use, *N*,*N*-dimethylacetamide (DMA) was dried on calcium hydride, distilled under reduced pressure, and stored over 4 Å molecular sieves. Triethylamine was dried on potassium hydroxide, distilled, and stored on 3 Å molecular sieves. Oligo(ethylene glycol) methyl ether methacrylate with average M_n of 300 Da ($OEGMA_{300}$) was passed over a column of basic alumina immediately prior to use. Tris[2-(dimethylamino)ethyl]amine (Me_6TREN) was prepared and purified according to a literature procedure.[36]

4.2.2. Analytical methods

HPLC was performed on a Waters 2695 system equipped with a dual wavelength UV absorption detector set to 210 and 254 nm. An Alltech ProSphere C18 column was used at 25 °C, employing a gradient of CH_3CN/H_2O/TFA 5/95/0.1 to 60/40/0.1 in 1 h. Unless noted otherwise, gel permation chromatography (GPC) was performed on a Waters 2695 system equipped with a differential refractive index detector using a MixedD column (Polymer laboratories). The column temperature was 40 °C, 10 mM LiCl in DMF was used as the eluent at a flow rate of 1 mL/min, and linear PEG standards were used for calibration. Samples were allowed to dissolve for at least 16 h prior to analysis.

NMR spectra were recorded on a Varian Mercury spectrometer operating at 300 MHz (^1H) or 75.5 MHz (^{13}C), and ESI-MS spectra were recorded on a Shimadzu QP8000 mass spectrometer. MALDI-TOF MS was performed on a Kratos Axima CFR apparatus using ACTH as external standard and α-cyano-4-hydroxycinnamic acid as matrix.

4.2.3. Synthesis of 2-(2-aminoethoxy)ethyl-2-bromoisobutyrate hydrobromide (linker 1)

The synthesis of linker **1** is shown in Scheme 1. In a round-bottom flask, 2-(2-aminoethoxy)ethanol (11.0 mL, 110 mmol) and di-tert-butyl dicarbonate (21.8 g, 100 mmol) were dissolved in CH_2Cl_2 (100 mL). The resulting mixture was stirred 16 h at room temperature. Then, the mixture was washed three times with 1 M $NaHSO_4$, three times with saturated $NaHCO_3$, and once with saturated NaCl. After drying on anhydrous $MgSO_4$, the CH_2Cl_2 layer was evaporated *in vacuo*, giving 2-(*N*-Boc-2-aminoethoxy)ethanol as a colorless oil in 78% yield (15.9 g, 78 mmol). ^{1}H NMR (300 MHz, $CDCl_3$): δ 5.28 (bs, 1H), 3.66 (t,2H), 3.50 (t, 2H), 3.48 (t, 2H), 3.25 (m, 2H), 3.10 (bs, 1H), 1.37 (s, 9H). ^{13}C NMR (75.5 MHz, $CDCl_3$): δ 156.3 (C=O), 79.4 ($\underline{C}(CH_3)_3$), 72.3 (CH_2), 70.3 (CH_2), 61.5 (CH_2), 40.4 (CH_2), 28.4 (CH_3).

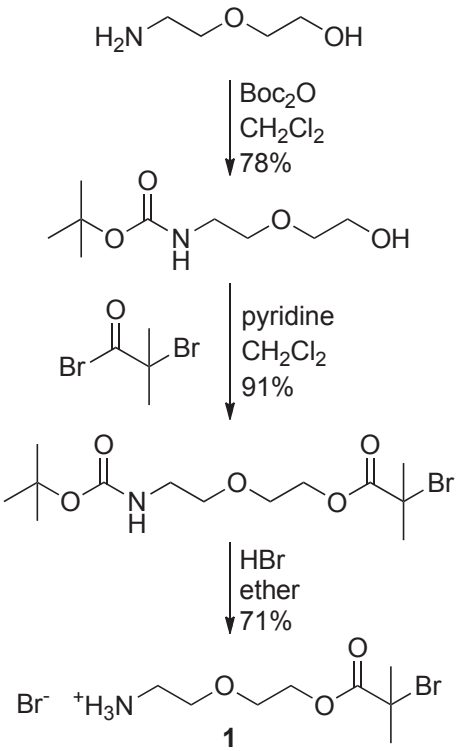

Scheme 1. Synthesis route of 2-(2-aminoethoxy)ethyl-2-bromoisobutyrate hydrobromide (linker **1**)

In the next reaction step, 2-(*N*-Boc-2-aminoethoxy)ethanol (14.3 g, 70 mmol) and pyridine (6.2 mL, 77 mmol) were dissolved in anhydrous CH_2Cl_2 (100 mL), and the solution was cooled on an ice bath. To this solution, 2-bromoisobutyryl bromide (9.5 mL, 77 mmol) was added dropwise while stirring. After addition, the mixture was allowed to reach room temperature and stirred for 30 min. The precipitated pyridinium bromide was filtered off. The filtrate was washed three times with 1 M $NaHSO_4$, three times with saturated $NaHCO_3$, and one time with saturated NaCl. After drying on anhydrous $MgSO_4$, the CH_2Cl_2 layer was evaporated *in vacuo*, giving 2-(*N*-Boc-2-aminoethoxy)ethyl-2-bromoisobutyrate in 91% yield (24.4 g, 69 mmol).The product was a colorless oil which slowly crystallized upon standing. ^{1}H NMR (300 MHz, $CDCl_3$): δ 4.93 (bs, 1H), 4.30 (t, 2H), 3.68 (t, 2H), 3.53 (t, 2H), 3.28 (m, 2H), 1.92 (s, 6H), 1.41 (s, 9H). ^{13}C NMR (75.5 MHz, $CDCl_3$): δ 171.8 (C=O), 156.1 (C=O), 79.4 ($\underline{C}(CH_3)_3$), 70.3 (CH_2), 68.6 (CH_2), 65.0 (CH_2), 55.7 (C–Br), 40.4 (CH_2), 30.9 ($C(\underline{C}H_3)_2$), 28.5 ($C(\underline{C}H_3)_3$).

In the last reaction step, 2-(*N*-Boc-2-aminoethoxy)ethyl-2-bromoisobutyrate (24 g, 68 mmol) was dissolved in diethyl ether (200 mL), and HBr (28 mL of a 33% solution in acetic acid) was added dropwise, after which the product precipitated out of solution. The reaction was left at room temperature for 16 h. The resulting white crystals of 2-(2-aminoethoxy)ethyl-2-bromoisobutyrate (**1**) were harvested by filtration, washed three times with a small volume of diethyl ether, and dried in a vacuum. Yield: 16.1 g (48 mmol, 71%). ^{1}H NMR (300 MHz, $CDCl_3$): δ 7.93 (bs, 3H), 4.39 (t, 2H), 3.89 (t, 2H), 3.81 (t, 2H), 3.32 (m, 2H), 1.94 (s, 6H). ^{13}C NMR (75.5 MHz, $CDCl_3$): δ 171.9 (C=O), 69.0 (CH_2), 66.5 (CH_2), 65.1 (CH_2), 56.0 (C–Br), 40.0 (CH_2), 30.9 ($C(\underline{C}H_3)_2$). ESI-MS: calcd for $C_8H_{17}NO_3Br$ $[M]^+$ 254.04; found 254.25.

4.2.4. Synthesis of N-(3-aminooxypropyl)-2-bromo-2-methylpropionylamide hydrochloride (linker 2)

The synthesis of linker **2** is shown in Scheme 2. In a round-bottom flask, *N*-3-bromopropylphthalimide (24.5 g, 91 mmol) and *N*-Boc-hydroxylamine (13.3 g, 100 mmol) were dissolved in toluene (100 mL). The solution was boiled under reflux, and 1,8-diazabicyclo[5.4.0]undec-7-ene (DBU) (15 mL,

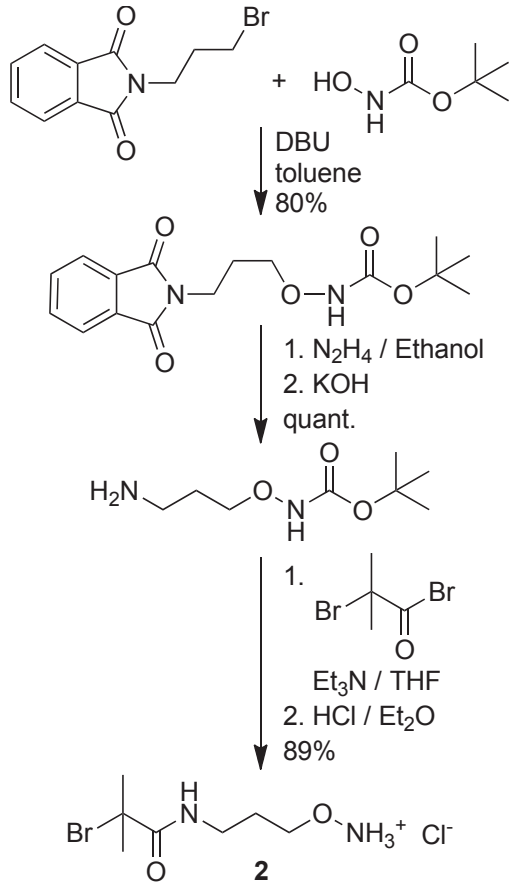

Scheme 2. Synthesis route of N-(3-aminooxypropyl)-2-bromo-2-methylpropionylamide hydrochloride (linker **2)**

100 mmol) was added dropwise. During the addition of DBU the desired product separated as a yellow oil. After stirring for 1 h, the mixture was concentrated *in vacuo*. The residue was redissolved in CH_2Cl_2 (200 mL) and washed with 10% citric acid (4 × 50 mL).[37] The organic phase was dried over MgSO4 and concentrated *in vacuo* to give *N*-(3-(*N*-Boc-aminooxy)propyl) phthalimide as a pale yellow solid in 80% yield (23.5 g, 73 mmol). ^{1}H NMR (300 MHz, $CDCl_3$): δ 7.85 (t, 2H), 7.72 (t, 2H), 7.35 (s, 1H), 3.94 (t, 2H), 3.84 (t, 2H), 2.02 (m, 2H), 1.48 (s, 9H). ^{13}C NMR (75.5 MHz, $CDCl_3$): δ 168.5 (imide C=O), 157.0 (urethane C=O), 134.1 (CH), 132.2 (C), 123.3 (CH), 81.8 ($\underline{C}(CH_3)_3$), 74.0 (CH_2), 35.1 (CH_2), 28.3 ($C(\underline{C}H_3)_3$), 27.3 (CH_2).

In the next step, *N*-(3-(*N*-Boc-aminooxy)propyl)phthalimide (13 g, 40 mmol) was dissolved in absolute ethanol (50 mL). Hydrazine hydrate (3 mL of an 85% aqueous solution) was added dropwise, and the mixture was boiled under reflux for 2 h. The product separated as its salt with phthalylhydrazide, from which it was liberated by adding KOH (2.5 g dissolved in 20 mL of absolute ethanol). After stirring vigorously for 1 h, the precipitate had turned into a fine white powder, the potassium salt of phthalylhydrazide. The mixture was concentrated *in vacuo*, resuspended in anhydrous $CHCl_3$ (100 mL) under vigorous stirring for 1 h, and filtered. The solids were washed three times with a small amount of $CHCl_3$. The combined filtrates were dried on $MgSO_4$ and concentrated *in vacuo* to give 3-(*N*-Boc-aminooxy)propyl)amine as an oil in quantitative yield (8 g, 40 mmol). ^{1}H NMR (300 MHz, $CDCl_3$): δ 3.93 (t, 2H), 3.84 (t, 2H), 1.96 (bs, 2H), 1.75 (m, 2H), 1.46 (s, 9H). ^{13}C NMR (75.5 MHz, $CDCl_3$): δ 157.5 (C=O), 82.0 ($\underline{C}(CH_3)_3$), 75.0 (CH_2), 39.1 (CH_2), 29.4 (CH_2), 28.4 ($C(\underline{C}H_3)_3$). ESI-MS: calcd for $C_8H_{19}N_2O_3$ $[M + H]^+$: 191.14; found 190.90.

Subsequently, 3-(*N*-Boc-aminooxy)propyl)amine (6.9 g, 36 mmol) and triethylamine (7.5 mL, 54 mmol) were dissolved in anhydrous THF (70 mL). The mixture was purged with N_2 and cooled on an ice bath, after which 2-bromoisobutyryl bromide (6.7 mL, 54 mmol) was added dropwise while stirring. Next, the ice bath was removed, and the mixture was stirred for 1 h at room temperature. The precipitated triethylammonium bromide was filtered off, and the filtrate was concentrated *in vacuo*. The residue was redissolved in EtOAc (300 mL), and this solution was washed with 1 M $NaHSO_4$ (3 × 50 mL), 1 M $NaHCO_3$ (3 × 50 mL), and saturated NaCl (2 × 50 mL). The organic layer was dried on $MgSO_4$ and concentrated *in vacuo* to give *N*-(3-(N′-Boc-aminooxy)propyl)-2-bromo-2-methylpropionylamide as a yellow oil. A fraction (8 g) of this oil was dissolved in Et_2O (25 mL), and the solution was cooled on ice. HCl gas was bubbled through the solution, upon which a white precipitate of *N*-(3-aminooxypropyl)-2-bromo-2-methylpropionylamide hydrochloride (**2**) was formed. The product was purified twice by trituration with CH_2Cl_2 and Et_2O at –20 °C. Yield: 4.4 g (16 mmol, 89% over two steps). ^{1}H NMR (300 MHz, DMSO-d_6): δ 10.92 (bs, 3H), 8.18 (t, 1H), 4.01 (t, 2H), 3.17

(q, 2H), 1.87 (s, 6H), 1.75 (m, 2H). ^{13}C NMR (75.5 MHz, DMSO-d_6): δ 170.8 (C=O), 72.0 (CH_2), 60.7 (C–Br), 35.9 (CH_2), 31.1 (C($\underline{C}H_3$)$_2$), 27.2 (CH_2). ESI-MS: calcd for $C_7H_{16}N_2O_2Br$ ([M]$^+$): 239.04; found 238.95.

4.2.5. Peptide synthesis

The peptide H-Ser-Gly-Pro-Gln-Gly-Ile-Phe-Gly-Gln-Met-Gly-NH_2 was synthesized by standard Fmoc solid phase peptide synthesis.[38] 350 mg of peptide (TFA salt, 0.30 mmol) was obtained, with a purity of >95% (HPLC). MALDI-TOF MS: calcd 1077.23 ([M + H]$^+$); found 1077.21. The product was used without further purification.

4.2.6. Functionalization of peptide C-terminus

To introduce a homoserine lactone functionality at the C-terminus (Scheme 3),[39-41] the peptide **3** (343 mg) was dissolved in 150 mL of N_2-flushed CH_3CN/H_2O/TFA (30/70/1). Under a nitrogen atmosphere, CNBr (12 mL of a 4 M solution in CH_3CN) was added, and the reaction mixture was stirred for 16 h in the dark. The mixture was evaporated to dryness *in vacuo* at 28 °C. The lactone-functionalized peptide **4** was then redissolved in CH_3CN/H_2O/TFA (30/70/0.1) and lyophilized. The yield after lyophilization was 383 mg. ESI-MS: calcd 973.47 ([M + H]$^+$); found 973.47.

Linker **1** (3.0 g, 0.9 mmol) was dissolved in CH_2Cl_2 (50 mL) and converted into the free amine by shaking with an equimolar amount of aqueous NaOH (9.0 mL, 1.0 M). The organic layer was dried on $MgSO_4$, followed by evaporation of the volatiles. Directly afterward, 1.2 mL of the resulting oil was added to the homoserine lactone-functionalized peptide **4** (325 mg, 0.30 mmol) together with 2-hydroxypyridine (200 μL of a 30 mg/mL solution in DMA). After vigorous stirring for 15 min, the reaction mixture became homogeneous, and it was then stirred for another 15 min. Excess linker and DMA were removed by precipitation of the product in MTBE (250 mL) containing 1% TFA. The resulting peptide macroinitiator **5** was purified by preparative HPLC (SunFire C18 preparative column, gradient: CH_3CN/H_2O/TFA 30/70/0.1 to

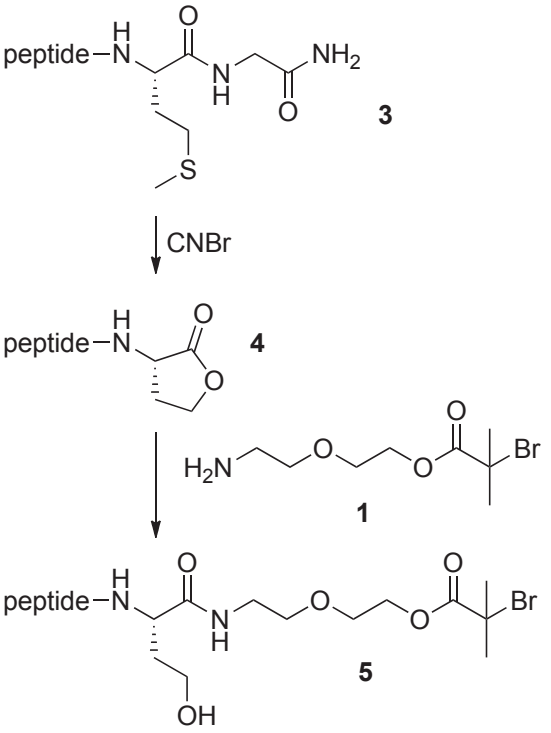

Scheme 3. Functionalization of the peptide C-terminus with linker **1**. "Peptide" indicates the sequence H-Ser-Gly-Pro-Gln-Gly-Ile-Phe-Gly-Gln-.

50/50/0.1, over 15 min) and subsequently lyophilized yielding 294 mg (0.22 mmol) of the TFA salt of the pure peptide macroinitiator **5** as a white powder. ESI-MS: calcd 1226.51 ($[M + H]^+$); found 1226.30.

4.2.7. ATRP of the C-terminal polymer block

Prior to use, all solvents and liquid reagents were deoxygenated by flushing with nitrogen gas for 15 min. A catalyst stock was prepared by weighing CuCl (12.0 mg, 120 μmol), $CuCl_2 \cdot 2H_2O$ (13.6 mg, 80 μmol), and 2,2′-bipyridyl (bpy) (62.4 mg, 400 μmol) into a 7 mL glass screw-capped vial equipped with a micro stirring bar. The vial was sealed with a septum and flushed with nitrogen gas for 15 min. Then, CH_3CN (0.6 mL) and H_2O (1.4 mL) were added through the septum, and the vial was held in an ultrasonic bath until all solids had dissolved forming the brown catalytic complex.

$OEGMA_{300}$ monomer (160, 320, or 640 μL for the aimed pOEGMA block lengths of 4, 8, and 16 kDa, respectively) was charged into an N_2-filled 2 mL septum vial equipped with a stirring bar. Then, 500 μL of the catalyst stock solution was added, followed by the peptide macroinitiator 5 (40 μmol, dissolved in a minimal volume of DMSO). Conversion was monitored during the reaction by ^{1}H NMR of samples diluted in air-saturated D_2O, comparing the integral of the region between 6.3 and 5.6 ppm (2H, H_2C=C) with the integral of the region between 4.5 and 4.0 ppm (2H, C(=O)OCH_2). Furthermore, at several time points samples were taken, which were quenched by diluting in air-saturated DMF, and the evolution of molecular weight was analyzed by GPC.

4.2.8. Azide substitution of the living chain end

When the monomer conversion was above 90%, NaN_3 (80 μL of an N_2-purged 1 M aqueous solution) was added to the reaction mixture, causing the chloride chain end to be substituted by an azide by means of the copper–bipyridyl catalyst.[42] Since the azide-functionalized chain end does not reinitiate, further OEGMA polymerization was prevented by this procedure. Azide functionalization also allows conjugation with a fluorescent probe.[42] The reaction mixture was left for 16 h to ensure complete substitution, after which the polymer was purified by 3× 10-fold concentration using a Vivaspin concentrator (MWCO of 2, 5, or 10 kDa for pOEGMA block lengths of 4, 8, and 16 kDa, respectively), each time diluting with 10 mM phosphate buffer, pH 7.0. The molecular weight of the polymers was determined by ^{1}H NMR based upon the ratio of the integrals of the aromatic phenylalanine protons and methoxy protons from pOEGMA.

4.2.9. Chain extension experiment

A sample (10 μL) of the peptide-$pOEGMA_{4\ kDa}$ polymer solution was taken before and after the substitution with NaN_3. The samples were diluted with CH_3CN (300 μL) and H_2O (700 μL) in a 2 mL septum vial. Subsequently, NIPAm (18 mg for target M_n = 32 kDa), CuBr (1.8 mg), and $CuBr_2$ (1.9 mg) were added. The vial was placed in an ice bath and purged with N_2 for 15 min. Then, the reaction was started by adding Me_6TREN (50 μL of a 0.4 M N_2-purged aqueous solution).

4.2.10. Functionalization of the N-terminus

To introduce an aldehyde functionality at the peptide's N-terminus (Scheme 4), 60 μL of a 1 M aqueous solution of $NaIO_4$ was added to the solution of peptide-pOEGMA **6** (40 mM in 1 mL of 10 mM phosphate buffer pH 7.4). Before and 15 min after addition, samples were taken for analysis. Disappearance of the amino group was confirmed by reaction with fluorescamine: 1 μL of sample was diluted in 1 mL of 50 mM phosphate buffer of pH 8.9. Subsequently, to 150 μL of this solution was added 50 μL of a freshly prepared 0.3 mg/mL solution of fluorescamine in dry acetone. The fluorescence was recorded (λ_{ex} = 380 nm, λ_{em} = 460 nm) in a FluoStar Optima well plate reader (BMG Labtech), and it was verified that after reaction with $NaIO_4$ no fluorescence was observable. To test for the development of an aldehyde functionality, a drop of sample was placed on a TLC plate and allowed to dry. The plate was then sprayed with a solution of 2.0 g of 2,4-dinitrophenylhydrazine and 4.0 mL of concentrated sulfuric acid in 100 mL of methanol. The development of a yellow spot indicated the formation of an aldehyde **7**.

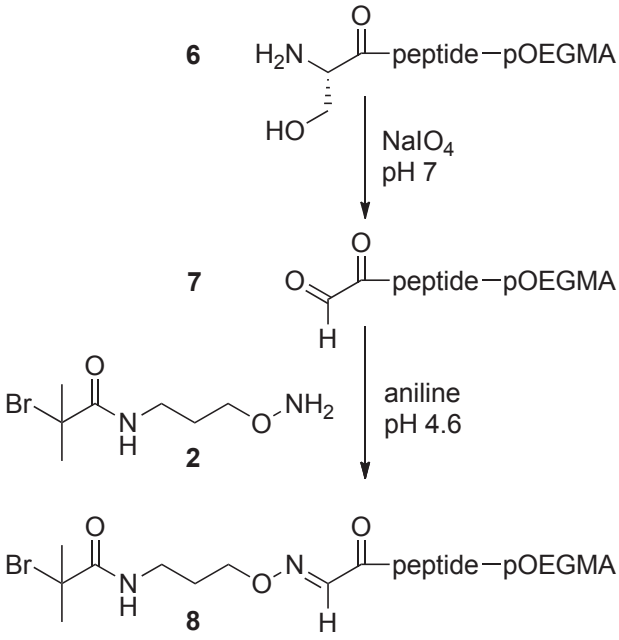

Scheme 4. Functionalization of the peptide N-terminus with linker **2**. "Peptide" indicates the sequence -Gly-Pro-Gln-Gly-Ile-Phe-Gly-Gln-.

After reaction with $NaIO_4$, the solution was diluted to 10 mL in 50 mM anilinium acetate buffer, pH 4.6.[43] Linker **2** (110 mg, 0.4 mmol) was added, and the reaction was allowed to proceed for 16 h at room temperature under nitrogen.

The polymer solution was again concentrated (4× 10-fold) using a Vivaspin concentrator (MWCO 2, 5, and 10 kDa), exchanging the buffer solution for demineralized water. The efficiency of coupling was assessed by ^{1}H NMR spectroscopy, comparing the integral of the proton on the oxime carbon of **8**, at 7.7 ppm, with the integral of the aromatic phenylalanine protons.

4.2.11. ATRP of the N-terminal polymer block

Following a published procedure,[44] CuBr (1.8 mg), $CuBr_2$ (1.9 mg), and *N*-isopropylacrylamide (NIPAm) (320 or 640 mg for a target M_n of 16 and 32 kDa, respectively) were weighed into a 2 mL septum vial. A stirring bar, CH_3CN (250 μL) and the N-terminally functionalized peptide-pOEGMA **8** (1 mL of a 20 mM aqueous solution) were added. For the target M_n of 32 kDa, it was necessary to add 1 extra mL of H_2O and 250 μL of CH_3CN to dissolve the NIPAm. The vial was placed in an ice bath, and the solution was purged with N_2 for 15 min. Then, the reaction was started by adding 50 μL of a 0.4 M N_2-purged aqueous solution of Me_6TREN. During the reaction, the conversion was monitored by ^{1}H NMR of samples diluted in air-saturated D_2O. Furthermore, at several time points samples were taken, which were quenched by diluting in air-saturated DMF and analyzed by gel permeation chromatography (GPC). The final polymers were dialyzed against water and lyophilized.

4.2.12. Polymer characterization

CPs of the polymers were determined using a Shimadzu UV-2450 spectrophotometer with temperature control by a Peltier element. The temperature of polymer solutions (1 mg/mL) was raised from 20 to 50 at 1 °C/min, and the CP was defined as the onset of the curve of extinction at 650 nm *vs* temperature.

For the determination of the critical micelle concentration (cmc), the different block copolymers were dissolved in water in concentrations ranging from 1 μg/mL to 1 mg/mL. Then, 5 μL of a 1.8×10^{-4} M solution

of pyrene in acetone was added to 1 mL of polymer solution. The micelles were formed by rapidly heating the solutions to 40 °C. After incubation for 16 h at this temperature, pyrene fluorescence was measured using a Horiba Fluorolog fluorometer at 37 °C. The emission was measured at 390 nm using excitation wavelengths of 333 and 338 nm. The ratio I_{338}/I_{333} was plotted against the logarithmic polymer concentration to determine the cmc.[45]

4.2.13. Formation of micelles

Micelles were formed using a heat shock procedure according to Neradovic *et al.*[46] by heating 900 µL of 0.22 µm-filtered water or phosphate buffered saline (PBS) to 40 °C and then adding 100 µL of a 1 mg/mL solution (at room temperature) of the polymer. The mixture was kept at 40 °C for 5 min before being equilibrated at 37 °C. Particle size was measured at 37 °C by dynamic light scattering (DLS) on an ALV CGS-3 system at a 90° scattering angle.

4.2.14. Fluorescent labeling of the polymer

To 1 mL of a 10 mg/mL aqueous solution of $pNIPAm_{32\ kDa}$-peptide-$pOEGMA_{8\ kDa}$ was added 3 µL of 0.1 mM copper(II) sulfate, 15 µL of 1 mg/mL Alexa Fluor 555 functionalized with an alkyne moiety in DMSO (Invitrogen), and 30 µL of 0.1 M ascorbic acid. The reaction mixture was purged with N_2 and stirred for 16 h in an N_2 atmosphere. The product was purified using a Vivaspin membrane with a molecular weight cutoff of 10 kDa (3× 10-fold concentration, each time diluting with H_2O). Labeling of the polymer was verified by GPC using a MesoPore column (Polymer Laboratories) at 40 °C, with DMF + 10 mM LiCl as the eluent and both refractive index (RI) and fluorescence detection.

4.2.15. Enzymatic degradation

Metalloprotease (type IV collagenase) from *C. histolyticum* was used as a model for MMP-2 and MMP-9. This enzyme has very similar substrate specificity and is commonly used as a readily available alternative to MMP-2 and MMP-9.[3, 4] The activity of the enzyme was determined colorimetrically by the *N*-(3-[2-furyl]acryloyl)-Leu-Gly-Pro-Ala (FALGPA) cleavage assay according to the manufacturer's protocol (Sigma-Aldrich) and was found to be 2300 units/mg (1 unit represents an activity of 1000 pmol

substrate/min). The fluorescently labeled polymer was diluted to a final polymer concentration of 10 μM in 0.22 μm-filtered HEPES buffer of pH 7.4 containing 20 mM $CaCl_2$ and 100 mM NaCl at room temperature. Then, a solution (0.22 μm-filtered) of 1000 units/mL of type IV collagenase in the same buffer was added to a final enzyme concentration of 10 units/mL, and the solution was incubated for 24 h at room temperature. GPC analysis with fluorescence detection was performed before and after the degradation (MesoPore column at 40 °C, DMF + 10 mM LiCl).

For the enzymatic degradation of intact micelles, micelles were formed by the above-mentioned heat shock procedure in HEPES buffer after which they were incubated with collagenase at 37 °C. At t = 0 and after 24 h a sample was diluted 10-fold in preheated buffer and injected into a Nanosight LM10-HS laser light scattering/fluorescence microscopy system, preheated to 37 °C. Using the Nanoparticle Tracking Analysis (NTA) software, images were taken to visualize the micelles and to determine whether their fluorescently labeled coronas had been cleaved off.

4.3. Results and discussion

4.3.1. Functionalization of the peptide C-terminus

To activate selectively the C-terminus of the peptide **3**, a reactive homoserine lactone was introduced by reaction of the penultimate methionine residue with CNBr (Scheme 3). This method, which is commonly used for the cleavage of recombinantly produced peptides from a carrier fusion protein,[41] allows for rapid and selective modification of the C-terminus of any peptide having methionine as the penultimate residue on the C-terminus.[39, 40] The only requirement is the absence of internal methionine residues, which would lead to cleavage of the peptide. However, since methionine is one of the least occurring amino acids in proteins,[47] this requirement is often easy to meet, making methionine a favorable target for site-specific peptide conjugation. The main advantage over other methodologies that target the C-terminus, *e.g.*, carbodiimide-based coupling,[48] is that CNBr functionalization is compatible with the presence of glutamate and aspartate residues. After reaction of the peptide with excess cyanogen bromide, 95% of the peptide was converted into the lactone form **4** (HPLC). Apart from the small amount

of unreacted peptide, there was also a trace impurity (<5%) of peptide in which the methionine residue had been oxidized to methionine sulfoxide, which renders it insensitive to lactonization with CNBr. The lactonized peptide was used without purification, as the main impurities are not reactive in the step of coupling the linker and could be removed after that step.

Linker **1**, which consists of a primary amine on one side and an efficient 2-bromoisobutyrate ATRP initiator on the other side, was synthesized in good yield and coupled to the peptide (Scheme 3). To catalyze aminolysis of the lactone, 10 mol % of 2-hydroxypyridine was added.[49] Nonreacted linker was easily removed after the reaction with the peptide, by selective precipitation, allowing the use of a large excess of linker. This yields a very short reaction time and negligible inter- and intramolecular reaction with the N-terminal amine. HPLC showed that after 15 min 95% of the peptide lactone had reacted. After preparative HPLC, the peptide macroinitiator **5** was obtained in 73% yield.

4.3.2. ATRP of $OEGMA_{300}$ starting from the C-terminus

The polymerization of $OEGMA_{300}$ yields brush-shaped PEG-like polymers which are frequently used as hydrophilic polymers in the biomedical field since they possess several of the advantages over the well-known PEG, *e.g.*, the fact that they are polymerizable by controlled radical polymerization.[50-53] Furthermore, because of the hydrophilic oligo(ethylene glycol) side chains and the hydrophobic polymethacrylate backbone, pOEGMA's have thermosensitive properties, which can be tuned by the average length of the oligo(ethylene glycol) side chains.[53] By using a monomer with an average molar mass of 300 Da, it was ensured that the resulting polymer has a lower critical solution temperature (LCST) above 68 °C,[52] meaning that the polymer is water-soluble at physiological temperature.

For the polymerization, a mild method compatible with the peptide was developed. Generally, ATRP of OEGMA is performed in alcohols at elevated temperatures,[51, 53] but it can also be performed in aqueous media at room temperature.[50] By addition of Cu(II) and a small amount of CH_3CN, a pseudoligand for Cu(I), the problem of disproportionation commonly faced in aqueous ATRP was eliminated.[54, 55] Furthermore, by varying the percentage CH_3CN (and consequently the polarity of the

solvent), it is possible to adjust the rate of the reaction.[56] In the present study, a fast reaction with sufficient control at ambient temperature was obtained in a CH_3CN/H_2O 3/7 (v/v) solvent mixture, which is a good solvent for the peptide used in the present study. As can be seen in Figure 1A, the residual monomer concentration decreased exponentially in time during the course of the reaction. This indicates a constant concentration of propagating radicals during the polymerization and thus effective and instantaneous initiation as well as negligible termination/combination; both are prerequisites for a controlled/living polymerization.[57] Furthermore, the number-averaged molecular weight (M_n) evolved linearly with conversion (Figure 1B), indicating a low rate of termination. These observations indicate that the polymerization was controlled.

^{1}H NMR spectroscopy of the polymers after purification showed that the pOEGMA blocks had M_n values of 3.2, 7.1, and 15.7 kDa, which are in good agreement with the expected molecular weights.

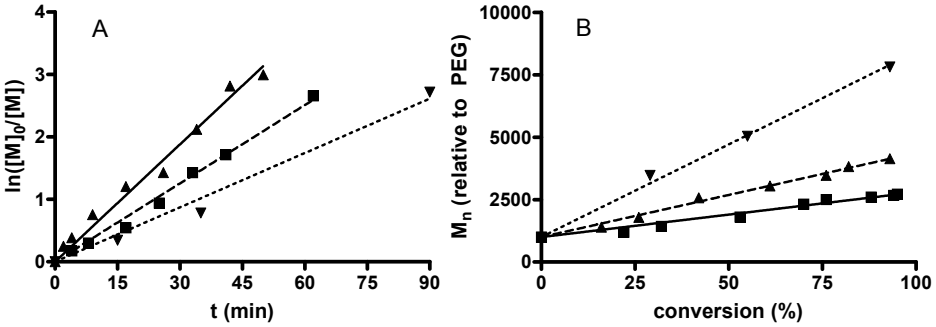

Figure 1. ATRP of $OEGMA_{300}$ using the synthesized peptide macroinitiator **5**: (A) semilogarithmic plot of monomer concentration [M] (as $[M]_0/[M]$) in time; (B) number-averaged molecular weight M_n (determined by GPC) as a function of monomer conversion. (▲) target M_n = 4 kDa, (■) target M_n = 8 kDa, (▼) target M_n = 16 kDa.

4.3.3. Inactivation of the living chain-end

One feature of ATRP is that the living chain end of the resulting polymers is able to reinitiate another polymerization, and this feature has been frequently used for the synthesis of block copolymers.[58-61] To be able to grow a different polymer chain from the other (N-) terminus of the peptide,

however, it must be ensured that the already existing polymer chain on the C-terminus will not reinitiate in a subsequent ATRP. Therefore, the chloride on the living chain end was substituted by azide using a recently developed copper-catalyzed azide substitution reaction.[42] The introduced azide functionality also renders it possible to attach in a later stage a fluorescent probe or a targeting ligand using azide/alkyne "click" chemistry.[42, 62-68] Figure 2 shows that the substitution with NaN_3, as expected, did not alter the molecular weight (distribution) of the polymer as determined by GPC analysis. Furthermore, the nonsubstituted pOEGMA chain could be extended with a pNIPAm block, which provides indeed evidence for the living character of the ATRP of OEGMA on the peptide macroinitiator. On the other hand, after substitution with NaN_3, pOEGMA was not able to reinitiate an ATRP (Figure 2). This demonstrates quantitative substitution of the Cl end-group by azide.

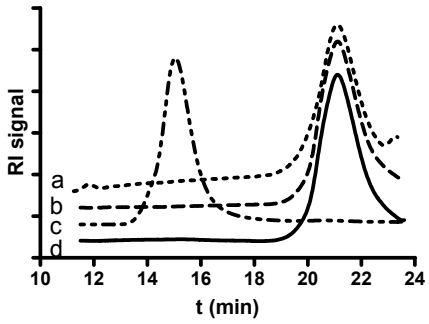

Figure 2. GPC chromatograms of peptide-pOEGMA$_{4\ kDa}$ hybrid polymer: (a) before substitution of the chloride chain end with azide, (b) after substitution with azide, (c) non-azidated polymer after chain extension with NIPAm, and (d) azidated polymer after chain extension.

4.3.4. Functionalization of the N-Terminus

Introduction of an aldehyde functionality into a peptide by mild periodate oxidation of an N-terminal serine residue followed by coupling of an O-substituted hydroxylamine is a highly selective, efficient, and well-known bioconjugation reaction.[69-71] The formed oxime bonds are acid-sensitive but stable at physiological pH.[72] The peptide-pOEGMA conjugates **6** were subjected to the above-mentioned oxidation with $NaIO_4$ in phosphate buffer (pH 7.4) (Scheme 4). Reaction with fluorescamine indicated disappearance

of the amine functionality of the N-terminal serine. Furthermore, a sample taken from the reaction mixture developed a yellow color after addition of 2,4-dinitrophenylhydrazine, indicating the formation of an aldehyde.

For further functionalization of the aldehyde-modified terminus of the peptide **7**, linker **2** was developed, carrying on one side a reactive aminooxy group and on the other side an ATRP initiator functionality. Linker **2** was synthesized as shown in Scheme 2. Subsequently, the aldehyde-functionalized peptide-pOEGMA conjugates **7** were incubated with linker **2** in 50 mM anilinium acetate buffer (pH 4.6) (Scheme 4), a known catalyst for the formation of oxime bonds.[71, 73, 74] After coupling of linker **2**, the appearance of a peak at δ 7.7 ppm in ^{1}H NMR (in D_2O) indicated the formation of an oxime bond (Figure 3). The degree of functionalization was >90% based on comparison of the integral of this peak with the integral of the peak of the phenyl protons of phenylalanine (δ 7.5–7.2 ppm).

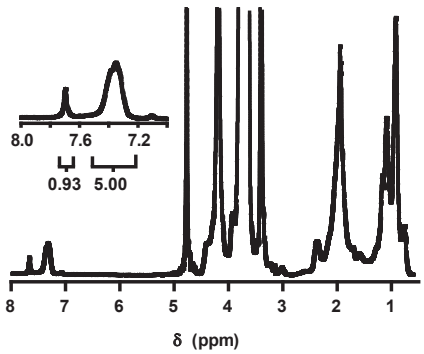

Figure 3. NMR spectrum of linker **2**-peptide-pOEGMA$_{4\ kDa}$ showing the peak of the proton on the oxime carbon at δ 7.7 ppm and the aromatic phenylalanine protons at δ 7.3–7.4 ppm.

4.3.5. ATRP of the N-Terminal Block

NIPAm was polymerized from the modified N-terminus of the peptide-pOEGMA conjugates **8** by ATRP in a CH_3CN/H_2O 3/7 (v/v) mixture at 0 °C.[44, 56, 75] The reaction was well controlled as evidenced by an exponential decrease of the residual monomer concentration (Figure 4A)

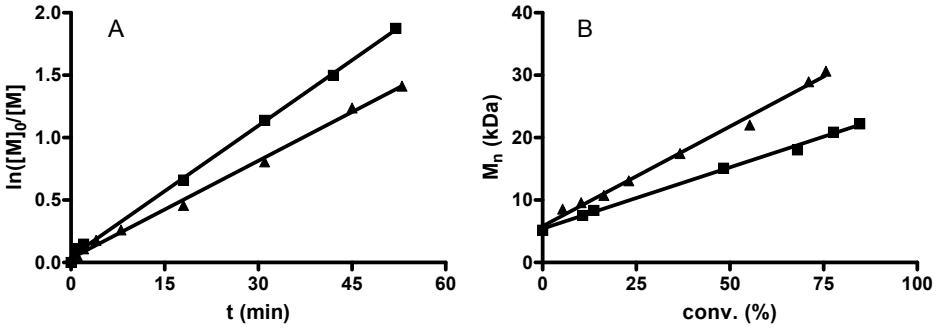

Figure 4. Kinetics of the polymerization of NIPAm onto peptide-pOEGMA$_{8\ kDa}$: (A) semilogarithmic plot of monomer concentration [M] (as $[M]_0/[M]$) in time; (B) number-averaged molecular weight M_n as a function of monomer conversion. (■) Target Mn = 16 kDa, (▲) target Mn = 32 kDa.

and a linear evolution of M_n with conversion, for both target molecular weights of the pNIPAm block (Figure 4B). This indicates successful growth of the pNIPAm block, starting from the peptide-pOEGMA macroinitiator **8**.

4.3.6. Characterization of the Polymers and Their Micelles

The structure of the final polymers is depicted in Figure 5. ^{1}H NMR analysis showed that the pNIPAm blocks had M_n values in good agreement with the expected molecular weight, based on the comparison of the integrals of the pOEGMA methoxy protons and pNIPAm methyl protons (Table 1). Furthermore, the dispersity of the synthesized polymers was low, with only polymers containing a pOEGMA$_{16\ kDa}$ block having a somewhat broader size distribution.

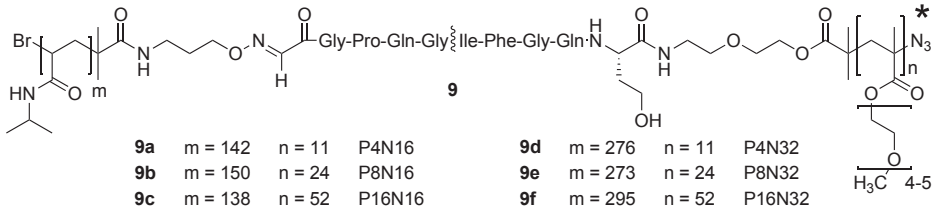

Figure 5. Structure of the final biohybrid triblock polymers. The wavy line indicates the bond that is cleavable by MMPs. The asterisk indicates the attachment point of the fluorescent probe in the P_8N_{32} polymer.

Table 1. Properties of the Polymers and Their Micelles

Abbreviation[a]	Polymers					Micelles		
	M_n[b] (kDa)		$Đ$[c]	CP[d] (°C)		CMC[e] (mg/mL)	R_h[f] (nm) (PDI)	
	pOEGMA	pNIPAm		H_2O	PBS		H_2O	PBS
P_4	3.2		1.20					
P_4N_{16}	3.2	16.0	1.25	35.5 ±0.1	33.0 ±0.2	0.03 ±0.01	29±1 (0.1)	173±2 (0.1)
P_4N_{32}	3.2	31.2	1.24	34.5 ±0.1	32.0 ±0.2	0.03 ±0.01	28±1 (0.1)	1756±138 (0.5)
P_8	7.1		1.32					
P_8N_{16}	7.1	17.0	1.24	35.6 ±0.1	33.1 ±0.1	0.03 ±0.01	27±1 (0.1)	35±1 (0.1)
P_8N_{32}	7.1	30.8	1.26	34.8 ±0.1	32.2 ±0.1	0.03 ±0.01	27±1 (0.1)	123±2 (0.1)
P_{16}	15.7		1.45					
$P_{16}N_{16}$	15.7	15.6	1.52	36.0 ±0.1	33.2 ±0.1	0.03 ±0.01	23±1 (0.2)	24±1 (0.1)
$P_{16}N_{32}$	15.7	33.3	1.64	34.7 ±0.1	32.1 ±0.1	0.03 ±0.01	22±1 (0.1)	33±1 (0.1)

[a]P denotes the aimed size of the pOEGMA block, N that of the pNIPAm block (both in kDa), [b]Number-averaged molecular weight based on ^{1}H NMR, [c]Dispersity from GPC, [d]Cloud Point, [e]Critical Micelle Concentration, [f]Z-averaged hydrodynamic radius (R_h) from DLS.

The CMC of the polymers dissolved in water was equal for all polymers. In general, a decrease in cmc with increasing hydrophobic block length would be expected, as well as an increase in cmc with increasing hydrophilic block length.[76, 77] Our observation of equal cmc's might be related to the fact that the found cmc values are very low, permitting an influence from the fluorescent probe (pyrene) itself.[78]

The CPs of the polymers dissolved in water were slightly higher than the published value of 32 °C of pNIPAm homopolymer in water due to the presence of large hydrophilic polymer blocks.[79, 80]

Consequently, Table 1 shows that the CP in water increased from 35.5 to 36.0 °C with increasing the pOEGMA block length from 4 to 16 kDa (P_4N_{16} *vs* $P_{16}N_{16}$) and decreased with increasing the pNIPAm length from 16 to 32 kDa. For self-assembly into micelles, a heat-shock protocol was used as it has been described that instantaneous heating of aqueous polymer solutions to above their CP leads to well-defined micelles.[46] Following this procedure, all polymers formed micelles with a size of 22–29 nm in water and narrow size distributions, which is favorable for drug delivery purposes.[81]

Increasing the pOEGMA length from 4 to 16 kDa leads to a larger surface area that is needed per polymer chain and thus to less polymer chains fitting in one micelle:[44] consequently, the size of the micelles decreased from 29 nm (P_4N_{16}) to 23 nm ($P_{16}N_{16}$). Interestingly, increasing the pNIPAm block from 16 to 32 kDa did not lead to an increase of the micellar size, but to a small decrease, *e.g.*, 29 nm (P_4N_{16}) *vs* 28 nm (P_4N_{32}). This effect has been observed before and has been attributed to greater hydrophobicity of the longer pNIPAm blocks, leading to more extensive dehydration of the micellar cores.[46, 82]

The difference in CP and size between micelles dispersed in water and PBS is also striking. The salting-out effect of PBS reduced the CPs by 2–3 °C, to values (32–33 °C) that are well below physiological temperature and thus compatible with drug delivery applications. Furthermore, PBS also led to a higher observed Z-averaged size. PEG is known to partially dehydrate upon addition of salt,[46, 83, 84] and the same behavior may be expected for pOEGMA. This partial dehydration may lead to the formation of larger particles due to a change in the ratio between the hydrodynamic volumes of the hydrophilic and hydrophobic blocks. For large pOEGMA blocks and/or small pNIPAM blocks, the hydrophilic/hydrophobic ratio in buffer is still enough to form small micelles (P_8N_{16}, $P_{16}N_{16}$, and $P_{16}N_{32}$); for smaller pOEGMA blocks, the increase in size was more pronounced. For the P_4N_{32} polymer, the (decreased) hydrodynamic volume of the pOEGMA blocks in buffer was not enough anymore to support stable nanoparticles, and aggregation resulted.

4.3.7. Enzymatic Degradation

The peptide separating the hydrophilic micelle corona from the thermosensitive micelle core has been designed to be cleaved by MMP-2 and MMP-9, as these enzymes are upregulated in diseased tissues (*e.g.*, in cancer and rheumatoid arthritis). For this reason, MMP-2/MMP-9 substrates have previously been utilized as building blocks of tissue-specific drug delivery systems.[85-90]

To verify that the peptide could still be cleaved by metalloproteases after growing the two polymer blocks on its N- and C-termini, the P_8N_{32} block copolymer was fluorescently labeled at the end of its hydrophilic block. Alkyne-functionalized Alexa Fluor 555 was coupled ("clicked") to the azide-functionalized chain end by Cu(I)-catalyzed azide–alkyne cycloaddition. A label to polymer molar ratio of 1:10 was used in order to minimize any effects of the label on micelle formation. As shown in Figure 6, the polymer was successfully labeled with Alexa Fluor 555 by this procedure.

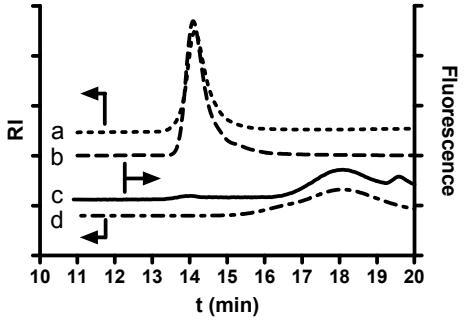

Figure 6. GPC traces of the fluorescently labeled polymer: (a) RI signal after labeling, (b) fluorescence signal (λ_{ex} = 555 nm, λ_{em} = 585 nm) after labeling, (c) fluorescence signal after enzymatic cleavage. For comparison, (d) shows the RI signal of peptide-$pOEGMA_{8\ kDa}$.

Subsequently, the polymer was incubated with collagenase for 24 h at room temperature. The cleaved polymer was then analyzed by GPC with fluorescence detection. It is well-known that pNIPAm (co)polymers elute in GPC at retention times corresponding to much higher molecular weights than expected, probably due to very persistent interchain hydrogen bonds.[91,92] This feature was exploited for the demonstration of cleavage of the peptide–polymer conjugate by collagenase. When a column with a narrow separation range was used, the fluorescently labeled intact polymer elutes in the void

volume (at 14 min, Figure 6), whereas the fluorescently labeled pOEGMA that is cleaved off elutes much later (at 18 min, the same retention time as peptide-$pOEGMA_{8\ kDa}$). Since the pNIPAm is unlabeled after cleavage, it is invisible using fluorescence detection. Thus, this method leads to a good separation of the uncleaved polymer and the cleaved-off hydrophilic blocks, while preventing interference from the cleaved thermosensitive blocks which coelute with the uncleaved polymer but are invisible using fluorescence detection.

To visualize the enzymatic degradation of the particles, micelles were formed by heat-shocking the fluorescently labeled polymer. Images of the solution were taken using a preheated Nanosight LM10-HS microscopy system which allows visualization of the nanoparticles by either their scattering of laser light or by their fluorescence. Images were obtained in both laser scattering and fluorescence mode directly before addition of the enzyme and after 24 h incubation at 37 °C (Figure 7). As can be seen in Figure 7C, particles are still present after degradation, but their fluorescence has vanished into the background noise (Figure 7D), indicating that the fluorescent and highly mobile hydrophilic pOEGMA chains have been cleaved off by the enzyme. On the basis of these findings, it can be

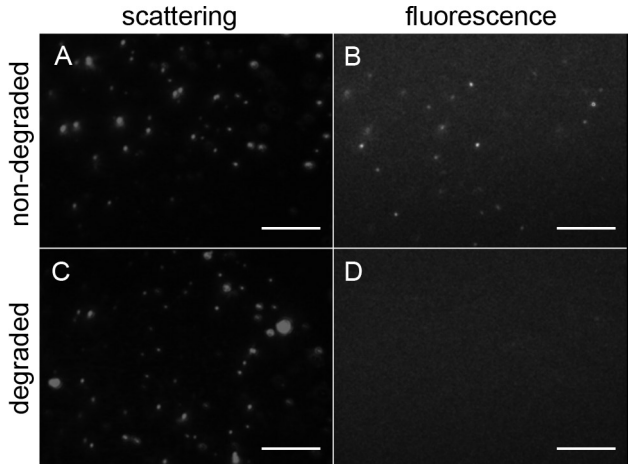

Figure 7. Images of the micellar dispersion of fluorescently labeled P_8N_{32} polymer, taken using a Nanosight system before (A and B) and after (C and D) enzymatic cleavage in HEPES buffer. (A) and (C) were recorded in scattering mode and (B) and (D) in fluorescence mode (λ_{ex} = 532 nm, λ_{em} > 565 nm), keeping the camera gain settings constant. Scale bars correspond to 10 μm; however, the apparent size of the micelles in these images reflects their scattering intensity rather than their actual size.

expected that when these micelles are used for drug delivery to tumors or inflamed tissues, their "stealth" corona will be cleaved off at the target site of action. We hypothesize that this "shedding" of the corona will impede further circulation of the micelles and facilitate cellular uptake.

4.4. Conclusion

We have demonstrated a suitable approach to grow two different polymer chains from a native peptide by ATRP, using two orthogonal methods to couple ATRP initiators to the N- and C-terminus. Furthermore, in this work a mild method is presented to inactivate the first living ATRP chain end, allowing the same polymerization chemistry for both polymerizations. Both polymerizations were well controlled, leading to a well-defined end product with control over the desired polymer block lengths.

Above the cloud point of one of the blocks, the polymers self-assembled into micelles. The micelles have been shown to "shed" the hydrophilic polymer blocks on their outside by the action of collagenase, a model for diseased tissue-specific matrix metalloproteases. Thus, the technology presented herein offers new possibilities for enzyme-triggered drug delivery.

References

(1) Ruiz-Hitzky, E.; Darder, M.; Aranda, P.; Ariga, K. *Adv. Mater*. **2010**, *3*, 323– 336

(2) Venkatesh, S.; Byrne, M. E.; Peppas, N. A.; Hilt, J. Z. *Expert Opin. Drug Delivery* **2005**, *6*, 1085– 1096

(3) Tsurkan, M. V.; Chwalek, K.; Levental, K. R.; Freudenberg, U.; Werner, C. *Macromol. Rapid Commun.* **2010**, *17*, 1529– 1533

(4) Seliktar, D.; Zisch, A. H.; Lutolf, M. P.; Wrana, J. L.; Hubbell, J. A. *J. Biomed. Mater. Res., Part A* **2004**, *4*, 704– 716

(5) Fuks, G.; Mayap Talom, R.; Gauffre, F. *Chem. Soc. Rev.* **2011**, *5*, 2475– 2493

(6) Xun, W.; Wu, D. Q.; Li, Z. Y.; Wang, H. Y.; Huang, F. W.; Cheng, S. X.; Zhang, X. Z.; Zhuo, R. X. *Macromol. Biosci.* **2009**, *12*, 1219– 1226

(7) Habraken, G. J.; Peeters, M.; Thornton, P. D.; Koning, C. E.; Heise, A. *Biomacromolecules* **2011**, *12*, 3761– 3769

(8) Oerlemans, C.; Bult, W.; Bos, M.; Storm, G.; Nijsen, J. F. W.; Hennink, W. E. *Pharm. Res.* **2010**, *27*, 2569– 2589

(9) Glinel, K.; Jonas, A. M.; Jouenne, T.; Leprince, J.; Galas, L.; Huck, W. T. *Bioconjugate Chem. 2009*, *1*, 71– 77

(10) Ku, T.; Chien, M.; Thompson, M. P.; Sinkovits, R. S.; Olson, N. H.; Baker, T. S.; Gianneschi, N. C. *J. Am. Chem. Soc.* **2011**, *22*, 8392– 8395

(11) Bencherif, S. A.; Gao, H.; Srinivasan, A.; Siegwart, D. J.; Hollinger, J. O.; Washburn, N. R.; Matyjaszewski, K. *Biomacromolecules* **2009**, *7*, 1795– 1803

(12) Katayama, Y.; Sonoda, T.; Maeda, M. *Macromolecules* **2001**, *24*, 8569– 8573

(13) Zhu, B.; Lu, D.; Ge, J.; Liu, Z. *Acta Biomater.* **2011**, *5*, 2131– 2138

(14) Broyer, R. M.; Quaker, G. M.; Maynard, H. D. *J. Am. Chem. Soc.* **2007**, *3*, 1041– 1047

(15) Pintauer, T.; Matyjaszewski, K. *Chem. Soc. Rev.* **2008**, *6*, 1087– 1097

(16) Fristrup, C. J.; Jankova, K.; Hvilsted, S. *Soft Matter* **2009**, *23*, 4623–4634

(17) Min, K.; Matyjaszewski, K. *Cent. Eur. J. Chem.* **2009**, *4*, 657– 674

(18) Boyer, C.; Bulmus, V.; Davis, T. P.; Ladmiral, V.; Liu, J.; Perrier, S. *Chem. Rev.* **2009**, *11*, 5402– 5436

(19) Gregory, A.; Stenzel, M. H. *Expert Opin. Drug Delivery* **2011**, *2*, 237– 269

(20) Stenzel, M. H. *Chem. Commun. (Cambridge, U. K.)* **2008**, *30*, 3486–3503

(21) Studer, A.; Schulte, T. *Chem. Rec.* **2005**, *1*, 27– 35

(22) Brinks, M. K.; Studer, A. *Macromol. Rapid Commun.* **2009**, *13*, 1043– 1057

(23) Bertin, D.; Gigmes, D.; Marque, S. R. A.; Tordo, P. *Chem. Soc. Rev.* **2011**, *5*, 2189– 2198

(24) Braunecker, W. A.; Matyjaszewski, K. *Prog. Polym. Sci.* **2007**, *1*, 93–146

(25) Grover, G. N.; Maynard, H. D. *Curr. Opin. Chem. Biol.* **2010**, *6*, 818– 827

(26) Topp, M. D. C.; Dijkstra, P. J.; Talsma, H.; Feijen, J. *Macromolecules* **1997**, *30*, 8518– 8520

(27) Neradovic, D.; van Nostrum, C. F.; Hennink, W. E. *Macromolecules* **2001**, *34*, 7589– 7591

(28) Netzel-Arnett, S.; Sang, Q. X.; Moore, W. G.; Navre, M.; Birkedal-Hansen, H.; Van Wart, H. E. *Biochemistry* **1993**, *25*, 6427– 6432

(29) Benassi, M. S.; Gamberi, G.; Magagnoli, G.; Molendini, L.; Ragazzini, P.; Merli, M.; Chiesa, F.; Balladelli, A.; Manfrini, M.; Bertoni, F.; Mercuri, M.; Picci, P. *Ann. Oncol.* **2001**, *1*, 75– 80

(30) Raithatha, S. A.; Muzik, H.; Muzik, H.; Rewcastle, N. B.; Johnston, R. N.; Edwards, D. R.; Forsyth, P. A. *Neuro-Oncology (Cary, NC, U. S.)* **2000**, *3*, 145– 150

(31) Kevorkian, L.; Young, D. A.; Darrah, C.; Donell, S. T.; Shepstone, L.; Porter, S.; Brockbank, S. M.; Edwards, D. R.; Parker, A. E.; Clark, I. M. *Arthritis Rheum.* **2004**, *1*, 131– 141

(32) Maeda, H.; Wu, J.; Sawa, T.; Matsumura, Y.; Hori, K. *J. Controlled Release* **2000**, *1–2*, 271– 284

(33) Khorsand Sourkohi, B.; Cunningham, A.; Zhang, Q.; Oh, J. K. *Biomacromolecules* **2011**.

(34) Habraken, G. J. M.; Koning, C. E.; Heise, A. *J. Polym. Sci., Part A: Polym. Chem.* **2009**, *24*, 6883– 6893

(35) Sun, P.; Zhang, Y.; Shi, L.; Gan, Z. *Macromol. Biosci.* **2010**, *6*, 621–631

(36) Ciampolini, M.; Nardi, N. *Inorg. Chem.* **1966**, *1*, 41– 44

(37) Salisbury, C. M.; Maly, D. J.; Ellman, J. A. *J. Am. Chem. Soc.* **2002**, *50*, 14868– 14870

(38) Chan, W. C.; White, P. D., Eds.; *Fmoc Solid Phase Peptide Synthesis: A Practical Approach*; Oxford University Press: New York, **2000**.

(39) Marcus, J. H. *Anal. Biochem.* **1975**, *2*, 583– 589

(40) Horn, M. J.; Laursen, R. A. *FEBS Lett.* **1973**, *3*, 285– 288

(41) LaVallie, E. R.; McCoy, J. M.; Smith, D. B.; Riggs, P.Enzymatic and Chemical Cleavage of Fusion Proteins. In *Current Protocols in Molecular Biology*; John Wiley & Sons, Inc.: New York, **2001**.

(42) de Graaf, A. J.; Mastrobattista, E.; Van Nostrum, C. F.; Rijkers, D. T. S.; Hennink, W. E.; Vermonden, T. *Chem. Commun. (Cambridge, U. K.)* **2011**, *24*, 6972– 6974

(43) Dirksen, A.; Dirksen, S.; Hackeng, T. M.; Dawson, P. E. *J. Am. Chem. Soc.* **2006**, *49*, 15602– 15603

(44) de Graaf, A. J.; Boere, K. W. M.; Kemmink, J.; Fokkink, R. G.; van Nostrum, C. F.; Rijkers, D. T. S.; van, d. G.; Wienk, H.; Baldus, M.; Mastrobattista, E.; Vermonden, T.; Hennink, W. E. *Langmuir* **2011**, *16*, 9843– 9848

(45) Wilhelm, M.; Zhao, C. L.; Wang, Y.; Xu, R.; Winnik, M. A.; Mura, J. L.; Riess, G.; Croucher, M. D. *Macromolecules* **1991**, *5*, 1033– 1040

(46) Neradovic, D.; Soga, O.; Van Nostrum, C. F.; Hennink, W. E. *Biomaterials* **2004**, *12*, 2409– 2418

(47) Wu, G.; Ott, T. L.; Knabe, D. A.; Bazer, F. W. *J. Nutr.* **1999**, *5*, 1031– 1038

(48) Valeur, E.; Bradley, M. *Chem. Soc. Rev.* **2009**, *2*, 606– 631

(49) Openshaw, H. T.; Whittaker, N. *J. Chem. Soc. C* **1969**, *1*, 89– 91

(50) Wang, X.; Armes, S. P. *Macromolecules* **2000**, *18*, 6640– 6647

(51) Lutz, J.-F.; Hoth, A. *Macromolecules* **2006**, *2*, 893– 896

(52) Ishizone, T.; Seki, A.; Hagiwara, M.; Han, S.; Yokoyama, H.; Oyane, A.; Deffieux, A.; Carlotti, S. *Macromolecules* **2008**, *8*, 2963– 2967

(53) Badi, N.; Lutz, J.-F. *J. Controlled Release* **2009**, *3*, 224– 229

(54) Tsarevsky, N. V.; Braunecker, W. A.; Matyjaszewski, K. *J. Organomet. Chem.* **2007**, *15*, 3212– 3222

(55) Tsarevsky, N. V.; Matyjaszewski, K. *Chem. Rev.* **2007**, *6*, 2270– 2299

(56) Ye, J.; Narain, R. *J. Phys. Chem. B* **2009**, *3*, 676– 681

(57) Matyjaszewski, K. *Curr. Opin. Solid State Mater. Sci.* **1996**, *6*, 769– 776

(58) Shipp, D. A.; Wang, J.; Matyjaszewski, K. *Macromolecules* **1998**, *23*, 8005– 8008

(59) Ma, Q.; Wooley, K. L. *J. Polym. Sci., Part A* **2000**, *Suppl.*, 4805– 4820

(60) Davis, K. A.; Matyjaszewski, K. *Macromolecules* **2000**, *11*, 4039– 4047

(61) Liu, S.; Weaver, J. V. M.; Tang, Y.; Billingham, N. C.; Armes, S. P.; Tribe, K. *Macromolecules* **2002**, *16*, 6121– 6131

(62) Tornøe, C. W.; Christensen, C.; Meldal, M. *J. Org. Chem.* **2002**, *9*, 3057– 3064

(63) Rostovtsev, V. V.; Green, L. G.; Fokin, V. V.; Sharpless, K. B. *Angew. Chem., Int. Ed.* **2002**, *14*, 2596– 2599

(64) Meldal, M.; Tornøe, C. W. *Chem. Rev.* **2008**, *8*, 2952– 3015

(65) Lutz, J.-F. *Angew. Chem., Int. Ed.* **2007**, *7*, 1018– 1025

(66) Binder, W. H.; Sachsenhofer, R. *Macromol. Rapid Commun.* **2007**, *1*, 15– 54

(67) Lutz, J.-F.; Börner, H. G.; Weichenhan, K. *Macromol. Rapid Commun.* **2005**, *7*, 514– 518

(68) Lutz, J.-F.; Börner, H. G.; Weichenhan, K. *Macromolecules* **2006**, *19*, 6376– 6383

(69) Gaertner, H. F.; Offord, R. E. *Bioconjugate Chem.* **1996**, *1*, 38– 44

(70) Rose, K.; Chen, J.; Dragovic, M.; Zeng, W.; Jeannerat, D.; Kamalaprija, P.; Burger, U. *Bioconjugate Chem.* **1999**, *6*, 1038– 1043

(71) Dirksen, A.; Hackeng, T. M.; Dawson, P. E. *Angew. Chem., Int. Ed.* **2006**, *45*, 7581– 7584

(72) Jin, Y.; Song, L.; Su, Y.; Zhu, L.; Pang, Y.; Qiu, F.; Tong, G.; Yan, D.; Zhu, B.; Zhu, X. *Biomacromolecules* **2011**, *10*, 3460– 3468

(73) Dirksen, A.; Dawson, P. E. *Bioconjugate Chem.* **2008**, *12*, 2543– 2548

(74) Thygesen, M. B.; Munch, H.; Sauer, J.; Cló, E.; Jørgensen, M. R.; Hindsgaul, O.; Jensen, K. J. *J. Org. Chem.* **2010**, *5*, 1752– 1755

(75) Millard, P. E.; Mougin, N. C.; Böker, A.; Müller, A. H. E. *Polym. Prepr. (Am. Chem. Soc., Div. Polym. Chem.)* **2008**, *49*, 121– 122

(76) van Hell, A. J.; Costa, C. I. C. A.; Flesch, F. M.; Sutter, M.; Jiskoot, W.; Crommelin, D. J. A.; Hennink, W. E.; Mastrobattista, E. *Biomacromolecules* **2007**, *9*, 2753– 2761

(77) Carstens, M. G.; van Nostrum, C. F.; Ramzi, A.; Meeldijk, J. D.; Verrijk, R.; de Leede, L. L.; Crommelin, D. J.; Hennink, W. E. *Langmuir* **2005**, *24*, 11446– 11454

(78) Jones, G.; Vullev, V. I. *Org. Lett.* **2001**, *16*, 2457– 2460

(79) Teodorescu, M.; Negru, I.; Stanescu, P. O.; Drăghici, C.; Lungu, A.; Sârbu, A. *React. Funct. Polym.* **2010**, *10*, 790– 797

(80) Xia, Y.; Yin, X.; Burke, N. A. D.; Stöver, H. D. H. *Macromolecules* **2005**, *14*, 5937– 5943

(81) Saha, R. N.; Vasanthakumar, S.; Bende, G.; Snehalatha, M. *Mol. Membr. Biol.* **2010**, *7*, 215– 231

(82) Soga, O.; van Nostrum, C. F.; Ramzi, A.; Visser, T.; Soulimani, F.; Frederik, P. M.; Bomans, P. H. H.; Hennink, W. E. *Langmuir* **2004**, *21*, 9388– 9395

(83) Louai, A.; Sarazin, D.; Pollet, G.; François, J.; Moreaux, F. *Polymer* **1991**, *4*, 713– 720

(84) Govender, T.; Stolnik, S.; Xiong, C.; Zhang, S.; Illum, L.; Davis, S. S. *J. Controlled Release* **2001**, *3*, 249– 258

(85) Yamada, R.; Kostova, M. B.; Anchoori, R. K.; Xu, S.; Neamati, N.; Khan, S. R. *Cancer Biol. Ther.* **2010**, *3*, 192– 203

(86) Wong, C.; Stylianopoulos, T.; Cui, J.; Martin, J.; Chauhan, V. P.; Jiang, W.; Popovíc, Z.; Jain, R. K.; Bawendi, M. G.; Fukumura, D. *Proc. Natl. Acad. Sci. U. S. A.* **2011**, *6*, 2426– 2431

(87) Garripelli, V. K.; Kim, J.; Son, S.; Kim, W. J.; Repka, M. A.; Jo, S. *Acta Biomater.* **2011**, *5*, 1984– 1992

(88) Kratz, F.; Drevs, J.; Bing, G.; Stockmar, C.; Scheuermann, K.; Lazar, P.; Unger, C. *Bioorg. Med. Chem. Lett.* **2001**, *15*, 2001– 2006

(89) Atkinson, J. M.; Siller, C. S.; Gill, J. H. *Br. J. Pharmacol.* **2008**, *7*, 1344– 1352

(90) Vartak, D. G.; Gemeinhart, R. A. *J. Drug Targeting* **2007**, *1*, 1– 20

(91) Ganachaud, F.; Monteiro, M. J.; Gilbert, R. G.; Dourges, M.; Thang, S. H.; Rizzardo, E. *Macromolecules* **2000**, *18*, 6738– 6745

(92) Smithenry, D. W.; Kang, M.; Gupta, V. K. *Macromolecules* **2001**, *24*, 8503– 8511

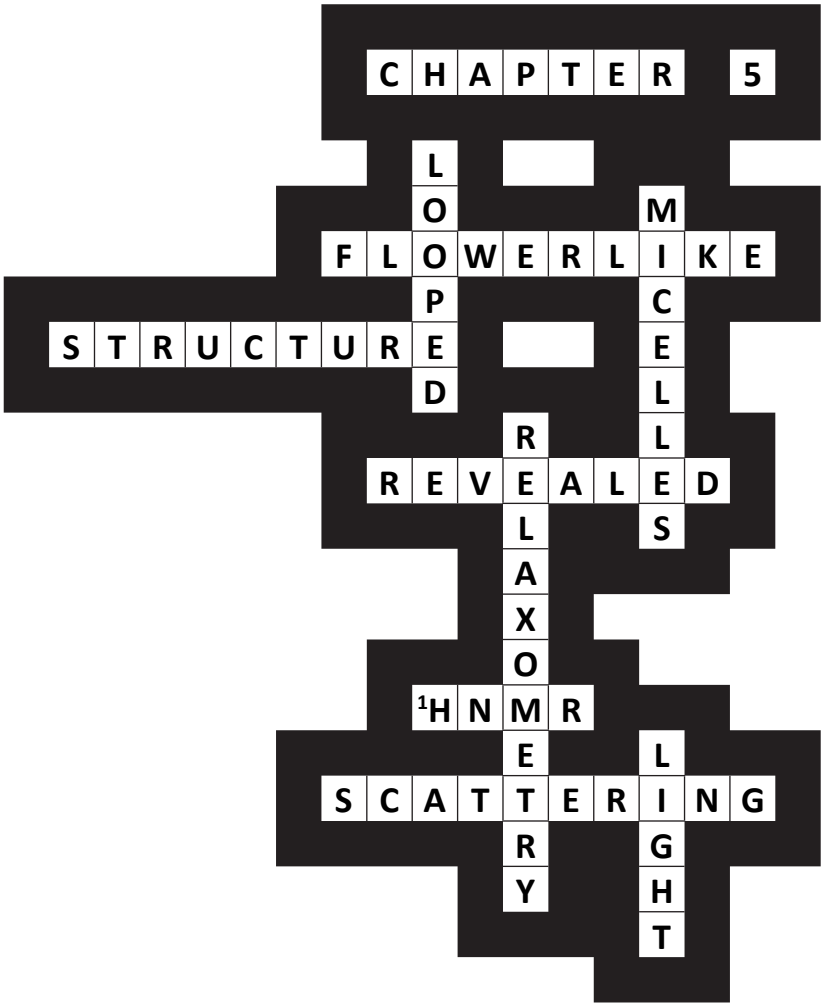

Looped structure of flowerlike micelles revealed by ^{1}H NMR relaxometry and light scattering

Albert J. de Graaf, Kristel W. M. Boere, Johan Kemmink, Remco G. Fokkink, Cornelus F. van Nostrum, Dirk T. S. Rijkers, Jasper van der Gucht, Hans Wienk, Marc Baldus, Enrico Mastrobattista, Tina Vermonden and Wim E. Hennink

Langmuir, **2011**, *27* (16), pp. 9843–9848

Copyright 2011, the American Chemical Society

Abstract

We present experimental proof that so-called "flowerlike micelles" exist and that they have some distinctly different properties compared to their "starlike" counterparts. Amphiphilic AB diblock and BAB triblock copolymers consisting of poly(ethylene glycol) (PEG) as hydrophilic A block and thermosensitive poly(*N*-isopropylacrylamide) (pNIPAm) B block(s) were synthesized via atom transfer radical polymerization (ATRP). In aqueous solutions, both block copolymer types form micelles above the cloud point of pNIPAm. Static and dynamic light scattering measurements in combination with NMR relaxation experiments proved the existence of flowerlike micelles based on $pNIPAm_{16kDa}$-PEG_{4kDa}-$pNIPAm_{16kDa}$ which had a smaller radius and lower mass and aggregation number than starlike micelles based on $mPEG_{2kDa}$-$pNIPAm_{16kDa}$. Furthermore, the PEG surface density was much lower for the flowerlike micelles, which we attribute to the looped configuration of the hydrophilic PEG block. ^{1}H NMR relaxation measurements showed biphasic T_2 relaxation for PEG, indicating rigid PEG segments close to the micelle core and more flexible distal segments. Even the flexible distal segments were shown to have a lower mobility in the flowerlike micelles compared to the starlike micelles, indicating strain due to loop formation. Taken together, it is demonstrated that self-assemblies of BAB triblock copolymers have their hydrophilic block in a looped conformation and thus indeed adopt a flowerlike conformation.

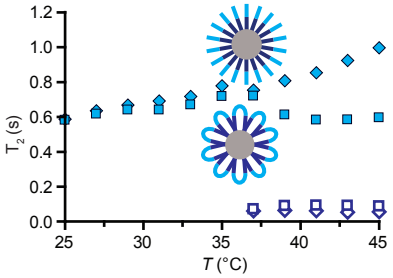

5.1. Introduction

Polymeric micelles are widely studied as delivery vehicles for hydrophobic, low molecular weight drugs.[1-8] Two important features are their generally low critical micelle concentration (CMC) as compared to low molecular weight amphiphiles and their small size (several tens of nanometers) which renders them suitable for passive targeting exploiting the enhanced permeability and retention effect.[9, 10] Furthermore, the highly hydrated shell of the micelles can shield them from recognition and uptake by cells of the immune system. Poly(ethylene glycol) (PEG), which is well-known for these stealthlike properties, is therefore often used to form the hydrophilic corona.[11] Polymeric micelles, with a hydrophobic core and a hydrophilic shell, are obtained by dispersing amphiphilic AB block copolymers in water.[1-8] BAB triblock copolymers with a hydrophilic midblock flanked by two hydrophobic blocks have been hypothesized to self-assemble into so-called "flowerlike micelles".[12-16] For drug delivery purposes, these flowerlike micelles might have several advantages over their starlike counterparts, like a potentially lower CMC and higher kinetic stability.[17-19] It must be noted that, although a flowerlike structure is intuitively logical, there is at present only indirect evidence to support its existence. It has been shown that theoretically flowerlike micelles can exist, if the entropic penalty of looping the hydrophilic blocks is smaller than the free energy decrease of micellization.[20-22] Small-angle X-ray and neutron scattering data on some BAB block copolymers could be fitted to a core–shell model under some assumptions.[23, 24] On the other hand, other authors claim based on simulations that self-assemblies of BAB block copolymers may not be "real" micelles having a well-separated core and corona.[25, 26]

The aim of the present study is to indisputably prove the existence of flowerlike micelles by proving that their hydrophilic blocks are in a looped conformation. Therefore, the size, aggregation number, and surface graft density of flowerlike and starlike micelles are compared. Furthermore, the segmental mobility of the hydrophilic PEG blocks in starlike and flowerlike micelles is studied by ^{1}H NMR relaxometry as a function of architecture, block length, and temperature.

5.2. Model system

As model system, we chose block copolymers of AB and BAB architecture consisting of a poly(ethylene glycol) (PEG) A block and thermosensitive poly(*N*-isopropylacrylamide) (pNIPAm) B block(s) (Figure 1). Above the cloud point (CP) of the thermosensitive blocks (32 °C for pNIPAm homopolymer in water[27]), these AB and BAB polymers form micelles. For a fair comparison between diblock and triblock copolymers, we compared $pNIPAm_{16kDa}$-PEG_{4kDa}-$pNIPAm_{16kDa}$ to $mPEG_{2kDa}$-$pNIPAm_{16kDa}$ so that the triblock copolymer can be considered as a double diblock copolymer. To study the influence of the PEG length on the loop structure, triblock copolymers with either a shorter (2 kDa) or longer (6 kDa) PEG block were prepared as well. The polymers were prepared by atom transfer radical polymerization (ATRP) of NIPAm onto (m)PEG macroinitiators.

5.3. Experimental section

5.3.1. Chemicals

N-Isopropylacrylamide (NIPAm; Aldrich, 97%) was recrystallized twice from a mixture of *n*-hexane and toluene (v/v = 1:1). Poly(ethylene glycol) (PEG) with molar masses of 2000, 4000, and 6000 Da and poly(ethylene glycol) monomethyl ether (mPEG) with molar mass of 2000 Da were purchased from Merck and dehydrated prior to use by coevaporation of water with toluene at 84–110 °C. Tris(2-dimethylaminoethyl)amine (Me_6TREN) was prepared according to reported procedures.[28] 2-Bromoisobutyryl bromide (Aldrich), copper bromide, and copper dibromide (Acros) were used as received.

5.3.2. Synthesis of (m)PEG macroinitiators

Dehydrated (m)PEG (5.0 g, different molecular weights) was dissolved in 100 mL of THF dried on molecular sieves and degassed by flushing with nitrogen. Subsequently, 1.1 equiv of triethylamine (to –OH groups) and 1.1 equiv of bromoisobutyryl bromide (to –OH groups) were added. The mixture was allowed to react overnight at room temperature, after which the bromide salt was filtrated off. The filtrate was concentrated and again dissolved in dichloromethane. The crude product was precipitated in cold diethyl ether and filtrated. A white product was formed with a yield of 80%. ^{1}H NMR (300

MHz, $CDCl_3$): mPEG macroinitiator, δ 4.3 ppm (t, 2H, OCH_2), δ 3.85 ppm (t, 2H, OCH_2), δ 3.65 ppm (t, 4*n*H, OCH_2), δ 3.35 ppm (t, 2H, OCH_2), δ 3.30 ppm (s, 3H, OCH_3), δ 1.85 ppm (s, 6H, CCH_3). PEG macroinitiator, δ 4.3 ppm (t, 4H, OCH_2), δ 3.85 ppm (t, 4H, OCH_2), δ 3.65 ppm (t, 4*n*H, OCH_2), δ 3.35 ppm (t, 4H, OCH_2), δ 1.85 ppm (s, 12H,CCH_3). Also, ^{1}H NMR spectra after addition of two droplets of trichloroacetyl isocyanate (TAIC) were taken to determine the degree of substitution. These spectra confirmed that the (m)PEG was >95% functionalized.

5.3.3. Synthesis of mPEG-pNIPAm and pNIPAm-PEG-pNIPAm copolymers

200 mg of (m)PEG macroinitiator, 18.1 mg of CuBr, and 18.8 mg of $CuBr_2$ and the correct amount of NIPAm for the aimed block length were dissolved in 10 mL of H_2O and 2.5 mL of acetonitrile. A stirring bar was introduced; the solution was degassed by flushing with N_2 for half an hour and placed in an ice bath for another 15 min. The reaction was started by adding 0.5 mL of 0.42 M Me_6TREN solution, which turned the mixture immediately blue. Periodically, 20 μL samples were taken, diluted in air-

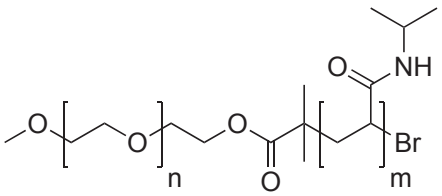

mPEG-pNIPAm

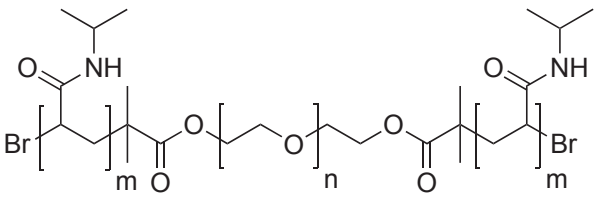

pNIPAm-PEG-pNIPAm

Figure 1. Structure of mPEG-pNIPAm and pNIPAm-PEG-pNIPAm. n = 44, n' ∈ {44, 90, 135}, m = 140.

saturated D_2O, and analyzed by ^1H NMR to determine the NIPAm conversion. When the conversion had reached 95%, the reaction was quenched by flushing with air for 1 min. The crude product was dialyzed against water overnight and subsequently freeze-dried. The yield was 90%.

The polymers were characterized by ^1H NMR with a Gemini 300 MHz spectrometer (Varian Associates Inc., NMR Instruments, Palo Alto, CA) and GPC. GPC was done using 2 PLgel 3 μm Mixed-D columns (Polymer Laboratories). The eluent was DMF containing 10 mM LiCl, the elution rate was set to 0.7 mL/min, and the temperature to 40 °C. Detection was done using a Viscotek TDA triple detector array. *dn*/*dc* was determined by the software based on the RI detector signal and the amount of injected polymer.

5.3.4. Formation of micelles

It has been shown that the size and polydispersity of thermosensitive micelles decrease with increasing the speed at which the cloud point (CP) is passed.[29] Therefore, micelles were formed by adding 100 μL of an aqueous polymer solution (1 mg/mL, at room temperature) to 900 μL water at 50 °C and equilibrating for 5 min. Using this "heat-shock" procedure, micelles having a small radius and low polydispersity were formed.

5.3.5. Determination of the Cloud Point (CP)

The CP's were determined by differential scanning calorimetry using a TA systems DSC-Q1000. The polymers were dissolved in a concentration of 3.3% in deionized water at room temperature. Samples of 10 μL were pipetted into aluminum pans which were subsequently hermetically closed, and the temperature was increased from 25 to 50 °C with 5 °C/min. The cloud point was taken as the onset point of the endotherm peak.

5.3.6. Determination of the Critical Micelle Concentration (CMC)

The CMC's of the block copolymers were measured using pyrene as a fluorescent probe.[30] The different block copolymers were dissolved in water in concentrations ranging from 1 μg/mL to 1 mg/mL. 15 μL of pyrene dissolved in acetone (1.8×10^{-4} M) was added to 4.5 mL of polymer solution. The micelles

were formed by rapidly heating the solutions to 45 °C. After incubation for 16 h at this temperature, pyrene fluorescence was measured using a Horiba Fluorolog fluorometer. Excitation spectra were recorded at 45 °C from 300 to 360 nm with the emission wavelength at 390 nm. The ratio I_{338}/I_{333} was plotted against the logarithmic polymer concentration to determine the CMC.

5.3.7. Dynamic Light Scattering (DLS)

DLS measurements were performed on a Malvern CGS-3 goniometer (Malvern Ltd., Malvern, U.K.) coupled to an LSE-5003 autocorrelator, a thermostated water bath, a He–Ne laser (25 mW, 633 nm, equipped with a model 2500 remote interface controller, Uniphase), and a computer with DLS software (PCS, version 3.15, Malvern). The measurement temperature was 40 °C, and the measurement angle was 90°. The solvent viscosity was corrected for the temperature by the software.

5.3.8. Static Light Scattering (SLS)

Static light scattering measurements were performed to determine the weight-average molecular weight of the micelles and the radius of gyration. Measurements were performed on an ALV 7002 correlator, ALV-SP/86 goniometer, RFIB263 KF photomultiplier detector with ALV 200 μm pinhole detection system and a Cobolt Samba-300 DPSS laser. The wavelength was set to 532 nm and the power to 300 mW, and the temperature was controlled by a Haake Phoenix II-C30P thermostatic bath. The second-order correlation function, $\Gamma_{2(t)}$, and total averaged scattered intensity were recorded 5 times per angle, for 21 angles, from 20° to 120° in increments of 5° to evaluate the angular dependence of the diffusion coefficient, D, and the excess Rayleigh ratio, R. This procedure was performed for five different concentrations near the CMC of the block copolymer. The SLS experiments were analyzed by a Zimm approximation (more details in the Supporting Information).

5.3.9. ^{1}H NMR relaxation measurements

For the relaxation measurements, micelles were formed using the above-mentioned heat-shock procedure as described under Formation of Micelles, with the exception that deuterium oxide was used as the solvent. T_1 and T_2 relaxation times were measured from 45 to 25 °C on

a Bruker 500 MHz spectrometer. At each temperature, a delay of 10 min allowed the stabilization of the sample temperature. The spin–lattice relaxation time, T_1, was studied by the inversion recovery method. The spin spin relaxation time, T_2, was studied by the Carr–Purcell–Meiboom–Gill pulse sequence. Relaxation times were obtained by nonlinear least-squares fitting of a monoexponential function except that T_2 values above the CP were determined by fitting a biexponential function.

5.4. Results and discussion

5.4.1. General properties of polymers

All polymerizations were well controlled (see Figure S1, Supporting Information). Table 1 summarizes the properties of the synthesized copolymers and their micelles. The molecular weights of the polymers agreed very well with the monomer/initiator feed ratio and their dispersity, as expected for a living polymerization, was low.

The CP's were higher than the well-known value of 32 °C for homopolymers of NIPAm. This is known to be due to the relatively short pNIPAm length of 16 kDa allowing the hydrophilic PEG to have a significant effect on the CP.[31, 32] The CMC of the different polymers was 0.02–0.03 mg/mL (Table 1), consistent with literature on mPEG-pNIPAm.[33] No significant differences in CMC were found between the diblock and triblock copolymers. This indicates that the expected effect of lowering the CMC by having two hydrophobic blocks in the BAB polymer is counteracted by the entropic penalty from the looped configuration of the PEG block. This unfavorable entropy contribution of the bending hydrophilic middle block was also reported in other studies, where triblock copolymers had even higher CMC's than corresponding diblock copolymers.[34, 35] Dynamic light scattering measurements showed that micelles of the triblock pNIPAm-PEG-pNIPAm polymers had a hydrodynamic radius (R_h) of 24–30 nm; the micelles of the diblock mPEG-pNIPAm revealed a significantly larger R_h of 35 nm (Table 1). The micelles remained stable for at least 24 h at 40 °C in water. The micelles were rather monodisperse as indicated by a polydispersity index

(PDI) < 0.1. Interestingly, the size of the flowerlike micelles decreases with increasing PEG length. We hypothesize that this is caused by an increased PEG "headgroup" area that causes less polymer chains to fit into one micelle.

Table 1. Characteristics of mPEG-pNIPAm and pNIPAm-PEG-pNIPAm Copolymers

	$M_{n,\,th}$[a] (kDa)	M_n[b] (kDa)	M_w/M_n[c]	CP[d] (°C)	CMC[e] (mg/mL)	R_h[f] (nm)	PDI[f]
$mPEG_{2K}$-$pNIPAm_{16K}$	18.0	18.2	1.03	36.2 ±0.1	0.03 ±0.01	35 ±2	0.04 ±0.02
$pNIPAm_{16K}$-PEG_{2K}-$pNIPAm_{16K}$	34.0	34.0	1.09	35.7 ±0.1	0.02 ±0.01	30 ±2	0.05 ±0.01
$pNIPAm_{16K}$-PEG_{4K}-$pNIPAm_{16K}$	36.0	35.7	1.14	36.7 ±0.1	0.02 ±0.01	27 ±2	0.08 ±0.03
$pNIPAm_{16K}$-PEG_{6K}-$pNIPAm_{16K}$	38.0	36.6	1.15	36.6 ±0.1	0.03 ±0.01	24 ±2	0.06 ±0.05

[a]Theoretical M_n, based on monomer/initiator ratio. [b]Determined by NMR. [c]Determined by GPC. [d]Determined by differential scanning calorimetry. [e]Determined from pyrene excitation spectra. [f]Measured with DLS at 0.1 mg/mL concentration, 40 °C and 90° scattering angle. Reported values are averages ±SD of three measurements.

5.4.2. Static Light Scattering

Static light scattering experiments were performed to investigate what effect the looped PEG conformation and the PEG length have on the surface area per PEG chain and aggregation number for the different micelles (Table 2). First of all, the R_g/R_h ratios (0.78–0.93) are within experimental errors similar for all micelles and are slightly higher than the value of $(3/5)^{1/2} = 0.775$ that can be calculated for a hard sphere.[36] This is compatible with micelles of which the corona is highly hydrated but still constitutes a significant fraction of the micelle's mass. When comparing the diblock $mPEG_{2kDa}$-$pNIPAm_{16kDa}$ with triblock $pNIPAm_{16kDa}$-PEG_{4kDa}-$pNIPAm_{16kDa}$, a 3.3 times lower aggregation number (N_{agg}) and 2.6 times higher surface area per PEG chain (S/N_{agg}) were found for the flowerlike micelles compared to the starlike micelles. In both cases, a factor of only 2 would be expected if the triblock would simply behave as a "double diblock". These findings can be explained by a looped conformation of the PEG chains in the flowerlike micelles, which forces them into a more mushroom- than brushlike conformation and therefore to

occupy a larger surface area. This in turn causes less pNIPAm chains to fit in the core of the micelle, as also represented by the lower overall density of the micelles composed of triblock copolymers as compared to those of diblocks.

Table 2. Characteristics of mPEG-pNIPAm and pNIPAm-PEG-pNIPAm Polymeric Micelles Measured by Simultaneous SLS and DLS

	R_g[a] (nm)	R_h[b] (nm)	R_g/R_h	$M_{w(mic)}$[b] (10^6 Da)	ρ_{mic}[c] (g/cm^3)	N_{agg}[d]	S/N_{agg}[e] (nm^2)
$mPEG_{2K}$-$pNIPAm_{16K}$	38 ±3	40 ±3	0.95 ±0.09	80 ±15	0.38 ±0.05	4426 ±818	4.8 ±0.9
$pNIPAm_{16K}$-PEG_{2K}-$pNIPAm_{16K}$	28 ±1	36 ±3	0.78 ±0.08	59 ±15	0.51 ±0.04	1745 ±432	9.4 ±0.8
$pNIPAm_{16K}$-PEG_{4K}-$pNIPAm_{16K}$	28 ±5	34 ±3	0.83 ±0.11	28 ±5	0.30 ±0.07	1324 ±535	12.5 ±4.2
$pNIPAm_{16K}$-PEG_{6K}-$pNIPAm_{16K}$	28 ±2	31 ±4	0.90 ±0.04	19 ±7	0.25 ±0.02	500 ±176	25.3 ±2.6

[a]Radius of gyration, extrapolated to zero concentration. [b]Extrapolated to zero concentration and zero scattering angle. [c]Density of the micelles. [d]Aggregation number of the micelles. [e]Surface area per PEG chain. All measurements were performed at 40 °C. Reported values are averages ±SD from three measurements.

Table 2 also shows that with increasing PEG block length the surface area per PEG chain in the flowerlike micelles increases and consequently their aggregation number decreases. Clearly, upon increasing the PEG molecular weight the PEG "headgroup" size thus increases not (only) in the radial direction but also in the tangential direction.

5.4.3. ^{1}H NMR Relaxometry

^{1}H NMR spectra were recorded for both $mPEG_{2kDa}$-$pNIPAm_{16kDa}$ and $pNIPAm_{16kDa}$-PEG_{4kDa}-$pNIPAm_{16kDa}$ at temperatures below and above the CP (Figure S2, Supporting Information). For both polymers, above the CP a clear loss of pNIPAm signals is visible while the integral of the PEG signal remains constant. This indicates the formation of micelles with a dense core and hydrated shell above the CP.[37] The PEG signal does, however, broaden at the base above the CP (see below). The micelles were further studied by ^{1}H NMR relaxation measurements, which provide a good measure of polymer chain flexibility.[38] Specifically, it has repeatedly been shown that restricting mobility of PEG chains leads to shorter T_2 times.[39, 40] To study

the relaxation behavior, ^{1}H NMR T_1 and T_2 relaxation measurements were performed at temperatures between 25 and 40 °C. All T_1 relaxation times were obtained from monoexponential fits (Figure S3, Supporting Information). The T_2 decay curves could also be well fitted by monoexponential decays below the CP ($R^2 > 0.99$). On the other hand, close inspection of the T_2 decay curves above the CP shows a deviation from monoexponential decay (Figure 2A), leading to low R^2 values for monoexponential fits. Instead, above the CP the decay of the PEG peak integral I with relaxation delay τ could be well fitted ($R^2 > 0.99$) by the biexponential equation

$$I_\tau = \left(f_{fast} \cdot e^{-\tau / T_{2\,fast}} + f_{slow} \cdot e^{-\tau / T_{2\,slow}} \right) \cdot I_0 \qquad \textbf{(1)}$$

yielding a fast (T_{2fast}) and slow (T_{2slow}) relaxation time. f_{fast} and f_{slow} represent the mole fractions of PEG protons that show fast and slow relaxation, respectively.

Although we do not expect the PEG chains to consist of well-separated segments each with a different T_2, but rather to show a gradient of T_2 times from the point of attachment to the pNIPAm core to the distal end, the experimental relaxation data could be well described by this simplification. This is also shown by the deconvolution of the PEG peak into a broad and a narrow peak (Figure 2B). As expected, the broad peak vanishes after a short relaxation delay τ, whereas the narrow peak decays more slowly.

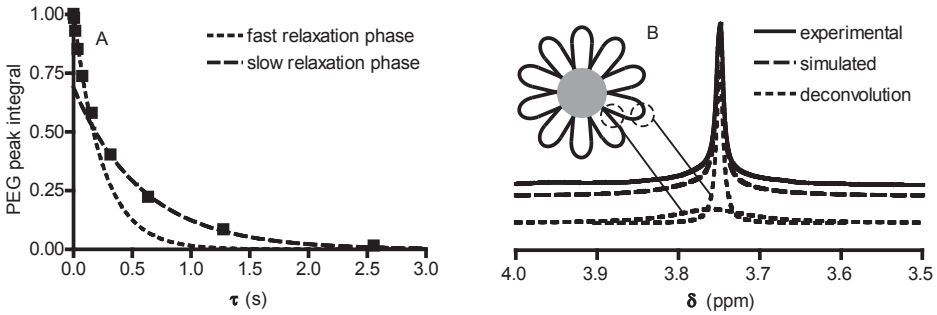

Figure 2. T_2 relaxation behavior of the PEG peak of $pNIPAm_{16kDa}$-PEG_{4kDa}-$pNIPAm_{16kDa}$ at 41 °C: (A) T_2 decay curve showing biphasic relaxation and (B) deconvolution of the PEG peak into a broad (fast relaxing) and narrow (slowly relaxing) component.

The appearance of a fast relaxing PEG fraction indicates the formation of more rigid, possibly less hydrated, segments[41, 42] which we assume to be the parts of the PEG chains that are closest to the micellar cores.[43]

The calculated relaxation times of diblock $mPEG_{2kDa}$-$pNIPAm_{16kDa}$ and triblock $pNIPAm_{16kDa}$-PEG_{4kDa}-$pNIPAm_{16kDa}$ are plotted in Figure 3 (other polymers in Figure S4, Supporting Information). The CP is clearly visible and appears about 1 °C higher in Figure 3 than in Table 1 due to the use of D_2O instead of H_2O.[44] Below the CP, the diblock and triblock show a similar linear relationship of T_1 and T_2 with temperature, with relaxation times that are typical for PEG in aqueous solution.[39, 41, 45, 46] Above the CP, however, there is a small difference in T_1 and a marked difference in T_2. As mentioned, the T_2 decay splits into a fast and slow component both for the diblock and the triblock copolymer. T_{2fast} is longer for the triblock compared to the diblock copolymer micelles (0.09 s *vs.* 0.06 s). This is probably a result of the different hydrodynamic radii of the two micelle types (27 nm *vs.* 35 nm). According to the Stokes–Einstein–Debye relation, this size difference causes the triblock copolymer micelles to have a shorter rotational correlation time than the normal micelles (12 μs *vs* 27 μs). For the parts of the PEG chains that are directly attached to the micellar core, rotational Brownian motion contributes significantly to T_2 relaxation. Therefore, T_{2fast} is longer for the (faster moving) triblock copolymer micelles.[47] On the other hand, the T_{2slow} of the triblock copolymer is

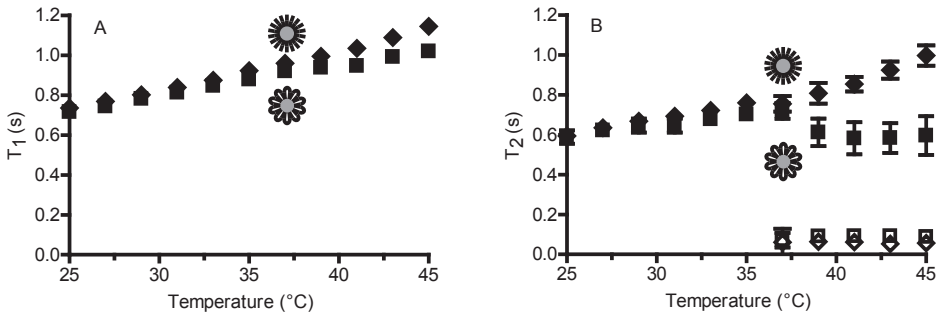

Figure 3. T_1 (A) and T_2 (B) relaxation times of protons in PEG for diblock $mPEG_{2kDa}$-$pNIPAm_{16kDa}$ and triblock $pNIPAm_{16kDa}$-$PEG_{4kDa}$$pNIPAm_{16kDa}$ as a function of temperature. Diamonds: diblock; squares: triblock. Error bars indicate the 95% confidence interval.

markedly shorter than the T_{2slow} of the diblock. As mentioned, we assume that T_{2slow} describes the relaxation of the distal parts of the PEG chains. The T_2 relaxation of these parts is reduced due to their high flexibility which leads to fast internal motions. Therefore, the observed difference indicates that the flexible distal part of PEG is less flexible in the flowerlike micelles formed by the triblock copolymer than in the starlike micelles formed by the diblock, caused by the formation of strained PEG loops in the former.

The relative contributions of PEG H atoms with fast and slow T_2 relaxation times, f_{fast} and f_{slow}, of the different block copolymers are shown in Figure 4. If the $pNIPAm_{16kDa}$-PEG_{4kDa}-$pNIPAm_{16kDa}$ triblock would behave as a double diblock, the same ratio between rigid and flexible chain segments would be expected as for the $mPEG_{2kDa}$-$pNIPAm_{16kDa}$ polymer.

However, all triblock copolymers clearly have a larger "rigid" fraction than the diblock copolymer. It is calculated that the diblock has one rigid segment of on average eight ethylene oxide (EO) units

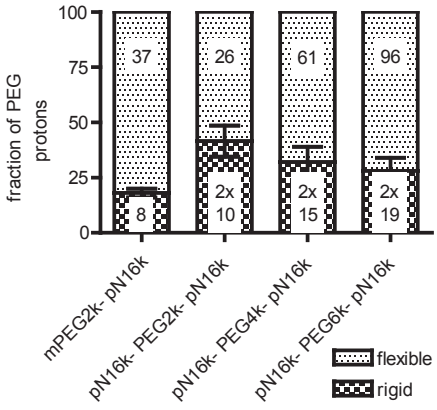

Figure 4. Vertical axis: relative mole fractions of rigid and flexible PEG chain segments for one diblock copolymer and three triblock copolymers measured at 41 °C. The numbers in the bars represent the length (in EO units) of these segments. Error bars represent the 95% confidence interval.

(18% of 45 units in total), whereas *e.g.* the PEG_{4kDa} triblock has two rigid segments of 15 EO units each (Figure 4). As expected, the relative amounts of flexible segments increase with increasing PEG length, although the absolute size of the rigid segments also increases slightly.

Taken together, these findings indicate that the PEG chains in the corona of the micelles can be regarded as having two parts: a rigid part that is directly attached to the micellar core, which has a fast T_2 decay, and a more flexible distal part, which has a slower T_2 decay.[46] In the flowerlike micelles the rigid part is larger and even the flexible part has a shorter T_2 than in the normal micelles (Figure 3), indicating that the PEG block in the flowerlike micelles is strained above the CP.

5.5. Conclusion

This work shows that the combination of NMR relaxometry and SLS provides a powerful way to probe the flowerlike conformation of triblock copolymer micelles experimentally. SLS indicated a major structural influence of the looping of the hydrophilic PEG block, whereas ^{1}H NMR T_2 relaxometry could be used to visualize the strain that this looping introduces into the PEG blocks. These data present a direct proof that flowerlike micelles exist and that they are distinctly different from starlike micelles.

Acknowledgment

The authors thank the SONNMRLSF in Utrecht, The Netherlands, for the use of a Bruker 500 MHz NMR spectrometer.

References

(1) Torchilin, V. P. *Cell. Mol. Life Sci*. **2004**, *61*, 2549-2559.

(2) Hu, X.; Jing, X. *Expert Opin. Drug Deliv*. **2009**, *6*, 1079-1090.

(3) Kumar, N.; Ravikumar, M. N.; Domb, A. J. *Adv. Drug Deliv. Rev*. **2001**, *53*, 23-44.

(4) Talelli, M.; Rijcken, C. J.; van Nostrum, C. F.; Storm, G.; Hennink, W. E. *Adv. Drug Deliv. Rev*. **2010**, *62*, 231-239.

(5) Chiappetta, D. A.; Sosnik, A. *Eur. J. Pharm. Biopharm*. **2007**, *66*, 303-317.

(6) O'Reilly, R. K.; Hawker, C. J.; Wooley, K. L. *Chem. Soc. Rev*. **2006**, *35*, 1068-1083.

(7) Read, E. S.; Armes, S. P. *Chem. Commun*. **2007**, *29*, 3021-3035.

(8) Oerlemans, C.; Bult, W.; Bos, M.; Storm, G.; Nijsen, J.F.; Hennink, W.E. *Pharm. Res*. **2010**, *27*, 2569-2589.

(9) Torchilin, V. P. *Pharm. Res*. **2007**, *24*, 1-16.

(10) Maeda, H.; Wu, J.; Sawa, T.; Matsumura, Y.; Hori, K. *J. Controlled Release* **2000**, *65*, 271-284.

(11) Owens, D. E. Peppas, N. A. *Int. J. Pharm*. **2006**, *307*, 93-102.

(12) Zhou, Z.; Chu, B. *Macromolecules* **1994**, *27*, 2025-2033.

(13) Chang, G.; Li, C.; Lu, W.; Ding, J. *Macromol. Biosci*. **2010**, *10*, 1248-1256.

(14) Honda, S.; Yamamoto, T.; Tezuka, Y. *J. Am. Chem. Soc*. **2010**, *132*, 10251-10253.

(15) Hua, S. -H.; Li, Y. -Y.; Liu, Y.; Xiao, W.; Li, C.; Huang, F. -W.; Zhang, X. -Z.; Zhuo, R. -X. *Macromol. Rapid Commun*. **2010**, *31*, 81-86

(16) Lee, E.S.; Oh, K.T.; Kim, D.; Youn, Y.S.; Bae, Y.H. *J. Controlled Release* **2007**, *123*, 19-26

(17) Gourier, C.; Beaudoin, E.; Duval, M.; Sarazin, D.; Maitre, S.; Francois J. *J. Colloid Interface Sci*. **2000**, *230*, 41-52.

(18) Creutz, S.; van Stam, J.; De Schryver, F. C.; Jerome, R. *Macromolecules* **1998**, *31*, 681-689.

(19) Xie, Z.; Lu, T.; Chen, X.; Lu, C.; Zheng, Y.; Jing, X. *J. Appl. Polym. Sci*. **2007**, *105*, 2271-2279.

(20) Balsara, N. P.; Tirrell, M.; Lodge, T. P. *Macromolecules* **1991**, *24*, 1975-1986.

(21) Linse, P. *Macromolecules* **1993**, *26*, 4437-4449.

(22) Sprakel, J.; Besseling, N. A.M.; Leermakers, F. A.M.; Cohen Stuart, M. A. *J. Phys. Chem. B* **2007**, *111*, 2903-2909.

(23) Giacomelli, F. C.; Riegel, I. C.; Petzhold, C. L.; da Silveira, N. P.; Stepanek, P. *Langmuir* **2009**, *25*, 3487-3493.

(24) Giacomelli, F. C.; Riegel, I. C.; Petzhold, C. L.; da Silveira, N. P.; Stepanek P. *Langmuir* **2009**, *25*, 731-738.

(25) Rodrigues, K.; Mattice, W. L. *Langmuir* **1992**, *8*, 456-459.

(26) Rodrigues, K.; Mattice, W.L. *Polym. Bull*. **1991**, *2*, 239-243.

(27) Schild H. G.; *Prog. Polym. Sci*. **1992**, *17*, 163-249.

(28) Ciampolini, M. and Nardi, N. *Inorg. Chem*. **1966**, *5*, 41-44.

(29) Neradovic, D.; Soga, O.; Van Nostrum, C.F.; Hennink, W.E. *Biomaterials* **2004**, *25*, 2409-2418

(30) Wilhelm, M.; Zhao, C.L.; Wang, Y.; Xu, R.; Winnik, M.A.; Mura, J.L.; Riess, G.; Croucher, M.D. *Macromolecules* **1991**, *24*, 1033-1040.

(31) Teodorescu, M.; Negru, I.; Stanescu, P. O.; Drăghici, C.; Lungu, A.; Sârbu, A. *React. Funct. Polym*. **2010**, *70*, 790-797.

(32) Xia, Y.; Yin, X.; Burke, N. A. D.; Stöver, H. D. H. *Macromolecules* **2005**, *38*, 5937-5943.

(33) Topp, M. D. C.; Dijkstra, P. J.; Talsma, H.; Feijen J. *Macromolecules* **1997**, *30*, 8518-8520.

(34) Van Butsele, K.; Cajot, S.; Van Vlierberghe, S.; Dubruel, P.; Passirani, C.; Benoit, J.; Jérôme, R.; Jérôme, C. *Adv. Funct. Mater*. **2009**, *19*, 1416-1425.

(35) Liu, T.; Kim, K.; Hsiao, B. S.; Chu, B. *Polymer* **2004**, *45*, 7989-7993.

(36) Aharoni, S. M. and Murthy, N. S. *Polym. Commun* **1983**, *24*, 132.

(37) Walderhaug, H. and Söderman, O. *Curr. Opin. Colloid Interface Sci*. **2009**, *14*, 171-177.

(38) Convertine, A. J.; Lokitz, B. S.; Vasileva, Y.; Myrick, L. J.; Scales, C. W.; Lowe, A. B.; McCormick, C. L. *Macromolecules* **2006**, *39*, 1724-1730.

(39) Cau, F. and Lacelle, S. *Macromolecules* **1996**, *29*, 170-178

(40) Poe, G.D.; Jarrett, W.L.;Scales, C.W.; McCormick, C.L. *Macromolecules* **2004**, *37*, 2603-2612.

(41) Bedu-Addo, F. K.;Tang, P.; Xu, Y.; Huang, L. *Pharm. Res*. **1996**, *13*, 710-717.

(42) Lüsse, S. and Arnold, K. *Macromolecules* **1996**, *29*, 4251-4257.

(43) Valentini, M; Napoli, A.; Tirelli, N.; Hubbell, J.A. *Langmuir* **2003**, *19*, 4852-4855.

(44) Ma, J.; Guo, C.; Tang, Y.; Xiang, J.; Chen, S.; Wang, J.; Liu, H. *J.Colloid. Interface Sci*. **2007**, *312*, 390-396.

(45) Heald, C. R.; Stolnik, S.; Kujawinski, K.S.; De Matteis, C.; Garnett, M. C.; Illum, L.; Davis, S. S.; Purkiss, S. C.; Barlow, R. J.; Gellert, P. R. *Langmuir* **2002**, *18*, 3669-3675.

(46) Garcia-Fuentes, M.; Torres, D.; Martín-Pastor, M.; Alonso M. J. *Langmuir* **2004**, *20*, 8839–8845.

(47) Törnblom, M.; Henriksson, U.; Ginley, M. *J. Phys. Chem*. **1994**, *98*, 7041-7051

5.6. Supporting information

5.6.1. Synthesis of block copolymers

The synthesis route of the triblock copolymers is depicted in Scheme S1. The synthesis of the diblock copolymer was analogous, using mPEG instead of PEG as starting material.

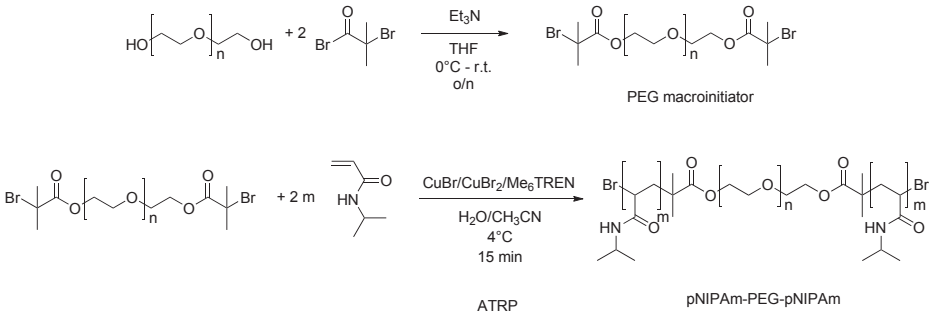

Scheme S1. Synthesis route and structure of pNIPAm-PEG-pNIPAm block copolymers

5.6.2. Detailed procedure for Static Light Scattering (SLS).

Static light scattering measurements were performed to determine the weight-average molecular weight of the micelles and the radius of gyration. Measurements were performed on an ALV 7002 Correlator, ALV-SP/86 goniometer, RFIB263KF Photo Multiplier Detector with ALV 200 μm Pinhole detection system and a Cobolt Samba-300 DPSS laser. The wavelength was set to 532 nm, power to 300 mW and the temperature was controlled by a Haake Phoenix II – C30P thermostatic bath. The intensity of scattered light was measured as a function of the wave vector

$$q = \frac{4\pi n_m}{\lambda}\sin\left(\frac{\theta}{2}\right) \qquad \textbf{(S1)}$$

with θ being the measurement angle, n_m the refractive index of the solvent and λ the wavelength of the light in vacuum.

The second-order correlation function, $\Gamma_2(t)$, and total averaged scattered intensity were recorded 5 times per angle, for 21 angles, from 20° to 120° in increments of 5° to evaluate the angular dependence of the diffusion coefficient, D, and the excess Rayleigh ratio, $R(q)$. This procedure was performed for five different concentrations above the CMC of the block copolymer.

The weight-averaged molecular weight M_w and the radius of gyration R_g were calculated based on the equation

$$\frac{K_R C}{R(q)} \approx \left(\frac{1}{M_w} + 2B_2 \frac{C}{M_w^2} \right) \left(1 + \frac{R_g^2}{3} q^2 \right) \quad \textbf{(S2)}$$

where C is the concentration, B_2 is the second virial coefficient and K_R is the optical constant, being

$$K_R \approx \frac{4\pi^2 n_m^2}{\lambda^4 N_{Av}} \left(\frac{dn}{dc} \right)^2 \quad \textbf{(S3)}$$

where dn/dc is the refractive index increment and N_{Av} is Avogadro's constant. dn/dc was calculated for each polymer based on the composition of the block copolymer and the dn/dc of pNIPAm (0.168) and PEG (0.132) in water.[S1]

The SLS experiments were analyzed by a Zimm approximation in which $K_RC/R(q)$ is plotted as a function of q^2 + Constant × C. $K_RC/R(q)$ was extrapolated both to zero concentration (C=0) and zero angle (q=0). The intercept of these two lines equals $1/M_w$. The radius of gyration, R_g, can be calculated from the slope of the concentration extrapolation. The density of the micelles was calculated by $\rho_{mic} = M_{w(mic)}/N_{Av}V$, where V is the average volume of the micelles, which can be calculated based on the hydrodynamic radius (R_h) determined by DLS. The aggregation number of micelles (N_{agg}) was calculated by dividing $M_{w(mic)}$ by the molecular weight of the polymers. The surface area per PEG chain (S/N_{agg}) was calculated by dividing S, the surface area of the shell of micelles calculated based on R_h, by N_{agg}.

5.6.3. Results

Kinetics of NIPAm ATRP

Millard *et al.* reported a controlled ATRP of NIPAm in water at low temperature.[S2] The ATRP of NIPAm in water only was found to be fast and uncontrolled, so termination could take place, yielding polymers with high dispersities. To prevent uncontrolled polymerization, a 4:1 water:acetonitrile solution was chosen and the reaction was performed at 4 °C, for which the reaction took approximately one hour to complete. Figure S1 shows the controlled/living characteristics of the NIPAm polymerization under these conditions. Figure S1A shows the pseudo first order kinetics of the polymerization. Figure S1B indicates that the molecular weight evolves linearly with conversion. Therefore, we conclude that a constant concentration of radicals was obtained and no termination by combination occurred. These results indicate that the polymerization of pNIPAm is well-controlled up to high conversion under the used conditions.

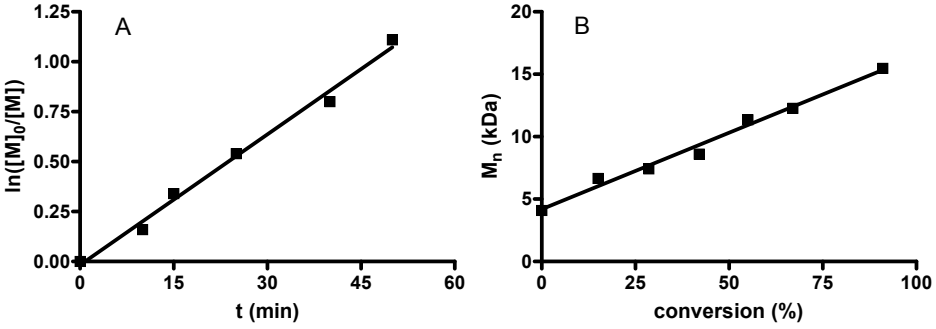

Figure S1. Kinetics of the ATRP of pNIPAm$_{16kDa}$-PEG$_{4kDa}$-pNIPAm$_{16kDa}$. A: Semilogarithmic time-conversion plot measured by ^{1}H NMR. B: Molecular weight-conversion plot measured by GPC.

NMR spectra above and below the CP

^{1}H NMR spectra were recorded in D_2O at 25 °C and 40 °C. A representative example is shown in Figure S2. Note the almost complete disappearance of the pNIPAM signals at 40 °C whereas the PEG peak integral remains constant. Although the integral of the PEG peak remains constant, its shape changes considerably. Above the CP the PEG peak is severely broadened at the base.

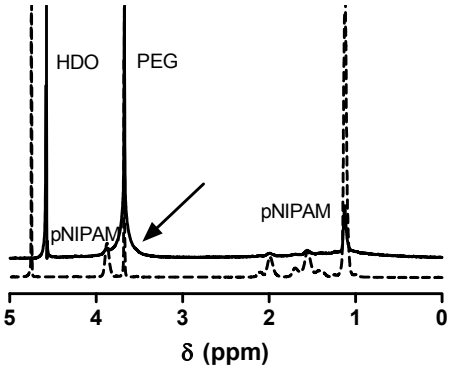

Figure S2. ^{1}H NMR spectra of pNIPAm-PEG-pNIPAm in D_2O (5 mg/mL) at 25 °C (dashed line) and 40 °C (solid line). The HDO peak shifts due to the temperature change. The arrow indicates the broadened base of the PEG peak at 40 °C.

T_1 and T_2 fits

T_1 and T_2 relaxation times were obtained by non-linear least squares fitting of a mono-exponential function (bi-exponential for T_2 above the CP). Figure S3 shows the T_1 and T_2 fits of PEG-pNIPAm diblock copolymer.

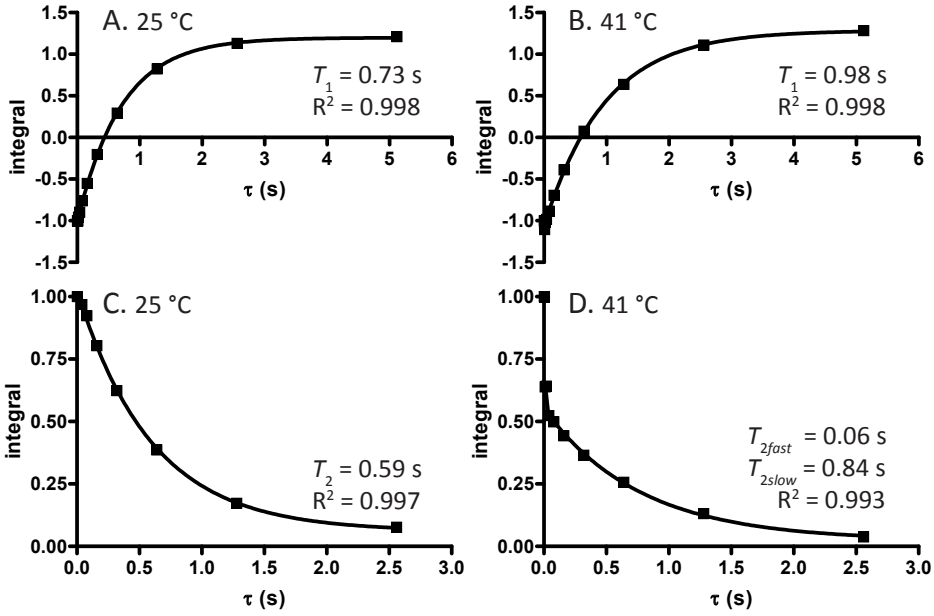

Figure S3. T_1 and T_2 exponential fits of the diblock $mPEG_{2kDa}$-$pNIPAm_{16kDa}$. Above the CP, a bi-exponential decay was fitted to the T_2 data; all other fits are mono-exponential.

All R^2 values of the fits were higher than 0.99. When applying a bi-exponential fit to the T_2 relaxation data below the CP, f_{fast} became negligibly small which justifies the use of mono-exponential fits below the CP.

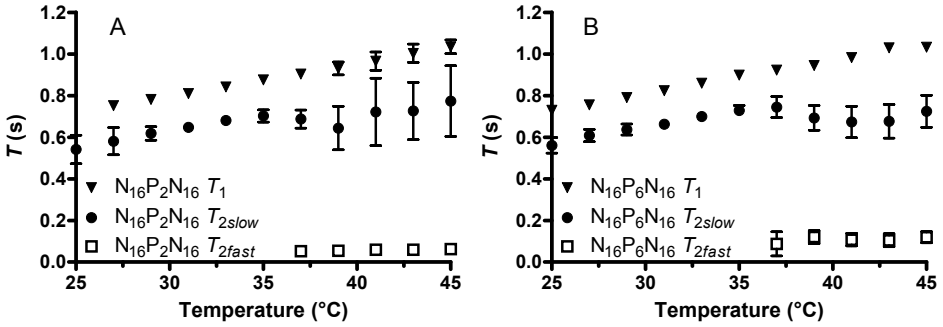

Figure S4. T_1 and T_2 relaxation times of PEG protons in (A) $pNIPAm_{16kDa}$-PEG_{2kDa}-$pNIPAm_{16kDa}$, and (B) $pNIPam_{16kDa}$-PEG_{6kDa}-$pNIPAm_{16kDa}$ as a function of temperature. Error bars indicate the 95% confidence interval.

5.6.4. Supporting References

(S1) Virtanen, J.; Baron, C.; Tenhu, H.: Grafting of poly(N-isopropylacrylamide) with poly(ethylene oxide) under various reaction conditions. *Macromolecules* **2000**, *33*, 336-341

(S2) Millard P-E.; Mougin N. C.; Böker, A.; Müller, A. H. E.: Fast ATRP of N-isopropylacrylamide in water and its application to bioconjugates . *Polym. Prepr*. **2008**, *49*, 127-137

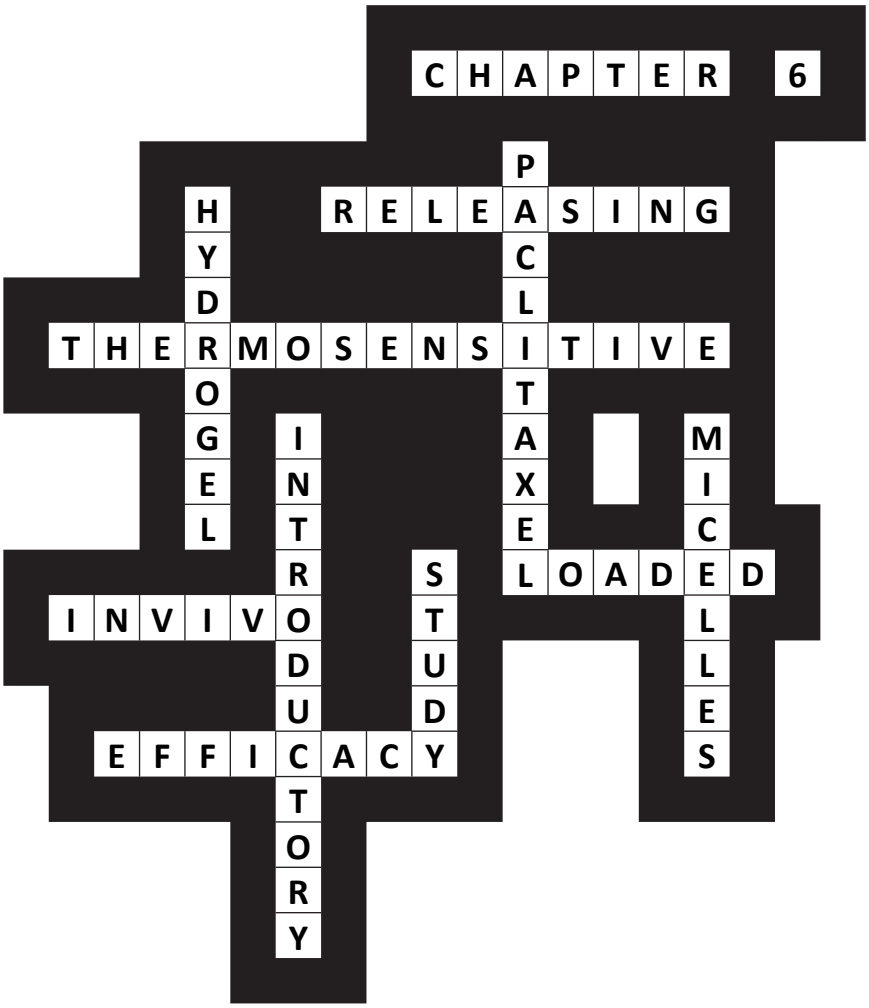

A thermosensitive hydrogel releasing paclitaxel-loaded micelles: an introductory in vivo efficacy study

Albert J. de Graaf, Inês I. Azevedo Próspero dos Santos, Ebel H. E. Pieters, Dirk T. S. Rijkers, Cornelus F. van Nostrum, Tina Vermonden, Robbert J. Kok, Wim E. Hennink and Enrico Mastrobattista

Abstract

In this chapter it is shown that when a hydrogel is transferred into water, it starts to release flower-like micelles. Experiments showed that micelles were continuously released as long as the medium was regularly refreshed. On the other hand, if the medium was not refreshed an equilibrium concentration of micelles was reached. When a gel was loaded with the cytostatic agent paclitaxel (PTX), micelles released in water were able to solubilize PTX, as evidenced by a PTX concentration in the release medium above its aqueous solubility. To test the applicability of these micelle-releasing gels for the delivery of cancer chemotherapeutics, an *in vivo* pilot experiment was performed. poly(*N*-isopropylacrylamide)-poly(ethylene glycol)-poly(*N*-isopropylacrylamide) gels (without and with 1.2% and 6.0% PTX loading) were administered *i.p.* in nude mice bearing 14C human squamous cell carcinoma tumor xenografts to obtain doses corresponding to 1× and 5× the maximum tolerated dose that has been determined for PTX when given *i.v.* as the standard formulation in Cremophor EL/ethanol. All gel formulations were well tolerated. After injection of the highest dose, PTX levels in serum could be determined for 48 h with a comparatively long elimination half-life of 7.4 h. These observations indicate a sustained release of PTX. A bioavailability of 100% was calculated from the area under the curve of plasma concentration *vs* time. Furthermore, at the highest dose, PTX was shown to completely inhibit tumor growth for at least 3 weeks with a single hydrogel injection. This promising concept may find application as a depot formulation of passively targeted anticancer drugs.

6.1. Introduction

The objective of the work presented in this chapter was to develop a drug-loaded thermosensitive hydrogel which slowly interconverts into drug-loaded polymeric micelles. The released micelles can solubilize a hydrophobic drug: the release kinetics of the drug are therefore likely controlled to a large extent by the dissolution rate of the gel.

This concept emerged from the notion that hydrophobic-hydrophilic-hydrophobic (BAB) triblock copolymers can self-assemble into hydrogels as well as flower-like micelles, depending on their concentration.[1-10] Polymeric micelles are widely studied as drug delivery vehicles for low-molecular weight hydrophobic drugs,[11-16] whereas (self-assembling) hydrogels are under investigation as depot formulations for various drugs, especially proteins.[17, 18] It has been shown in a number of studies that at high concentrations of BAB block copolymers in water there is always an equilibrium between a gel (consisting of bridged micelles) and free micelles.[7-9] This equilibrium implies that, if such a hydrogel would be formed *in vivo*, it will release micelles over time.

Recently, there have been a number of reports on hydrogel/micelle composite systems, *i.e.* hydrogels which release micelles that were made of different materials and were incorporated into the hydrogel.[19-22] Two hydrogel systems have been described that can be degraded by glutathione, leaving behind polymeric micelles made of the same material as the parent gel.[23, 24] However, in the latter publications this micelle formation was only noted as a peculiarity and was not discussed in terms of applicability for making a gradually releasing micellar drug delivery system. No papers have been published yet, which describe a drug-loaded hydrogel that gradually and spontaneously interconverts into drug-loaded micelles.

It might be envisioned that such a system is beneficial for the delivery of cytostatic drugs, as (i) it could reduce the often used long infusionsto a single injection and (ii) cytostatic drugs have repeatedly shown a longer plasma half-life and increased tumor accumulation (due to the enhanced permeability and retention effect) when formulated in polymeric micelles as compared to the free drugs.[11-16, 25-27] Furthermore, over the last decade there has been an increasing interest in the use of so-called metronomic dosing schedules for chemotherapeutics. With metronomic dosing a continuous (up to weeks)

dose of one or more chemotherapeutic agents is given at a rate which is much lower than for conventional chemotherapy. It has been shown that, when given in this way, many cytostatic agents have an additional beneficial anti-angiogenic effect.[28-31] A hydrogel, which continuously releases cytostatics for a long time could be advantageous in such a metronomic therapy.

In the present study, poly(*N*-isopropylacrylamide)-poly(ethylene glycol)-poly(*N*-isopropylacrylamide) (pNIPAm-PEG-pNIPAm) thermosensitive block polymers were used as model polymers for the investigation of the release of flower-like micelles from thermosensitive (in situ gelling) hydrogels. The lower critical solution temperature of pNIPAm (32 °C) allowed dissolution of the polymers at room temperature and gel formation at 37 °C. Furthermore, these polymers have already been shown to form gels at high concentrations and flower-like micelles at low concentrations.[32, 33]

The hydrogels were loaded with the cytostatic drug paclitaxel (PTX), which is frequently used to treat patients suffering from breast- or ovarian cancer.[34] It is a suitable candidate for metronomic dosing since it is effective at low concentrations[35-38] and it has been shown to be anti-angiogenic at low, prolonged concentrations (10 ng/mL for 3 days *in vitro*).[29, 34, 39]

In this paper, we report the *in vitro* release of micelles and PTX from pNIPAm-PEG-pNIPAm gels. Furthermore, release kinetics and efficacy were studied in an *in vivo* mouse model. As route of administration for the PTX-loaded hydrogels, *i.p.* injection was chosen as it allowed administration of a suitable amount of hydrogel leading to rapid in situ gel formation. PTX *i.p.* is under investigation as local therapy for ovarian cancer,[40, 41] but there are several reports that after *i.p.* injection PTX is also able to reach the systemic circulation via the lymphatic system, with reported bioavailabilities between 5% and 37%.[37, 42-45] When used as local therapy, high plasma levels of PTX are considered undesirable. Only recently, a sustained systemic release after *i.p.* injection of the related compound docetaxel, was recognized as advantageous for treatment of distal metastases.[46] Based on these data, we hypothesize that PTX, solubilized in micelles that are released from a gel, can be transported to the circulation and has an effect on tumor growth.

6.2. Experimental methods

6.2.1. Synthesis of polymers

Chemicals

PEG with molar mass of 6000 Da was purchased from Merck and dehydrated prior to use by azeotropic distillation of water using toluene. *N*-isopropylacrylamide (NIPAm; Aldrich, >99%), 2-bromoisobutyrylbromide (Aldrich), CuBr (Aldrich) and $CuBr_2$ (Acros) were used as received. Tris(2-dimethylaminoethyl)amine (Me_6TREN) was prepared according to a reported procedure.[47]

Synthesis of PEG initiator

The synthesis is summarized in Scheme 1. Dehydrated PEG (5.0 g) was dissolved in 50 mL of dichloromethane (CH_2Cl_2) dried on molecular sieves and degassed by flushing with nitrogen. The flask was put in an ice bath and subsequently 1.2 eq triethylamine (to –OH groups) and 1.2 eq 2-bromo-isobutyrylbromide (to –OH groups) were added. The mixture was allowed to react overnight at room temperature. Afterwards, dichloromethane was removed *in vacuo*. Tetrahydrofuran (THF, 50 ml) was added and the bromide salt was filtrated off. The filtrate was concentrated *in vacuo* and dissolved in a minimum amount of dichloromethane. The crude product was precipitated in cold diethylether and then centrifuged (1000× g, 5 min, 4 °C) and the obtained white precipitate was filtrated and dried by flushing with nitrogen to yield a white powder. The product was further dried overnight in a desiccator. ^{1}H NMR analysis was performed after drying. A second spectrum was recorded after adding two droplets of trichloroacetyl isocyanate to the sample to derivatize the unreacted OH-groups and thereby enable determination of the degree of substitution.

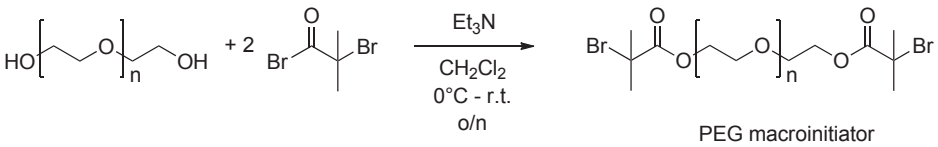

Scheme 1. Synthesis of PEG macroinitiator.

The final yield was 85%. ^{1}H NMR spectrometry indicated that 85% of the PEG –OH groups were functionalized and no excesss 2-bromo-isobutyrylbromide was left. ^{1}H NMR (300 MHz, $CDCl_3$): δ 4.32 ppm (t, 4H, OCH_2), δ 3.63 ppm (t, 4nH, OCH_2), δ 1.93 ppm (s, 12H, $C(CH_3)_2$).

Synthesis of pNIPAm-PEG-pNIPAM

The polymerization reaction is summarized in Scheme 2. Screw-capped septum vials with the following content were prepared: 0.3 g of PEG_{6000} macroinitiator (0.05 mmol PEG; 0.1 mmol initiating sites), 9.0 mg CuBr, 9.4 mg $CuBr_2$ and 1.6 g or 3.2 g NIPAm (target M_n: 16000 Da resp. 32000 Da). A stirring bar was introduced in each vial and the vials were capped with a septum. The solutions were degassed by flushing with N_2 and placed in an ice bath. When NIPAm was dissolved, the reaction was started by adding 0.25 mL 0.42 M Me_6TREN solution in water (degassed by flushing with N_2 prior to addition), which immediately turned the reaction mixture blue. Periodically, 20 μL samples were taken, diluted in air-saturated D_2O and analyzed by ^{1}H NMR to determine the NIPAm conversion. When the conversion had reached >95%, the reaction was quenched by flushing with air for several minutes. The crude product was dialyzed (with dialysis cassettes of 10,000 Da MWCO) against water at 4 °C overnight and subsequently lyophilized.

The polymers were characterized by ^{1}H NMR with a Varian Mercury Plus 300 MHz NMR instrument and by GPC. GPC was performed using Mixed-D columns (Polymer Laboratories), a solution of 10 mM LiCl in DMF as eluent, a flow of 0.7 mL/min and a temperature of 40 °C. A refractive index detector was used and linear PEG standards were used for calibration.

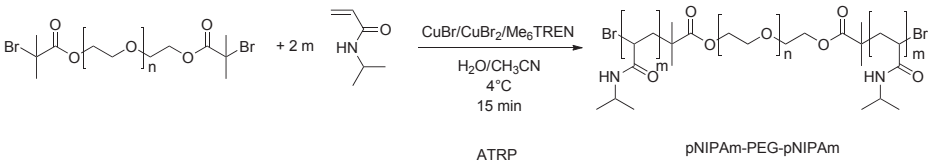

Scheme 2. Schematic representation of polymerization reaction of NIPAm onto the PEG macroinitiator.

6.2.2. Characterization of polymers and gels

Determination of the CP

Samples of the polymers were prepared at a concentration of 1 mg/mL in water and phosphate-buffered saline (PBS). A Shimadzu UV 2450 spectrophotometer equipped with a Peltier heating element was used with the Tm analysis software to measure the CP at a wavelength of 650 nm, raising the temperature from 20 °C to 50 °C at 1 °C/min.

DLS

Micelles were formed by a heat shock procedure.[48] In short, an aqueous polymer solution (100 μL, 1 mg/mL) at room temperature was added to 900 μL of water which was pre-heated to 50 °C. The micellar dispersions were equilibrated at 40 °C for 5 min before being measured in a Malvern CGS-3 goniometer (Malvern Ltd., Malvern, U.K.) coupled to an LSE-5003 autocorrelator, a thermostated water bath (set to 40 °C), a He-Ne laser (25 mW, 633 nm, equipped with a Uniphase 2500 remote interface controller,) and a computer with DLS software (PCS, version 3.15, Malvern). The measurement angle was 90°. The solvent viscosity was corrected for the temperature by the software.

Gel formation

For all gels, unless noted otherwise, the following procedure was used. Polymer was dissolved to a final concentration of 25% (w/w) in water. This concentration was chosen because it offers a suitable balance between fluidity at room temperature, gelation kinetics and gel strength above the CP. The required volume of polymer solution was placed on the bottom of a vial and kept for 10 min at 50 °C in a water bath, before being equilibrated at 37 °C.

Temperature-sweep rheology

To study the gel formation, 60 μL of a polymer solution (25% (w/w) in water or PBS) was introduced into an AR-G2 rheometer (TA Instruments Ltd) equipped with a Peltier plate for temperature control using a cone-plate geometry (steel, 20 mm diameter with an angle of 1°) and Rheology Advantage Instrument Control AR software. A solvent trap was used to prevent evaporation of the solvent. The storage (G') and loss (G'') moduli

were measured for a range of temperatures from 20 °C to 60 °C with a heating rate of 1 °C/min. A strain of 1% and a frequency of 1 Hz were used. The data were analyzed through Rheology Advantage Data Analysis software.

Temperature-dependent NMR analysis of gels

To investigate whether the hydrogels can indeed be regarded as an assembly of flower-like micelles with bridged chains, ^{1}H NMR spectra of the polymer solution or gels (25% (w/w) in D_2O) were recorded at 25 °C and 40 °C, respectively.

6.2.3. *In vitro* release

Imaging the release of micelles from in situ formed gels

One mL of filtered demineralized water was equilibrated at 40 °C in the measurement chamber of a Nanosight LM14-HS laser light scattering microscopy system equipped with a 532 nm laser and an actively cooled EMCCD camera. Approximately 0.1 mL of a 25% (w/w) aqueous solution of polymer of around 20 °C was injected to form a hydrogel in situ, comparable to the way a hydrogel would be formed upon *i.p.* injection *in vivo*. Diffusion of the micelles released from the gel was followed in time, and their size distribution was determined from their Brownian motion using nanoparticle tracking analysis (NTA) software.

Release kinetics of micelles from gels measured with DLS

Hydrogels were formed by heating 50 μL of a 25% (w/w) polymer solution from room temperature to 50 °C. After 10 minutes, 2 mL of PBS (filtered through 0.2 μm and preheated to 37 °C) was added to the hydrogel. Samples of 1 mL were collected every 15 minutes and transferred into a pre-heated DLS cuvette, and the initial solution was refilled with 1 mL of pre-heated PBS to maintain the volume. The samples were analyzed by DLS measurements at 40 °C.

Loading of the gel with PTX

An aqueous polymer solution (6 mL, 50 mg/mL) was filtered through a 0.2 μm filter. To the polymer solution (at room temperature) was quickly added the required volume of a 30 mg/mL solution of PTX in CH_3CN by a microliter syringe. Either 0, 120 or 600 μL was added

to yield PTX/polymer ratios of 0.0%, 1.2% and 6.0% (w/w), respectively. The mixture was briefly vortexed, after which an equal volume of sterile filtered water (preheated to 60 °C) was added at once. The resulting micellar dispersion was again briefly vortexed and equilibrated at 40 °C in a water bath for 15 min. Then, the micellar dispersion was snap-frozen by transferring it dropwise to a 50 mL polypropylene tube filled with liquid nitrogen. The resulting ice beads were freeze dried for 48 h and stored at -20 °C until use. Just before the experiment, the freeze dried micelles were allowed to thaw and dissolved in sterile-filtered water (900 µL) at room temperature. Air bubbles were removed by shortly keeping the tube in an ultrasonic bath. The gels without or with 1.2% PTX loading were clear, whereas the gel with 6.0% PTX loading had a slight bluish tinge.

Release of PTX in water

A volume of $N_{16}P_6N_{16}$ gel (20 µL) loaded with PTX (1.2% (w/w) to polymer) was prepared as described above. Then, water of 40 °C (1 mL) was placed on top. After 1, 2 and 3 h the concentration of PTX in the supernatant aqueous phase was determined as described below.

In vitro release of PTX in serum

Gels were loaded with PTX as described in the previous section. A volume of gel (10 µL) was brought into 200 µL bovine serum which was preheated to 37 °C. The vials were shaken at 37 °C in a water bath. Every 15 min half of the serum was removed and replaced with fresh, preheated serum. PTX concentration in the samples was determined as described below.

Analysis of PTX by UPLC

CH_3CN (40 µL) was added to each sample (20 µL). The samples were vortexed for 10 seconds and centrifuged for 5 min at 12,000 rpm, 4 °C to remove precipitated plasma components. PTX amounts were determined by UPLC on a Waters Acquity UPLC system using a Waters HSS T3 1.7 µm, 2.1 × 50 mm column at 50 °C. The eluent was CH_3CN/H_2O/HCOOH 45/55/0.1 (v/v) at a flow rate of 1 mL/min. After each run of 4 min the column was cleaned for 1.5 min with CH_3CN/H_2O/HCOOH 90/10/0.1 (v/v) at 1 mL/min (ramp times 0.5 min) and re-equilibrated for 2.5 min with the starting eluent. Per sample, 7 µL was

injected. PTX was detected at awavelength of 227 nm. Calibration was done using standard solutions of PTX (0.05-20 μg/mL) in CH_3CN. In every sample set, a recovery test of PTX from spiked serum was included. Observed recoveries were consistently between 90-110%.

6.2.4. *In vivo* experiment

In vivo release of PTX

The animal experiment was performed in accordance with local regulations and with consent of the local animal welfare committee. 14C cells (human head and neck squamous cell carcinoma cells, 1×10^6 in 0.1 mL cold PBS) were injected *s.c.* into the flank of female CD1-Foxn1 nude mice. When tumors had become palpable (average tumor volume 37 mm^3), the mice were divided over three groups (5 mice per group). Each mouse received an *i.p.* injection of 200 μL of a 25% (w/w) solution of $N_{16}P_6N_{16}$ at room temperature containing 0%, 1.2% or 6% PTX (w/w relative to polymer). These amounts correspond to 0, 20 or 100 mg/kg body weight and to 0×, 1× or 5× the maximum tolerated dose (MTD) of PTX in mice when it is given as *i.v.* injection formulated in cremophor EL/ethanol.[43] After 1 h, 5 h, 24 h and 48 h, blood samples (approx. 200 μL) were obtained via cheek punction (2 mice per group per time point), collected in K_4-EDTA tubes and kept on ice. Within 30 minutes, the samples were centrifuged for 10 min at 10,000 rpm, 4 °C. The supernatant plasma was stored at -20 °C until analysis. PTX concentrations in plasma were determined by UPLC as described above. The equation

$$\ln(C_t) = \ln(C_0) - k \cdot t \qquad \textbf{(1)}$$

was fitted by a linear least squares method to the plasma concentrations C_t at timepoints t = 5 h, 24 h and 48 h of the high dose PTX formulation. From the obtained rate constant k, the half-life of the plasma concentrations $t_{½}$ was calculated as

$$t_{½} = \frac{\ln(2)}{k} \qquad \textbf{(2)}$$

The area under the curve (AUC) was calculated using the trapezoidal approximation. From the AUC and the given dose D, the bioavailability F was estimated using 2.5 $L \cdot h^{-1} \cdot kg^{-1}$ as a reference value for the clearance Cl of PTX:[49,50]

$$F = \frac{AUC}{D} \cdot Cl \quad \textbf{(3)}$$

Measurement of the effect on tumor growth

Tumor growth was monitored daily using digital calipers. By measuring the largest diameter l and the smallest diameter b, tumor volume V could be estimated as

$$V = \tfrac{1}{2} l \cdot b^2 \quad \textbf{(4)}$$

Tissue homogenization

The excised tissue was transferred into a 2 mL polypropylene tube containing zirconia beads. Cold phosphate buffer (100 μL of 0.5 M, pH 7.4) was added and the tube was placed in a Precellys 24 homogenizer. A program consisting of 3 runs of 20 s at 5000 rpm, with 5 s between the runs, was used to homogenize the tissue. After homogenization, CH_3CN (200 μL) was added, the tube was vortexed and then centrifuged for 5 min at 12,000 rpm. The supernatant was analyzed as described above.

6.3. Results and discussion

6.3.1. Synthesis of polymers

The characteristics of the triblock polymers are summarized in Table 1. Molecular weights corresponded to the calculated values based on the feed and the dispersities were rather narrow, as expected for polymers synthesized by controlled radical polymerization.

Table 1. Characteristics of the synthesized pNIPAm-PEG-pNIPAm copolymers.

Polymer	$M_{n\ (th)}$ [a] (kDa)	M_n [b] (kDa)	$Đ$ [c]
$pNIPAm_{16kDa}$-PEG_{6kDa}-$pNIPAm_{16kDa}$ ($N_{16}P_6N_{16}$)	38.0	38.2	1.36
$pNIPAm_{32kDa}$-PEG_{6kDa}-$pNIPAm_{32kDa}$ ($N_{32}P_6N_{32}$)	70.0	69.8	1.45

[a]Theoretical M_n based on monomer/initiator ratio. [b]Determined by ^{1}H NMR. [c]Dispersity, determined by GPC.

6.3.2. Characterization of polymers and gels

Self-assembly behavior of the polymers

The properties of gels and micelles formed from the synthesized polymers are summarized in Table 2.

The CP of $N_{32}P_6N_{32}$ was lower than the CP of $N_{16}P_6N_{16}$ (33.0 *vs.* 35.2 °C in PBS). It has been shown before that the effect of a coupled hydrophilic PEG block on the thermal properties becomes significant for polymers containing small pNIPAm blocks.[32, 33] For both polymers it can be observed that the presence of ions (as in PBS) leads to a decrease in CP of around 2.5 °C due to salting out. The polymers self-assembled into micelles above their CP and above their critical micelle concentration, which is 0.03 mg/mL for $N_{16}P_6N_{16}$.[33] Micelles of $N_{32}P_6N_{32}$ were slightly larger than those of $N_{16}P_6N_{16}$ (24 *vs* 23 nm in PBS). Furthermore (mainly for $N_{32}P_6N_{32}$) using PBS leads to an increase in hydrodynamic radius R_h, probably due to a decrease in hydration of the PEG chains leading to an increased aggregation number per micelle.

Table 2. Characteristics of micelles and gels of the polymers.

Polymer	Diluent	CP (°C)	R_h [a] (nm)	$T_{onset,visc}$	GP (°C)	G', G'' [b] (kPa)
$N_{16}P_6N_{16}$	PBS	35.2	24±1	30.5	36.1	2.5
	Water	37.7	23±1	35.0	40.4	1.7
$N_{32}P_6N_{32}$	PBS	33.0	39±1	30.5	32.6	0.8
	Water	35.8	24±1	34.0	36.0	0.8

[a]at 40 °C; [b]at the GP

When 25% (w/w) polymer solutions were heated (Figure 1), at a certain temperature ($T_{onset,visc}$) the viscosity started to increase rapidly. Upon further heating, a gel point (GP) was reached, defined here as the point where tan δ ≡ G"/G' became smaller than 1. For both polymers, the GP (as well as the CP) was below 37 °C in PBS. The dependency of GP and $T_{onset,visc}$ on the polymer composition and diluent was the same as for the CP, with GP ≥ CP > $T_{onset,visc}$ (Table 2). Due to its larger hydrophobic character, the $N_{32}P_6N_{32}$ gel in PBS started to partly dehydrate at temperatures above 34 °C, causing it to lose contact with the rheometer (Figure 1).

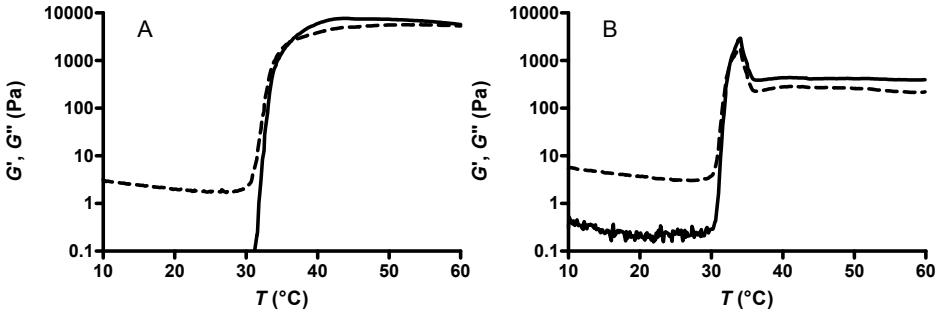

Figure 1. Rheograms of 25% (w/w) gels of (A) $N_{16}P_6N_{16}$ and (B) $N_{32}P_6N_{32}$, in PBS as a function of temperature. Solid lines: storage modulus (G'), dashed lines: loss modulus (G").

Gels of $N_{16}P_6N_{16}$ were translucent, whereas those made of $N_{32}P_6N_{32}$ had a white appearance (Figure 2), possibly because the "micelles" in the gel are more strongly dehydrated.

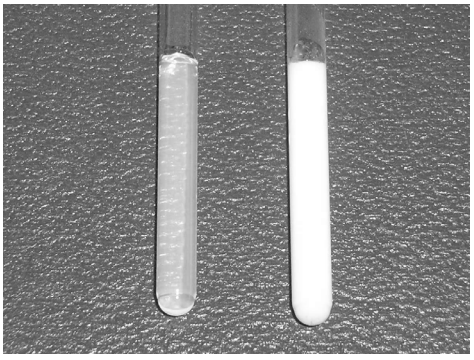

Figure 2. Gels formed by heating 25% (w/w) solutions of $N_{16}P_6N_{16}$ (left) and $N_{32}P_6N_{32}$ (right) in water to 40 °C.

Temperature-dependent NMR of gels

^{1}H NMR spectra of the polymer solutions at 25 °C and the gels at 40 °C are shown in Figure 3. As the ratio between the integrals of the PEG peaks and the HDO peaks at 40 °C is equal to the ratio at 25 °C, it can be concluded that in both gels the PEG chains are still fully hydrated above the GP. In contrast, the signals of the core-forming pNIPAm segments almost completely disappeared above the GP indicating that the pNIPAm segments self-assembled in hydrophobic domains. For both polymers at 40 °C the PEG peak has a narrow top (caused by a long T_2) and a broad base (caused by a short T_2) corresponding to observations of dilute dispersions of pNIPAm-PEG-pNIPAm flower-like micelles. The narrow top and broad base have been attributed to the PEG segments which are distal and proximal (respectively) to the cores of the flower-like micelles.[33]

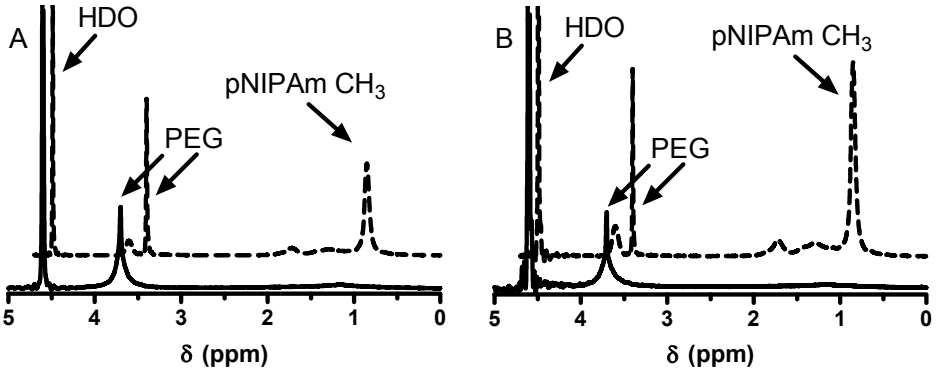

Figure 3. ^{1}H NMR spectra (in D_2O) of 25% (w/w) solutions of (A) $N_{16}P_6N_{16}$ and (B) $N_{32}P_6N_{32}$. Dashed traces: 25 °C (shifted 0.3 ppm upfield for clarity), solid traces: 40 °C.

6.3.3. *In vitro* release

Imaging the release of micelles from in situ formed gels

Upon slow injection of the polymer solutions into the pre-heated (40 °C; above the LCST of the NIPAm blocks) measurement chamber of the Nanosight apparatus, instantaneous gel formation was observed. The intenisity of scattered laser light was monitored and Figure 4 shows that after 10 min increased scattering was observed close to the gel edge, diffusing from the gel in time. This observation indicates that micelles are present in the aqueous phase that is in direct contact with the gel. The

size distribution of the micelles was determined from their Brownian motion (Figure 6 B, C) once they reached the detection spot and showed homogeneous distributions of particles with average diameters of 86 nm ($N_{16}P_6N_{16}$) and 91 nm ($N_{32}P_6N_{32}$). Converted to hydrodynamic radius, this corresponds to R_h = 43 and 46 nm, *i.e.* about 2 times larger than the values found for dilute, heat-shocked dispersions of micelles.

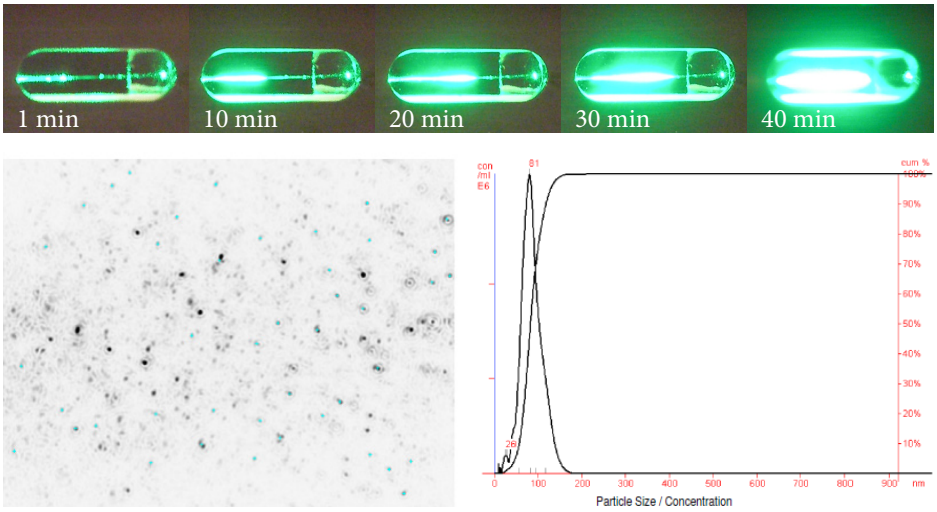

Figure 4. Release of micelles from an *in situ* formed gel of $N_{16}P_6N_{16}$. (A) Diffusion of the micelles from the hydrogel (from left to right). The hydrogel is positioned on the far left, outside the visible area. The area on the right side is the entry point of the laser beam. (B) Microscopic image of the light scattering by individual micelles released from the in situ formed gel. The apparent particle size in this image reflects the scattering intensity of the particles rather than their actual size. (C) Size distribution of the released micelles as calculated by nanoparticle tracking analysis software.

This finding may indicate that a significant proportion of the released micelles are still 'bridged', which is a normal phenomenon for flower-like micelles unless they are observed at very low concentrations (such as in the DLS experiment). In addition, the lower threshold of the NanoSight system (approximately 40-60 nm) may have attributed to a higher average size distribution compared to DLS (Table 2).

Release kinetics of micelles from gels measured with DLS

To mimic physiological conditions, the release kinetics of micelles from the gels was studied in PBS. When gels were brought into PBS (pre-heated to 37 °C), release of micelles could be observed by eye after approximately 1 h (Figure 5).

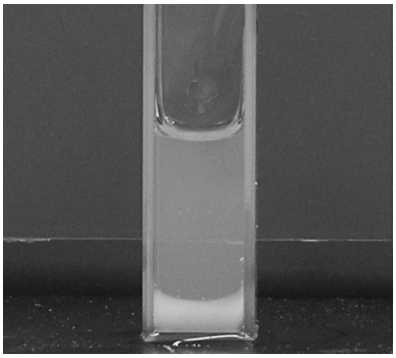

Figure 5. Release of micelles from the $N_{16}P_6N_{16}$ gel (at the bottom of the tube) in PBS at 37 °C. The Rayleigh scattering which is observed above the gel indicates the presence of micelles.

When the medium was refreshed every 15 min, it was observed by DLS that every time new micelles were released. The amount of released micelles (as indicated by the ratio of scattered versus incident light) increased during the first 1.5 h (6 medium refreshings) and then the release leveled off (Figure 6A). There was a notably faster release from the $N_{16}P_6N_{16}$ gel than from the $N_{32}P_6N_{32}$ gel. To release a micelle from a gel, all 'bridging' chains need to be extracted from its core (or from its neighbor's core). It

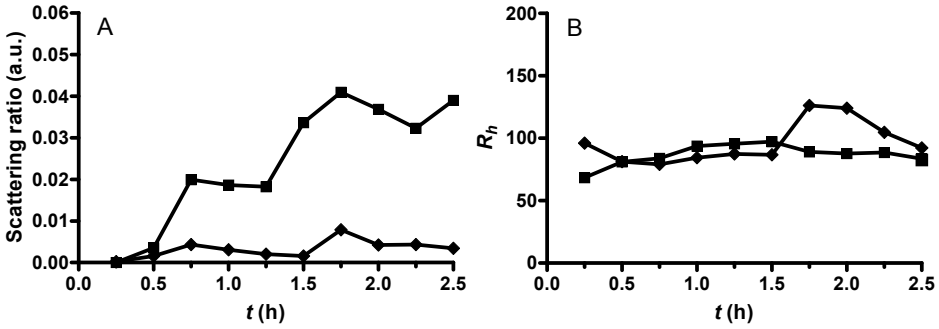

Figure 6. Characterization of the scattering ratio (A) and hydrodynamic radius (B) of the micelles that were released from the hydrogel. Squares: $N_{16}P_6N_{16}$, diamonds: $N_{32}P_6N_{32}$. Data are averages of two independent samples.

can be imagined that extracting a pNIPAm block of 16 kDa is easier than extracting a block of 32 kDa. Furthermore, the difference between the GP of the $N_{32}P6N_{32}$ gel and the experimental temperature is larger than for the $N_{16}P_6N_{16}$ gel, and the $N_{32}P_6N_{32}$ gel is more dehydrated than the $N_{16}P_6N_{16}$ gel. The size of the released micelles remained constant throughout the whole experiment, and was equal for both polymers (Figure 6B).

When an $N_{16}P_6N_{16}$ gel was kept in a DLS cuvette overnight without refreshing the medium, an equilibrium scattering intensity was reached within an hour, after which the scattering intensity did not increase significantly (results not shown). Furthermore, the gel was still present after the overnight incubation. These observations led to the conclusion that the release of micelles from the hydrogels is an equilibrium process, which can only be driven completely to the side of micelles by continuously refreshing the release medium.

PTX encapsulation and release

PTX was loaded into the gels by forming PTX-loaded micelles, lyophilizing these and subsequently redissolving them in a small volume of water (25% (w/w) polymer). Due to its hydrophobic character, PTX likely partitions into the hydrophobic pNIPAm domains of the gels. The $N_{16}P_6N_{16}$, gel which showed the fastest release in the DLS experiment, was loaded with 1.2% (w/w to polymer) PTX and was incubated in water at 40 °C. The concentration of PTX in the water phase above the gel after 1 h was only 0.6 μg/mL, which corresponds to its maximum solubility in water.[50-52] After 2 h, however, the concentration had increased to 5.7 μg/mL, *i.e.* almost 10 times the solubility of free PTX. Clearly, the micelles which were released from the gel solubilized the PTX which was also released from the gel.

Two mechanisms can be envisioned by which the PTX ends up in the micelles. In the first mechanism, intact micelles containing PTX bud off from the hydrogel. Another possible mechanism is that unimers and PTX dissolve separately from the hydrogel, followed by self-assembly of the unimers into micelles once the concentration exceeds the CMC. The dissolved PTX then partitions into these micelles. For *in vivo* application, the first mechanism would be desired as it would protect PTX against aggregation or interaction with plasma components. The present data can be explained by both mechanisms. The observation of a lag time in the release is best explained by

mechanism 2, as it would take some time before the CMC is reached only after which PTX can be solubilized in micelles. On the other hand, the observation that the released particles are larger than micelles prepared from a dilute solution, may indicate that they are in fact pieces of hydrogel (each consisting of a few bridged micelles) that are released from the hydrogel in intact form.

In vitro release of PTX in serum.

Figure 7 shows the cumulative release of PTX from hydrogels made of the two polymers. In line with the DLS measurements of the release, it can be observed that the hydrogels of $N_{32}P_6N_{32}$ showed the slowest release. $N_{16}P_6N_{16}$ hydrogels with different PTX loadings showed a nearly complete release in 4 h (*i.e.* after 15 times refreshing the medium), whereas the release from $N_{32}P_6N_{32}$ gels was much slower, amounting to only 10% release over the 4 h time period. After this time, no $N_{16}P_6N_{16}$ hydrogels could be observed anymore, while the $N_{32}P_6N_{32}$ gels were still present. The $N_{16}P_6N_{16}$ gel with high PTX loading showed faster release kinetics than the same gel with lower PTX loading. The reason for this difference is unclear. The release behavior of the $N_{16}P_6N_{16}$ gel with the low PTX loading is nearly zero-order, in line with the light scattering release experiment which also showed zero order release of micelles. Again, there was hardly any release in a control experiment in which samples were taken without refreshing the medium but only pipetting it up and down (Figure 7, diamonds): the final concentration of PTX was 1.2 μg/mL, whereas its solubility in serum is at least 5 μg/mL.[49] At any time point, the PTX concentrations in serum that was in contact with the $N_{32}P_6N_{32}$

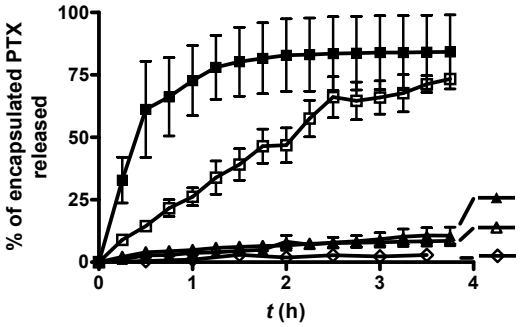

Figure 7. *In vitro* release of PTX in serum. Squares: $N_{16}P_6N_{16}$, triangles: $N_{32}P_6N_{32}$, closed symbols: 6.0% loading, open symbols: 1.2% loading. Diamonds represent the release from $N_{16}P_6N_{16}$ 1.2% loading when the medium was not refreshed. Values are indicated as mean ±SD of three replicates.

gels were also well below this value. These data indicate that (i) PTX is stably entrapped in the hydrogels, from which it is hardly extracted by serum, (ii) the faster a hydrogel releases micelles, the faster it also releases PTX, and (iii) both PTX and micelles are released simultaneously, in an erosion-controlled fashion which is governed by the rate at which the release medium is refreshed.

6.3.4. *In vivo* experiment

In vivo release of PTX

The $N_{16}P_6N_{16}$ gels were selected for use in an *in vivo* experiment, as it was anticipated that the low flow rate of intraperitoneal fluid combined with the low release rate of $N_{32}P_6N_{32}$ would lead to undetectably low PTX levels in plasma and thus to low (if any) therapeutic efficacy. The hydrogels were well tolerated by the mice, even the formulation which contained 100 mg/kg PTX (*i.e.* 4-5× the MTD of PTX formulated in Cremophor EL/ethanol, when given *i.p.* resp. *i.v.*).[43, 53, 54]

One of the mice in the 100 mg/kg group and one in the control group died after 1 and 5 days, respectively, whereas the other mice showed no signs of distress. The tumor of the mouse from the 100 mg/kg group was excised and the concentration of PTX in it was determined to be 0.1 mg/g (around 0.1% of the injected dose) which indicates that PTX released from the hydrogel is able to reach the tumor via the systemic circulation.

Figure 8 shows the levels of PTX in the blood plasma of mice after injection of PTX-containing hydrogels. It can be concluded from these data that PTX (possibly packed in micelles) is able to be carried by the lymphatic flow via the lymph nodes to the circulation. It has been shown before that both free PTX and PTX in micelles or other nanoparticles are able to be gradually transported (within several hours) from the intraperitoneal cavity to the circulation, whereas PTX in microparticles is hardly transported.[44, 45] For at least 48 h the plasma PTX concentrations stayed well above the minimal effective (*in vitro*) concentration which has been reported to be around 10 ng/mL.[35-38] From the data points at 5, 24 and 48 h the half-life $t_{½}$ of the plasma concentrations was calculated to be 7.4 h, about twice as long as literature values for PTX/Cremophor *i.p.* in mice (range 2.9-3.7 h).[37, 50] This finding can be explained by either

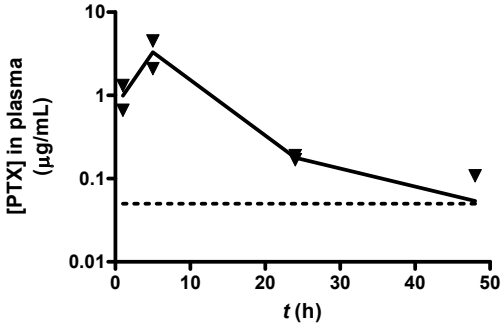

Figure 8. Plasma PTX levels of mice injected with the $N_{16}P_6N_{16}$ hydrogel at a dose of 100 mg/kg PTX. The dotted line indicates the detection limit of 0.05 µg/mL. Data points represent individual mice (2 per timepoint); the curve is drawn through the averaged values.

or both of two explanations. The first possible explanation is that the released PTX is encapsulated in long-circulating micelles, which increases $t_{½}$ due to reduced clearance. The second possible explanation is that the hydrogel gave a continuous release of PTX during this period. The apparent half-life $t_{½}$ is then the result of the balance between release and clearance.

Using the trapezoidal method, an $AUC_{0\text{-}48h}$ of 45 µg·mL^{-1}·h was calculated. In order to calculate the bioavailability of PTX, the obtained AUC was compared to literature pharmacokinetic data on PTX/Cremophor formulations at relatively low doses, which in fact produced similar maximal plasma concentrations as found in our experiment.[43, 49] In this way, a bioavailability of 106% was calculated for the 100 mg/kg formulation. Interestingly, literature values for the bioavailability after *i.p.* injection of PTX formulated in Cremophor/ethanol or in nanoparticles lie between 5% and 37%.[37, 42-45] The high bioavailability found in our study may be related to the fact that the PTX was shown to be on one hand stably incorporated in the hydrogel, preventing aggregation or diffusion into local tissues (mainly intestines, leading to toxicity[45]) before it can reach the circulation, and on the other hand to be completely released over time.

The plasma levels of the 20 mg/kg group at 1 and 5 h amounted to 13% of the plasma concentrations of the 100 mg/kg group, whereas 20% of the dose was given. This is in line with the observation from the *in vitro* release experiment which showed that the 1.2% loaded gel released its

contents slower than the 6% loaded gel. Unfortunately, the plasma levels of the 20 mg/kg group dropped below the detection threshold after 24 h so no further pharmacokinetic data could be obtained from this group.

Inhibition of tumor growth.

The effect of the PTX-loaded hydrogels on the growth of the tumors is shown in Figure 9. A 300% increase in tumor volume (average tumor volume 144 mm^3) was taken as the threshold point for the Kaplan-Meier plot in Figure 9A, whereas Figure 9B displays the relative tumor volume after 20 days. No significant difference could be observed between the 20 mg/kg group and the control. Apparently, the plasma PTX concentrations that were reached in this group were not sufficiently high, whether or not they were sustained for a long time. In the 100 mg/kg group, however, no mice showed any measurable tumor growth for the entire period of the experiment. The fact that this inhibitory effect is observed, although the plasma concentrations of PTX are quite low, may indicate that the sustained release of PTX was indeed beneficial, in line with already existing evidence and theories on the advantages of metronomic dosing.[28-31, 34]

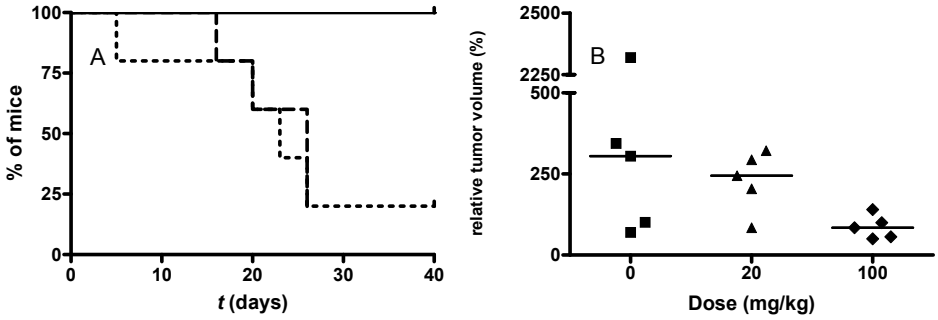

Figure 9. A: Kaplan-Meier plot showing the percentage of mice of which the tumor size had increased less than 300%. Dotted line: 0 mg/kg, dashed line: 20 mg/kg, solid line: 100 mg/kg. B: Distribution of the relative tumor sizes of the three groups at 20 days after the start of treatment. Indicated is the median of each group.

6.4. Conclusion

Taken together, these findings showed that thermosensitive triblock copolymer hydrogels slowly interconverted into flower-like micelles when in contact with an aqueous environment. A hydrophobic drug (PTX) could be released in a sustained manner together with these micelles and be solubilized in the micelles. The release rate of micelles and PTX was governed by the refreshing frequency of the release medium, and a nearly quantitatively release was obtained both *in vitro* and *in vivo*. *In vivo*, this system gave a sustained release of PTX over at least 48 h and allowed to give at least a 5 times higher dose of PTX than the maximum tolerated dose of the commonly used formulation in Cremophor EL/ethanol. Although the exact mechanism of the release remains to be elucidated, as well as the question whether or not the released PTX circulates in micelles *in vivo*, the concept of a hydrogel which interconverts into micelles has been proven. Furthermore, this article indicates that this concept may find application as a depot formulation of (passively targeted) anticancer drugs.

References

(1) Zhou, Z.; Chu, B. *Macromolecules* **1994**, *8*, 2025-2033.

(2) Chang, G.; Li, C.; Lu, W.; Ding, *J. Macromol. Biosci*. **2010**, *10*, 1248-1256.

(3) Honda, S.; Yamamoto, T.; Tezuka, Y. *J. Am. Chem. Soc*. **2010**, *30*, 10251-10253.

(4) Hua, S.; Li, Y.; Liu, Y.; Xiao, W.; Li, C.; Huang, F.; Zhang, X.; Zhuo, R. *Macromol. Rapid Commun*. **2010**, *1*, 81-86.

(5) Lee, E. S.; Oh, K. T.; Kim, D.; Youn, Y. S.; Bae, Y. H. *J. Controlled Release* **2007**, *1*, 19-26.

(6) Bae, S. J.; Suh, J. M.; Sohn, Y. S.; Bae, Y. H.; Kim, S. W.; Jeong, B. *Macromolecules* **2005**, *12*, 5260-5265.

(7) Semenov, A. N.; Joanny, J.; Khokhlov, A. R. *Macromolecules* **1995**, *4*, 1066-1075.

(8) Fumihiko, T. *J. Non-Cryst. Solids* **2002**, *0*, 688-697.

(9) Kujawa, P.; Watanabe, H.; Tanaka, F.; Winnik, F. M. *Eur. Phys. J. E: Soft Matter* **2005**, *2*, 129-137.

(10) McCormick, C. L.; Sumerlin, B. S.; Lokitz, B. S.; Stempka, J. E. *Soft Matter* **2008**, *9*, 1760-1773.

(11) Torchilin, V. P. *AAPS J*. **2007**, *2*, E128-E147.

(12) Blanco, E.; Kessinger, C. W.; Sumer, B. D.; Gao, J. *Exp. Biol. Med. (Maywood, NJ, U. S.)* **2009**, *2*, 123-131.

(13) Torchilin, V. P. *Pharm. Res*. **2007**, *1*, 1-16.

(14) Torchilin, V. P. *Cell Mol. Life Sci*. **2004**, *19-20*, 2549-2559.

(15) Hu, X.; Jing, X. *Expert Opin. Drug Delivery* **2009**, *10*, 1079-1090.

(16) Oerlemans, C.; Bult, W.; Bos, M.; Storm, G.; Nijsen, J. F.; Hennink, W. E. *Pharm. Res*. **2010**, *12*, 2569-2589.

(17) Van Tomme, S. R.; Storm, G.; Hennink, W. E. *Int. J. Pharm*. **2008**, *1-2*, 1-18.

(18) Peppas, N. A.; Bures, P.; Leobandung, W.; Ichikawa, H. *Eur. J. Pharm. Biopharm*. **2000**, *1*, 27-46.

(19) Kim, J.; Won, Y.; Lim, K.; Kim, Y. *Pharm. Res*. **2012**, *29*, 1-10.

(20) Tang, Y.; Heaysman, C. L.; Willis, S.; Lewis, A. L. *Expert Opin. Drug Delivery* **2011**, *9*, 1141-1159.

(21) Chen, M.; Tsai, H.; Liu, C.; Peng, S.; Lai, W.; Chen, S.; Chang, Y.; Sung, H. *Biomaterials* **2009**, *11*, 2102-2111.

(22) Wei, L.; Cai, C.; Lin, J.; Chen, T. *Biomaterials* **2009**, *13*, 2606-2613.

(23) Li, C.; Madsen, J.; Armes, S. P.; Lewis, A. L. *Angew. Chem., Int. Ed*. **2006**, *21*, 3510-3513.

(24) Madsen, J.; Armes, S. P.; Bertal, K.; Lomas, H.; MacNeil, S.; Lewis, A. L. *Biomacromolecules* **2008**, *8*, 2265-2275.

(25) Alexis, F.; Pridgen, E.; Molnar, L. K.; Farokhzad, O. C. *Mol. Pharmaceutics* **2008**, *4*, 505-515.

(26) Matsumura, Y.; Maeda, H. *Cancer Res*. **1986**, *12 Pt 1*, 6387-6392.

(27) Maeda, H.; Wu, J.; Sawa, T.; Matsumura, Y.; Hori, K. *J. Controlled Release* **2000**, *1-2*, 271-284.

(28) Kerbel, R. S.; Kamen, B. A. *Nat. Rev. Cancer* **2004**, *6*, 423-436.

(29) De Souza, R.; Zahedi, P.; Moriyama, E. H.; Allen, C. J.; Wilson, B. C.; Piquette-Miller, M. *Mol. Cancer Ther*. **2010**, *6*, 1820-1830.

(30) Gasparini, G. *Lancet Oncol*. **2001**, *12*, 733-740.

(31) Browder, T.; Butterfield, C. E.; Kräling, B. M.; Shi, B.; Marshall, B.; O'Reilly, M. S.; Folkman, J. *Cancer Res*. **2000**, *7*, 1878-1886.

(32) Teodorescu, M.; Negru, I.; Stanescu, P. O.; Drăghici, C.; Lungu, A.; Sârbu, A. *React. Funct. Polym*. **2010**, *10*, 790-797.

(33) de Graaf, A. J.; Boere, K. W. M.; Kemmink, J.; Fokkink, R. G.; van Nostrum, C. F.; Rijkers, D. T. S.; van, d. G.; Wienk, H.; Baldus, M.; Mastrobattista, E.; Vermonden, T.; Hennink, W. E. *Langmuir* **2011**, *16*, 9843-9848.

(34) Nabholtz, J.; Gligorov, J. *Expert Opin. Pharmacother*. **2005**, *7*, 1073-1094.

(35) Lopes, N. M.; Adams, E. G.; Pitts, T. W.; Bhuyan, B. K. *Cancer Chemother. Pharmacol*. **1993**, *3*, 235-242.

(36) Jordan, M. A.; Wendell, K.; Gardiner, S.; Brent Derry, W.; Copp, H.; Wilson, L. *Cancer Res*. **1996**, *4*, 816-825.

(37) Innocenti, F.; Danesi, R.; Di Paolo, A.; Agen, C.; Nardini, D.; Bocci, G.; Del Tacca, M. *Drug Metab. Dispos*. **1995**, *7*, 713-717.

(38) Rowinsky, E. K.; Donehower, R. C.; Jones, R. J.; Tucker, R. W. *Cancer Res*. **1988**, *14*, 4093-4100.

(39) Belotti, D.; Vergani, V.; Drudis, T.; Borsotti, P.; Pitelli, M. R.; Viale, G.; Giavazzi, R.; Taraboletti, G. *Clin. Cancer Res*. **1996**, *11*, 1843-1849.

(40) Bajaj, G.; Yeo, Y. *Pharm. Res*. **2010**, *5*, 735-738.

(41) Francis, P.; Rowinsky, E.; Schneider, J.; Hakes, T.; Hoskins, W.; Markman, M. *J. Clin. Oncol*. **1995**, *12*, 2961-2967.

(42) Soma, D.; Kitayama, J.; Ishigami, H.; Kaisaki, S.; Nagawa, H. *J. Surg. Res*. **2009**, *1*, 142-146.

(43) Eiseman, J. L.; Eddington, N. D.; Leslie, J.; MacAuley, C.; Sentz, D. L.; Zuhowski, M.; Kujawa, J. M.; Young, D.; Egorin, M. J. *Cancer Chemother. Pharmacol*. **1994**, *6*, 465-471.

(44) Gelderblom, H.; Verweij, J.; van Zomeren, D. M.; Buijs, D.; Ouwens, L.; Nooter, K.; Stoter, G.; Sparreboom, A. *Clin. Cancer Res*. **2002**, *4*, 1237-1241.

(45) Tsai, M.; Lu, Z.; Wang, J.; Yeh, T.; Wientjes, M.; Au, J. *Pharm. Res*. **2007**, *9*, 1691-1701.

(46) Zahedi, P.; Stewart, J.; De Souza, R.; Piquette-Miller, M.; Allen, C. *J. Controlled Release* **2011**, in press. doi:10.1016/j.jconrel.2011.11.025.

(47) Ciampolini, M.; Nardi, N. *Inorg. Chem*. **1966**, *1*, 41-44.

(48) Neradovic, D.; Soga, O.; Van Nostrum, C. F.; Hennink, W. E. *Biomaterials* **2004**, *12*, 2409-2418.

(49) Sparreboom, A.; van Tellingen, O.; Nooijen, W. J.; Beijnen, J. H. *Cancer Res*. **1996**, *9*, 2112-2115.

(50) Sparreboom, A.; van Tellingen, O.; Nooijen, W. J.; Beijnen, J. H. *Anticancer Drugs* **1998**, *1*, 1-17.

(51) Mathew, A. E.; Mejillano, M. R.; Nath, J. P.; Himes, R. H.; Stella, V. J. *J. Med. Chem*. **1992**, *1*, 145-151.

(52) Swindell, C. S.; Krauss, N. E.; Horwitz, S. B.; Ringel, I. *J. Med. Chem*. **1991**, *3*, 1176-1184.

(53) Bajaj, G.; Kim, M. R.; Mohammed, S. I.; Yeo, Y. *J. Controlled Release* **2011**, in press. doi:10.1016/j.jconrel.2011.12.001.

(54) Auzenne, E.; Ghosh, S. C.; Khodadadian, M.; Rivera, B.; Farquhar, D.; Price, R. E.; Ravoori, M.; Kundra, V.; Freedman, R. S.; Klostergaard, J. *Neoplasia* **2007**, *6*, 479-486.

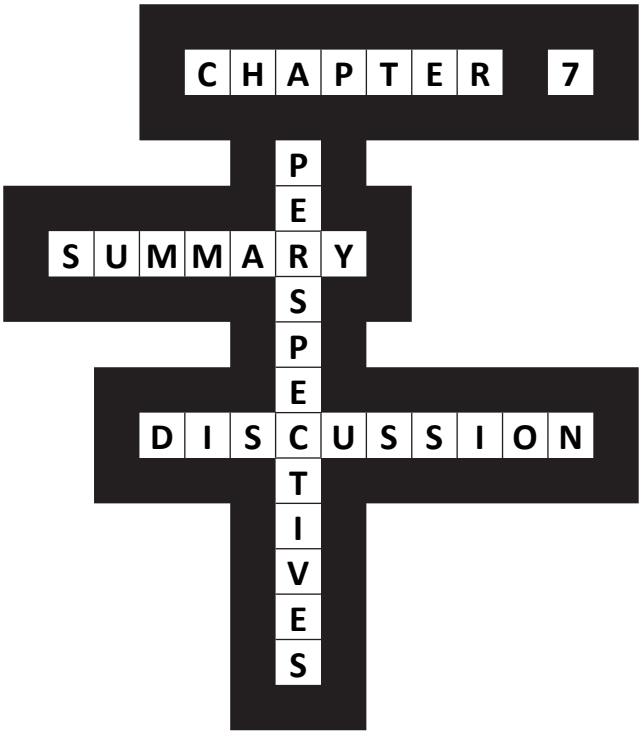
CHAPTER 7
PERSPECTIVES
SUMMARY
DISCUSSION

7.1. Summary

This thesis reports on the synthesis and characterization of several block copolymers for pharmaceutical applications. All block copolymers were thermosensitive and self-assembled at 37 °C into structures like micelles and hydrogels, which can be used for innovative drug delivery purposes, *e.g.* hydrogels releasing a cytostatic agent encapsulated in flower-like micelles. Methods were explored for the synthesis of polymer (bio)conjugates, which among others resulted in the development of matrix metalloprotease-cleavable micelles formed by peptide hybrid block copolymers.

Chapter 1 introduces the main concepts that are investigated in this thesis. It is explained that encapsulating therapeutic drugs in nanoparticles with a diameter between 10 and 100 nm leads to an increased residence time in the blood stream due to decreased degradation and clearance. Furthermore, the enhanced permeability and retention (EPR) effect is described, which gives nanoparticles the possibility to extravasate through the leaky vasculature of inflamed tissues including tumors and to accumalate there. One important class of nanoparticles that can be exploited to this end is polymeric micelles, formed by self-assembly of amphiphilic block copolymers above their critical micelle concentration (CMC). For the preparation of these polymers, the technique of atom transfer radical polymerization (ATRP) has been used, which is an example of a controlled or "living" radical polymerization. ATRP is based on a copper-catalyzed equilibrium between growing and dormant chains, which can be exploited for other reactions as well (see **Chapter 3**). Benefits of controlled radical polymerizations over conventional free radical polymerizations include simultaneous growth of all polymer chains in a batch reaction and negligible termination, thus leading to polymers with a narrow molecular weight distribution. The living character opens the possibility to synthesize block coplymers. Controlled radical polymerizations are widely used for the preparation of biomedically relevant materials. Specifically, they are well suited for the generation of biohybrid polymers *i.e.* polymers that are conjugated to sensitive biomolecules such as peptides or proteins.

Chapter 2 reviews the state-of-art of a relatively new way of preparing such polymer bioconjugates, namely by introducing non-natural amino acids with bio-orthogonal reactivity, into proteins and peptides. Subsequently, a

polymer (or any desired moiety) can be coupled site-specifically to such an incorporated non-natural amino acid. This strategy can overcome the problem of poor site-specificity associated with existing techniques for conjugation to natural amino acids (*e.g.* NHS-based coupling to lysine and maleimide-based coupling to cysteine), which are currently employed among others for the conjugation of poly(ethylene glycol) (PEG) to therapeutic proteins. Several strategies have been developed for the incorporation of non-natural amino acids with bio-orthogonal reactivity into proteins and peptides. In short peptides, virtually any non-natural amino acid can be incorporated using solid phase peptide synthesis. For large proteins, one possibility could be semisynthetic incorporation of the non-natural amino acid, meaning that a small part of the protein containing the non-natural amino acid is produced by solid phase peptide synthesis. This fragment is then coupled to the (recombinantly produced) rest of the protein by any of a series of conjugation reactions including native chemical-, expressed protein-, imine- and Staudinger ligations. For entirely recombinant production of non-natural amino acid-containing proteins, an often used approach is to produce the proteins in a bacterial strain which is auxotrophic for a certain natural amino acid, most commonly the relatively rare amino acid methionine. If these bacteria are grown in methionine-free medium and are given a non-natural amino acid, which resembles methionine (azide- or alkyne-containing analogues are often used) they will incorporate this one instead of methionine into the recombinantly produced protein. Another popular approach is the use of a genetically engineered bacterial strain expressing both a tRNA, which specifically recognizes the rare stop codon UAG, and a specifically engineered orthogonal aminoacyl-tRNA synthetase which specifically loads this tRNA with the non-natural amino acid of choice. In this way, the UAG codon is reassigned to code for an additional, 21st amino acid. Using these approaches, a wide variety of non-natural amino acids has been incorporated into proteins. Bio-orthogonal reactivities that have been introduced in this way include azide- and alkyne functionalities, which can be used in the popular copper-catalyzed azide-alkyne cycloaddition 'click' reaction. Other popular non-natural amino acids contain ketone- or aldehyde functionalities, which have been used in carbonyl condensations

(another class of 'click' reactions). Even amino acids containing ATRP initiator moieties have been introduced, allowing for the growing of polymers from a recombinant protein (the so-called 'grafting-from' approach).

As outlined above, a suitable and popular reaction for synthesizing polymer bioconjugates is the copper-catalyzed azide-alkyne cycloaddition (CuAAC) 'click' reaction. In **Chapter 3**, a novel method is introduced to introduce a reactive azide functionality on polymers after their synthesis by ATRP. The mechanism of ATRP relies on a highly dynamic, copper-catalyzed equilibrium between chains having a radical or a halogen atom at their living chain end. By simply adding sodium azide to the reaction mixture, it was shown that the halogen atoms at the living chain ends are rapidly substituted by azide groups. Starting from a bromide-ended polymer and using a 2-fold excess of azide, the reaction was complete within 5 min at room temperature. On the other hand, a control reaction without the copper complex showed negligible substitution after 18 h, proving that the reaction is indeed catalyzed by the same copper complex that catalyzes the ATRP process. No substitution was observed in the presence of the radical scavenger TEMPO, which indicates that the substitution process, very much like the process of ATRP, occurs via an intermediate radical. The reaction from a chloride-ended polymer was slower than from a bromide-ended polymer but could be accelerated by employing a higher temperature, larger excess of azide and/or by addition of ascorbic acid. Apart from its reaction rate under mild conditions, the discovered copper-catalyzed reaction has another benefit over the traditional method of S_N2 substitution of the living chain end, since the ATRP catalyst is also able to couple subsequently an alkyne-functionalized molecule via CuAAC 'click' chemistry. Therefore, it was shown that the sequence of polymerization, substitution and 'clicking' could be performed in one pot with all three reactions catalyzed by the same copper complex. All reactions proceeded in aqueous environment at room temperature. Furthermore, the system was shown to work for different monomer/catalyst pairs, demonstrating its broad scope and applicability. The need for a dipolar aprotic solvent to facilitate an S_N2 reaction is obviated by this procedure, resulting in facile work-up and compatibility with sensitive polymer bioconjugates.

Growing polymers from a peptide or protein ('grafting-from') presents an interesting way to synthesize polymer bioconjugates. **Chapter 4** reports on the synthesis of peptide-hybrid polymers using this approach. A peptide containing an enzymatic cleavage site for a biologically relevant protease was functionalized at its C-terminus with an ATRP initiator, followed by the polymerization of oligo(ethylene glycol) methyl ether methacrylate to form a hydrophilic polymer block. At the end of the polymerization, the living chain end was inactivated by the method as developed in **Chapter 3**. Subsequently, another ATRP initiator was conjugated to the N-terminus of the peptide followed by the polymerization of *N*-isopropylacrylamide to form a thermosensitive block. Both polymerizations were controlled, and polymers of several block lengths were prepared (hydrophilic block: 4, 8 and 16 kDa, thermosensitive block: 16 and 32 kDa). By this procedure, amphiphilic block copolymers were obtained, which had a peptide separating the hydrophilic and thermosensitive blocks. At 37 °C in water, all polymers formed micelles with a favorable size for drug delivery purposes (R_h 22 – 29 nm). One of the polymers was fluorescently labeled at the installed azide functionality at the end of its hydrophilic block (which was grown from the C-terminus of the peptide). In this way, fluorescent micelles were obtained. After incubation of these micelles with a metalloprotease (a model for several matrix metalloproteases, which are upregulated in tumors), it was observed that their fluorescently labeled coronas were cleaved off. This system may function as a long-circulating drug delivery vehicle with enzyme-triggered destabilization in the target tissue to release *e.g.* a cytotoxic payload.

Apart from amphiphilic diblock copolymers, amphiphilic triblock copolymers have also been investigated as micelle-forming agents for drug delivery applications. **Chapter 5** describes a study of physico-chemical differences between micelles formed from diblock and triblock copolymers. To this end, diblock methoxy-poly(ethylene glycol)-poly(*N*-isopropylacrylamide) (mPEG-pNIPAm) and triblock pNIPAm-PEG-pNIPAm polymers were prepared by ATRP of NIPAm from (m)PEG macroinitiators. The polymerization yielded well-defined polymers in which the thermosensitive pNIPAm block was kept constant (16 kDa) but the hydrophilic (m)PEG block was varied: 2 kDa for the diblock copolymer and 2, 4 and 6 kDa for the triblock copolymers. Above the critical micelle

concentration (CMC), and above the cloud point temperature (CP) of the pNIPAm blocks, all polymers self-assembled into micelles having pNIPAm blocks in the core and (m)PEG blocks in the corona. When comparing "star-like" micelles from the $mPEG_{2kDa}$-$pNIPAm_{16kDa}$ diblock copolymer with "flower-like" micelles from the $pNIPAm_{16kDa}$-PEG_{4kDa}-$pNIPAm_{16kDa}$ triblock copolymer (which can be regarded as a "double diblock" copolymer), it was found that the latter had a significantly smaller hydrodynamic radius (27 nm *vs* 35 nm). It was hypothesized that this effect is due to the looping of the PEG blocks in the flower-like micelles, which causes every triblock chain to occupy more than twice the surface area of a diblock chain on the outside of the micelles. This leads to less chains fitting in one micelle, and consequently a reduced micellar size. The data on the other triblock copolymers matched this hypothesis: upon increasing the PEG block size, the micellar hydrodynamic radius decreased rather than increased. The number of chains per micelle was quantified by means of static light scattering, which revealed that the flower-like micelles of $pNIPAm_{16kDa}$-PEG_{4kDa}-$pNIPAm_{16kDa}$ indeed contained less than half the number of chains that the star-like micelles of $mPEG_{2kDa}$-$pNIPAm_{16kDa}$ contained (1300 *vs* 4400), and every chain occupied more than twice as much surface area (13 *vs* 5 nm^2). Furthermore, the number of chains per micelle was shown to decrease upon increasing the PEG block length, while the surface area per chain increased. Above the CP, ^1H NMR relaxometry was able to distinguish between the signals of the PEG segments that were close to the micellar cores ($T_2 \approx 0.1$ s, more rigid) and those of the more distal segments ($T_2 \approx 0.6$-1.0 s, more flexible). The proportion of rigid segments was shown to be higher in the flower-like micelles than in the star-like micelles and decrease with increasing PEG block length. Furthermore, it was shown that in the flower-like micelles even the distal PEG segments are less flexible than in the star-like micelles. This observation provided, for the first time, experimental proof for the flower-like conformation of triblock copolymer micelles.

Besides flower-like micelles, triblock copolymers like pNIPAm-PEG-pNIPAm can also self-assemble into hydrogels. At low concentration, micelles are formed whereas hydrogels occur at high polymer concentration. **Chapter 6** describes that when a hydrogel is transferred into water, it starts to release flower-like micelles. Experiments showed that micelles were

continuously released as long as the medium was regularly refreshed. On the other hand, if the medium was not refreshed an equilibrium concentration of micelles was reached. Gels consisting of $pNIPAm_{16kDa}$-PEG_{6kDa}-$pNIPAm_{16kDa}$ ($N_{16}P_6N_{16}$) showed a faster release than gels consisting of $N_{32}P_6N_{32}$. When a gel was loaded with the cytostatic agent paclitaxel (PTX), micelles released in water were able to solubilize PTX, as evidenced by a PTX concentration in the release medium above its aqueous solubility. In serum, the $N_{16}P_6N_{16}$ gel loaded with 1.2% PTX (w/w ratio to polymer) showed an almost zero-order drug release, releasing 80% of incorporated PTX in 4 h. On the other hand, $N_{32}P_6N_{32}$ gels released their contents much slower (only 10% release in 4 h). To test the applicability of these micelle-releasing gels for the delivery of cancer chemotherapeutics, an *in vivo* pilot experiment was performed. $N_{16}P_6N_{16}$ gels (without and with 1.2% and 6.0% PTX loading) were administered *i.p.* in nude mice bearing 14C human squamous cell carcinoma tumor xenografts to obtain doses of 0, 20 and 100 mg/kg PTX, respectively. These PTX doses correspond to 1× and 5× the maximum tolerated dose that has been determined for PTX when given *i.v.* as the standard formulation in Cremophor EL/ethanol. All gel formulations were well tolerated. After injection of the highest dose, PTX levels in serum could be determined for 48 h with a comparatively long elimination half-life of 7.4 h. These observations indicate a sustained release of PTX. A bioavailability of 100% was calculated from the area under the curve of plasma concentration *vs* time. Furthermore, at the highest dose, PTX was shown to completely inhibit tumor growth for at least 3 weeks with a single hydrogel injection. This promising concept may find application as a depot formulation of passively targeted anticancer drugs.

7.2. Discussion and perspectives

7.2.1. Choice of thermosensitive polymer

It must be noted that the PEG-pNIPAm and pOEGMA-pNIPAm block copolymers employed in this thesis should be regarded as model polymers since the molecular weights of the intact polymers are above the threshold for renal clearance, which is around 30-50 kDa.[1] The ester bonds connecting the blocks will eventually degrade, reducing the molecular weights to below the

threshold. However, in our experience this reaction proceeds only very slowly at neutral pH. Therefore, these polymers would presumably not be suitable for repeated administration to patients due to the risk of accumulation in the body. Nevertheless, the *in vivo* experiment described in **Chapter 6** showed that relatively large amounts of these polymers were well tolerated by mice.

In our group, thermosensitive copolymers of *N*-(2-hydroxypropyl) methacrylamide mono- and dilactate (HPMAm(lac)$_n$ are often used rather than pNIPAm-based constructs because (i) their CP can be tuned by varying the ratio of HPMAm(lac)$_1$ and HPMAm(lac)$_2$, (ii) their CP increases after hydrolysis of the lactate side chains, eventually leading to a polymer, which is completely water-soluble at 37 °C and (iii) their molecular weight decreases considerably by this hydrolysis.[2-4]

The reason that HPMAm(lac)$_n$ monomers were not employed in this thesis is that at present they have only been polymerized by free radical polymerization. Attempts to polymerize them by controlled radical polymerization have not succeeded yet: both techniques of reversible addition-fragmentation chain transfer (RAFT) polymerization and ATRP have shown only limited conversion. Theories to explain this difficulty include the attack of the penultimate amide nitrogen on the radial chain end during polymerization, and (in the case of ATRP) catalyst poisoning due to complexation of the activating copper(I) species by the formed polymer chains.[5]

7.2.2. Polymerization technique

Recently, however, preliminary experiments in our group have shown promising results by employing single electron transfer living radical polymerization (SET-LRP) to polymerize HPMAm(lac)$_n$. SET-LRP is very similar to ATRP, except that activation occurs by reaction between a halogen-capped polymer chain and metallic copper(0) rather than copper(I).[6] Therefore, the growing chain cannot form a complex with the activator species. Furthermore, by using SET-LRP, very high polymerization rates are usually obtained at low temperatures while the polymerization is still controlled.[7] These characteristics imply that amide attack on the radical would be less competitive. SET-LRP has already been successfully used for the polymerization of acrylamide-based monomers.[8]

Applying SET-LRP, HPMAm(lac)$_1$, HPMAm(lac)$_2$ and a 1:1 mixture of these two monomers have been polymerized up to 80-90% conversion in water/methanol 70/30 and water/DMSO 70/30. Unfortunately, however, the produced polymers precipitated from these mixtures at high conversions. Currently, other solvent compositions are under investigation.

7.2.3. Core-crosslinking

It has been shown that thermosensitive micelles have limited stability in serum, probably due to interactions with proteins.[9] If they are to be used for drug delivery purposes, this may lead to premature release of the payload. Core crosslinking has been proven to be an effective way of stabilizing polymeric micelles, and indeed, it has been shown to significantly enhance their blood residence times.[9] The most frequently employed method for core crosslinking in our group is the coupling, post polymerization, of methacryloyl moieties to hydroxyl groups in the side chains of thermosensitive HPMAm(lac)$_n$ polymer blocks. After micelle formation, the methacryloyl groups are then polymerized.[9, 10] The coupling reaction, which employs methacryloylchloride or methacrylic anhydride, should be carried out under anhydrous conditions. Furthermore, this method is of course only applicable to monomers having a hydroxyl group in their side chain. Another core-crosslinking method which is currently under investigation in our group, relies on the copolymerization, together with NIPAm, of a small amount (5-10 mol%) of the azide-bearing monomer *N*-(3-azidopropyl)acrylamide (AzPAm). After polymerization and micelle formation, core-crosslinking can achieved by a CuAAC 'click' reaction between the incorporated AzPAm moieties and dipropargyl ether.[11]

7.2.4. Reversible covalent coupling of drugs

Unfortunately, however, even from core-crosslinked micelles a considerable amount of the encapsulated drug may leak out before the target site is reached. Recently, promising results have been obtained in our group by coupling drug molecules (doxorubicin) to the micelle-forming PEG-pHPMAm(lac)$_n$ polymers via pH sensitive linkers, which are stable at the normal physiological pH of 7.4 but rapidly degrade in a more acidic environment which is found in tumors.[10, 12]

7.2.5. Micelle topology

One advantage of flower-like micelles (**Chapter 5**) over star-like micelles is the fact that they can be released from physically crosslinked hydrogels, as explored in **Chapter 6**. Apart from that feature, in terms of drug delivery purposes flower-like micelles seem to be just as applicable as star-like micelles, based on the results from **Chapter 5**. Others have even found a lower CMC for triblock copolymer micelles,[13] although we did not observe this effect. Furthermore, a higher kinetic stability has been reported previously for triblock copolymer micelles,[14] which is intuitively logical since two blocks need to be removed from the core to extract a unimer from the micelle. Such an increased kinetic stability would also be advantageous, since this may contribute significantly to a micelle's residence time in the circulation.[15] The kinetic stability of micelles was not studied in this thesis. In a preliminary experiment, however, a dispersion of flower-like micelles was diluted 10-fold (to a final concentration below the CMC). The light scattering intensity dropped rapidly to much less than 10% of its initial value (330 → 2 kHz), indicating limited kinetic stability of pNIPAm-PEG-pNIPAm micelles. The contribution of kinetic stability to the overall stability of polymeric micelles can be expected, however, to be dependent on the type and characteristics of the polymers. Other, more hydrophobic polymers than pNIPAm may be more suitable for drug delivery in this regard.[15]

Another advantage of flower-like micelles over star-like micelles could arise if peptides are used as hydrophilic blocks. The conformation of peptides can have a large influence on their interaction with, especially, membrane proteins. For example, restricting flexibility of peptides by cyclization is an often employed strategy to increase their affinity for receptors.[16] In this way, peptide-polymer hybrid micelles can be designed with applications for targeted drug delivery in mind.

7.2.6. Micelle-releasing gels

Considering the micelle-releasing hydrogel system (**Chapter 6**), two main questions remain open: (i) do intact micelles "bud off" from the gel or is the release mechanism based on dissolution of unimers that later combine into micelles? And (ii) if PTX is indeed released inside micelles, how stably is it entrapped and how stable are the micelles in the circulation? These

interesting questions cannot be definitively answered by the results obtained in **Chapter 6**, but are interesting and relevant enough to be investigated further. One way to ensure having a release of intact and stable micelles could be to make a system like the one developed by the group of Armes:[17, 18] they describe a hydrogel in which the cores of the micelles are in situ crosslinked upon injection and the bridging hydrophilic blocks (and the loops) can be cleaved over time to release core-crosslinked micelles. This cleavage can occur *e.g.* through hydrolysis or reduction, and can be either chemically or enzymatically. As mentioned in **Chapter 6**, such a system has not yet been investigated as a depot for drug-loaded micelles. However, this method would enable the development of very intelligent stimuli-responsive drug delivery systems.

7.2.7. Growing polymers from proteins/peptides

The last years have witnessed an increasing interest in the "grafting-from" approach due to the advantages it has over conjugating a pre-made polymer to a protein. First of all, the reaction rate of a coupling reaction is limited by the diffusion rate of the two high-molecular weight reactants. On the other hand, for the reaction rate of a polymerization only the diffusion rate of the low molecular weight monomer matters. Secondly, after polymerization (especially after controlled radical polymerization, in which initiator efficiencies often approach 100%), the product conjugate can easily be separated from low molecular weight reactants such as monomer and catalyst, by dialysis. In the case of a coupling reaction, both the starting materials and the product are of high molecular weight, making separation by dialysis often impossible. Recently, non-natural amino acid ATRP initiators have been developed that enabled growing a polymer from a protein with full control over the conjugation site within the protein.[19, 20] We anticipate that the flexibility of this approach, combined with the advantages outlined above and the still continuing improvement in controlled radical polymerization techniques, will lead to a further growth of the field of polymerizations by "grafting from" proteins. Projects in this direction have recently been initiated in our group.

7.3. Conclusion

To conclude, this thesis reports on the preparation, characterization and application of amphiphilic and biohybrid polymers and self-assembled structures thereof. Practical applications of concepts such as grafting of polymers from peptides, one-pot functionalization of polymers prepared by ATRP, micelles having flower-like topology and hydrogels releasing such flower-like micelles, have been demonstrated in this thesis.

References

(1) Seymour, L. W.; Duncan, R.; Strohalm, J.; Kopeçek, J. *J. Biomed. Mater. Res*. **1987**, *11*, 1341-1358.

(2) Soga, O.; van Nostrum, C. F.; Fens, M.; Rijcken, C. J.; Schiffelers, R. M.; Storm, G.; Hennink, W. E. *J. Controlled Release* **2005**, *2*, 341-53.

(3) Soga, O.; van Nostrum, C. F.; Hennink, W. E. *Biomacromolecules* **2004**, *3*, 818-821.

(4) Soga, O.; van Nostrum, C. F.; Ramzi, A.; Visser, T.; Soulimani, F.; Frederik, P. M.; Bomans, P. H. H.; Hennink, W. E. *Langmuir* **2004**, *21*, 9388-9395.

(5) Teodorescu, M.; Matyjaszewski, K. *Macromolecules* **1999**, *15*, 4826-4831.

(6) Percec, V.; Guliashvili, T.; Ladislaw, J. S.; Wistrand, A.; Stjerndahl, A.; Sienkowska, M. J.; Monteiro, M. J.; Sahoo, S. *J. Am. Chem. Soc*. **2006**, *43*, 14156-14165.

(7) Rosen, B. M.; Percec, V. *Chem. Rev*. **2009**, *11*, 5069-5119.

(8) Nguyen, N. H.; Rosen, B. M.; Percec, V. *J. Polym. Sci., Part A: Polym. Chem*. **2010**, *8*, 1752-1763.

(9) Rijcken, C. J.; Snel, C. J.; Schiffelers, R. M.; van Nostrum, C. F.; Hennink, W. E. *Biomaterials* **2007**, *36*, 5581-5593.

(10) Talelli, M.; Iman, M.; Varkouhi, A. K.; Rijcken, C. J. F.; Schiffelers, R. M.; Etrych, T.; Ulbrich, K.; van Nostrum, C. F.; Lammers, T.; Storm, G.; Hennink, W. E. *Biomaterials* **2010**, *30*, 7797-7804.

(11) Jiang, X.; Zhang, J.; Zhou, Y.; Xu, J.; Liu, S. *J. Polym. Sci., Part A: Polym. Chem*. **2008**, *3*, 860-871.

(12) Talelli, M.; Iman, M.; Rijcken, C. J.; van Nostrum, C. F.; Hennink, W. E. *J. Controlled Release* **2010**, *1*, e121-122.

(13) Gourier, C.; Beaudoin, E.; Duval, M.; Sarazin, D.; Maitre, S.; Francois, J. *J. Colloid Interface Sci*. **2000**, *1*, 41-52.

(14) Creutz, S.; van Stam, J.; De Schryver, F. C.; Jerome, R. *Macromolecules* **1998**, *3*, 681-689.

(15) Lu, J.; Owen, S. C.; Shoichet, M. S. *Macromolecules* **2011**, *15*, 6002-6008.

(16) White, C. J.; Yudin, A. K. *Nat. Chem*. **2011**, *7*, 509-524.

(17) Li, C.; Madsen, J.; Armes, S. P.; Lewis, A. L. *Angew. Chem., Int. Ed*. **2006**, *21*, 3510-3513.

(18) Madsen, J.; Armes, S. P.; Bertal, K.; Lomas, H.; MacNeil, S.; Lewis, A. L. *Biomacromolecules* **2008**, *8*, 2265-2275.

(19) Broyer, R. M.; Quaker, G. M.; Maynard, H. D. *J. Am. Chem. Soc*. **2007**, *3*, 1041-1047.

(20) Averick, S. E.; Magenau, A. J. D.; Simakova, A.; Woodman, B. F.; Seong, A.; Mehl, R. A.; Matyjaszewski, K. *Polym. Chem*. **2011**, *7*, 1476-1478.


APPENDICES
AFFILIATIONS
COLLABORATING
AUTHORS
SAMENVATTING
NEDERLANDSE
CURRICULUM VITAE
PUBLICATIONS LIST
DANKWOORD

Nederlandse samenvatting

Hoofdstuk 1. Introductie

Dit proefschrift beschrijft het maken en bestuderen van een aantal polymeren[1] met mogelijk farmaceutische toepassingen. Eén van die toepassingen is het maken van nanodeeltjes. Nanodeeltjes, bolletjes met een afmeting tussen één tienduizendste en één honderdduizendste van een millimeter, worden momenteel veel onderzocht voor farmaceutische toepassingen. Het is namelijk gebleken dat als je zulke deeltjes bij een patiënt injecteert, deze deeltjes heel lang in het lichaam blijven. Door nu geneesmiddelen te verpakken in nanodeeltjes zullen deze ook heel lang actief blijven: ze worden slechts heel langzaam uitgescheiden en ze worden veel minder snel afgebroken dan vrije geneesmiddelen. Verder is het bekend dat ontstoken weefsel (bijvoorbeeld kankergezwellen oftewel tumoren) lekke bloedvaten hebben, terwijl gezond weefsel dat niet heeft. De nanodeeltjes met geneesmiddelen er in kunnen dan specifiek in het ontstoken weefsel uit de bloedbaan treden om het geneesmiddel alleen dáár af te geven en zo bijwerkingen op andere plaatsen in het lichaam te vermijden.[2]

Een veel onderzochte soort nanodeeltjes zijn de polymere micellen. Deze worden spontaan gevormd als je een oplossing maakt van amfifiele polymeren in water. Amfifiele polymeren zijn polymeren waarvan de ene helft van iedere keten wél oplosbaar is in water, maar de andere helft niet. Er vormen zich dan spontaan kleine bolletjes (micellen) van elk tientallen tot duizenden

1. Polymeren zijn stoffen die bestaan uit hele lange keten-vormige moleculen. Bekende voorbeelden van polymeren zijn plastics en rubber, maar ook zetmeel, gelatine, wol en zijde behoren hier toe. Ieder keten-vormig polymeer-molecuul is opgebouwd uit aan elkaar gekoppelde kleinere moleculen, de zogenaamde monomeren. Het vormen van polymeren uit monomeren heet polymerisatie.

2. Uiteindelijk zullen alsnog de meeste nanodeeltjes terecht komen in de lever en de milt, omdat deze organen erg goed zijn in het 'wegvangen' van bacteriën en virussen (die net zo groot zijn als nanodeeltjes). Het gaat er echter om dat de verhouding tussen geneesmiddel in gezond en in ziek weefsel beter wordt dan zonder het gebruik van nanodeeltjes. Ook worden veel geneesmiddelen afgebroken in de lever in plaats van daar tot bijwerkingen te leiden.

polymeerketens. Van iedere keten zit de water-onoplosbare helft aan de binnenkant en de water-oplosbare helft aan de buitenkant (Figuur 1). Veel geneesmiddelen lossen een stuk beter op in de kern van zo'n micel dan in water.

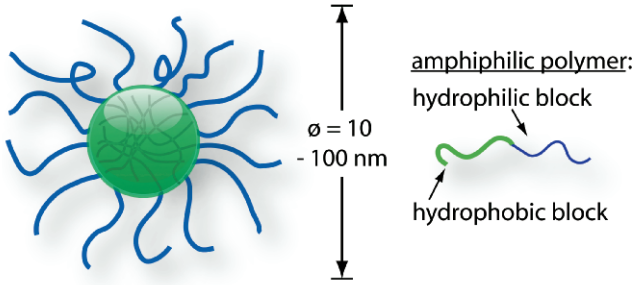

Figuur 1. Schematische weergave van een amfifiel polymeer (rechts) en een polymere micel (zonder geneesmiddel er in). Met toestemming overgenomen uit Blanco *et al.*, *J. Exp. Biol. Med. (Maywood, NJ, U. S.)* **2009**, *2*, 123-131. Copyright 2009, the Society for Experimental Biology and Medicine.

Naast amfifiele polymeren, komen in dit proefschrift ook biohybride polymeren aan bod. Dit zijn polymeren die vastgemaakt zijn aan bijvoorbeeld een eiwitmolecuul, een peptide (een stukje van een eiwitmolecuul) of aan een stukje DNA. Veel van de moderne geneesmiddelen die in ontwikkeling zijn, bestaan uit eiwitten, peptiden of DNA. Door polymeren hier aan vast te laten groeien, zou je dus nanodeeltjes kunnen maken met eiwitten, peptiden of DNA er aan vast gekoppeld.

Zulke nanodeeltjes zouden hele geavanceerde farmaceutische toepassingen kunnen hebben, omdat het lichaam heel specifiek reageert op met name bepaalde eiwitten en peptiden. Door slim te kiezen welk eiwit of peptide je aan een nanodeeltje koppelt, kun je er voor zorgen dat alleen de cellen waar het nanodeeltje (met geneesmiddel er in) naartoe moet, zo'n nanodeeltje vastpakken of zelfs 'opeten'. Ook kun je peptiden gebruiken die geknipt kunnen worden door bepaalde enzymen die alleen op bepaalde plekken in het lichaam actief zijn. Zo kun je er voor zorgen dat alleen op die plekken de nanodeeltjes uit elkaar vallen en het geneesmiddel vrij komt.

Hoofdstuk 2. Niet-natuurlijke aminozuren

Hoofdstuk 2 is een samenvatting van de bestaande literatuur over een relatief nieuwe manier om polymeren (of andere stoffen) aan peptiden en eiwitten vast te maken. In de natuur worden eiwitten en peptiden opgebouwd uit combinaties van 20 verschillende soorten aminozuren. Voor enkele aminozuren (voornamelijk lysine en cysteïne) bestaan er al lange tijd chemische reacties waarmee polymeren of andere stoffen aan die aminozuren gekoppeld kunnen worden. Maar als zo'n aminozuur meerdere keren voorkomt in een eiwit, dan is niet te sturen op welke plek de koppeling plaatsvindt. Daarom zijn er een aantal methoden ontwikkeld om ook niet-natuurlijke aminozuren in te bouwen. Deze niet-natuurlijke aminozuren hebben specifieke chemische reactiviteiten, waardoor een polymeer of een andere stof specifiek aan zo'n niet-natuurlijk aminozuur gekoppeld kan worden en niet reageert met de natuurlijke aminozuren in het eiwit of peptide.

Peptiden bestaan uit een klein aantal aminozuren en kunnen eenvoudig synthetisch gemaakt worden. Daarbij is het erg eenvoudig om ook niet-natuurlijke aminozuren in te bouwen. Bij eiwitten, die veel te groot zijn om synthetisch te kunnen maken, is het moeilijker. Meestal worden farmaceutische eiwitten door genetisch gemodificeerde bacteriën, schimmels of gekweekte zoogdiercellen geproduceerd: zogenaamde recombinante eiwitproductie. Eén mogelijke oplossing is om het grootste deel van een eiwit recombinant te produceren, en alleen een klein stukje (een peptide dus) synthetisch te maken. Het niet-natuurlijke aminozuur kan dan eenvoudig in dat kleine peptide worden ingebouwd, waarna het recombinant geproduceerde eiwitdeel en het synthetische peptide aan elkaar gekoppeld worden om het volledige eiwit te vormen met het niet-natuurlijke aminozuur er in.

Een vaker gebruikte methode is om een niet-natuurlijk aminozuur te kiezen dat lijkt op een weinig voorkomend natuurlijk aminozuur (meestal methionine). Door gebruik te maken van een bacteriestam die methionine niet zelf kan maken, en deze in plaats van methionine het niet-natuurlijke aminozuur te voeren, kan een recombinant eiwit geproduceerd worden dat een niet-natuurlijk aminozuur bevat.

Een derde methode, die sterk in opkomst is, is gebruik te maken van bacteriën die genetisch zo gemodificeerd zijn dat ze 21 in plaats van 20 aminozuren kunnen hanteren. Als 21e aminozuur kan dan, in principe, elk gewenst niet-natuurlijk aminozuur worden gebruikt. Dit is een veelzijdige methode, maar elk nieuw niet-natuurlijk aminozuur vereist opnieuw genetisch modificeren van bacteriën.

Veel gebruikte niet-natuurlijke aminozuren zijn bijvoorbeeld aminozuren die een azide bevatten. Na inbouwen van zo'n azide in een eiwit, kan hier aan bijvoorbeeld een polymeer gekoppeld worden dat een alkyn bevat. Andersom kan ook, als het aminozuur een alkyn bevat en het polymeer een azide bevat. Aziden en alkynen kunnen namelijk heel snel en heel specifiek met elkaar reageren onder invloed van koper-ionen. Koper treedt hierbij op als katalysator. Deze reactie tussen een azide en een alkyn wordt heeft als bijnaam de 'klik'-reactie, en in de volgende hoofdstukken komt deze verder aan bod. Een zeer recente ontwikkeling is het gebruik van een niet-natuurlijk aminozuur dat een initiator bevat voor een polymerisatie. Zo kun je polymeren 'groeien' vanaf een eiwit.

Hoofdstuk 3. Drie opeenvolgende reacties met dezelfde koper-katalysator

In dit proefschrift worden amfifiele polymeren gemaakt met een bepaalde techniek, genaamd Atom Transfer Radical Polymerization (ATRP). Met behulp van een koper-katalysator produceert deze techniek op een heel gecontroleerde manier polymeren: alle polymeerketens groeien tegelijk en even snel, waardoor ze ook allemaal bijna even lang worden. Bovendien zijn deze polymerisatie-reacties mogelijk bij kamertemperatuur met water als oplosmiddel. Technieken zoals ATRP worden daarom veel gebruikt voor het maken van polymeren voor biomedische toepassingen, zoals amfifiele polymeren en biohybride polymeren.

Het is al langer bekend dat dezelfde koper-katalysatoren die voor ATRP gebruikt worden, ook als katalysatoren kunnen optreden voor de eerder genoemde 'klik'-reacties tussen aziden en alkynen. Het is ook bekend dat het mogelijk is om na ATRP het gevormde polymeer

te voorzien van een azide, zodat het polymeer daarna ergens aan vast 'geklikt' kan worden, bijvoorbeeld aan een alkyn-bevattend eiwit. De combinatie van ATRP en 'klik'-chemie wordt daarom steeds populairder.

Het enige nadeel is echter dat het polymeer voorzien moet worden van een azide in een aparte reactie, die langzaam verloopt en waarbij een onprettig oplosmiddel, hoge temperatuur en/of een grote overmaat van het giftige natriumazide gebruikt moeten worden.

Hoofdstuk 3 beschrijft de ontwikkeling van een nieuwe reactie om het polymeer te voorzien van een azide. Het elegante is dat ook deze reactie gekatalyseerd wordt door weer dezelfde koper-katalysatoren. De reactie is heel snel (enkele minuten) en verloopt ook in water, bij kamertemperatuur en met slechts een hele kleine overmaat natriumazide. Deze ontwikkeling maakt het mogelijk om ATRP, functionalisering van het gevormde polymeer met azide en 'klik'-koppeling van een ander molecuul aan het gevormde polymeer, achtereenvolgens in hetzelfde potje uit te voeren zonder van oplosmiddel of katalysator te hoeven wisselen en zonder tussenproducten te hoeven opzuiveren.

Hoofdstuk 4. Enzymatisch afbreekbare micellen

Hoofdstuk 4 komt weer terug op de eerder genoemde biohybride polymeren. In dit hoofdstuk worden aan de twee uiteinden van een peptide twee verschillende polymeren gegroeid. Eerst aan de ene kant (de zgn. C-terminus) en dan aan de andere kant (de zgn. N-terminus). Deze polymeren worden gegroeid door aan het betreffende uiteinde van het peptide een initiator te koppelen, waarna het polymeer er aan vast 'groeit' via een ATRP polymerisatie.

Eerst wordt aan de C-terminus een initiator gekoppeld waarna hieraan een wateroplosbaar polymeer wordt gegroeid, genaamd pOEGMA (poly(oligo(ethylene glycol) methyl ether methacrylate). Na de polymerisatie wordt aan het uiteinde van dit polymeer een azide geplaatst d.m.v. de in hoofdstuk 3 ontwikkelde reactie. Vervolgens wordt aan de N-terminus een initiator gekoppeld waarna hieraan een temperatuurgevoelig polymeer wordt gegroeid, genaamd pNIPAm (poly(N-isopropylacrylamide)).

Het feit dat het eerste polymeer gefunctionaliseerd is met azide, verhindert dat het tweede polymeer aan dit eerste polymeer vast groeit i.p.v. aan de N-terminus van het peptide. Het is namelijk een

eigenschap van ATRP dat een eenmaal gevormd polymeer in een tweede polymerisatie-reactie normaal gesproken gewoon weer verder groeit. Deze eigenschap wordt vaak gebruikt om amfifiele polymeren te maken.

Terugkomend op het gemaakte peptide met de twee polymeerketens er aan: zoals gezegd is één van deze ketens wateroplosbaar terwijl de andere temperatuurgevoelig (thermosensitief) is. Dit wil zeggen dat bij lage temperatuur dit eveneens een wateroplosbaar polymeer is, maar dat het bij hoge temperatuur onoplosbaar wordt in water. Bij het gebruikte pNIPAm ligt dit omslagpunt, het zogenaamde Cloud Point, ongeveer bij 32 °C. Omdat dit omslagpunt zo dicht bij de menselijke lichaamstemperatuur ligt, wordt pNIPAm veel onderzocht voor biomedische toepassingen.

In ons geval heeft de thermosensitiviteit van pNIPAm als gevolg dat de polymeer-peptide-polymeer ketens bij kamertemperatuur volledig wateroplosbaar zijn, maar bij lichaamstemperatuur amfifiel zijn. Zoals eerder uitgelegd vormen ze dan micellen (Figuur 2) waar eventueel geneesmiddelen in geladen kunnen worden.

Het peptide tussen het pOEGMA en het pNIPAm blok is zó gekozen dat het specifiek geknipt kan worden door enzymen (MMP-2 en MMP-9) die veel actiever zijn in tumoren dan in gezond weefsel. Dit houdt in dat de micellen in theorie specifiek in tumoren uit elkaar zouden moeten vallen: het geneesmiddel zou zich dan in de tumor moeten ophopen.

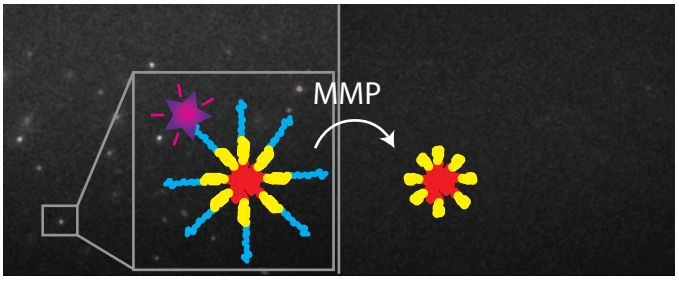

Figuur 2. Schematische weergave van de enzymatisch afbreekbare micellen. Rood = hydrofoob (thermosensitief) polymeer blok. Blauw = hydrofiel polymeer blok. Geel = peptide. Paars = fluoresent molecuul. In de achtergrond is het beeld van de fluorescentie-microscoop te zien. Links: voor degradatie. Rechts: na degradatie.

Om te laten zien dat de buitenkant (de corona) van de micellen inderdaad er af geknipt wordt, is er eerst een alkyn-bevattend fluorescent molecuul gekoppeld aan het azide dat aan het hydrofiele blok vast zat, d.m.v. de 'klik'-reactie. De gevormde fluorescente micellen waren onder een microscoop zichtbaar. Na toevoeging van een enzym uit dezelfde familie als MMP-2 en MMP-9 (maar dan geproduceerd door bacteriën), was te zien dat er nog steeds wel deeltjes waren, maar dat deze niet meer fluorescent waren (Figuur 2). De fluorescerende corona was er dus af geknipt. Hoewel het nog niet met een geneesmiddel is uitgetest en nog niet in tumoren, blijkt het principe van afbreekbare micellen wel te werken.

Hoofdstuk 5. Bloem-vormige micellen

Behalve amfifiele polymeren die aan één kant wateroplosbaar (hydrofiel) zijn en aan de andere kant onoplosbaar in water (hydrofoob), bestaan er ook polymeren waarvan het midden van de keten hydrofiel is en de twee uiteinde hydrofoob. Dit zijn de zogenaamde amfifiele triblok copolymeren. Net als de 'gewone' diblok copolymeren vormen ook deze triblok copolymeren micellen in water. Alle uiteinden van de polymeerketens zitten in de kern van een micel, en de hydrofiele middenstukken vormen een soort 'lussen' aan de buitenkant (zie ook Figuur 3 op pagina 208). De zo gevormde micellen worden vaak aangeduid als 'bloem-vormige' (engels: flower-like) micellen. Hoewel niet zo vaak bestudeerd, zouden deze bloem-vormige micellen ook toepassingen kunnen vinden in de toediening van geneesmiddelen. Op een mogelijke toepassing zal in hoofdstuk 6 in gegaan worden.

In hoofdstuk 5 worden experimenten gedaan met zowel bloem-vormige als 'gewone' (oftewel 'ster-vormige') micellen, met als doel te onderzoeken of de polymeerketens in de bloem-vormige micellen er hinder van ondervinden dat ze gebogen zitten in een lus.

Di- en triblok copolymeren werden gemaakt via ATRP door pNIPAm te groeien aan één of twee kanten van een hydrofiel polymeer. Als hydrofiel polymeer werd PEG (poly(ethylene glycol)) gekozen: dit is een eenvoudig polymeer dat al heel veel gebruikt wordt in de farmacie. De pNIPAm blokken werden steeds even lang gehouden, maar de lengte van het PEG blok werd

gevarieerd. Een diblok copolymeer werd vergeleken met een triblok copolymeer waarvan het PEG blok twee keer zo lang was: zo zou je het triblok copolymeer kunnen beschouwen als twee aan elkaar bevestigde diblok copolymeren.

Het bleek dat bloem-vormige micellen van het triblok copolymeer kleiner waren dan ster-vormige micellen van het diblok copolymeer. We vermoedden dat dit komt doordat de PEG-lussen er voor zorgen dat een triblok copolymeer méér plek nodig heeft aan het oppervlak van een micel, dan twee losse diblok copolymeren. Hierdoor passen er minder polymeer-moleculen per micel en worden de micellen dus kleiner. Ons vermoeden werd bevestigd toen we de PEG-blokken in de triblok copolymeren groter maakten: dit leidde tot nog kleinere micellen.

Nanodeeltjes verstrooien licht: melk is bijvoorbeeld wit door natuurlijke eiwit- en vet-nanodeeltjes. De hoeveelheid verstrooid licht hangt af van de gemiddelde massa van de nanodeeltjes. Met lichtverstrooiings-experimenten hebben we bepaald hoe zwaar de ster-vormige en bloem-vormige micellen zijn. Het bleek dat inderdaad de bloem-vormige micellen minder dan de helft van het aantal ketens bevatten dan de ster-vormige micellen. Als je een triblok copolymeer beschouwt als een dubbel diblok copolymeer, dan zou je verwachten dat ze *precies* half zo veel ketens bevatten. Ook bleken de triblok copolymeren per keten inderdaad meer dan twee keer zo veel plek op het oppervlak van een micel nodig te hebben dan de diblok copolymeren, door het vormen van lussen.

Tenslotte hebben we gekeken naar de beweeglijkheid van de hydrofiele ketens in de ster-vormige en bloem-vormige micellen. Hiervoor maakten we gebruik van een techniek genaamd NMR (nuclear magnetic resonance oftewel kernspin-resonantie). Met behulp van een magneetveld en radiofrequentie-signalen brachten we orde aan tussen de kernen van de waterstofatomen in de PEG-ketens. De tijd die het duurde voordat deze orde weer verstoord werd (de zogenaamde T_2 relaxatietijd) namen we als maat voor de beweeglijkheid van de PEG-ketens.

Het bleek dat bij lage temperatuur (waar de thermosensitieve polymeren nog geen micellen vormen) deze relaxatietijd voor alle ketens hetzelfde was. Maar bij verhogen van de temperatuur (waardoor micellen gevormd werden) waren er duidelijke verschillen te zien.

Ten eerste bleken van iedere PEG keten de waterstofatomen dicht bij de kern van de micel veel minder beweeglijk te zijn dan de waterstofatomen verder weg van de kern. In de bloem-vormige micellen had een veel groter deel van de waterstofatomen een verminderde beweeglijkheid dan in de ster-vormige micellen.

Ten tweede bleken de waterstofatomen die wél nog beweeglijk waren (dus de stukken PEG-keten helemaal aan de buitenkant van de micellen), toch een stuk minder beweeglijk te zijn in de bloem-vormige micellen dan in de ster-vormige micellen.

Uit de combinatie van de lichtverstrooiings-experimenten en de NMR-experimenten leidden we af dat de polymeerketens in bloem-vormige micellen inderdaad enigszins hinder ondervinden van het feit dat ze lussen moeten vormen. Omgekeerd is het feit dat wij deze hinder konden waarnemen, een bewijs dat de triblok copolymeren inderdaad bloem-vormige micellen vormen. Het was wel bekend dat ze nanodeeltjes vormen, maar dat die er uit zien als bloem-vormige micellen was tot nu toe maar een theorie.

Hoofdstuk 6. Een hydrogel die micellen afgeeft met geneesmiddel er in

Behalve bloem-vormige micellen, kunnen triblok copolymeren ook een zogenaamde hydrogel vormen. Bij lage concentratie vormen ze micellen terwijl een hydogel ontstaat bij hogere concentratie. Zo'n hydrogel kan beschouwd worden als een groot aantal bloemvormige micellen dicht bij elkaar, die aan elkaar vast 'plakken' doordat er ook polymeerketens zijn die 'bruggen' vormen (Figuur 3 op pagina 208). Eén hydrofoob blok zit dan in de kern van de ene micel, terwijl het andere hydrofobe blok in de kern van een andere micel zit. Hoofdstuk 6 laat zien dat als je een stukje van zo'n hydrogel in een groter volume water brengt, er zich spontaan bloem-vormige micellen afsplitsen van de gel. Micellen blijven vrijkomen totdat er een soort evenwichts-concentratie van micellen ontstaat in het water. Als het water dan ververst wordt, komen er weer nieuwe micellen vrij, enzovoort.

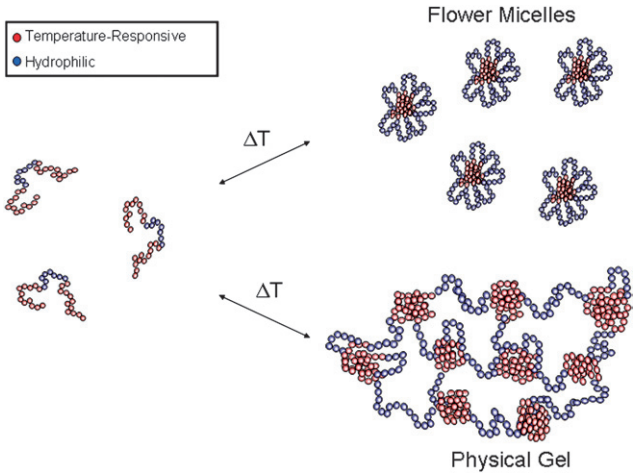

Figuur 3. Thermosensitieve triblok copolymeren kunnen bij lage concentratie bloemvormige micellen vormen (boven). Bij hoge concentratie vormen ze hydrogels (onder). Met toestemming overgenomen uit McCormick *et al.*, *Soft Matter* **2008**, *9*, 1760-1773. Copyright 2008, the Royal Society of Chemistry.

De zelfde polymeren als in hoofdstuk 5 werden ook in hoofdstuk 6 gebruikt, namelijk pNIPAm-PEG-pNIPAm. Hydrogels werden gevormd door een geconcentreerde polymeer-oplossing te verwarmen tot 37 °C. Het bleek dat hydrogels van polymeren met korte pNIPAm blokken veel sneller micellen af gaven dan hydrogels van polymeren met lange pNIPAm blokken.

Als het kanker-geneesmiddel (cytostaticum) paclitaxel in de hydrogel opgelost werd voordat de hydrogel in water gebracht werd, dan kon na enige tijd een hoge concentratie paclitaxel in het water gemeten worden, veel hoger dan de oplosbaarheid van paclitaxel in water. Dit geeft aan dat het paclitaxel in de kernen van de micellen zat, waarin het veel beter oplosbaar is dan in water. Ook hier bleek dat polymeren met korte pNIPAm blokken sneller paclitaxel afgaven dan polymeren met lange pNIPAm blokken: de snelheid van afgifte van paclitaxel volgt dus de snelheid van afgifte van micellen.

We wilden onderzoeken of dit systeem ook echt gebruikt zou kunnen worden voor de afgifte van geneesmiddelen. Zoals uitgelegd is het verpakken van geneesmiddelen in nanodeeltjes (micellen) een veel onderzochte manier om ze specifiek in tumoren terecht te laten komen. Maar micellen moeten per injectie toegediend worden. Eén keer een hydrogel injecteren die vervolgens langere tijd micellen met geneesmiddel af geeft, zou dus handig kunnen zijn.

Onze hydrogelen hebben we daarom toegediend aan muizen die tumoren hadden. Bij kamertemperatuur waren het gewoon polymeeroplossingen die eenvoudig geïnjecteerd konden worden. Na de injectie warmden de thermosensitieve polymeren op tot lichaamstemperatuur, waardoor hydrogels vanzelf gevormd werden. Eén hydrogel was niet beladen met paclitaxel, één hydrogel bevatte de hoeveelheid paclitaxel die een muis normaal gesproken maximaal kan verdragen en één hydrogel bevatte 6 keer zo veel paclitaxel. Zelfs deze laatste hydrogel werd goed verdragen door de muizen, wat een indicatie is dat het paclitaxel inderdaad verpakt was in de hydrogel en later in de micellen die er uit vrij kwamen.

Na injectie van de hoogste dosis paclitaxel, kon dit nog 48 uur lang in het bloed van de muizen aangetoond worden. Berekeningen gaven aan dat al het paclitaxel vrij kwam, maar de snelheid waarmee het uit het bloed verdween was lager dan bekend is voor vrij paclitaxel. Deze waarnemingen duiden er op dat het paclitaxel langzaam vrij komt uit de hydrogels en dat het mogelijk inderdaad vrijkomt in micellen.

Bovendien bleek één injectie van de hydrogel met de hoogste dosering paclitaxel in staat te zijn de groei van de tumoren drie weken lang te verhinderen. Dit was slechts een allereerste experiment, maar het nieuwe toedienings-concept blijkt te werken: het is mogelijk dat dit uiteindelijk een toepassing vindt voor de langzame afgifte van cytostatica.

List of publications

Albert J. de Graaf, Marlous Kooijman, Wim E. Hennink and Enrico Mastrobattista: Nonnatural Amino Acids for Site-Specific Protein Conjugation, *Bioconjugate Chemistry*, **2009**, *20* (7), pp 1281-1295

Albert J. de Graaf, Enrico Mastrobattista, Cornelus F. van Nostrum, Dirk T. S. Rijkers, Wim E. Hennink and Tina Vermonden: ATRP, subsequent azide substitution and 'click' chemistry: three reactions using one catalyst in one pot, *Chemical Communications*, **2011**, *47*, pp. 6972-6974

Albert J. de Graaf, Kristel W. M. Boere, Johan Kemmink, Remco G. Fokkink, Cornelus F. van Nostrum, Dirk T. S. Rijkers, Jasper van der Gucht, Hans Wienk, Marc Baldus, Enrico Mastrobattista, Tina Vermonden and Wim E. Hennink: Looped Structure of Flowerlike Micelles Revealed by ^{1}H NMR Relaxometry and Light Scattering, *Langmuir*, **2011**, *27* (16), pp 9843–9848

Albert J. de Graaf, Enrico Mastrobattista, Tina Vermonden, Cornelus F. van Nostrum, Dirk T. S. Rijkers, Rob M. J. Liskamp, and Wim E. Hennink: Thermosensitive Peptide-Hybrid ABC Block Copolymers Obtained by ATRP: Synthesis, Self-Assembly, and Enzymatic Degradation, *Macromolecules* **2012**, *45*, 842-851

Affiliations of collaborating authors

Inês I. Azevedo Próspero dos Santos, Escola Superior de Tecnologia da Saúde de Lisboa, Instituto Politécnico de Lisboa, Portugal.

Marc Baldus, Bijvoet Center for Biomolecular Research, NMR Spectroscopy Research Group, Utrecht University, The Netherlands.

Kristel W. M. Boere, Utrecht Institute for Pharmaceutical Sciences, Pharmaceutics, Utrecht University, The Netherlands.

Remco G. Fokkink, Laboratory of Physical Chemistry and Colloid Science, Wageningen University, The Netherlands

Jasper van der Gucht, Laboratory of Physical Chemistry and Colloid Science, Wageningen University, The Netherlands

Wim E. Hennink, Utrecht Institute for Pharmaceutical Sciences, Pharmaceutics, Utrecht University, The Netherlands.

Johan Kemmink, Utrecht Institute for Pharmaceutical Sciences, Medicinal Chemistry & Chemical Biology, Utrecht University, The Netherlands.

Robbert J. Kok, Utrecht Institute for Pharmaceutical Sciences, Pharmaceutics, Utrecht University, The Netherlands.

Marlous Kooijman,Utrecht Institute for Pharmaceutical Sciences, Pharmaceutics, Utrecht University, The Netherlands.

Rob M. J. Liskamp, Utrecht Institute for Pharmaceutical Sciences, Medicinal Chemistry & Chemical Biology, Utrecht University, The Netherlands.

Enrico Mastrobattista, Utrecht Institute for Pharmaceutical Sciences, Pharmaceutics, Utrecht University, The Netherlands.

Cornelus F. van Nostrum, Utrecht Institute for Pharmaceutical Sciences, Pharmaceutics, Utrecht University, The Netherlands.

Ebel H. E. Pieters, Utrecht Institute for Pharmaceutical Sciences, Pharmaceutics, Utrecht University, The Netherlands.

Dirk T. S. Rijkers, Utrecht Institute for Pharmaceutical Sciences, Medicinal Chemistry & Chemical Biology, Utrecht University, The Netherlands.

Tina Vermonden, Utrecht Institute for Pharmaceutical Sciences, Pharmaceutics, Utrecht University, The Netherlands.

Hans Wienk, Bijvoet Center for Biomolecular Research, NMR Spectroscopy Research Group, Utrecht University, The Netherlands

Dankwoord

Een promotietraject wordt door sommigen wel “de mooiste tijd van je leven” genoemd. Of dat waar is weet ik natuurlijk nog niet (ik zou ’t niet erg vinden als het nóg mooier wordt) maar een feit is: ik heb het erg naar mijn zin gehad. Ik ben tot de conclusie gekomen dat, wat mij betreft, het niet eens zo heel erg uit maakt wat je precies doet. Als je er maar je creativiteit in kwijt kunt en, minstens zo belangrijk, als je gezellige mensen om je heen hebt, komt het wel goed. Een heel aantal mensen wil ik daarom hartelijk bedanken.

Allereerst mijn vele studenten. Zonder jullie handen stond ik nu waarschijnlijk nog op het lab. Marlous, met ons review-artikel kreeg mijn project een kick-start. In *no time* verzamelde jij een enorme berg literatuur en bracht daar structuur in. Ik was er vast van overtuigd dat ik op dat onderwerp verder zou gaan: zo zie je maar hoe dat gaat. Kristel, dankjewel voor het doorzettingsvermogen waarmee je de flowermicelles uiteindelijk getemd hebt. Ik ben blij dat jullie allebei, Marlous en Kristel, collega’s in onze groep geworden zijn en ik heb er alle vertrouwen in dat jullie heel succesvol gaan zijn. Inês, you came from the sunny Portugal all the way to the Dutch snow to elaborate a ‘wild idea’ that had come out of Kristel’s project. Your structured way of working is still an example for me. Rima, jij kwam helemaal in het begin toen ik ook nog niet wist hoe het allemaal in elkaar zat. In jouw project hebben we gemerkt wat er allemaal niet kan: dat is later heel waardevol gebleken. Redouan en Rob, jullie werk aan niet-natuurlijke aminozuren en recombinante eiwitproductie is niet in dit boekje terecht gekomen, maar ik (en jullie hopelijk ook) heb er wel veel plezier aan beleefd. Een promotieonderzoek duurt nu eenmaal vier en geen acht jaar, dus je moet een keer keuzes maken.

Ik had ook het geluk een heel team van uitstekende begeleiders te hebben: Wim, Enrico, Tina, Dirk en René, elke maand kwamen jullie met zijn allen met mij om de tafel zitten om mij de juiste vragen te stellen en me met goede raad terzijde te staan. Wim, een goed team bestaat uit mensen die complementair zijn. Op jou en mij is dat zeker van toepassing. Bovenal wil ik je daarom bedanken voor je vertrouwen: waar het kon liet je me dingen altijd op mijn manier doen al moet het je soms gejeukt hebben.

Je eist van je AIO's bijna net zo veel als van je zelf, maar als het er op aan komt staat niemand zo vierkant achter zijn mensen als jij. Enrico, jouw niet aflatende stroom ideeën en bovenal je onverbeterlijke optimisme hebben me altijd als dat nodig was er aan herinnerd dat we wetenschap bedrijven omdat het zo spannend is. Ook buiten jouw expertise ben je een geweldige dagelijks begeleider. Tina, het project ging steeds meer in jouw richting en ik ben heel blij dat jij ook co-promotor bent geworden. Hoe bescheiden je ook bent, als het er op aan komt geef jij openhartig je mening. Dank daar voor. Dirk, een goede buur is beter dan een verre vriend. Jij bent *de* buurman van onze vakgroep. Jouw engelengeduld in het beantwoorden van domme vragen is uitzonderlijk, net als de precisie waarmee je manuscripten nakijkt. René, als stille kracht van het team was het juist op de onverwachte momenten dat jouw grote ervaring me verder hielp. Rob, al verdween je mettertijd op de achtergrond, toch hoor je ook in dit rijtje thuis. Jouw energie en pragmatische instelling hebben me op een cruciaal moment verder geholpen. Synthesizer - *E. coli* 1 - 0, wordt vervolgd.

Mies, jouw onschatbare waarde behoeft geen betoog. Maar bovenal waardeer ik je om je levensinstelling. Zoals alles is ook wetenschap mensenwerk en draait het er om dat je er voor elkaar bent, samen lol hebt en vooral jezelf niet te serieus neemt. Dank voor je hulp en alle gezelligheid, en voor het paranimf-zijn. Işıl, my other paranimf, like Mies you're also always there for the people around you. I still owe you a Mars bar. Thanks for being a great colleague and for being my paranimf.

Alle andere vroegere en huidige collega's van het lab verdienen hier ook een plekje. Wouter van de Unclear Medicine/Advanced NUclear Science, het is allemaal jouw schuld dat ik bij BioFarm terecht ben gekomen. The ex-Z521 crew: Roberta, Francesca, Laura, Yang and Luís, you were great lab-mates. Cristianne (i.t.t. mij een echte Limburger) dank voor de muizen, het vele advies en het gezelschap op de vroege ochtend. Also the other members of the *early bird club* Karin, Grzegorz, of course also Işıl and Tina, and later Hajar: I was never alone early in the morning. If one comes to work in the weekend, he is always welcomed by the *weekend crew* Yahya, Farshad and Mazda, and previously Amir G. Also the other Iranians Afrouz, Amir V., Maryam, Mehrnoosh, Mercedeh, Neda, Negar, Sima and Shima: thanks for

the cultural exchange. Maryam (and Mercedeh), I really enjoyed working with you. As I said, complementary characters make up a good team. Thanks for the flowermicelles idea, and I'm sure your project will give fantastic results.

De "oude garde" Ellen, Ethlinn, Frank, Joris, Joost, Marcel, Niels, Rolf, Sabrina, Twan en naamgenoot Albert Jan, jullie hebben de weg voorbereid. Abdul, Alex, Anastasia, Andhyk, Bart, Burcin, Chris, Eduardo, Erik, Filis, Georgi, Jia, Kim, Kimberley, Kohei, Louis, Inge, Maria, Marina, Markus, Medha, Merel, Naushad, Paul, Peter B., Peter vM., Pieter, Rachel, Roy, Sander, Susan, Sylvia, Vera, bedankt voor van alles en nog wat en vooral de gezelligheid. De *eminence grise* Daan, Gert, Huub, Herman en nu ook Raymond, zo ver heb ik niet gezien maar reuzenschouders in de buurt zijn toch handig. Van de onderwijs-staf wil ik met name Marie-Louise, Nel en Thom bedanken voor de gezelligheid bij de labuitjes.

Emmy, er zijn nog veel biertjes niet gedronken. Roel, bedankt voor de geweldige sfeer die jij bracht. Veel geluk in Zweden. Audrey, klimmen met jou was steeds een geweldige manier om alles even te vergeten. Barbara, dank voor alle ondersteuning en vooral natuurlijk voor Tyra. Ebel, al is muizen pesten niet het leukste wat er is (en dat vind jij gelukkig ook), toch was het met jou in de stal erg gezellig. Robbert-Jan, jij was altijd bereid over van alles mee te brainstormen. Dank voor de *crash course* farmacokinetiek. Herre, niet alleen ben jij de computer- en kwaliteits-opzichter, ook heb je mij op weg geholpen met hoe je eigenlijk goed een student begeleidt. Dank daar voor.

Zoals gezegd zijn goede buren belangrijk, en tot de goede buren behoort eigenlijk iedereen van "MadChem". Allereerst Steffen voor veel discussies, advies en flauwekul. Alle bewoners van het Metal-lab voor de goede muziek, lol en "geleende" chemicaliën. Hans J. voor de peptiden, Hans H. voor de MS, en Johan voor de NMR. Ook de samenwerkingen buiten het Went- en Wiedgebouw waren erg prettig: Jasper en Remco uit Wageningen: hartelijk dank voor de SLS-metingen en ondersteuning. Marc, Sabine, Christian en Hans (en later Jan): geweldig om met jullie samen te mogen werken aan NMR relaxatie. Sert en Peter, dank voor de gezellige gesprekken en voor mij naar huis sturen als het te laat werd. Iedereen van de instrumentele dienst, het magazijn en schoonmakers: zonder jullie gebeurde er niets.

Buiten de universiteit zijn er ook tal van mensen die ik wil bedanken voor de vele momenten van ontspanning en gezelligheid waarin het weer duidelijk werd waar het echt om draait in het leven. Het Smulhuis: Esther, Diny, Jos, alle vrijwilligers en de gasten. Iedereen van Spontaan, Proton Elementair, de Trumantrawanten, huisgenoot Maartje en natuurlijk Aissatou + dochters: jullie zijn schatten. Opa en oma's, ooms en tantes, neefjes en nichtjes: het is altijd gezellig met jullie. Dank voor alle belangstelling. Pa, hoe ben jij ooit gepromoveerd met twee koters om je heen? Ik ben blij dat ik jouw voorbeeld had om te volgen (wat betreft promoveren dan, die koters nog niet). Ik hou me aanbevolen als opstapper naar Engeland. Christel en Dione, Bram, Christien, Anne en al jullie aanhang, ik ben heel blij met jullie. Ook bij de familie Flameling heeft die rare *homo kinetus* zich altijd heel welkom gevoeld. Dank voor het ontspannende bomenzagen en autosleutelen.

En ten slotte natuurlijk mijn allerliefste Roos: bergen beklimmen is vooral leuk als jij er bij bent. Deze beklimming had ik niet gekund zonder jou. Het heeft lang genoeg geduurd en is nu afgelopen, maar samen gaan we nog heel veel avonturen beleven!

Curriculum vitae

Albert de Graaf was born on the 29th of January 1983 in Delft, the Netherlands. After finishing pre-university education (Gymnasium *cum laude*) at the Bernardinus College in Heerlen in 2000, he started studying chemistry and physics at Utrecht University. Continuing after the first year with only with chemistry, he obtained his Master's degree in chemistry (master programme Drug Innovation) in 2007, *cum laude*. During his studies, he performed research internships at the NMR spectroscopy research group, Utrecht University; the department of nuclear medicine, Utrecht University Medical Centre; and the department of pharmaceutics, N.V. Organon, Oss, the Netherlands. In december 2007 he started his PhD research project at the department of Pharmaceutics, Utrecht University under the supervision of prof. dr. ir. W. E. Hennink. The results of this research project are presented in this thesis.